TESE DE DOUTORAMENTO

DEVELOPMENT OF NOVEL ARYNES AND APPLICATION TO THE SYNTHESIS OF POLYCYCLIC AROMATIC HYDROCARBONS

Iago Pozo Míguez

ESCOLA DE DOUTORAMENTO INTERNACIONAL

PROGRAMA DE DOUTORAMENTO EN CIENCIA E TECNOLOXÍA QUÍMICA

SANTIAGO DE COMPOSTELA

2020

USC
UNIVERSIDADE
DE SANTIAGO
DE COMPOSTELA

DECLARACIÓN DO AUTOR DA TESE

Development of novel arynes and application to the synthesis of polycyclic aromatic hydrocarbons

D. Iago Pozo Míguez

Presento a miña tese, seguindo o procedemento axeitado ao Regulamento, e declaro que:

1) A tese abarca os resultados da elaboración do meu traballo.
2) Na tese faise referencia ás colaboracións que tivo este traballo.
3) A tese é a versión definitiva presentada para a súa defensa e coincide coa versión enviada en formato electrónico.
4) Confirmo que a tese non incorre en ningún tipo de plaxio doutros autores nin de traballos presentados por min para a obtención doutros títulos.

En Santiago de Compostela, 18 de xuño de 2020

Asdo. Iago Pozo Míguez

USC
UNIVERSIDADE
DE SANTIAGO
DE COMPOSTELA

AUTORIZACIÓN DOS DIRECTORES DA TESE

Development of novel arynes and application to the synthesis of polycyclic aromatic hydrocarbons

Dona María Dolores Pérez Meirás e Don Diego Peña Gil, Catedrática e Profesor Titular, respectivamente, do Departamento de Química Orgánica e Investigadores Principais do *Centro Singular de Investigación en Química Biolóxica e Materiais Moleculares* (CiQUS) da Universidade de Santiago de Compostela,

INFORMAN:

Que a presente tese, correspóndese co traballo realizado por D. Iago Pozo Míguez, baixo a nosa dirección, e autorizamos a súa presentación, considerando que reúne os requisitos esixidos no Regulamento de Estudos de Doutoramento da USC, e que como directores desta non incorre nas causas de abstención establecidas na Lei 40/2015.

En Santiago de Compostela, 18 de xuño de 2020

Asdo. María Dolores Pérez Meirás

Asdo. Diego Peña Gil

USC
UNIVERSIDADE
DE SANTIAGO
DE COMPOSTELA

Agradecimientos

Durante el transcurso de esta tesis doctoral he coincidido con grandes personas que me han inspirado y ayudado, y sin las cuales su realización no hubiera sido posible. Además, he recibido el apoyo de instituciones que me han provisto de los medios necesarios. A todos ellos me gustaría agradecer sinceramente su valiosa contribución a este trabajo.

A mis directores de Tesis, la Profa. Dolores Pérez y el Prof. Diego Peña, y al Prof. Enrique Guitián, por darme esta gran oportunidad. Su entusiasmo, paciencia y dedicación han sido esenciales para completar este proyecto. Las experiencias vividas bajo su supervisión serán determinantes para mi futuro.

Al Prof. Agustín Cobas, por su ayuda desinteresada y por su trabajo en la realización y supervisión de cálculos teóricos.

Al Prof. Alois Fürstner (Max-Planck-Institut für Kohlenforschung, Mülheim an der Ruhr, Alemania), por permitirme formar parte de su grupo de investigación y por su dedicación durante tres meses. Además de a Felix, Sebastian, Julius, Minh, Bart, Lauren, Xiaobin, Johanna, Alexander, Bernhard, Karin, Roswitha, Saskia, Christian, Sebastian A. y al resto del grupo por haberme acogido amablemente. Especialmente a Monika Lickfeld y al Dr. Luis Martínez-Rodríguez por su gran ayuda.

Al Prof. Miquel A. Pericàs (ICIQ, Tarragona, España), por darme la oportunidad de unirme a su grupo de investigación y por su supervisión durante un mes. También a su grupo de investigación y a Alba, Montse, y los demás integrantes de ERTFLOW, particularmente a la Dr. Esther Alza.

Al Dr. Zsolt Majzik, Dr. Niko Pavliček, y Dr. Leo Gross (IBM Research, Zürich), y al Prof. Manuel Melle-Franco (CICECO, Universidad de Aveiro, Portugal), por hacer posible una brillante colaboración.

A Rafal Zuzak, Prof. Marek Szymonski y Prof. Szymon Godlewski (NANOSAM, University of Kraków, Poland), Dr. Mads Engelund (Espeen, Luxemburgo) y Dra. Aran García-Lekue (DIPC, San Sebastián), por una genial colaboración.

A mis compañeros y amigos de laboratorio, Lojo, García, Jenni, Sulleiro, Andrea, Juampe, Dulce, Fátima M., Celia, Silvia, Antía, Javier, Laura, Fabio, Gonzalo, Marta, Rebeca, Anxo, Jose María, David, Daniel, Jesús J., Sabela A. y Venancio que han hecho de esta una gran experiencia. Especialmente a Sara, Jose y Fátima G., por haberme enseñado tanto, y a Manu,

Sabela Q., Berta, Jesús y Saleta, por haber creado un buen ambiente en el laboratorio e incontables buenos momentos durante estos años.

A Damián, Álvaro y Eva, por los interesantes debates mantenidos y por su alentadora dedicación, y a los demás compañeros del P1L2 y P1L3. Del mismo modo, a Lucas, Núñez, Calvelo y el resto de colegas del CiQUS.

Al personal del CiQUS, incluyendo estudiantes, investigadores postdoctorales e IPs que contribuyen generando una atmósfera agradable, imprescindible para el desarrollo científico y personal. También a Laura, Noela, Pablo, Mari Carmen, Flora, Carmen, Lucía, Elena y distinguidamente a Arcadio, por asegurar el funcionamiento del centro. También a las personas que constituyen las unidades de apoyo a la investigación, sobre todo a la unidad de RX y a Ramón y Mencha.

A mis compañeros de carrera, Samuel, Cartas, Roi, Beni, Cris, Martín, Torres, Andrea, Manuel y Alberto, por muchos buenos momentos en la cafetería, y a Iria y Alba por haberme acompañado tanto dentro como fuera del aula.

A los miembros de la Sociedade Xuvenil Galega de Química (SXGQ), particularmente a Marta y Sergio, por haber compartido divertidísimas actividades de divulgación, chocolatadas y tardes de Dixit.

A Juanito, Luigi, Cepeda, Denis, Carlos, Diego, Cristian, Lucas, Xabier, García, Marco, Damián, Adriana, Varela, Pombo, Xaquín, Mario, Manuel, Jorge, Lucía, Tania, Antón, Kike y otros amigos, por estar siempre dispuestos a disfrutar y compartir los mejores momentos.

A mis padres y a mi hermana, por su apoyo incondicional y su confianza, que me han permitido abordar este desafío.

A Nuria, por ser mi principal apoyo durante esta etapa. Gracias por acompañarme en cada momento y en cada decisión.

A la Xunta de Galicia y al Fondo Social Europeo (FSE) por haberme concedido una beca predoctoral. Así como al Ministerio de Economía y Empresa (MINECO) por el apoyo económico concedido a través a los proyectos CTQ2013-44142-P y CTQ2016-78157-R (IP: Profa. Dolores Pérez).

List of publications

Catalytic Asymmetric Fluorination of Copper Carbene Complexes: Preparative Advances and a Mechanistic Rationale

M. Buchsteiner, L. Martinez-Rodriguez, P. Jerabek, I. Pozo, M. Patzer, N. Nöthling, C. W. Lehmann, A. Fürstner

Chem. Eur. J. **2020**, *26*, 2509–2515.

Revisiting Kekulene: Synthesis and Single Molecule Imaging

I. Pozo, Z. Majzik, N. Pavliček, M. Melle-Franco, E. Guitián, D. Peña, L. Gross, D. Pérez

J. Am. Chem. Soc. **2019**, *141*, 15488–15493.

Synthesis of nanographenes, starphenes and sterically congested polyarenes by aryne cyclotrimerization

I. Pozo, E. Guitián, D. Pérez, D. Peña

Acc. Chem. Res. **2019**, *52*, 2472–2481.

Synthesis and reactivity of a trigonal porous nanographene on a gold surface

R. Zuzak, I. Pozo, M. Engelund, A. Garcia-Lekue, M. Vilas-Varela, J. M. Alonso, M. Szymonski, E. Guitián, D. Pérez, S. Godlewski, D. Peña

Chem. Sci. **2019**, *10*, 10143–10148.

1,7-Naphthodiyne: A New Platform for the Synthesis of Novel, Sterically Congested PAHs

I. Pozo, A. Cobas, D. Peña, E. Guitián, D. Pérez

Chem. Commun. **2016**, *52*, 5534–5537.

USC
UNIVERSIDADE
DE SANTIAGO
DE COMPOSTELA

Table of contents

Table of contents I

Abbreviations and symbols V

Abstract VII

1 Introduction 1

1.1 Polycyclic Aromatic Hydrocarbons 1

1.1.1 Structure and properties 2

1.1.2 Classification and potential applications 6

1.2 Arynes 9

1.2.1 Structure and reactivity 11

1.2.2 Generation methods 17

1.2.3 Hetarynes 19

1.2.4 Polyarynes: bisarynes, trisarynes and beyond 22

1.3 Application of arynes in materials chemistry 27

2 2-Thiophyne 33

2.1 Backgroud information 33

2.1.1 Contributions from Wittig's group 33

2.1.2 Contributions from Reinecke's group 35

2.1.3 Contributions by other authors 36

2.2 Objectives 38

2.3 Results and discussion 39

2.3.1 Synthesis of 2-(trimethylsilyl)-3-thiophenyl triflate 39

2.3.2 Study of reactivity 41

2.3.3 Mechanistic studies 43

2.4 Conclusions 48

3 1,7-Naphthodiyne 49

3.1 Background information 49

3.2 Objectives 51

3.3 Results and discussion 52

3.3.1 Synthesis of a precursor of 1,7-naphthodiyne 52

3.3.2 Study of reactivity 55

3.3.3 Study of a novel reaction: formal aryne insertion into a C-H bond 59

3.4 Conclusions 62

USC UNIVERSIDADE DE SANTIAGO DE COMPOSTELA

4 2,6,10-Triphenylenotriyne 63
4.1 Background information 63
4.1.1 1,3,5-Benzotriyne 63
4.1.2 Other trisaryne synthons 66
4.2 Objectives 68
4.3 Results and discussion 69
4.3.1 Synthesis of precursors of 2,6,10-triphenylenotriyne 69
4.3.2 Study of reactivity with other dienes 74
4.4 Conclusions 77

5 Aryne-based synthesis of heteroacenes 79
5.1 Background information 79
5.1.1 Substituted acenes 80
5.1.2 π-Extended acenes 80
5.1.3 Heteroatom-containing acenes 81
5.1.4 Aryne-mediated synthesis of acenes 82
5.2 Objectives 84
5.3 Synthesis of heteroacenes: acenotriazoles and acenoisoxazoles 85
5.4 Preliminary study of electronic properties of heteroacenes 89
5.5 Conclusions 93

6 Kekulene 95
6.1 Background information 95
6.1.1 Benzene and annulenes 95
6.1.2 Story of kekulene 96
6.1.3 Other cycloarenes 99
6.2 Objectives 101
6.3 Synthesis of kekulene 102
6.4 Structural study of kekulene 110
6.4.1 AFM 110
6.4.2 Calculations 111
6.5 Conclusions 113

7 Experimental section 115
7.1 General procedures 115
7.2 Experimental procedures for Chapter 2 117
7.2.1 Synthesis of 2-(trimethylsilyl)-3-thiophenyl trifluoromethanesulfonate (2) 117

7.2.2 Reactivity of 2-(trimethylsilyl)-3-thiophenyl trifluoromethanesulfonate (2) 119
7.2.3 Computational details 121
7.3 Experimental procedures for Chapter 3 125
7.3.1 Synthesis of 1,8-bis(trimethylsilyl)naphthalene-2,7-diyl bistriflate (32) 125
7.3.2 Reactivity of 1,8-bis(trimethylsilyl)naphthalene-2,7-diyl bistriflate (32) 128
7.3.3 Study of the novel reactivity: formal C-H bond aryne insertion 133
7.3.4 Computational details 136
7.4 Experimental procedures for Chapter 4 138
7.4.1 Synthesis of tris(trifluoromethanesulfonate)s 55 138
7.4.2 Reactivity of tris(trifluoromethanesulfonate)s 55 144
7.5 Experimental procedures for Chapter 5 147
7.5.1 General procedure for the synthesis of heteroacenes 147
7.5.2 Synthesis of heteroacenes 148
7.5.3 Computational details 156
7.6 Experimental procedures for Chapter 6 157
7.6.1 Synthesis of 5,6,8,9-tetrahydrobenzo[m]tetraphene (103) 157
7.6.2 AFM imaging 159
7.6.3 Computational details 159

Appendix 161
A.1 Selected spectra 161
A.2 Arynes: chronology 215
A.3 Diederich and Staab's synthesis of kekulene 219
A.4 Cover image 221

Resumen de la tesis doctoral 223

USC
UNIVERSIDADE
DE SANTIAGO
DE COMPOSTELA

Abbreviations and symbols

Ac	Acetyl
AFM	Atomic Force Microscopy
APCI	Atmospheric Pressure Chemical Ionisation
Bn	Benzyl
Bu	Butyl
CBP	4,4'-bis(*N*-carbazolyl)-1,1'-biphenyl
CCDC	Cambridge Crystallographic Data Centre
CNT	Carbon nanotubes
Cp	Cyclopentadienyl
CPCM	Conductor-like Polarisation Continuum Model
Cp*	1,2,3,4,5-Pentamethyl cyclopentadienyl
Cy	Cyclohexyl
CV	Cyclic voltammetry
d	Doublet (in NMR)
dd	Doublet of doublets (in NMR)
DABCO	1,4-Diazabicyclo[2.2.2]octane
DBU	1,8-Diazabicyclo[5.4.0]undec-7-ene
DDQ	2,3-Dichloro-5,6-dicyano-para-benzoquinone
DFT	Density Functional Theory
DMAD	Dimethyl acetylenedicarboxylate
DMF	*N*,*N*-Dimethylformamide
E	Energy
EI	Electron Ionisation
Et	Ethyl
Fc	Ferrocene
FLG	Few-Layer Graphene
HBC	Hexabenzocoronene
HMDS	Hexamethyldisilazane
HOMO	Highest Occupied Molecular Orbital
HPLC	High Performance Liquid Chromatography
HRMS	High Resolution Mass Spectrometry
h/ν	Light
i-	*iso*-
IR	Infrared spectroscopy
J	Coupling constant (in NMR)
LG	Leaving Group
LTMP	Lithium 2,2,6,6-tetramethylpiperidide
LRMS	Low Resolution Mass Spectrometry
LUMO	Lowest Unoccupied Molecular Orbital
m	Multiplet (in NMR)
m-	*meta*-
MCPBA	*meta*-Chloroperoxybenzoic acid
Me	Methyl
MALDI	Matrix-Assisted Laser Desorption/Ionisation
MM	Molecular Mechanics
MO	Molecular Orbitals
Ms	Mesyl
m/z	Mass/Charge ratio
n-	*normal*-

NALDI	Nanotechnology-Assisted Laser Desorption/Ionisation
NBS	*N*-Bromosuccinimide
NICS	Nucleus Independent Chemical Shift
NMR	Nuclear Magnetic Resonance
NHE	Normal Hydrogen Electrode
Nu	Nucleophile
o-	*ortho*-
OFET	Organic Field-Effect Transistor
OLED	Organic Light Emitting Diodes
OTf	Trifluoromethanesulfonate
Ox	Oxidation or oxidant
p-	*para*-
PAH	Polycyclic Aromatic Hydrocarbon
Ph	Phenyl
PPM	Probe Particle Model
Pr	Propyl
Py	Pyridine
q	quartet
Red	Reduction or reducing agent
rt	Room temperature
s	Singlet (in NMR)
SFC	Supercritical Fluid Chromatography
t-	*tert*-
TBAF	Tetra-*n*-butylammonium fluoride
TBS	Tert-Butyldimethylsilyl
td	Triplet of doublets (in NMR)
TD	Time-Dependent
TES	Triethylsilyl
THF	Tetrahydrofuran
TIPS	Triisopropylsilyl
TLC	Thin-Layer Chromatography
TMEDA	Tetramethylethylenediamine
TMS	Trimethylsilyl
TOF	Time Of Flight
Tol	Toluene
Ts	Tosyl
UV	Ultra-Violet
Vis	Visible
XDR	X-Ray Difraction
δ	Chemical shift
Δ	Reflux temperature

Abstract

This dissertation collects the most relevant results obtained by the author in the development of novel arynes and their application to the synthesis of polycyclic aromatic hydrocarbons (PAHs) of potential use in nanotechnology. It is organised in seven chapters, being the first the Introduction and the last the Experimental Section. Intermediate chapters correspond to five independent sub-projects discussed below:

The Introduction, Chapter 1, provides a general overview of the chemistry of arynes and of the synthesis of polycyclic aromatic hydrocarbons (PAHs). Specially, the section reviews some of the most relevant examples in the junction of both topics.

Chapter 2, entitled “2-Thiophyne”, entails the synthesis of a potential precursor of this particularly elusive hetaryne, and the study of its reactivity.

Chapter 3, “1,7-Naphthodiyne”, is focused on the development of a precursor of mentioned bisaryne. Moreover, the chapter describes the study of its reactivity and examples of its ability as platform for the synthesis of angular-shaped PAHs.

Chapter 4, “2,6,10-Triphenylenotriyne”, relates to the synthesis of two precursors of this novel trisaryne and the study of their suitability to afford star-shaped nanographenes and other triphenylene-based arenes.

Chapter 5, “Aryne-based approach to heteroacenes”, describes the synthesis of two novel families of heteroacenes by means of aryne chemistry, and the preliminary study of their electronic properties.

Chapter 6, “Kekulene”, describes our contribution to the optimisation of the synthesis of this emblematic molecule, and the resolution of its structure at the single molecular level by using state-of-the-art atomic force microscopy.

Chapter 7, “Experimental section” collects a detailed description of the procedures used in Chapters 2 to 6.

USC
UNIVERSIDADE
DE SANTIAGO
DE COMPOSTELA

1 Introduction

1.1 Polycyclic Aromatic Hydrocarbons

The discovery of graphene in 2004 by Geim and Novoselov[1] sparked unprecedented expectations among the scientific community worldwide, followed by a huge stimulus of research across different fields in order to address the relevant scientific questions and technological challenges associated to this 'wonder material'.[2] From the chemical perspective, it meant that many research groups focused their efforts on obtaining tiny fragments of this material (nanographenes) with defined sizes and shapes, two features tightly related with the properties of graphene molecules and materials.[3] It is worth to note that these graphene substructures are nothing but extended **arenes**, constituted by the fusion of aromatic rings.

Arenes, defined as monocyclic and polycyclic aromatic hydrocarbons,[4] constitute a large family of molecules containing at least one cyclic π-delocalised system, usually benzene, as common structural unit. Arenes comprised by two or more fused rings are known as **p**olycyclic **a**romatic **h**ydrocarbons (PAHs) (Figure 1).

[1] K. S. Novoselov, A. K. Geim, S. V Morozov, D. Jiang, Y. Zhang, S. V. Dubonos, I. V Grigorieva, A. A. Firsov, *Science* **2004**, *5*, 1–12.
[2] A. Geim, *Science* **2009**, 324, 1530–1534.
[3] a) L. Chen, Y. Hernandez, X. Feng, K. Müllen, *Angew. Chem. Int. Ed.* **2012**, *51*, 7640–7654.
[4] G. P. Moss, P. A. S. Smith, D. Tavernier, *Pure Appl. Chem.* **1995**, *67*, 1307–1375.

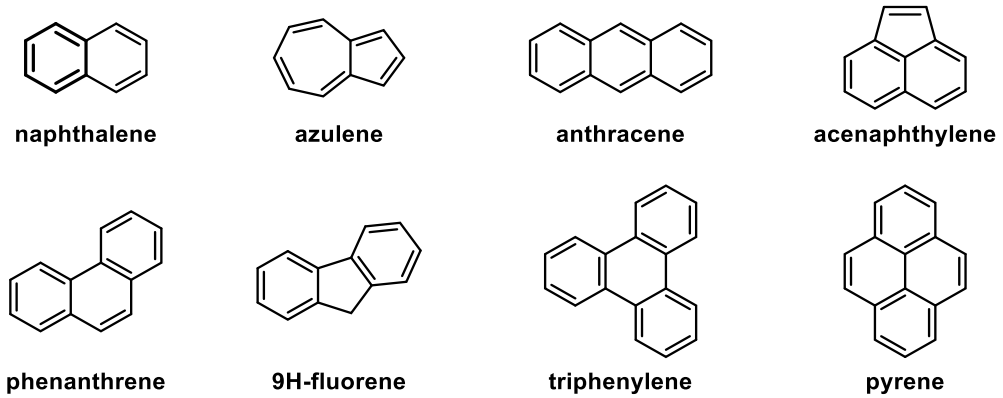


Figure 1. Examples of PAHs.

Some compounds of this family are badly reputed due to their potential carcinogenic activity.[5] This hazard arises a particular concern since many PAHs are usually generated in combustion processes and, thus, they are ubiquitous air pollutants. PAHs can be found abundantly in nature forming part of fossil fuels, such as coal and petrol.[6] Polycyclic arenes are also practically omnipresent across the Universe and could represent up to a 30% of the carbon in the Galaxy,[7] being detected by characteristic IR bands in a variety of astrophysical regions[8] and also in meteorites.[9]

1.1.1 Structure and properties

The structure of PAHs is consisted of π-conjugated (usually benzenoid) rings fused in different topological arrangements. When the fused rings share two atoms and one bond, they are referred as *ortho*-fused or *cata*-condensed, whereas if they have three atoms in common are considered *peri*-fused (Figure 2).[10]

[5] A. Lunch, *The Carcinogenic Effects of Polycyclic Aromatic Hydrocarbons*, Imperial College. Press, London, **2005**.
[6] H. Richter, J. B. Howard, *Prog. Energy Combust. Sci.* **2000**, *26*, 565–608.
[7] T. P. Snow, A. N. Witt, *Science* **1995**, *270*, 1455–1460.
[8] A. G. Li, *Nat. Astron.* **2020**, *4*, 339–351.
[9] a) B. S. & R. J. S. D. J. Cook, S. Schlemmer, N. Balucani, D. R. Wagner, *Nature* **1996**, *380*, 227–229; b) L. Becker, D. P. Glavin, J. L. Bada, *Geochim. Cosmochim. Acta* **1997**, *61*, 475–481.
[10] G. P. Moss, *Pure Appl. Chem.* **1998**, *70*, 143–216.

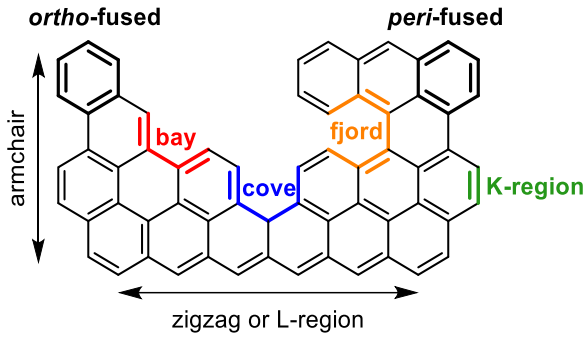


Figure 2. Common structural motifs in arenes.

Other topologic motives are those related with the shape of the periphery. In the case of nanographenes, the terms *zigzag* and *armchair* are widely used to define their edges. Conversely, PAHs' regions can also be named employing a different jargon. Thus, the peripheral shape obtained from the linear fusion of benzenic rings is also known as *L-region*, while *K-region* is the convex part of an armchair edge (Figure 2).[11] On the other hand, the areas limited by the concave edges are called *bay*, *cove* or *fjord* regions, depending on the number of C-C bonds determining these concave rims (3, 4 or 5 bonds respectively).[10,11]

Structure and properties are strongly related in monocyclic and polycyclic π-conjugated systems, in fact, some features related with their stability and properties can be qualitatively predicted following few simple rules. Thereby, it is possible to know if a fully conjugated monocyclic system is aromatic (4n+2 π-electrons) or antiaromatic (4n π-electrons) using the Hückel's rules.[12] These kind of qualitative methods have been extended for specific cases, such as Möbius topologies,[13] the excited-state of conjugated cycles[14] or spherical systems.[15] The thus predicted conclusions often match perfectly with experimental data (e.g. NMR shifts)

---

[11] a) F. S. Ehrenhauser, *Polycycl. Aromat. Comp.* **2015**, *35*, 161–176. For recent examples on the use of this nomenclature see: b) K. Ozaki, K. Kawasumi, M. Shibata, H. Ito, K. Itami, *Nat. Commun.* **2015**, *6*, 1–8; c) D. Lungerich, O. Papaianina, M. Feofanov, J. Liu, M. Devarajulu, S. I. Troyanov, S. Maier, K. Amsharov, *Nat. Commun.* **2018**, *9*, 1–8.

[10] G. P. Moss, *Pure Appl. Chem.* **1998**, *70*, 143–216.

[12] a) E. Hückel, *Z. Physik* **1931**, *70*, 204–286; b) E. Hückel, *Z. Physik* **1931**, *72*, 310–337; c) E. Hückel, *Z. Physik* **1932**, *76*, 628–648; d) E. Hückel, *Grundzüge der Theorie ungesättiger und aromatischer Verbindungen*, Berlin: Verlag Chem., **1938**.

[13] a) H. S. Rzepa, *Chem. Rev.* **2005**, *105*, 3697–3715; b) G. Naulet, L. Sturm, A. Robert, P. Dechambenoit, F. Röricht, R. Herges, H. Bock, F. Durola, *Chem. Sci.* **2018**, *9*, 9830–8936.

[14] a) N. C. Baird, *J. Am. Chem. Soc.* **1972**, *94*, 4941–4948; b) H. Ottosson, *Nat. Chem.* **2012**, *4*, 969–971; c) M. Rosenberg, C. Dahlstrand, K. Kilså, H. Ottosson, *Chem. Rev.* **2014**, *114*, 5379–5425.

[15] A. Hirsch, Z. Chen, H. Jiao, *Angew. Chem. Int. Ed.* **2000**, *39*, 3915–3917.

and theoretically calculated parameters (e.g. **n**ucleus **i**ndependent **c**hemical **s**hift, NICS).[16] An extended summary of all these concepts, rules and theories is collected in the fantastic book "*Aromaticity and other Conjugation Effects*".[17] Another characteristic presented by aromatic rings is the bond length equalisation. While antiaromatic rings clearly show an alternation between double and single bonds, aromatic cycles exhibit similar bond distances. This feature has been experimentally measured [e.g. by **X**-**r**ay **d**iffraction (XRD) analysis] and quantified by different methods and indexes over the years.[18]

In 1972 Erich Clar published a model to qualitatively predict which is the most relevant resonance form contributing to the structure of PAHs and to discuss their aromatic character.[19] Clar's rule states that the Kekulé resonance structure with the largest number of disjointed aromatic π-sextets, i.e., benzene-like moieties, is the most important for characterisation of properties of PAHs. Aromatic π-sextets (inspired by the Armit and Robinson's proposed term, *the aromatic π-sextet*)[20] are defined as six π-electrons localised in a single benzene-like ring separated from adjacent rings by formal C-C single bonds, and can be represented by a circle inscribed in the cyclic framework. As an example of the application of Clar's rule, the analysis of two *cata*-fused four-ring PAHs, triphenylene and tetracene, is shown in Figure 3. Tetracene has two possible resonant forms, although both of them contain only one aromatic sextet (Figure 3a). However, triphenylene can be represented by two different electronic structures, one displaying only one aromatic sextet, while the other bears three (Figure 3b). Therefore, the second resonant form contributes stronger of its structure. Comparing both PAHs' structures, is clear that triphenylene have more aromatic sextets, and thus, it is the most stable.

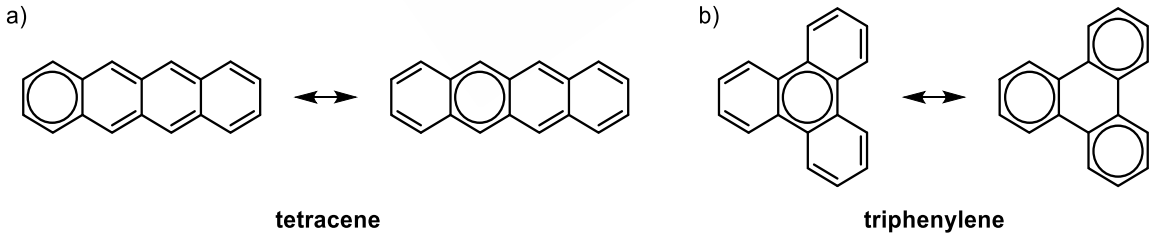


Figure 3. Resonant forms of triphenylene and tetracene.

---

[16] a) P. V. R. Schleyer, C. Maerker, A. Dransfeld, H. Jiao, N. J. R. Van Eikema Hommes, *J. Am. Chem. Soc.* **1996**, *118*, 6317–6318; b) Z. Chen, C. S. Wannere, C. Corminboeuf, R. Puchta, P. von Ragué Schleyer, *Chem. Rev.* **2005**, *105*, 3842–3888.

[17] R. Gleiter, G. Haberhauer, *Aromaticity and Other Conjugation Effects,* Wiley-VCH, **2012**.

[18] T. M. Krygowski, M. K. Cyrański, *Chem. Rev.* **2001**, *101*, 1385–1419.

[19] E. Clar, *The Aromatic Sextet*, Wiley, London, **1972**.

[20] a) M. Solà, *Front. Chem.* **2013**, *1*, 4–11; b) J. W. Armit, R. Robinson, *J. Chem. Soc. Trans.* **1925**, *127*, 1604–1618.

The relevance of Clar's structure is exposed by the correlation between the predicted resonant form and the experimental data. Thereby, in pentacene only one aromatic sextet can be placed, originating three possible resonant forms. Their combination indicates higher bond orders for C^3-C^4 and C^5-C^6, in agreement with the distances measured by X-ray diffraction analysis (Figure 4a).[21] In case of **h**exa**b**enzo**c**oronene (HBC), it is achievable to place up to seven aromatic sextets on its structure, only in one resonant form. Remarkably, the longest bonds are those located out of them (C^3-C^7 and C^4-C^5), according again with the results obtained by X-ray diffraction analysis.[21]

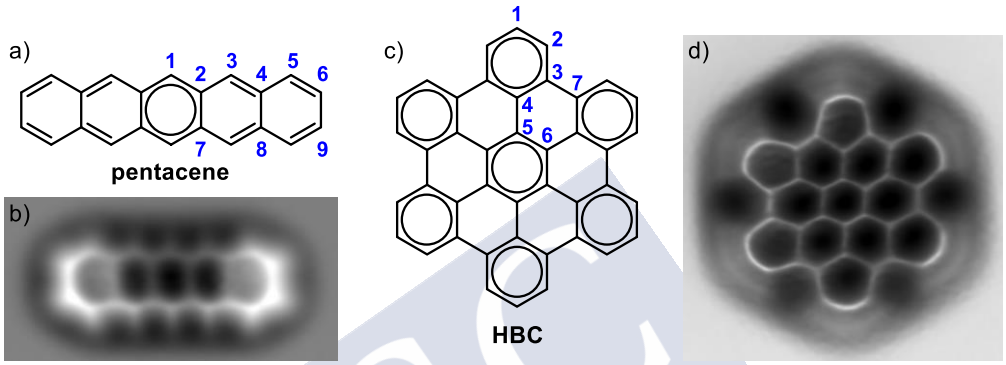


Figure 4. a) Pentacene structure, C-C bond distances (in Å) obtained from X-ray diffraction analysis; C^1-C^2: 1.44, C^2-C^3: 1.42; C^2-C^7: 1.46, C^3-C^4: 1.38; C^4-C^5: 1.43, C^4-C^8: 1.45; C^5-C^6: 1.35 and C^6-C^9: 1.43. b) Constant-height AFM images of pentacene acquired with a CO-modified tip on Cu(111). c) HBC structure, C-C bond distances (in Å) obtained from X-ray diffraction analysis; C^1-C^2: 1.37, C^2-C^3: 1.40; C^3-C^4: 1.41; C^3-C^7: 1.46, C^4-C^5: 1.45 and C^5-C^6: 1.42. b) Constant-height AFM images of HBC acquired with a CO-modified tip on Cu(111).

In recent years, the development of advanced microscopies, such as ultra-high resolution **a**tomic **f**orce **m**icroscopy (AFM), allowed to obtain clarifying single molecule images of some of these polycyclic planar compounds.[22] Detailed analysis of the contrast allows qualitative resolution of bond-order differences, particularly with regard to the inner C-C bonds. The results of these studies, applied to individual molecules, are in agreement with those obtained by bulk techniques, such as XRD.

---

[21] a) For pentacene: C. C. Mattheus, A. B. Dros, J. Baas, A. Meetsma, J. L. De Boer, T. T. M. Palstra, *Acta Crystallogr. Sect. C Cryst. Struct. Commun.* **2001**, *57*, 939–941; b) S. Xiao, M. Myers, Q. Miao, S. Sanaur, K. Pang, M. L. Steigerwald, C. Nuckolls, *Angew. Chem. Int. Ed.* **2005**, *44*, 7390–7394; c) For HBC: R. Goddard, M. W. Haenel, W. C. Herndon, C. Krueger, M. Zander *J. Am. Chem. Soc.* **1995**, *117*, 30–41.

[22] a) L. Gross, F. Mohn, N. Moll, P. Liljeroth, G. Meyer, *Science* **2009**, *325*, 1110–1114; b) L. Gross, F. Mohn, N. Moll, B. Schuler, A. Criado, E. Guitián, D. Peña, A. Gourdon, G. Meyer, *Science* **2012**, *337*, 1326–1329.

1.1.2 Classification and potential applications

The vast structural diversity of PAHs makes them classifiable under many different criteria. Traditionally, they were grouped in families with specific features in common, such as those shown in Figure 5 as representative examples of benzenoid PAHs which are relevant in the in the context of this work. Acenes, such as pentacene (Figure 4) or rubrene (5,6,11,12-tetraphenyltetracene), are among the most used *p*-type semiconductors in **o**rganic **f**ield-**e**ffect **t**ransistors (OFETs). They exhibit suitable HOMO and LUMO energy levels and high hole mobilities.[23] Furthermore, larger acenes have a great theoretical interest due to their proposed diradical ground state.[24] The paddle-wheel structure of iptycenes makes them particularly useful in the field of molecular machines and in supramolecular crystal engineering.[25] Iptycene-derived porous networks could be used as membranes or gas storage materials. Other two families of arenes whose functionality arises from their shape are starphenes and cycloarenes. Starphenes are basically three acenes fused through a trigonal junction, that can be considered as extended triphenylenes. Taking advantage of its geometry and electronic properties, they have demonstrated potential as logic gates.[26] On the other hand the circularly fused PAHs, cycloarenes (Figure 5), are difficult to synthesise, representing an historical challenge in organic synthesis. The electronic structure and properties of this family of PAHs have been subject of extensive theoretical research.[27] More recently, renewed interest in cycloarenes can be related to their structural similarity with graphene pores,[28] serving as models to provide a better understanding about the influence of these kind of defects in graphene.

---

[23] Q. Ye, C. Chi, *Chem. Mater.* **2014**, *26*, 4046–4056.
[24] a) M. Bendikov, H. M. Duong, K. Starkey, K. N. Houk, E. A. Carter, F. Wudl, *J. Am. Chem. Soc.* **2004**, *126*, 7416–7417; b) B. Hajgató, M. Huzak, M. S. Deleuze, *J. Phys. Chem. A* **2011**, *115*, 9282–9293.
[25] J. H. Chong, M. J. MacLachlan, *Chem. Soc. Rev.* **2009**, *38*, 3301–3315.
[26] W.-H. Soe, C. Manzano, N. Renaud, P. De Mendoza, A. De Sarkar, F. Ample, M. Hliwa, A. M. Echavarren, N. Chandrasekhar, C. Joachim, *ACS Nano* **2011**, *5*, 1436–1440.
[27] J. C. Buttrick, B. T. King, *Chem. Soc. Rev*. **2017**, *46*, 7−20.
[28] A. W. Robertson, G.-D. Lee, K. He, C. Gong, Q. Chen, E. Yoon, A. I. Kirkland, J. H. Warner *ACS Nano* **2015**, *9*, 11599−11607.

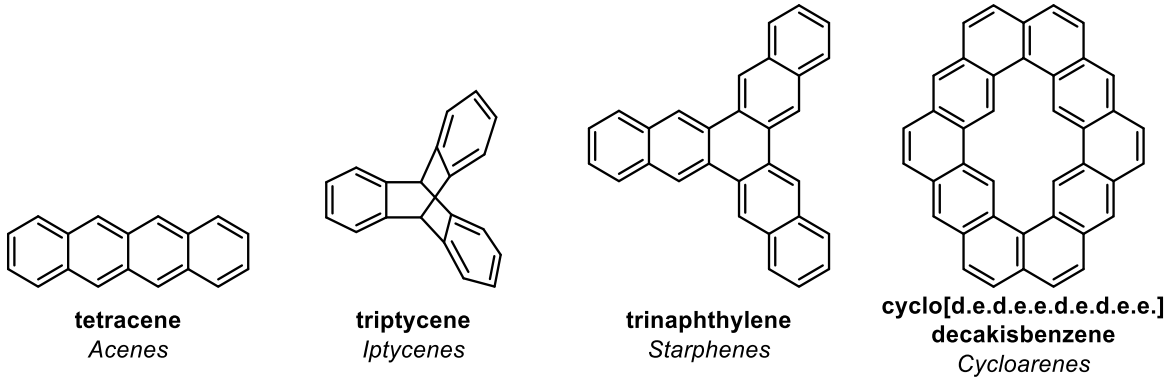


Figure 5. Examples of relevant PAHs and their corresponding *family names*.

The presence of specific chemical motives in graphene and PAHs can determine their properties. This phenomenon is usually referred as *doping*. As examples of this relationship, the addition of 5, 7 or 8 membered cycles in PAHs, originates curved scaffolds.[29] Of special interest is the case of heteroarenes, which contain at least one heteroatom (e.g. N, O, S, P, etc.).[30] Not only the number of heteroatoms and its nature affect to the properties of these compounds, but also their position is crucial (Figure 6).[31] A clarifying example is constituted by the family of HBC derivatives. Comparing the parent HBC with the *peripheral*-tetraazaHBC, both exhibit a similar electronic structure and aromatic character, although the aza-derivative displays a higher electron acceptor character. On the contrary, *internal*-diazaHBC, has two extra electrons, and for this reason, shows antiaromatic character in the central ring (4n π-electrons) and low stability.[32]

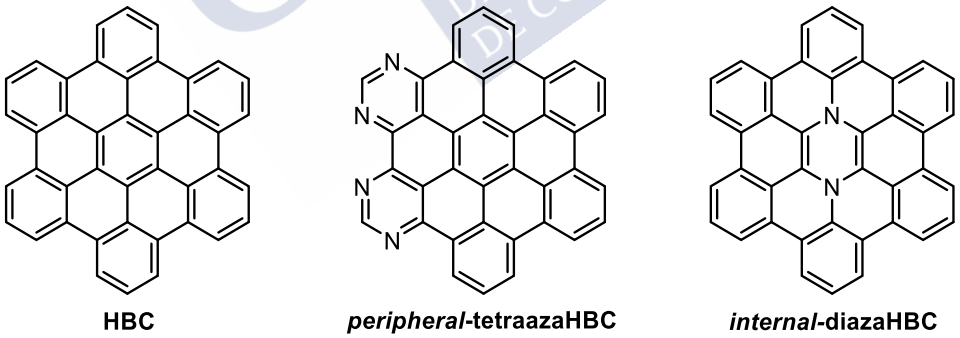


Figure 6. Examples *N*-doped HBC derivatives.

---

[29] a) M. Rickhaus, M. Mayor, M. Juríček, *Chem. Soc. Rev.* **2017**, *46*, 1643–1660; b) S. H. Pun, Q. Miao, *Acc. Chem. Res.* **2018**, *51*, 1630–1642; c) C. M. Cruz, I. R. Márquez, I. F. A. Mariz, V. Blanco, C. Sánchez-Sánchez, J. M. Sobrado, J. A. Martín-Gago, J. M. Cuerva, E. Maçôas, A. G. Campaña, *Chem. Sci.* **2018**, *9*, 3917–3924.

[30] M. Stępień, E. Gońka, M. Żyła, N. Sprutta, *Chem. Rev.* **2017**, *117*, 3479–3716.

[31] A. N. Lakshminarayana, C. Chi, *N-Containing Polycyclic Heteroarenes*, 225–226, in *Polycyclic Arenes and Heteroarenes, Q. Miao,* Wiley-VCH, **2016**.

[32] X.-Y. Wang, M. Richter, Y. He, J. Björk, A. Riss, R. Rajesh, M. Garnica, F. Hennersdorf, J. J. Weigand, A. Narita, R. Berger, X. Feng, W. Auwärter, J. V. Barth, C.-A. Palma, K. Müllen, *Nat. Commun.* **2017**, *8*, 4–10.

Heteroarenes have been widely used in organic electronics.[33] Among the most representative compounds are *N*-doped arenes (or nitrogenated arenes), such as the 4,4'-bis(*N*-**c**arbazolyl)-1,1'-**bip**henyl (CBP) (Figure 7), which works as hole transport material in **o**rganic **l**ight-**e**mitting **d**iodes (OLEDs),[34] and porphyrins, acting as dyes in dye-sensitised solar cells.[35] Whereas, oligothiophenes often play the role of semiconductors in OFETs.[36]

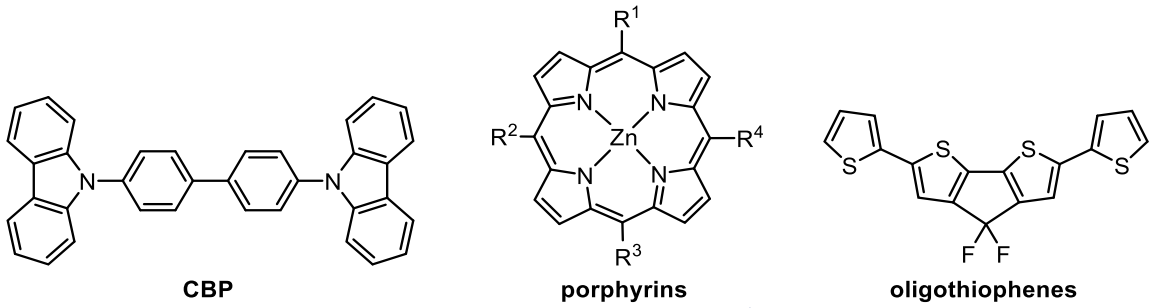


Figure 7. Examples of functional heteroarenes.

The wide structural diversity of heteroarenes and their tunable properties, make them highly interesting targets. The understanding of their structure-properties relationships will allow the design of functional materials with unprecedented applications.

[33] a) *Organic Optoelectronic Materials*, Ed.: Y. Li; Springer, **2015**; b) G. de la Torre, G. Bottari, T. Torres, *Adv. Energy Mater.* **2017**, *7*, 1601700.
[34] T. Chatterjee, K. T. Wong, *Adv. Opt. Mater.* **2019**, *7*, 1–34.
[35] M. Urbani, M. Grätzel, M. K. Nazeeruddin, T. Torres, *Chem. Rev.* **2014**, *114*, 12330–12396.
[36] Y. Ie, M. Nitani, M. Ishikawa, K. I. Nakayama, H. Tada, T. Kaneda, Y. Aso, *Org. Lett.* **2007**, *9*, 2115–2118.

1.2 Arynes

Arynes can be defined as ephemeral, neutral reaction intermediates formally derived from arenes by abstraction of two hydrogen atoms. For this reason, they have been also historically named as didehydroarenes. In 1902 Stoermer and Kahlert proposed for the first time an aryne, the *2,3-didehydrobenzofuran* (or 2-benzofuryne), as reaction intermediate,[37] Apparently, this pioneering article received minimal attention for decades. The *ortho*-benzyne was postulated as a diradical species 25 years later (Figure 8a).[38] The existence of benzyne was firmly supported by Roberts and coworkers in 1953 employing ^{14}C labelling experiments (Figure 8b).[39] Towards the second half of the twentieth century, numerous authors contributed to the understanding of the nature of these intermediates, specially of *o*-benzyne, whose spectral characterisation (IR,[40] UV[41] and mass spectra[42]) in the gas phase or in cryogenic matrices has been reported. The ^{1}H and ^{13}C NMR spectra in solution of benzyne generated inside a hemicarcerand molecular container was also described in the late 90's.[43] It should be noted the remarkable labour of Wittig and Huisgen studying arynes reactivity.[44] The fascinating story of arynes is collected in the excellent review "*One century of aryne chemistry*"[45] and in the essential book "*Dehydrobenzene and Cycloalkynes*".[46]

USC UNIVERSIDADE DE SANTIAGO DE COMPOSTELA

[37] R. Stoermer, B. Kahlert, *Ber. Dtsch. Chem. Ges.* **1902**, *35*, 1633–1640.
[38] W. E. Bachmann, H. T. Clarke, *J. Am. Chem. Soc.* **1927**, *49*, 2089–2098.
[39] J. D. Roberts, H. E. Simmons, L. A. Carlsmith, C. W. Vaughan, *J. Am. Chem. Soc.* **1953**, *75*, 3290–3291.
[40] a) O. L. Chapman, K. Mattes, C. L. Mcintosh, J. Pacansky, G. V. Calder, G. Orr, *J. Am. Chem. Soc.* **1973**, *95*, 6134–6135; b) J. G. Radziszewski, B. A. Hess, R. Zahradnik, *J. Am. Chem. Soc.* **1992**, *114*, 52–57.
[41] R. S. Berry, G. N. Spokes, M. Stiles, *J. Am. Chem. Soc.* **1962**, *84*, 3570–3577.
[42] I. P. Fisher, F. P. Lossing, *J. Am. Chem. Soc.* **1963**, *85*, 1018–1019.
[43] R. Warmuth, *Angew. Chem. Int. Ed. Engl.* **1997**, 1347–1350.
[44] a) G. Wittig, *Naturwissenschaften* **1942**, *30*, 696–703; b) G. Wittig, *Angew. Chem. Int. Ed. Engl.* **1965**, *4*, 731–737; c) R. Huisgen, H. Rist, *Naturwissenschaften* **1954**, *41*, 358–359; d) R. Huisgen, R. Knorr, *Tetrahedron Lett.* **1963**, *16*, 1017–1021; e) R. Huisgen, R. Knorr, *Naturwiss.***1961**, *48*, 715–716.
[45] H. H. Wenk, M. Winkler, W. Sander, *Angew. Chem. Int. Ed.* **2003**, *42*, 502–528.
[46] R. W. Hoffmann, *Dehydrobenzene and Cycloalkynes*, Academic Press, New York, **1967**.

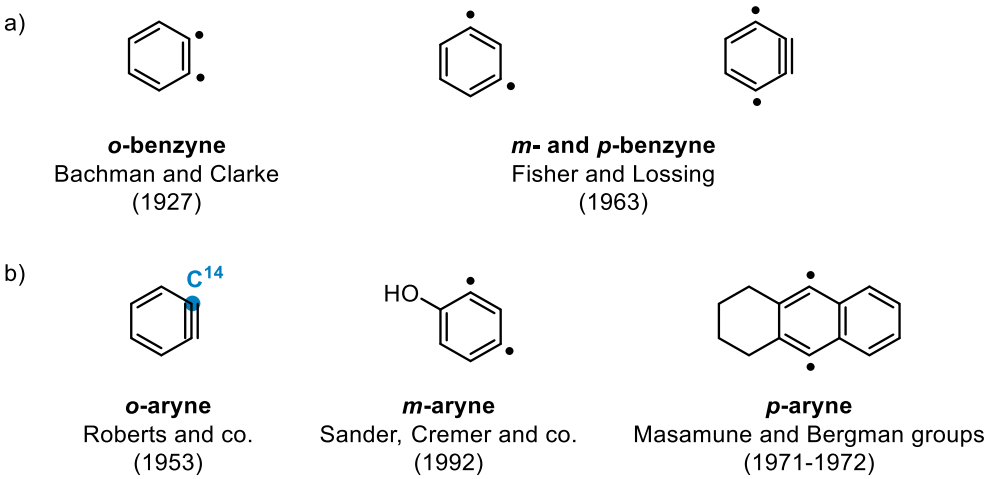


Figure 8. a) Postulated *o*-, *m*- and *p*-benzynes. b) Examples of experimentally detected *o*-, *m*- and *p*-arynes.

During the late sixties and early seventies, several articles were published describing attempts to generate *m*- and *p*-benzynes (Figure 8a),[42] even though, their existence was finally demonstrated in 1992 and 1972 respectively (Figure 8b).[47] Recently, it has become possible to visualise individual molecules of *o*-aryne,[48] *m*-aryne[49] and *p*-aryne[50] by means of ultra-high resolution nc-AFM (Figure 9).

[42] I. P. Fisher, F. P. Lossing, *J. Am. Chem. Soc.* **1963**, *85*, 1018–1019.
[47] a) For the first solid proof of a *m*-aryne see: G. Bucher, W. Sander, E. Kraka, D. Cremer, *Angew. Chem. Int. Ed. Engl.* **1992**, *31*, 1230-1233; b) For the first evidence of *p*-aryne existence see: N. Darby, C. U. Kim, J. A. Salaun, K. W. Shelton, S. Takada, S. Masamune, *Chem. Commun.* **1971**, 1516–1517; c) R. R. Jones, R. G. Bergman, *J. Am. Chem. Soc.* **1972**, *94*, 660–661; d) For an excellent overview of *meta*- and *para*- arynes story see: W. Sander, *Acc. Chem. Res.* **1999**, *32*, 669–676; e) M. Winkler, H. H. Wenk, W. Sander, *Arynes* in *Reactive Intermediate Chemistry*, Willey, **2003**.
[48] N. Pavliček, B. Schuler, S. Collazos, N. Moll, D. Pérez, E. Guitián, G. Meyer, D. Peña, L. Gross, *Nat. Chem.* **2015**, *7*, 623–628.
[49] N. Pavliček, Z. Collazos, G. Meyer, D. Pérez, E. Guitián, D. Pena, L. Gross, *ACS Nano* **2017**, *11*, 10768–10773.
[50] B. Schuler, S. Fatayer, F. Mohn, N. Moll, N. Pavliček, G. Meyer, D. Penã, L. Gross, *Nat. Chem.* **2016**, *8*, 220–224.

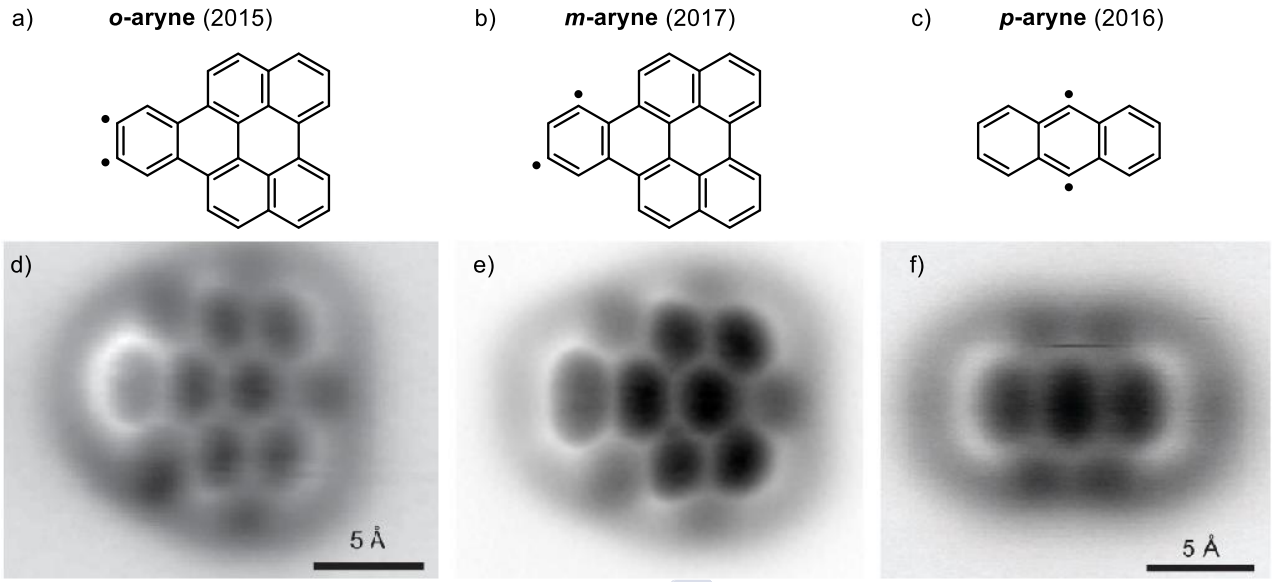


Figure 9. Structures and high-resolution AFM images of on-surface generated *ortho*- (a, d), *meta*- (b, e) and *para*-arynes (c, f).

1.2.1 Structure and reactivity

By far, the best studied aryne is 1,2-didehydrobenzene, usually named *o*-benzyne or, simply, **benzyne**. The structure of benzyne can be represented by the resonant forms depicted in Figure 10. Despite some controversy, there is a general agreement on the major contribution of the structure containing a strained formal triple bond between two adjacent carbon atoms, although significant cumulenic character has been evidenced by some experiments.[43]

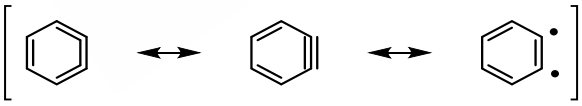


Figure 10. Resonant forms of benzyne.

A diagram corresponding to the **m**olecular **o**rbitals (MO) of *o*-benzyne is shown in Figure 11. Significantly, the third π-bond of benzyne lies in the nodal plane of the aromatic system, and thus, the six π-electrons do not intervene in its reactivity. Moreover, the particularly low LUMO energy value, makes benzyne a good electrophile and dienophile in cycloaddition reactions.[51]

---

[43] R. Warmuth, *Angew. Chem. Int. Ed. Engl.* **1997**, 1347–1350.
[51] A. Rauk, Orbital Interaction Theory of Organic Chemistry, Second Edition, Willey, **2001**.

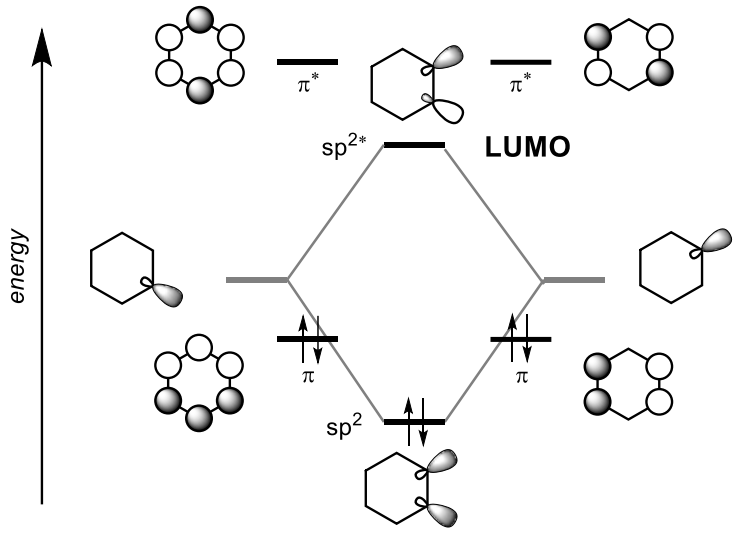


Figure 11. Diagram of molecular orbitals of benzyne.

Benzyne is the parent member of the family of *o*-arynes (*o*-didehydroarenes), which are extremely interesting short-lived species with a rich reactivity and huge versatility in organic synthesis. In the following figure, some representative examples of monocyclic and polycyclic *o*-aryne systems which have been developed and used as building blocks in synthesis are shown (Figure 12).

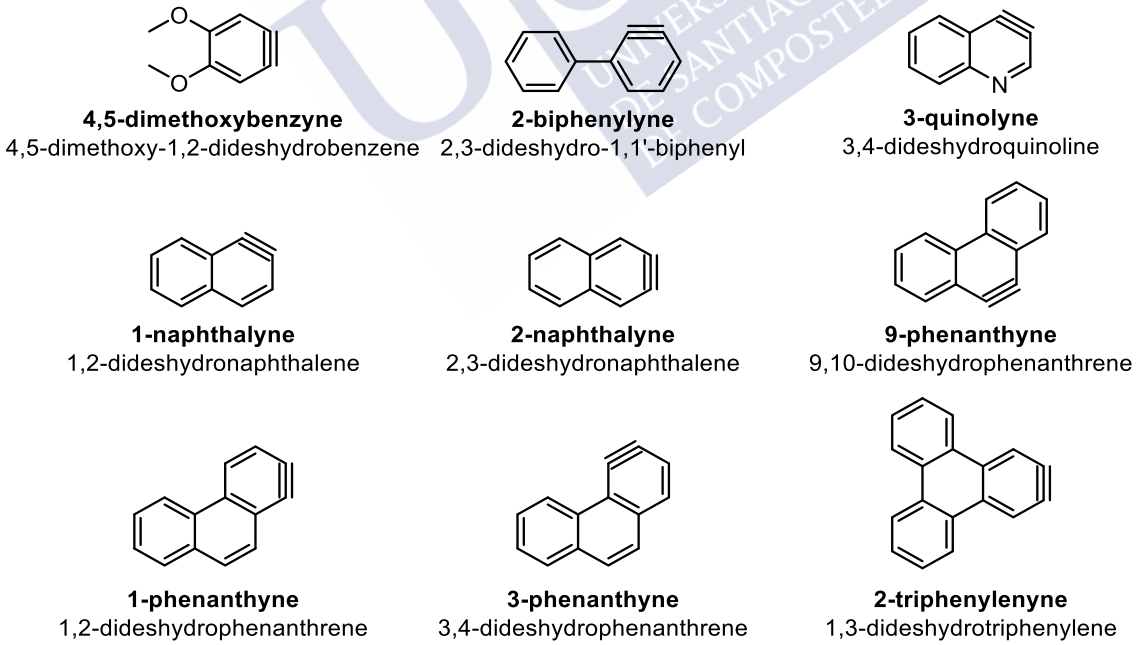
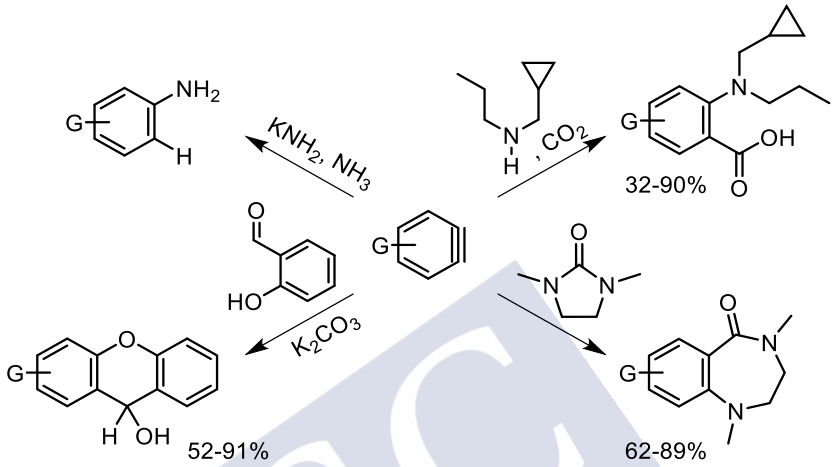


Figure 12. Examples of *o*-arynes.

With regard to the reactivity,[52] arynes are strong electrophiles, so they can undergo attacks by a wide variety of nucleophiles, leaving a negative charge in the vicinal carbon. The resulting anions can evolve by capturing a proton[39] or other electrophile, *inter*-[53] o *intra*-[54] molecularly (Scheme 1). Some of these processes are considered as formal σ-bond insertions. A great example of this reactivity was provided by Hiyama and co., who obtained benzodiazepines from aryne precursors in one step and high yield (Scheme 1).[55]



Scheme 1. Selected examples of the reactivity of arynes as electrophiles.

The presence of substituents may influence the reactivity of the aryne and, in the case of asymmetrically substituted benzynes, also the regioselectivity of the nucleophilic addition. Thus, in the presence of electronegative atoms next to the triple bond (e.g. *o*-OMe), the attack of a nucleophile occurs mainly in position C(1), *meta*- to the existing substituent (Figure 13). By contrast, substituents with electropositive atoms (e.g. TMS) direct the nucleophilic attack to the *ortho* position. The presence of substituents al position C(4) has scarce effect in the reactions, weakly prioritising attacks to position C(2).[56] Intuitively, bulky groups placed in C(3) usually lead to nucleophilic addition to the distant arynic C(1). In addition, nucleophilic attack to C(2) is usually preferred in the reactions of 1-naphthalynes (Figure 13). Traditionally, these observations had been explained as the result of a combination of electronic and steric effects.

---

[52] a) H. Hart, *Arynes and Heteroarynes Suppl. C2: The Chemistry of Triple-Bonded Functional Groups*, Wiley, Chichester, **1994**, p. 1017; b) H. Pellisier, M. Santelli, *Tetrahedron*, **2003**, *59*, 701–730; c) A. Bhunia,S. R. Yetra, A. T. Biju,*Chem. Soc. Rev.* **2012**, *41*, 3140–3152.

[39] J. D. Roberts, H. E. Simmons, L. A. Carlsmith, C. W. Vaughan, *J. Am. Chem. Soc.* **1953**, *75*, 3290–3291.

[53] H. Yoshida, T. Morishita, J. Ohshita, *Org. Lett.* **2008**, *10*, 3845–3847.

[54] K. Okuma, A. Nojima, N. Matsunaga, K. Shioji, *Org. Lett.* **2009**, *11*, 169–171.

[55] H. Yoshida, E. Shirakawa, Y. Honda, T. Hiyama, *Angew. Chem. Int. Ed.* **2002**, *41*, 3247–3249.

[56] H. J. H. and W. C. M. G. B. R. Graaff, *Tetrahedron Lett.* **1965**, *15*, 963–968.

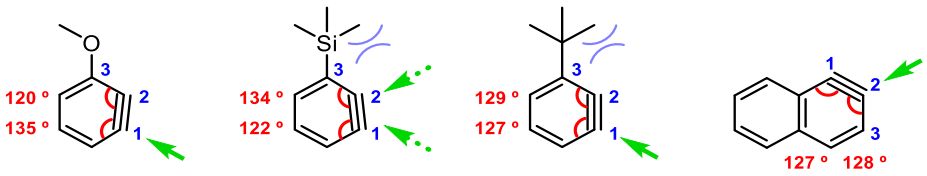
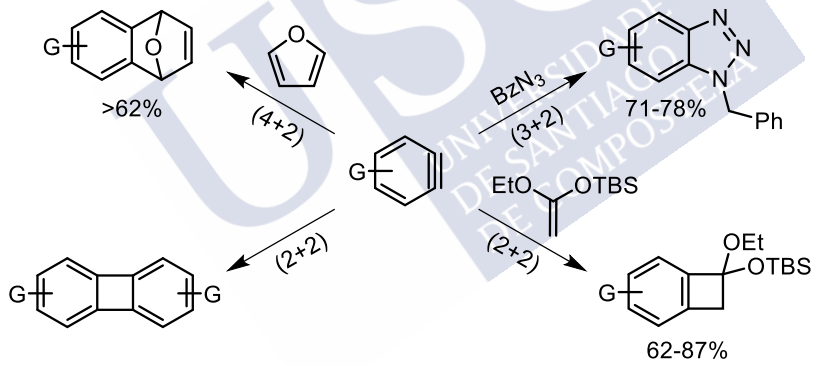


Figure 13. Selectivity in arynes.

Recently, Garg, Houk and coworkers published the "*distortion model*",[57] aimed to explain the regioselectivity of nucleophilic additions and cycloadditions to arynes. It establishes that the most electrophilic carbon is the one bearing the larger internal angle, determined by theoretical calculations (Figure 13). The efficacy of this model to easily predict selectivity in arynes, requiring only short-time calculations, makes it extremely useful.

Arynes can also participate in (n+2) cycloaddition reactions. Diels-Alder reactions with cyclic electron rich dienes usually afford the corresponding adducts in high yields, and thus, they can be used as trapping experiments to demonstrate the generation of arynic species. In fact, the first of example of an aryne trapping reaction with furan was reported by Wittig as early as in 1955.[58]



Scheme 2. Examples of cycloaddition reactions involving arynes.

Aryne also participate in 1,3-dipolar cycloadditions and, although the first evidences were published during the early sixties, the *arynic version* of the *click chemistry* was developed by Larock and co. in 2008, obtaining the corresponding triazole derivatives in good yields.[59] Finally, in spite of [π2*s*+π2*s*] reactions being forbidden according to the Woodward and

---

[57] a) S. M. Bronner, J. L. MacKey, K. N. Houk, N. K. Garg, *J. Am. Chem. Soc.* **2012**, *134*, 13966–13969; b) J. M. Medina, J. L. MacKey, N. K. Garg, K. N. Houk, *J. Am. Chem. Soc.* **2014**, *136*, 15798–15805; c) P. H.-Y. Cheong, R. S. Paton, S. M. Bronner, G. J. Im, N. K. Garg, K. N. Houk, *J. Am. Chem. Soc.* **2010**, *132*, 1267–1269.
[58] G. Wittig, L. Pohmer, *Angew. Chem.* **1955**, *67*, 348.
[59] F. Shi, J. P. Waldo, Y. Chen, R. C. Larock, *Org. Lett.* **2008**, *10*, 2409–2412.

Hoffmann rules, benzyne dimerise affording biphenylene[60] and react with alkenes, in some cases with high regioselectivity, probably through radical reaction pathways.[61]

As other unstable species, arynes can be stabilised by complexation with transition metals. Thereby, during the great expansion of organometallic chemistry in the 80's, the first metal complexes of benzyne were prepared and unambiguously characterised by X-ray diffraction analysis.[62] Nevertheless, the reactivity of these complexes was quite limited and their application in synthesis was also hampered by the lack of stability of some of them and by the need of stoichiometric amounts of metals and ligands to proceed (Figure 14).

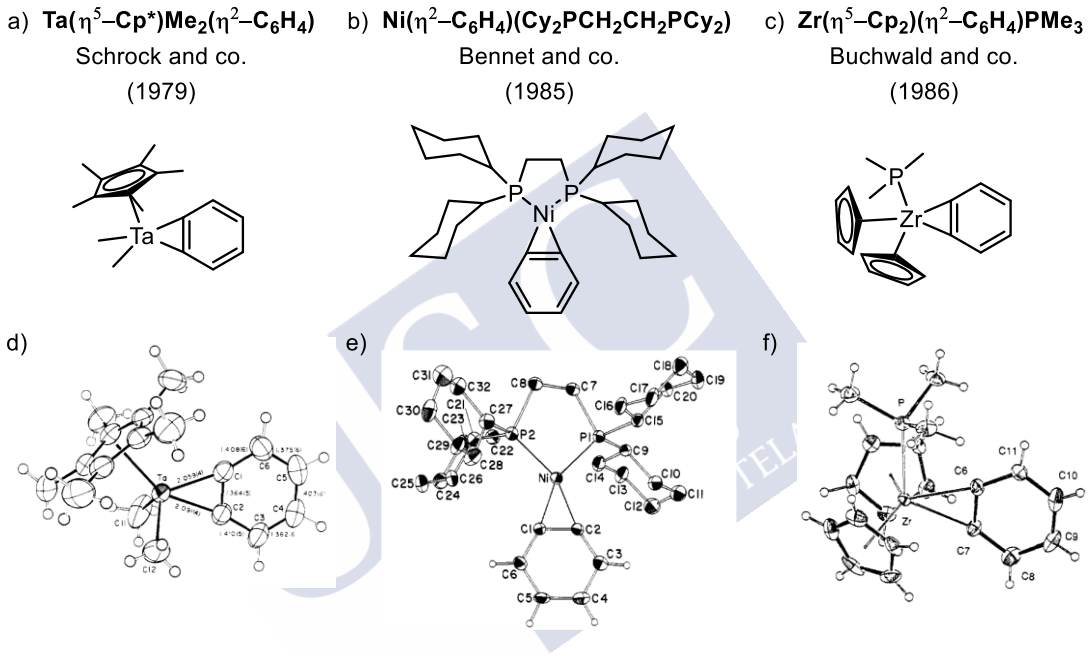


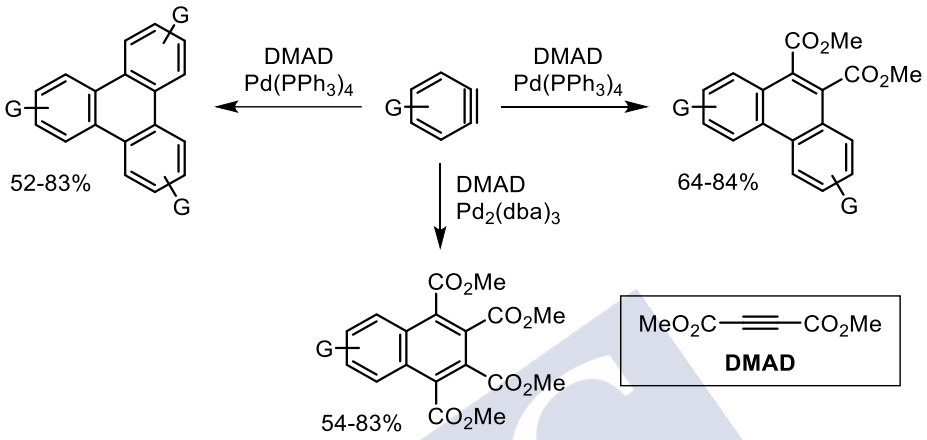
Figure 14. Examples of early metal-aryne complexes reported; Structure of a) Ta(η^5-Cp*)Me$_2$(η^2-C$_6$H$_4$), b) Ni(η^2-C$_6$H$_4$)(Cy$_2$PCH$_2$CH$_2$PCy$_2$) and c) Zr(η^5-Cp$_2$)(η^2-C$_6$H$_4$)PMe$_3$. X-ray structure of mentioned complexes d), e) and f) respectively.

In 1998, our research group developed the first metal-catalysed reaction involving these intermediates, the (2+2+2) Pd-catalysed cyclotrimerisation of arynes (Scheme 3).[63] This reaction was further developed later, and applied to synthesise a wide variety of star-shaped PAHs. In the following years, the (2+2+2) co-cycloaddition of arynes with electron poor

---

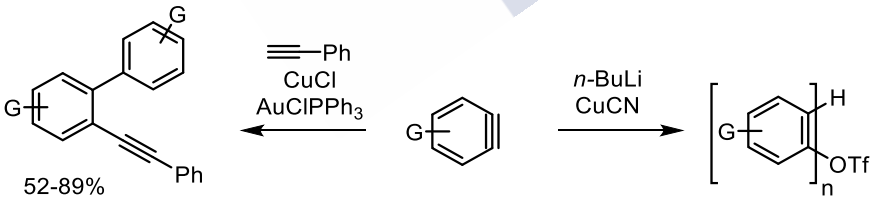
[60] A. Lüttringhaus, K. Schubert, *Naturwissenschaften* **1955**, *42*, 17.
[61] T. Hosoya, T. Hasegawa, Y. Kuriyama, K. Suzuki, *Tetrahedron Lett.* **1995**, *36*, 3377–3380.
[62] a) S. J. McLain, R. R. Schrock, P. R. Sharp, M. R. Churchill, W. J. Youngs, *J. Am. Chem. Soc.* **1979**, *101*, 263–265; b) M. A. Bennett, T. W. Hambley, N. K. Roberts, G. B. Robertson, *Organometallics* **1985**, 1992–2000; c) S. L. Buchwald, B. T. Watson, J. C. Huffman, *J. Am. Chem. Soc.* **1986**, *108*, 7411–7413.
[63] D. Peña, S. Escudero, D. Pérez, E. Guitián, L. Castedo, *Angew. Chem. Int. Ed.* **1998**, *37*, 2659–2661.

alkynes, such as **d**imethyl **a**cetylene**dic**arboxylate (DMAD) was reported.[64] Remarkably, the chemoselectivity of the reaction can be controlled by changing the ligands on the palladium catalyst. Thus, the use of triphenylphosphine drives the reaction to the addition of two arynes and one alkyne, while the **dib**enzylidene**a**cetone (dba) promotes the introduction of one aryne and two alkynes.



Scheme 3. Palladium-catalysed (2+2+2)-cycloaddition reactions involving arynes.

These pioneering works published during the late nineties by our research group, soon inspired the development of other catalytic reactions involving arynes. Examples of this legacy are, the gold-catalysed tandem assembly between terminal alkynes and arynes[65] or the copper-catalysed aryne polymerisation, which allowed the synthesis of poly-*o*-arylenes (Scheme 4).[66]

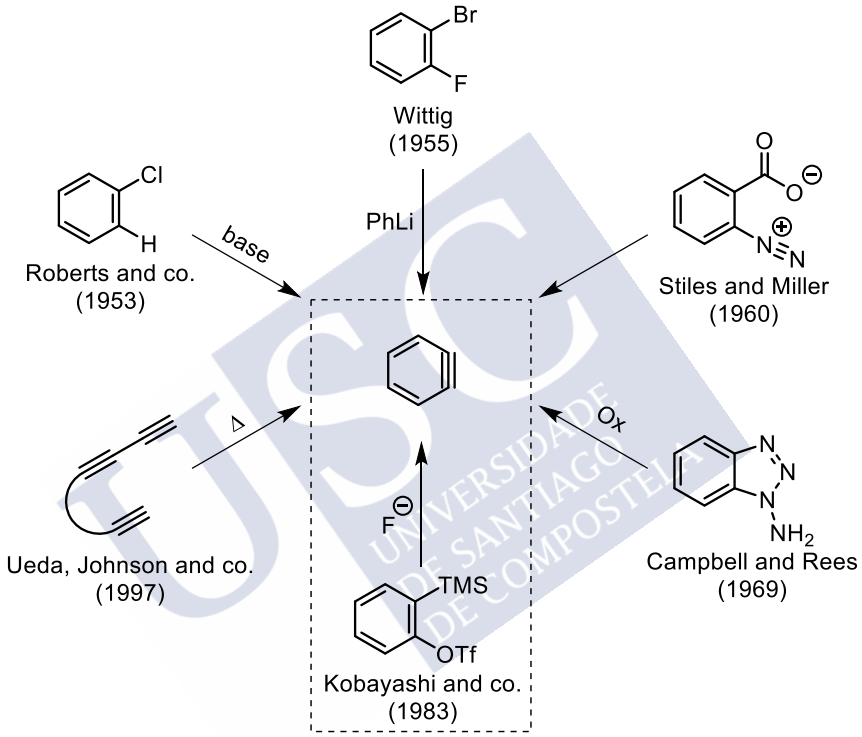


Scheme 4. Examples of other metal-catalysed reactions of arynes.

[64] Peña, D.; Pérez, D.; Guitián, E.; Castedo, L. *J. Am. Chem. Soc*. **1999**, *121*, 5827–5828.
[65] C. Xie, Y. Zhang, Y. Yanga, *Chem. Commun.* **2008**, 4810-4812.
[66] Y. Mizukoshi, K. Mikami, M. Uchiyama, *J. Am. Chem. Soc.* **2015**, *137*, 74–77.

1.2.2 Generation methods

Arynes are extremely short-lived reaction intermediates (in the range of μs-ms),[45] and thus, their use in synthesis requires them to be generated *in situ*. Early developed methods for aryne generation required harsh reaction conditions, explosive precursors or the use of highly reactive reagents (strong bases, organolithium reagents, oxidants…), being incompatible with many functional groups and inappropriate for long synthetic routes (Scheme 5). An overview of aryne precursors and their applications in natural product synthesis has been collected in the fantastic review recently published by Suzuki's group.[67]

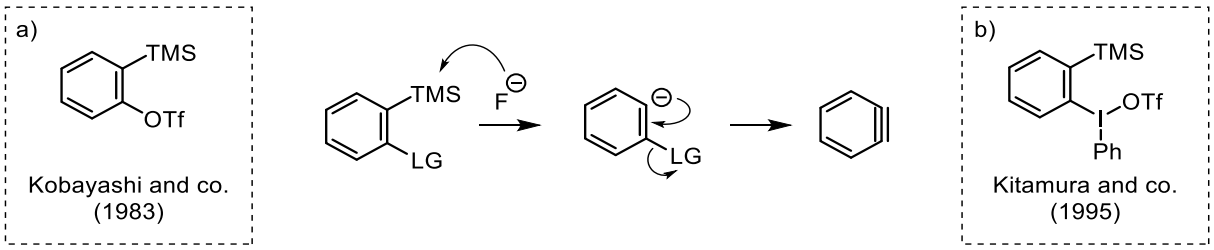


Scheme 5. Examples of representative aryne precursors.

The discovery of Kobayashi's method of aryne generation (1983, Scheme 5)[68] went practically unnoticed for almost 15 years, but in the long term resulted to be a landmark achievement in the field of aryne chemistry. Utilising *ortho*-(trimethylsilyl)aryl triflates (Scheme 6a) is possible to generate the corresponding arynes using a fluoride source, selectively and under mild reaction conditions (Scheme 6). In 1998 our group used this method for the development of the previously mentioned palladium-catalysed (2+2+2) cycloadditions and,

[45] H. H. Wenk, M. Winkler, W. Sander, *Angew. Chem. Int. Ed.* **2003**, *42*, 502–528.
[67] H. Takikawa, A. Nishii, T. Sakai, K. Suzuki, *Chem. Soc. Rev.* **2018**, *47*, 8030–8056.
[68] Y. Himeshima, T. Sonoda, H. Kobayashi, *Chem. Lett.* **1983**, 1211–1214.

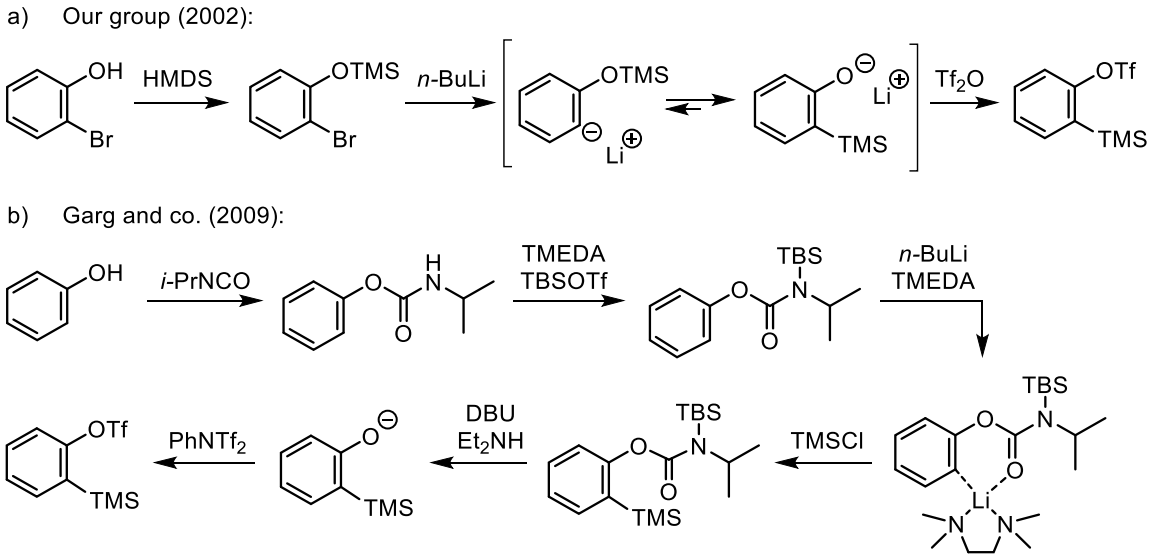
since then, it became the method of choice for the generation of arynes in synthesis.[69] Other closely related precursors containing alkylsilyl groups have been developed later, such as the useful Kitamura precursors (Scheme 6b).[70]



Scheme 6. Proposed mechanism of fluoride induced benzyne generation.

In 2002, our research group developed an optimised protocol for the preparation of *o*-(trimethylsilyl)aryl triflates from the corresponding *o*-bromophenols in one-pot (Scheme 7a),[71] which also contributed to convert the Kobayashi's method into the most employed methodology for aryne generation, according to the literature. The synthetic strategy begins with the protection of an *ortho*-bromophenol using **h**exa**m**ethyl**dis**ilazane (HMDS). Then, the lithium-halogen exchange at low temperature induces a reversible retro-Brook type rearrangement. The equilibrium is irreversibly displaced towards the formation of the desired product by esterification with triflic anhydride (Scheme 7a). Thereafter, Greaney's group published the *flow version* of this robust synthetic protocol, obtaining the aryne precursors in high yields and avoiding the use of low temperatures.[72]

[69] S. Liu, Y. Li, Y. Lan, *Eur. J. Org. Chem.* **2017**, 6349–6353.
[70] T. Kitamura, M. Yamane, *J. Chem. Soc., Chem. Commun.* **1995**, 983–984.
[71] D. Peña, A. Cobas, D. Pérez, E. Guitián, *Synthesis* **2002**, *10*, 1454–1458.
[72] B. Michel, M. F. Greaney, *Org. Lett.* **2014**, *16*, 2684–2687.

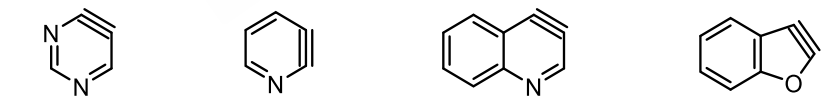


Scheme 7. Common synthesis of TMS/OTf aryne precursors.

Few years later, Garg and coworkers published a synthetic strategy[73] based on the Hoppe's protocol.[74] It consisted in the protection of a phenol with a directing group to guide the direct silylation to the *ortho*-position (Scheme 7b).

1.2.3 Hetarynes

Hetarynes can be defined as arynes which contain at least one heteroatom on the same aromatic ring where they bear the *arynic* unsaturation. However, other arynes derived from heteroarenes have been generally included in this term. These intermediates have caught the attention of many chemists due to their synthetic potential.



4-pyrimidyne **2-pyridyne** **3-quinolyne** **2-benzofuryne**

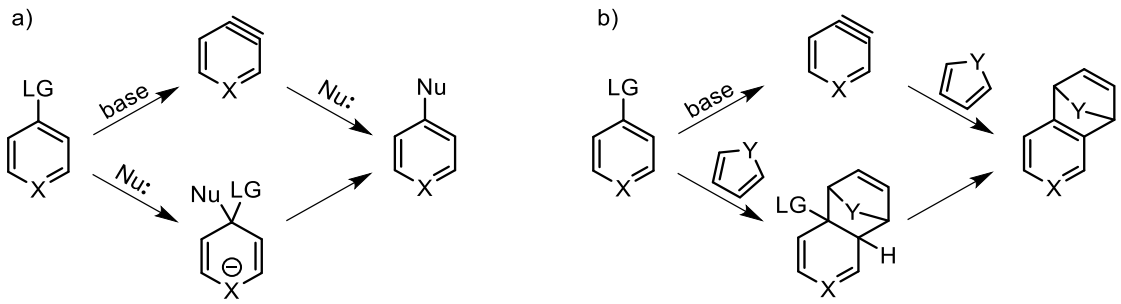
Figure 15. Examples of hetarynes.

Their stability and reactivity strongly depend on the ring size, and on the nature, number, and position of the heteroatoms. The aromatic stabilisation in heteroaromatic rings is lower than in benzene, leaving some room for side reactions, such as nucleophilic aromatic

---

[73] S. M. Bronner, K. B. Bahnck, N. K. Garg, *Org. Lett.* **2009**, *11*, 1007–1010.
[74] a) M. Kauch, V. Snieckus, D. Hoppe, *J. Org. Chem.* **2005**, *70*, 7149–7158; b) M. Kauch, D. Hoppe, *Synthesis* **2006**, 1575–1577.

substitutions (Scheme 8a) or cycloadditions (Scheme 8b).[75] Hence, hetaryne trapping experiments can be confusing and sometimes lead to incorrect conclusions.



Scheme 8. *Arynic* pathway and mechanistic alternatives.

Despite the large number of publications on this topic, most of hetarynes are still waiting for an appropriate precursor.[76] Probably, the best studied of these intermediates are pyridynes, which can present the *arynic* bond in three different positions (Figure 16). 1-Pyridyne behaves essentially as a pyrimidyl cation, on the contrary, 2- and 3- pyridynes, whose Kobayashi precursors were reported in 1997 and 1998 respectively,[77] have been used in organic synthesis (Figure 16).

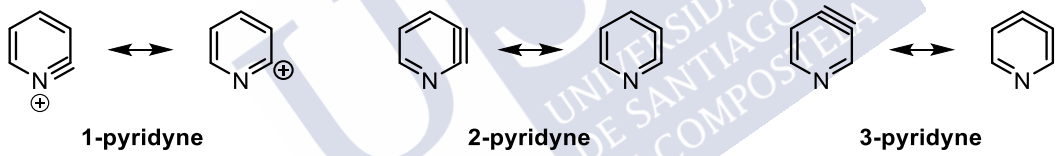


Figure 16. Resonance forms of 1-, 2- and 3-pyridynes.

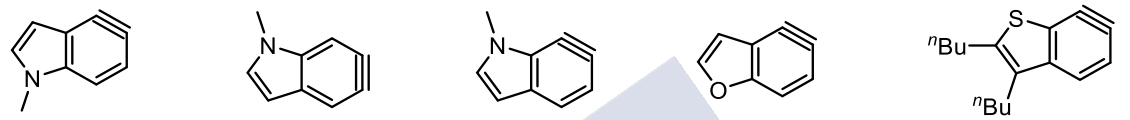
In terms of selectivity, 2-pyridynes undergo the attack of nucleophiles mainly in position 2, while 3-pyridynes are weakly influenced by the heteroatom, affording preferably the *para*-substituted product. Their structure and selectivity were thoroughly studied by Garg, Houk and coworkers.[78]

[75] M. G. Reinecke, *Tetrahedron* **1982**, *38*, 427–498.
[76] A. E. Goetz, T. K. Shah, N. K. Garg, *Chem. Commun.* **2015**, *51*, 34–45.
[77] a) For 2-pyridyne see: M. A. Walters, J. J. Shay, *Synth. Commun.* **1997**, *27*, 3573–3579; b) For 3-pyridyne see: M. T. Díaz, A. Cobas, E. Guitián, L. Castedo, *Synlett* **1998**, 157–158.
[78] A. E. Goetz, N. K. Garg, *Nat. Chem.* **2013**, *5*, 54–60.



Figure 17. Selectivity of 1- and 2-pyridynes.

Several examples of hetarynes containing the arynic unsaturation and the heteroatom in different rings have been reported in the literature. In these cases the triple bond is scarcely affected by the heteroatom ring substitution.[79] Few of these species have a suitable precursor available for their generation (Figure 18), most of them being developed by Garg's group.[73,80]



4-indolyne Garg and co. (2009) | **5-indolyne** Garg and co. (2010) | **6-indolyne** Garg and co. (2010) | **4-benzofuryne** Garg and co. (2016) | **6-benzothiophyne** Hosoya and co. (2018)

Figure 18. Selected examples of hetarynes.

5-Membered hetarynes are particularly intriguing. Indeed, their triple bond is even more strained than those placed in 6-membered rings. Remarkably, the first heteroatom-containing didehydroarene postulated was a 5-membered hetaryne (2-benzofuryne),[37] although its generation was later questioned.[75] Many of these species have been proposed (Figure 19),[81] although only few authors could provide solid evidences of their generation. The strongest support for the formation of any of these intermediates was provided by Wong and co. using Kobayashi and Kitamura aryne precursors.[82] Hence, 3-thiophyne and the 3-pyrrolyne generation, was presumed due to the isolation of the corresponding furan trapping adducts

---

[79] Y. Nakamura, S. Yoshida, T. Hosoya, *Heterocycles* **2019**, *98*, 1623–1677.
[73] S. M. Bronner, K. B. Bahnck, N. K. Garg, *Org. Lett.* **2009**, *11*, 1007–1010.
[80] a) For 5- and 6-indolynes see: G. J. Im, S. M. Bronner, A. E. Goetz, R. S. Paton, P. H.-Y. Cheong, K. N. Houk, N. K. Garg, *J. Am. Chem. Soc.* **2010**, *132*, 17933–17944; b) For 4-benzofuryne see: T. K. Shah, J. M. Medina, N. K. Garg, *J. Am. Chem. Soc.* **2016**, *138*, 4948–4954; c) For 6-benzothiophyne see: S. Yoshida, T. Kuribara, T. Morita, T. Matsuzawa, K. Morimoto, T. Kobayashi, T. Hosoya, *RSC Adv.* **2018**, *8*, 21754–21758.
[37] R. Stoermer, B. Kahlert, *Ber. Dtsch. Chem. Ges.* **1902**, *35*, 1633–1640.
[75] M. G. Reinecke, *Tetrahedron* **1982**, *38*, 427–498.
[81] a) For 2-indolyne see: S. C. Conway, G. W. Gribble, *Heterocycles* **1992**, *34*, 2095–2018; b) For 2-thiophyne see: G. Wittig, V. Wahl, *Angew. Chem.* **1961**, *14*, 492; c) For 3-furyne see: Y.-M. Wu, X.-P. Yang, F. Xue, T. C. W. Mak, H. N. C. Wong, *J. Chin. Chem. Soc.* **1999**, *46*, 463–468.
[82] a) For 3-thiophyne see: X. Ye, W.-K. Li, H. N. C. Wong, *J. Am. Chem. Soc.* **1996**, *118*, 2511–2512; b) For 3-pyrrolyne see: J.-H. Liu, H.-W. Chan, F. Xue, Q.-G. Wang, T. C. W. Mak, H. N. C. Wong, *J. Org. Chem.* **1999**, *64*, 1630–1634.

(31% and 1% yield respectively). These precedents make 5-membered hetarynes to be as challenging as interesting.

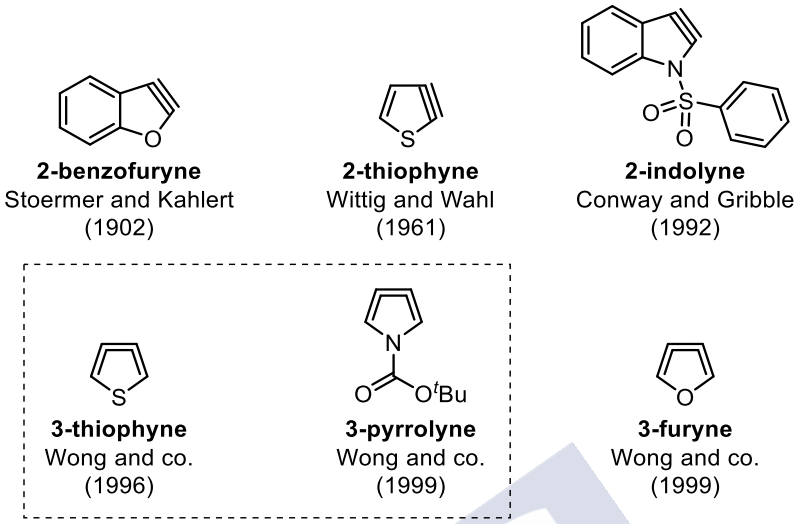


Figure 19. Selected examples of postulated 5-membered hetarynes.

In 2012 Goetz et al. published an interesting article to computationally predict the synthetic viability of arynes and hetarynes, based on the calculation of the energy of dehydrogenation of the corresponding heterocyclic arene.[83] The study confirmed that benzynes, indolynes (with the triple bond in the benzene ring) and pyridynes should be accessible, with estimated energy differences <115 Kcal mol^{-1}, while 2-indolyne and 2-benzofuryne, with values >130 Kcal mol^{-1}, should not. Noteworthy, 2- and 3-thiophynes were classified in an intermediate category as "hetarynes that can likely be generated", with energies of dehydrogenation in the range between 115 and 130 Kcal mol^{-1}.

1.2.4 Polyarynes: bisarynes, trisarynes and beyond

The introduction of additional arynic unsaturations in the same aromatic core opens a new branch in the field of aryne chemistry, plenty of opportunities. We consider polyarynes as those species resulting from the formal generation of two or more triple bonds in an aromatic ring. These intermediates are usually named by indicating the number of the first carbon of each triple bond and the corresponding suffix (-diyne, -triyne).

---

[83] A. E. Goetz, S. M. Bronner, J. D. Cisneros, J. M. Melamed, R. S. Paton, K. N. Houk, N. K. Garg, *Angew. Chem. Int. Ed.* **2012**, *51*, 2758–2762.

The first reference to the sequential generation of two arynic unsaturations in a benzene derivative, and the isolation of the corresponding furan bisadducts, was reported by Wittig and Härle in 1959 (Figure 20).[84] Few years later, Fields and Meyerson proposed the generation of 1,3-benzodiyne and their attempts to obtain 1,3,5-benzotriyne.[85]

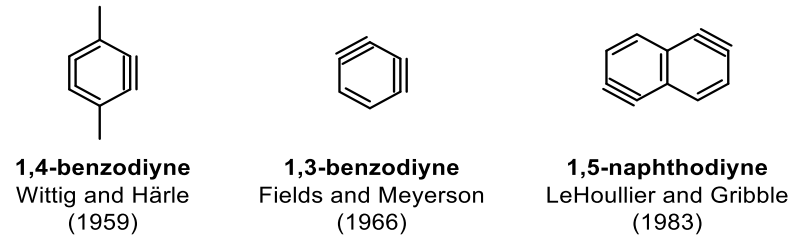
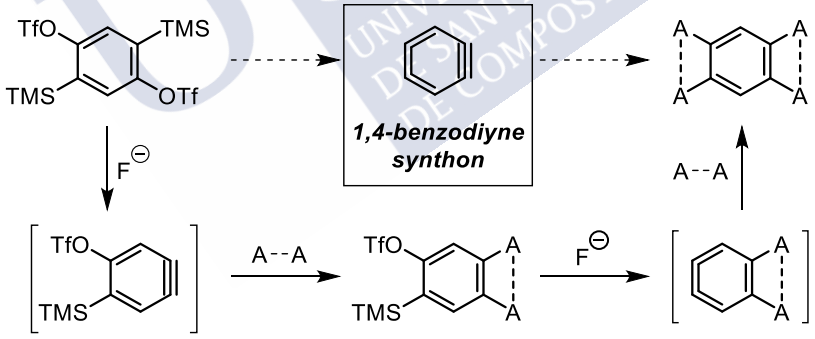


Figure 20. Examples of first bisarynes postulated.

Although a few authors have claimed the detection of polyarynes in special conditions (argon matrix, 10K),[86] in solution chemistry they should be considered as synthons rather than as actual reaction intermediates (Scheme 9). In fact, most reports suggest the sequential generation and trapping of each of the two (or three) triple bonds in stepwise processes (Scheme 9). Taking advantage of this behaviour, the generation of only one of the potential triple bonds, and subsequent reaction with an appropriate partner, allows to obtain structurally complex aryne precursors



Scheme 9. Sequential generation of 1,4-benzodiyne.

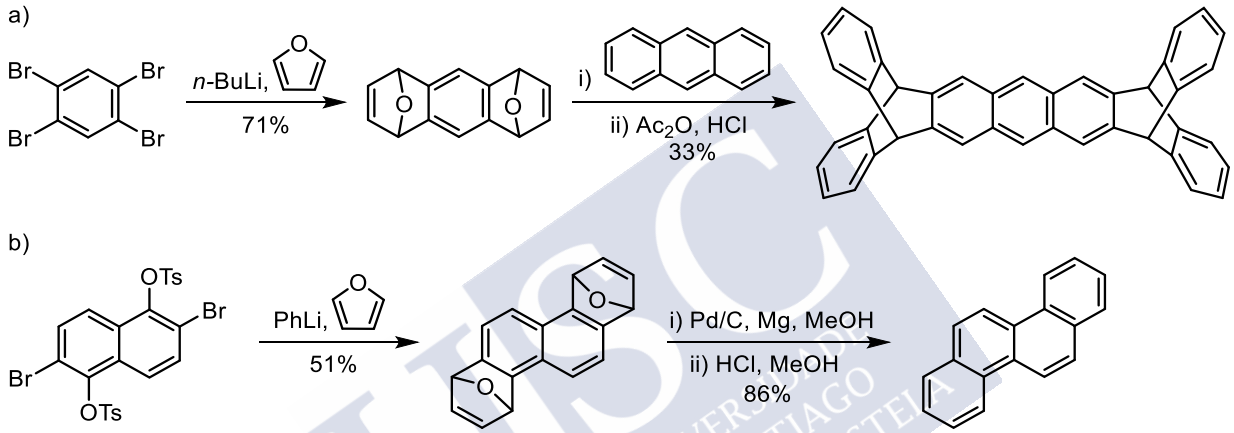
Other species that have been grouped with polyarynes are, for instance, those which contain arynes in independent aromatic rings linked by σ-bonds,[87] masked bisaryne

---

[84] G. Wittig, H. Härle, *Liebigs Ann. Chem.* **1959**, *623*, 17–34.
[85] E. K. Fields, S. Meyerson, *J. Org. Chem.* **1966**, *31*, 3307–3309.
[86] a) M. Moriyama, T. Ohana, A. Yabe, *J. Am. Chem. Soc.* **1997**, *119*, 10229–10230; b) T. Sato, S. Arulmozhiraja, H. Niino, S. Sasaki, T. Matsuura, A. Yabe, *J. Am. Chem. Soc*. **2002**, *124*, 4512–4521.
[87] B. Knieriem, K. Rauch, *Chem. Ber.* **1993**, *126*, 2531–2534.

precursors[88] and compounds able to generate consecutive arynes.[89] Similarly, any arene with two or more leaving groups properly located could be potentially a polyaryne precursor. However, we consider polyaryne precursors exclusively those compounds which can generate all their arynic units (probably stepwise) in one synthetic shot.

During the early eighties polyaryne synthons were introduced in the literature as useful tools in PAHs synthesis. Hart et al. published the synthesis of anthracene and iptycene derivatives employing the 1,4-benzodiyne synthon (Scheme 10a).[90] Thereafter, the 1,5-naphthodiyne synthon was used by LeHoullier and Gribble to obtain chrysene (1983, Scheme 10b).[91]



Scheme 10. Selected examples of early use of bisaryne synthons in PAHs synthesis.

Some years later, Buchwald's and Bennett's groups, published the X-ray structure of two organometallic complexes of 1,4-benzodiyne, in 1987 and 1988 respectively. As in the case of metal complexes of monoarynes, these complexes found scarce application in synthesis.

---

[88] a) C.-J. F. Du, H. Hart, K.-K. D. Ng, *J. Org. Chem.* **1986**, *51*, 3162–3165; b) J. Shi, Y. Li, Y. Li, *Chem. Soc. Rev.* **2017**, *46*, 1707–1719.

[89] a) X. Xiao, T. R. Hoye, *Nat. Chem.* **2018**, *10*, 838–844; b) H. Haneda, S. Eda, M. Aratani, T. Hamura, *Org. Lett.* **2014**, *16*, 286–289; c) J. He, Z. Jia, H. Tan, X. Luo, D. Qiu, J. Shi, H. Xu, Y. Li, *Angew. Chem. Int. Ed.* **2019**, *58*, 18513–18518.

[90] a) H. Hart, C. Lai, G. Nwokogu, S. Shamouilian, A. Teuerstein, C. Zlotogorski, *J. Am. Chem. Soc.* **1980**, *102*, 6649–6651; b) H. Hart, N. Raju, M. A. Meador, D. L. Ward, *J. Org. Chem.* **1983**, *48*, 4357–4360.

[91] C. S. LeHoullier, G. W. Gribble, *J. Org. Chem.* **1983**, *48*, 1682–1685.

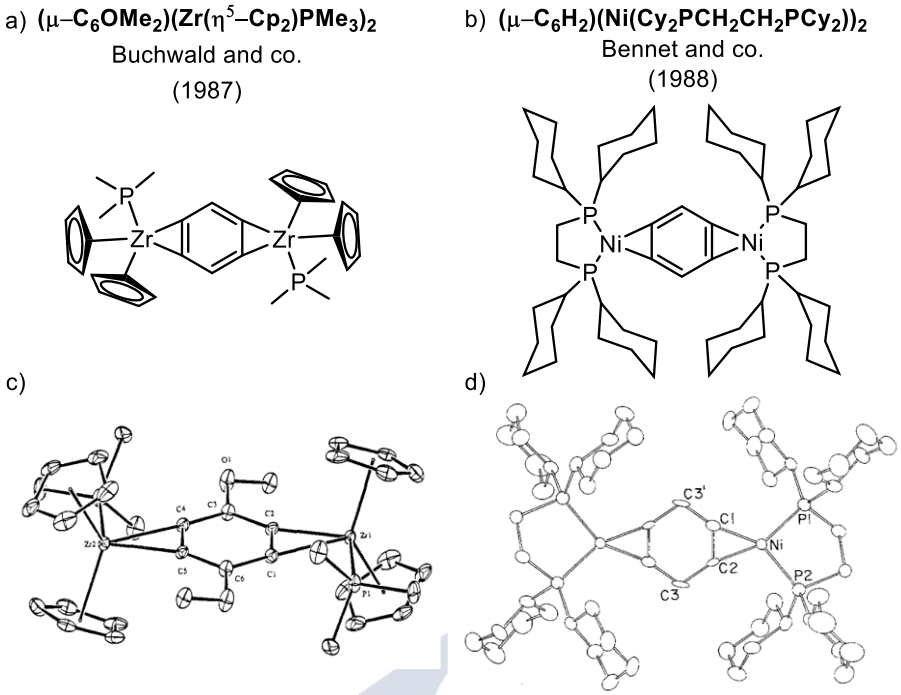
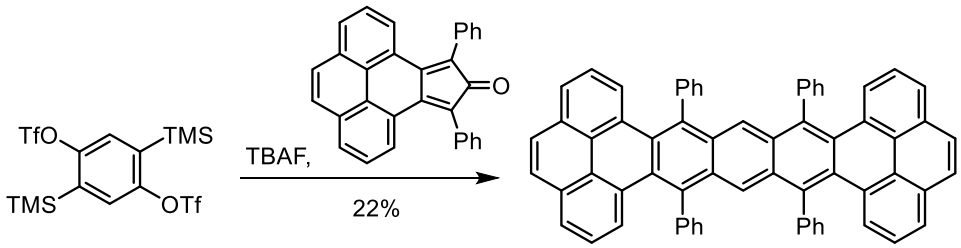


Figure 21. Examples of early organometallic 1,4-bezodiyne complexes reported; Structure of a) (μ-$C_6(OMe)_2$)(Zr(η^5-Cp_2)$PMe_3)_2$ and b) (μ-C_6H_2)(Ni($Cy_2PCH_2CH_2PCy_2$)). X-ray structure of mentioned complexes c) and d) respectively.

During the following decades, several examples of bisarynes have been reported, most of them for benzene and naphthalene, although, they have been also developed for larger arenes.[92] However, the lack of suitable bisaryne precursors driven to poor yields. It was not until 2003, when Wudl and coworkers published the first Kobayashi precursor of the 1,4-benzodiyne synthon (Scheme 11). This compound gave a straightforward access to pentacene and heptacene derivatives.[93] Recent examples about the evolution of bisarynes field are collected in the introduction of Chapter 3, which is directly related with this topic.



Scheme 11. Synthesis of an heptacene derivative using bisaryne chemistry.

---

[92] a) G. E. Morton, A. G. M. Barrett, *J. Org. Chem.* **2005**, *70*, 3525–3529; b) H. Hart, S. Shamouilian, Y. Takehira, *J. Org. Chem.* **1981**, *46*, 4427–4432; c) D. Chun, Y. Cheng, F. Wudl, *Angew. Chem. Int. Ed.* **2008**, *47*, 8380–8385.
[93] H. M. Duong, M. Bendikov, D. Steiger, Q. Zhang, G. Sonmez, J. Yamada, F. Wudl, *Org. Lett.* **2003**, *5*, 4433–4436.

Other polyarynes, such as trisarynes, have scarcely been used in synthesis. Even though a certain number of articles claimed their generation, few proofs have been provided so far. The very limited number of articles on trisarynes found in the literature, are commented in the background information of Chapter 4, which is specifically focused on this topic.

A general view about the story of bisarynes, trisarynes and polyarynes is included in a detailed review published by Sato and Niino.[94]

USC UNIVERSIDADE DE SANTIAGO DE COMPOSTELA

[94] T. Sato, H. Niino, *Aust. J. Chem.* **2010**, *63*, 1048–1060.

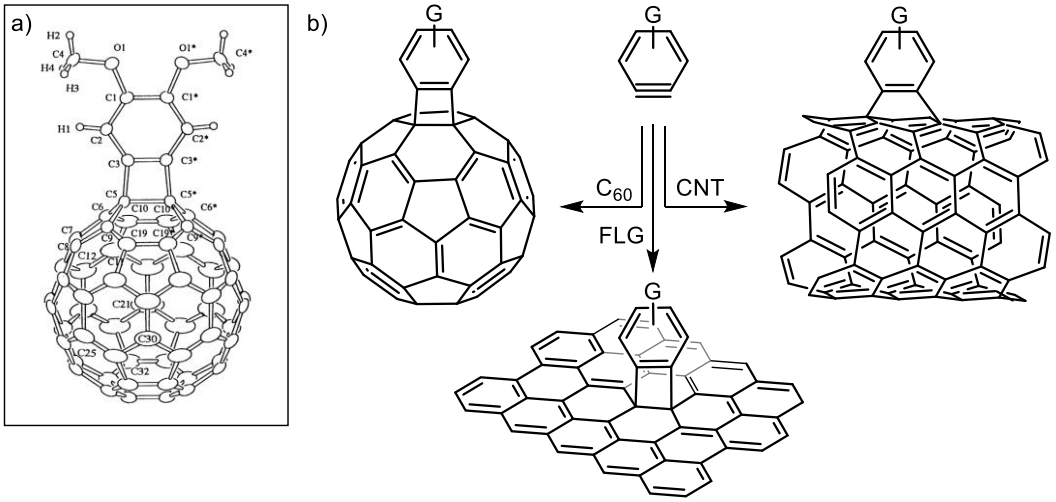
1.3 Application of arynes in materials chemistry

Several unique features of arynes make them tremendously useful building blocks for the construction of extended π-conjugated molecules and other carbon nanostructures of interest in materials science.[95] Thanks to their rich chemistry and, in particular, to their efficient participation in cycloaddition reactions, the use of arynes allow the incorporation of benzene rings (or larger benzologue moieties) through the formation of two or more carbon–carbon bonds in one step, thus providing convergent synthetic strategies towards complex structures containing aromatic rings.[96]

On the one hand, arynes have been used to achieve the direct functionalisation of carbon nanostructures, such as, fullerene (C_{60}),[97] **c**arbon **n**ano**t**ubes (CNT)[98] and **f**ew-**l**ayer **g**raphene (FLG).[99] Theoretical calculations support that (4+2) and (2+2) cycloaddition reactions occur in CNTs depending on the periphery and diameter,[100] whereas the reactivity of arynes with C_{60} take place notably through (2+2) cycloadditions (Scheme 12).

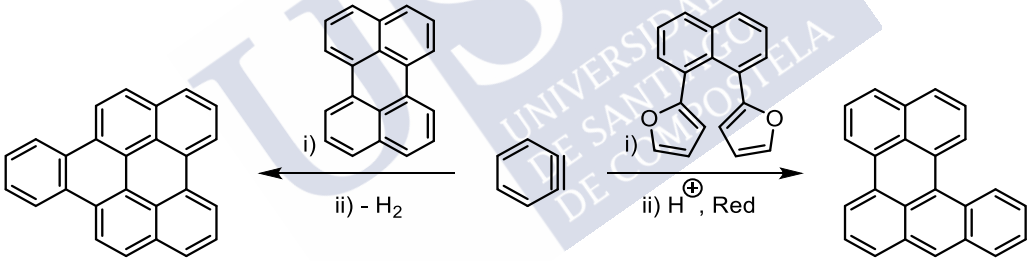
USC UNIVERSIDADE DE SANTIAGO DE COMPOSTELA

[95] F. García, D. Peña, D. Pérez, E. Guitián, *Aryne Cycloadditions for the Synthesis of Functional Polyarenes*, in *Modern Aryne Chemistry*. Ed: A. Biju. Wiley-VCH (In Press).
[96] a) D. Pérez, D. Peña, E. Guitian, *Eur. J. Org. Chem.* **2013**, *27*, 5981–6013; b) S. Fatayer, N. B. Poddar, S. Quiroga, F. Schulz, B. Schuler, S. V. Kalpathy, G. Meyer, D. Pérez, E. Guitián, D. Peña, M. J. Wornat, L. Gross, *J. Am. Chem. Soc.* **2018**, *140*, 8156–8161; c) H. Ito, Y. Segawa, K. Murakami, K. Itami, *J. Am. Chem. Soc.* **2019**, *141*, 3–10.
[97] a) S. H. Hoke, J. Molstad, D. Dilettato, M. J. Jay, D. Carlson, B. Kahr, R. G. Cooks, *J. Org. Chem.* **1992**, *57*, 5069–5071; b) T. Ishida, K. Shinozuka, T. Nogami, S. Sasaki, M. Iyoda, *Chem. Lett.* **1995**, *24*, 317–318; c) D. García, L. Rodríguez-Pérez, M. A. Herranz, D. Peña, E. Guitián, S. Bailey, Q. Al-Galiby, M. Noori, C. J. Lambert, D. Pérez, N. Martín, *Chem. Commun.* **2016**, *52*, 6677–6680.
[98] a) A. Criado, M. J. Gómez-Escalonilla, J. L. G. Fierro, A. Urbina, D. Peña, E. Guitián, F. Langa, *Chem. Commun.* **2010**, *46*, 7028–7030; b) A. Criado, M. Vizuete, M. J. Gómez-Escalonilla, S. García-Rodriguez, J. L. G. Fierro, A. Cobas, D. Peña, E. Guitián, F. Langa, *Carbon* **2013**, *63*, 140–148.
[99] a) X. Zhong, J. Jin, S. Li, Z. Niu, W. Hu, R. Li, J. Ma, *Chem. Commun.* **2010**, *46*, 7340–7342; b) M. V. Sulleiro, S. Quiroga, D. Peña, D. Pérez, E. Guitián, A. Criado, M. Prato, *Chem. Commun.* **2018**, *54*, 2086–2089.
[100] J. P. Martínez, F. Langa, F. M. Bickelhaupt, S. Osuna, M. Solá *J. Phys. Chem. C* **2016**, *120*, 1716−1726.



Scheme 12. a) X-ray structure of 4,5-dimethoxybenzyne fullerene cycloadduct. b) Reactivity of arynes with carbon nanostructures.

The selective Diels-Alder reaction of arynes with the bay-region of perylene was published by Scott's group in 2011 (Scheme 13).[101] Otherwise, *K*-region extended perylenes can be obtained by a cascade process, involving two tandem Diels-Alder reactions of arynes with adequately designed oligoacenes.[102]



Scheme 13. Synthesis of π-extended perylene derivatives.

The synthesis of the largest unsubstituted or perphenylated acenes (Figure 22) have been also achieved by using different aryne-based strategies.[103] The story of acene derivatives is splendidly summarised in the review "*Unusual stabilization of larger acenes and heteroacenes*"[104] and "*Strategies for the Synthesis of Higher Acenes*".[105]

---

[101] E. H. Fort, L. T. Scott, *Tetrahedron Lett.* **2011**, *52*, 2051–2053.
[102] a) A. Criado, D. Peña, A. Cobas, E. Guitián, *Chem. Eur. J.* **2010**, *16*, 9736–9740; b) A. Criado, A. Cobas, M. Vilas Varela, D. Pérez, D. Peña. E. Guitián *J. Org. Chem.* **2013**, *78*, 12673–12649.
[103] a) For perphenyltetracene see: Y. Xiao, J. T. Mague, R. H. Schmehl, F. M. Haque, R. A. Pascal, Jr., *Angew. Chem. Int. Ed.* **2019**, *58*, 2831–2833; b) For dodecacene see: F. Eisenhut, T. Kühne, F. García, S. Fernández, E. Guitián, D. Pérez, G. Trinquier, G. Cuniberti, C. Joachim, D. Peña, F. Moresco, *ACS Nano* **2020**, *14*, 1011–1017.
[104] M. Müller, L. Ahrens, V. Brosius, J. Freudenberg, U. H. F. Bunz, *J. Mater. Chem. C* **2019**, *7*, 14011–14034.
[105] R. Dorel, A. M. Echavarren, *Eur. J. Org. Chem.* **2017**, *2017*, 14–24.

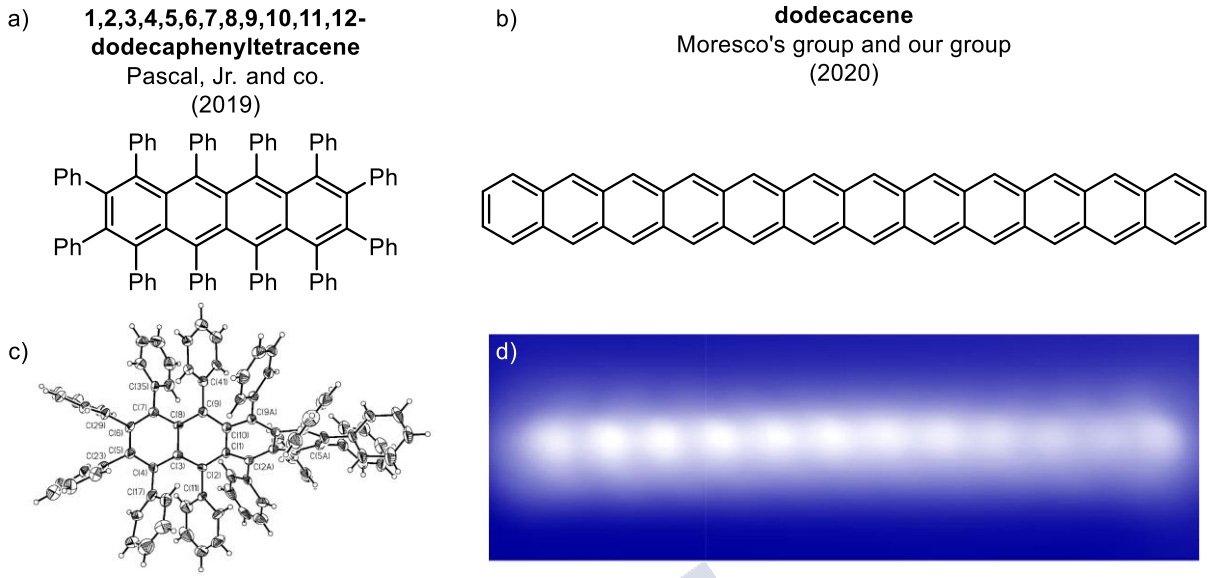


Figure 22. Structure of largest acenes a) perphenylated and b) unsubstituted. c) X-ray structure of perphenyltetracene. d) Constant height **s**canning **t**unneling **m**icroscopy (STM) image using a CO-functionalised tip of dodecacene.

Since the development of (2+2+2) metal-catalysed cyclotrimerisation reactions of arynes in 1998,[63] several examples of three-fold symmetric arenes have been reported. For instance, the hindered cloverphene[106] and hexapole helicene shown in Figure 23. The synthesis of this molecule was published by two different groups concurrently, using a (2+2+2) palladium-catalysed cyclotrimerisation reaction[107] and Yamamoto type reaction.[108] At the same time, it was also prepared independently in our research group (Figure 23b).[109]

---

[63] D. Peña, S. Escudero, D. Pérez, E. Guitián, L. Castedo, *Angew. Chem. Int. Ed.* **1998**, *37*, 2659–2661.
[106] J. M. Alonso, A. E. Díaz-Álvarez, A. Criado, D. Pérez, D. Peña, E. Guitián, *Angew. Chem. Int. Ed.* **2012**, *51*, 173–177.
[107] T. Hosokawa, Y. Takahashi, T. Matsushima, S. Watanabe, S. Kikkawa, I. Azumaya, A. Tsurusaki, K. Kamikawa, *J. Am. Chem. Soc.* **2017**, *139*, 18512–18521.
[108] V. Berezhnaia, M. Roy, N. Vanthuyne, M. Villa, J. V. Naubron, J. Rodriguez, Y. Coquerel, M. Gingras, *J. Am. Chem. Soc.* **2017**, *139*, 18508–18511.
[109] R. Zuzak, J. Castro-Esteban, P. Brandimarte, M. Engelund, A. Cobas, P. Piątkowski, M. Kolmer, D. Pérez, E. Guitián, M. Szymonski, D. Sánchez-Portal, S. Godlewski, D. Peña, *Chem. Commun.* **2018**, *54*, 10256–10259.

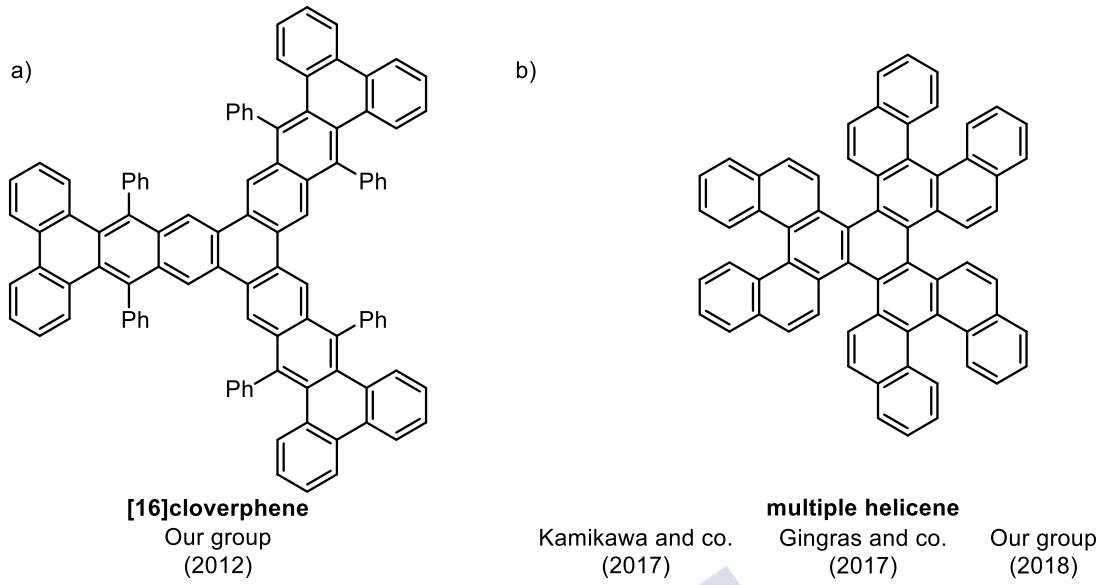
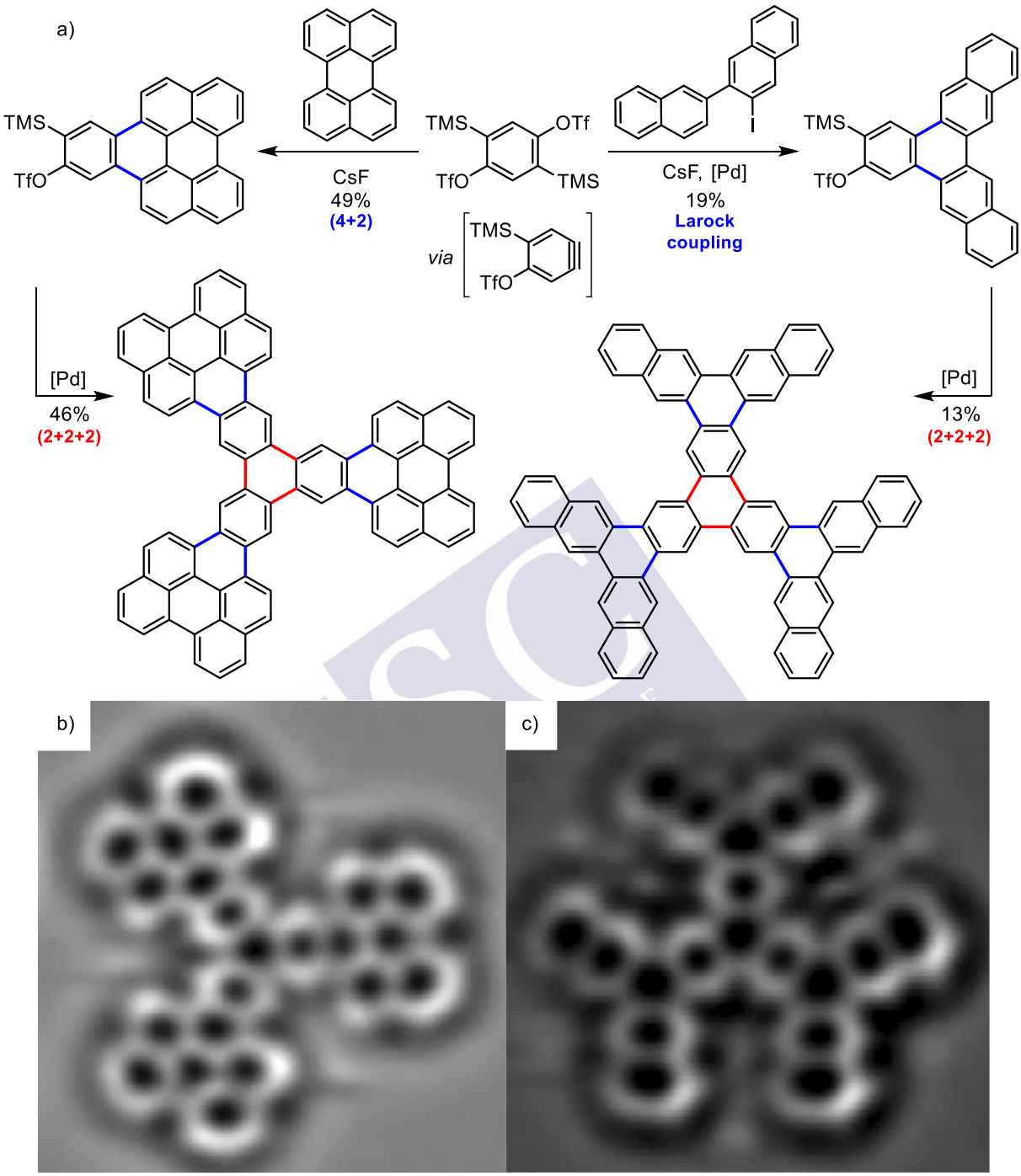


Figure 23. Example of three-fold symmetric shaped arenes: a) [16]cloverphene and b) three-fold multiple helicene.

It is possible to synthesise complex molecules by exploiting the bisarynes' ability of generate independently their two arynic unsaturations. This kind of methodologies have been widely employed in our research group to obtain PAHs. The power of these strategies can be illustrated by two remarkable examples shown in Scheme 14. They both start with the synthesis of novel, complex aryne precursors by selective generation of one single arynic unsaturation from a commercially available bistriflate, and subsequent reaction with an appropriate arynophile. In the case shown in the left, the naphthoperylene triflate was obtained by a Diels-Alder reaction/dehydrogenation sequence, in a 49%.[110] The aryne precursor on the right was obtained in a 19% yield, using a Larock coupling reaction (Scheme 14a).[111]

[110] B. Schuler, S. Collazos, L. Gross, G. Meyer, D. Pérez, E. Guitián, D. Peña, *Angew. Chem. Int. Ed.* **2014**, *53*, 9004–9006.
[111] M. Vilas-Varela, S. Fatayer, Z. Majzik, D. Pérez, E. Guitián, L. Gross, D. Peña, *Chem. Eur. J.* **2018**, *24*, 17697–17700.



Scheme 14. a) Synthesis of starphenes using bisarynes, b) and c) AFM images of flat starphenes on NaCl (2 monolayers)/Cu(111) using a CO-functionalised tip.

Once having these new *o*-(trimethylsilyl)aryl triflates, the corresponding aynes could be generated and reacted through (2+2+2) palladium-catalysed cyclotrimerisation to afford the expected nanographenes in 46% and 13% yield, respectively. Due to their extremely low solubility, their full characterisation in solution was precluded, being preliminarily identified by mass spectrometry. However, thanks to the long-term collaboration of our group with L. Gross

(IBM Research, Zurich), individual molecules of these three-fold symmetric planar nanographenes could be beautifully imaged with atomic resolution by non-contact AFM with functionalised tips (Scheme 14b and c).

The examples mentioned in this section 1.3 are clearly illustrative of the potential of aryne chemistry for the synthesis of extended PAHs, functional nanographenes and other carbon nanostructures. The current scientific interest on these families of compounds, mainly associated to their potential application in organic electronics, has been reviewed in section 1.1, while section 1.2 highlighted the current relevance of aryne chemistry. This PhD dissertation aims to further develop this exciting area of research, through significant contributions to both the development of new aryne species and the synthesis of PAHs of interest. The specific objectives of the thesis are detailed in each of the following chapters

2 2-Thiophyne

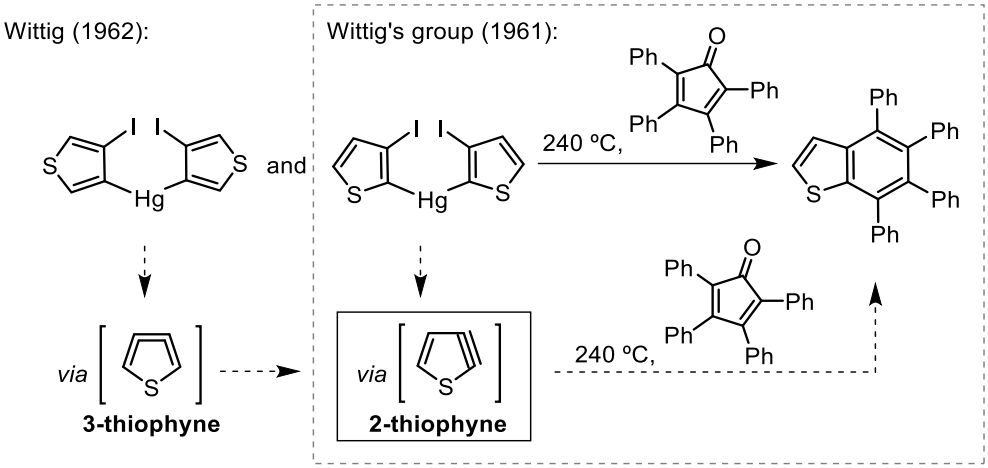
2.1 Background information

2-Thiophyne (2,3-didehydrothiophene) is among the most intriguing aryne intermediates proposed to date. Its generation has been postulated by a number of authors by using different methods, however, unambiguous proofs of its actual existence remain elusive. Although pyridynes are currently the most used and the best studied hetarynes, before the 80's thiophynes attracted more experimental efforts.[112] Some of the most representative contributions published on this topic are summarised below.

2.1.1 Contributions from Wittig's group

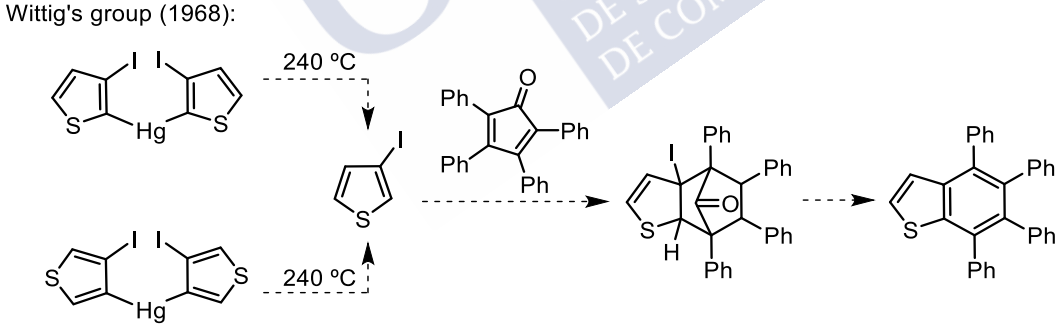
In 1960 Wittig and coworkers developed a new method to generate benzyne by heating (*o*-iodophenyl)mercury iodide.[113] The next year, this group used the novel strategy to obtain a new hetaryne, 2-thiophyne.[114] In this first attempt they placed bis(3-iodo-2-thiophenyl)mercury in presence of tetraphenylcyclopentadienone under aryne forming conditions and obtained the expected 4,5,6,7-tetraphenylbenzothiophene in 9% yield (Scheme 15). The isolation of the expected reaction product led them to postulate the generation of 2-thiophyne for the first time. However, in 1962 Wittig realised that another isomeric organomercury compound bis(4-iodo-3-thiophenyl)mercury, also gives the same reaction product (Scheme 15),[115] and proposed the isomerisation of 3-thiophyne, possibly unstable due to its cumulenic character, to 2-thiophyne.

[112] L. Radom, R. H. Nobes, D. J. Underwood, W. K. Li, *Pure Appl. Chem.* **1986**, *58*, 75–88.
[113] G. Wittig, H. F. Ebel, *Angew. Chem.* **1960**, *72*, 564.
[114] G. Wittig, V. Wahl, *Angew. Chem.* **1961**, *73*, 492.
[115] G. Wittig, *Angew. Chem. Int. Ed. Engl.* **1962**, *1*, 415–419.



Scheme 15. First attempts of thiophynes generation by Wittig's group.

Few years later, the same group tried to demonstrate the generation of this elusive intermediate once again with a study involving different aryne precursors and generation methods.[116] They found that organomercury compounds could have originated 3-iodothiophene by thermal decomposition and proposed an alternative reaction pathway in order to explain the formation of 4,5,6,7-tetraphenylbenzothiophene (Scheme 16), not involving the intermediate hetaryne. The conclusion of this article underlines the need for other aryne precursors, which could provide more solid evidences of the existence of this five-membered hetaryne.

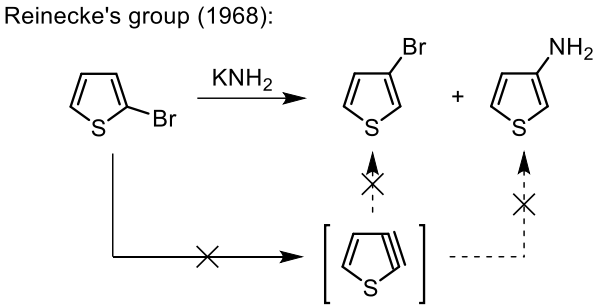


Scheme 16. Plausible non-aryne mechanism proposed.

[116] G. Wittig, M. Rings, *Justus Liebigs Ann. Chem.* **1968**, *719*, 127–144.

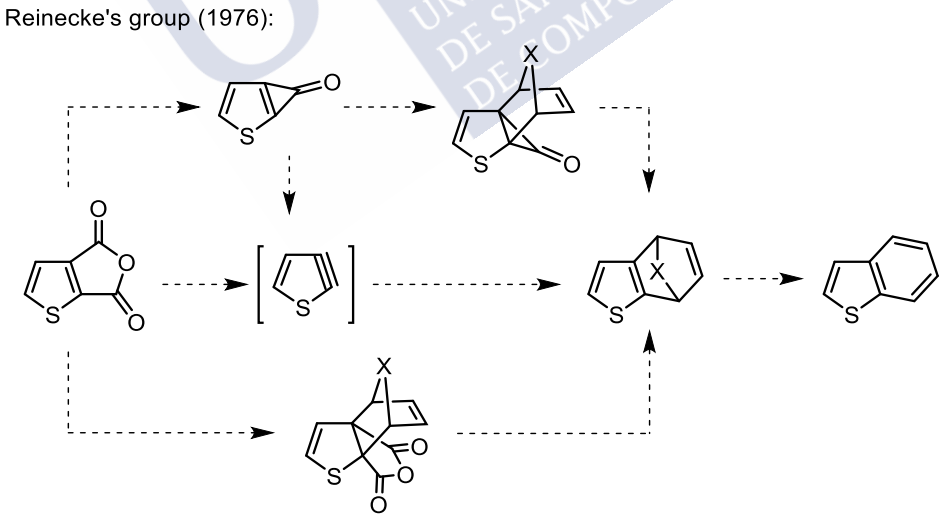
2.1.2 Contributions from Reinecke's group

In 1968, the aromatic substitution of 2-bromothiophene with different amides was studied by Reinecke and Adickes.[117] Apparently, they isolated products which could be explained through an aryne-based mechanism, although this possibility was finally dismissed (Scheme 17).[118]



Scheme 17. Study of the aromatic substitution on 2-bromothiophene with potassium amide.

Reinecke's group published in 1976 the **f**lash **v**acuum **t**hermolysis (FVT) of the thiophene-2,3-dicarboxylic acid anhydride (Scheme 18),[119] a method that had been previously validated to generate benzyne from phthalic anhydride, in the presence of several trapping agents. They obtained products apparently derived from 2-thiophyne, although alternative mechanism were not ruled out. They concluded: "*Taken in toto the above results constitute the most convincing evidence to date for the generation of a five-membered hetaryne, thiophyne*".



Scheme 18. Mechanistic alternatives proposed for the reaction of thiophene-2,3-dicarboxylic anhydride with dienes under FVT conditions.

---

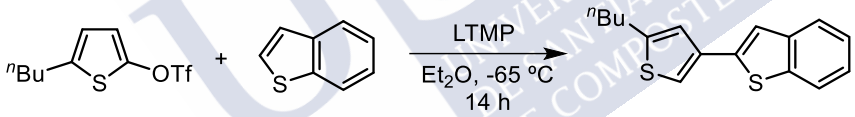
[117] M. G. Reinecke, H. W. Adickes, *J. Am. Chem. Soc.* **1968**, *90*, 511–513.
[118] T. Kauffmann, R. Wirthwein, *Angew. Chem. Int. Ed. Engl.* **1971**, *10*, 20–33.
[119] M. G. Reinecke, J. G. Newsom, *J. Am. Chem. Soc.* **1976**, *98*, 3021–3022.

In 1981 the same group published additional examples of the unusual reactivity of the supposed 2-thiophyne generated by FVT methods,[120] e.g. reaction with the diene through (2+2) cycloaddition rather than through Diels-Alder reaction.[121] In this work they reaffirmed that the arynic interpretation of the results remained to be the most plausible. The next year, Reinecke published a fantastic review on the study of hetarynes, specially focused on thiophynes.[75]

2.1.3 Contributions by other authors

In 1966, Fields and Meyerson claimed the generation of 2-thiophyne by pyrolysis (690 °C) of phthalic anhydride in presence of thiophene, as a conclusion derived from the study of the reaction by mass spectrometry and gas chromatography.[122]

In a recent report (2014), Daugulis' group published a novel methodology for the arylation of arenes and aromatic heterocycles, based on aryne chemistry.[123] In one example they postulate the intermediacy of a 2-thiophyne in the synthesis of a substituted 2-(3-thiophenyl)benzothiophene, but a detailed study of this mechanism has not been reported yet (Scheme 19).



Scheme 19. Synthesis of substituted 2-(3-thiophenyl)benzothiophene.

Finally, Miura and coworkers were able to obtain the X-ray structure of a nickel complex of 2-thiophyne (Figure 24).[124] However, as with regard to other stoichiometric aryne-metal complexes (Chapter 1, Figure 14 and Figure 21), its synthetic utility is rather limited. Despite the publication of this organometallic complex, the generation of the "*free"* aryne remains still unreported.

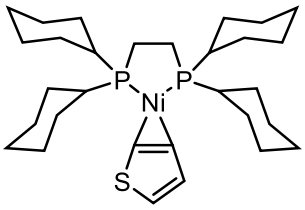
---

[120] M. G. Reinecke, J. G. Newsom, L. J. Chen, *J. Am. Chem. Soc.* **1981**, *103*, 2760–2769.
[121] M. G. Reinecke, J. G. Newsom, K. A. Almqvist, *Tetrahedron* **1981**, *37*, 4151–1457.
[75] M. G. Reinecke, *Tetrahedron* **1982**, *38*, 427–498.
[122] E. K. Fields, S. Meyerson, *Chem. Commun.* **1966**, 708–710.
[123] T. Truong, M. Mesgar, K. K. A. Le, O. Daugulis, *J. Am. Chem. Soc.* **2014**, *136*, 8568–8576.
[124] M. Terada, Y. Nishii, M. Miura, *Chem. Commun.* **2018**, *54*, 2918–2921.

a) **Ni(η^2–C_4H_2S)($Cy_2PCH_2CH_2PCy_2$)** b)

Miura and co.

(2013)



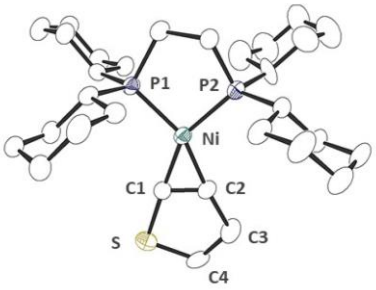


Figure 24. a) Organo-nickel complex; Ni(η^2-C_4H_2S)($Cy_2PCH_2CH_2PCy_2$) and b) its X-ray structure.

To sum up, despite the efforts of several groups along the years, the actual generation of the 2-thiophyne is still being questioned.

USC UNIVERSIDADE DE SANTIAGO DE COMPOSTELA

2.2 Objectives

The original objective of this part of the thesis was the synthesis of a suitable precursor of 2-thiophyne, and the study of the generation and trapping of this extremely elusive 5-membered hetaryne.

The curious story behind 2-thiophyne had captured our interest and encouraged us to tackle this challenge. As an additional factor, we envisaged the potential application of this intermediate to the synthesis of sulphur-doped arenes and *S*-heteroacenes, of undoubted interest as π-functional materials.[125]

Additionally, our motivation was supported by two facts: on the one hand, the extensive experience of our group in the chemistry of *o*-(trimethylsilyl)aryl triflates, precursors of choice to generate arynes under mild conditions; on the other hand, computational work published in 2012 by Goetz et al.[83] suggesting the synthetic viability of 2-thiophyne.

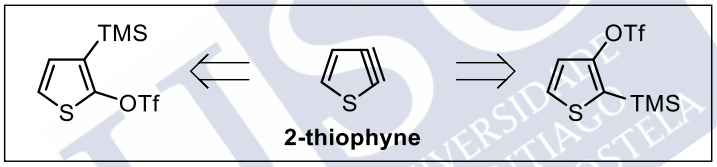


Figure 25. Potential Kobayashi's type precursors of 2-thiophyne.

[125] J. E. Anthony, *Chem. Rev.* **2006**, *106*, 5028-5054.
[83] A. E. Goetz, S. M. Bronner, J. D. Cisneros, J. M. Melamed, R. S. Paton, K. N. Houk, N. K. Garg, *Angew. Chem. Int. Ed.* **2012**, *51*, 2758–2762.

2.3 Results and discussion

In the last two decades aryne chemistry experienced an unprecedented outbreak due to the emergence of silyl-based precursors (Chapter 1, Scheme 5 and Scheme 6). The first examples and the most common so far, are the Kobayashi's type aryne precursors, *o*-(trimethylsilyl)aryl triflates, which are usually able to generate the corresponding arynes upon reaction with a fluoride source under mild reaction conditions. Our experience in the field led us to believe that these kind of functionalised thiophenes could be excellent candidates to demonstrate the existence of the 2-thiophyne (**1**).

2.3.1 Synthesis of 2-(trimethylsilyl)-3-thiophenyl triflate

Among the two possible Kobayashi's type precursors of 2-thiophyne (**1**) (see Figure 25), we targeted the 2-(trimethylsilyl)-3-thiophenyl triflate (**2**) because we found it more accessible synthetically.

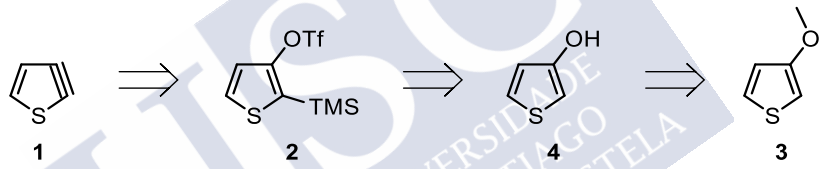
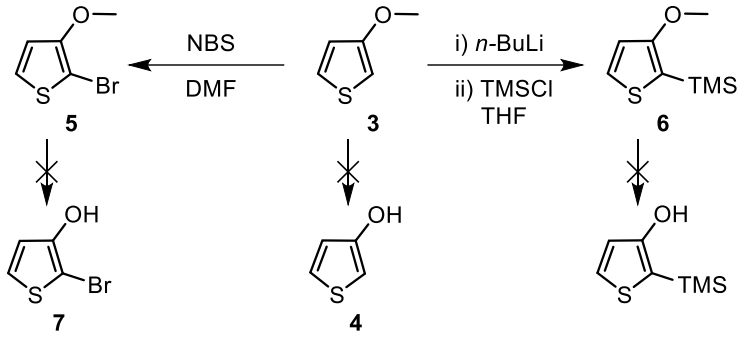


Figure 26. Retrosynthetic analysis of 2-thiophyne (**1**).

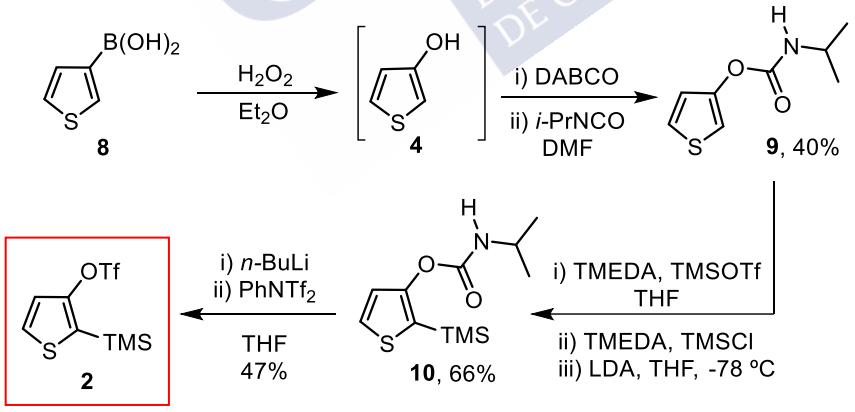
We envisioned a plausible synthesis employing the standard protocol developed in our laboratory (Chapter 1, Scheme 7)[71] for the efficient synthesis of *o*-(trimethylsilyl)aryl triflates from the corresponding *o*-bromophenols. We started our study with the commercially available 3-methoxythiophene (**3**), which could serve as a protected derivative of 3-thiophenol (**4**). We were able to functionalise this product at the C(2) position to afford 2-bromo-3-methoxythiophene (**5**)[126] and 2-(trimethylsilyl)-3-methoxythiophene (**6**).[127] However, all the performed attempts to deprotect the hydroxy groups by cleaving the O-CH_3 bonds resulted in decomposition.

[71] D. Peña, A. Cobas, D. Pérez, E. Guitián, *Synthesis* **2002**, *10*, 1454–1458.
[126] E. V. Canesi, D. Fazzi, L. Colella, C. Bertarelli, C. Castiglioni, *J. Am. Chem. Soc.* **2012**, *134*, 19070–19083.
[127] L. Albertin, C. Bertarelli, M. C. Gallazzi, S. V. Meille, S. C. Capelli, *J. Chem. Soc., Perkin Trans. 2* **2002**, 1752–1759.



Scheme 20. First attempts on the synthesis of a 2-thiophyne precursor.

According to our experience, *o*-bromophenols are usually rather unstable, hence, we decided to avoid the need of prepare **7**. Thus, we designed a new synthetic route based on the protocol developed by Garg for other arynes (Chapter 1, Scheme 7). In this occasion we prepared an ethereal solution of thiophenol **4** by oxidation of the corresponding boronic acid **8** following a described procedure.[128] Then, the hydroxy group was protected *in situ* with isopropyl isocyanate. Having the carbamate **9** in hands, we used the conditions reported for direct *o*-silylation,[73,74] obtaining compound **10** in a 66% yield. Finally, the carbamate was cleaved by treatment with *n*-BuLi and the resulting lithium alkoxide was treated with *N*-phenylbistriflimide to give the 2-(trimethylsilyl)-3-thiophenyl triflate (**2**) in a 47% yield. The protons on the thiophene in compound **2** showed a coupling constant ($J_{H\text{-}H}$ = 5.1 Hz) and chemical shifts (7.1 and 7.5 ppm) according to their 3,4-*ortho* positions.



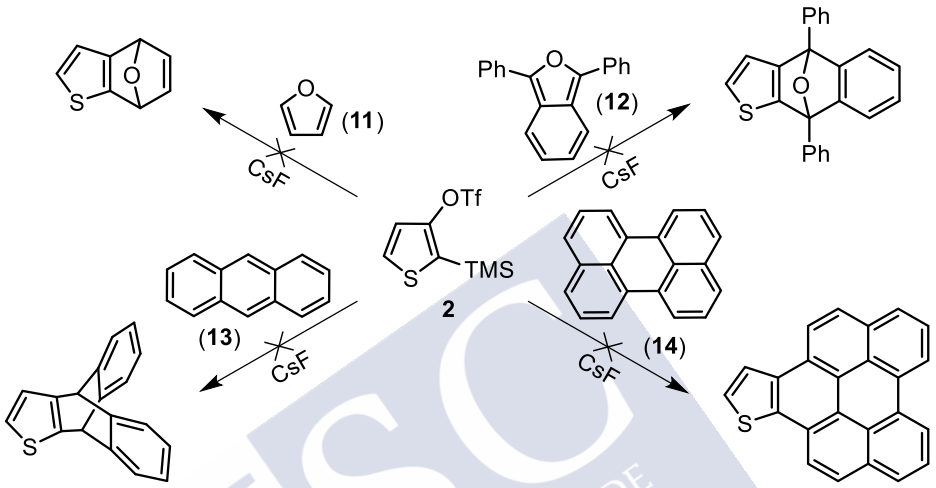
Scheme 21. Synthesis of a potential Kobayashi 2-thiophyne precursor.

---

[128] I. Vendina, A. Parkova, P. Trapencieris, *Heterocycles* **2014**, *8*, 1565–1572.
[73] S. M. Bronner, K. B. Bahnck, N. K. Garg, *Org. Lett.* **2009**, *11*, 1007–1010.
[74] a) M. Kauch, V. Snieckus, D. Hoppe, *J. Org. Chem.* **2005**, *70*, 7149–7158; b) M. Kauch, D. Hoppe, *Synthesis* **2006**, 1575–1577.

2.3.2 Study of reactivity

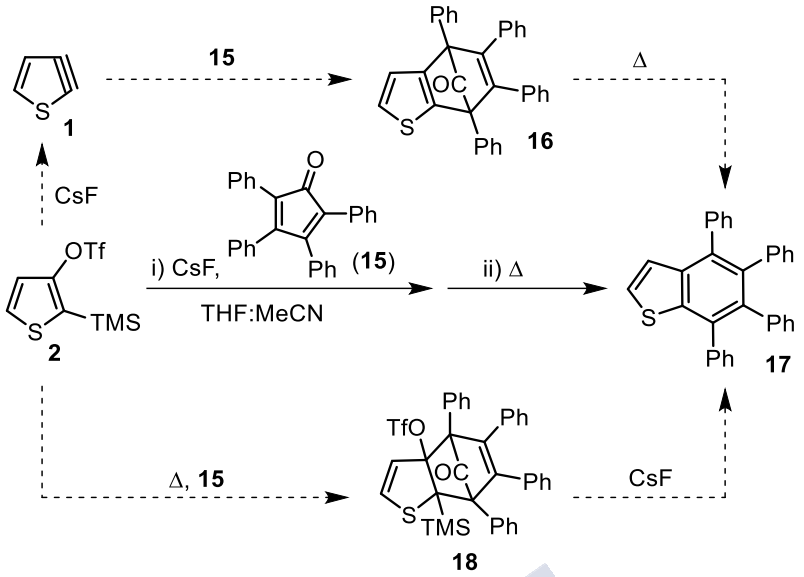
Once we had the potential aryne precursor **2** in hands, we studied its ability to generate 2-thiophyne. Therefore, we essayed its reaction with CsF in presence of different dienes, such as furan (**11**), 1,3-diphenylisobenzofuran (**12**), anthracene (**13**) and perylene (**14**). In these reactions we observed the consumption of **2** by TLC and ^{1}H NMR of the reaction crude, but the expected reaction products were not detected.



Scheme 22. Reaction of **2** with CsF in presence of dienes.

Then, we decided to emulate the first trapping reaction attempted by Wittig in 1961,[114] and thus, compound **2** was reacted in presence of 2,3,4,5-tretraphenylcyclopentadienone (**15**) under our aryne forming conditions, followed by heating at reflux for 16h. If 2-thiophyne were formed, it should afford the Diels-Alder adduct **16**, which under heating should undergo cheletropic extrusion of CO. In the first experiment performed, we successfully isolated **17** in low yield (Scheme 23). The characterisation was confirmed comparing the spectroscopic data with those described in the literature for this compound.[129]

[114] G. Wittig, V. Wahl, *Angew. Chem.* **1961**, *73*, 492.
[129] A. Bej, A. Chakraborty, A. Sarkar, *RSC Adv.* **2013**, *3*, 15812–15819.



Scheme 23. Preliminary study of 2-thiophyne generation, and plausible mechanisms.

At first sight, the most plausible mechanism to explain the formation of **17** should be through the 2-thiophyne (**1**) as intermediate, but due to the historical controversy about the generation of this elusive species, we decided study the reaction in depth. Determined to clarify the reaction mechanism, we tried to detect any reaction intermediate. Hence, we repeated the reaction stepwise, expecting to isolate the feasible adducts **16** or **18** under mild conditions. When the reaction was conducted at room temperature, we isolated a compound with NMR (22 aromatic protons, two of them with the characteristic coupling constant of *ortho* positions on thiophene, $J_{H\text{-}H}$ = 5.3 Hz), IR (a sharp peak at 1703 cm^{-1}) and mass spectra which could be in agreement with the structure of the intermediate **16**. However, X-ray diffraction analysis revealed the totally unexpected structure shown in Figure 27.

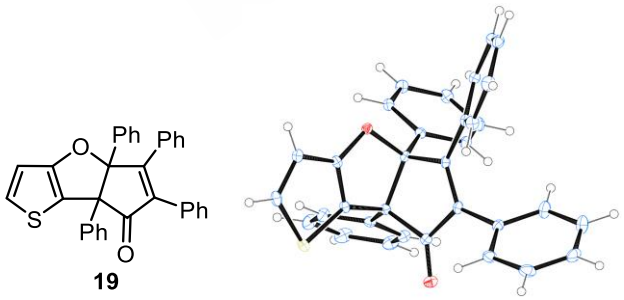
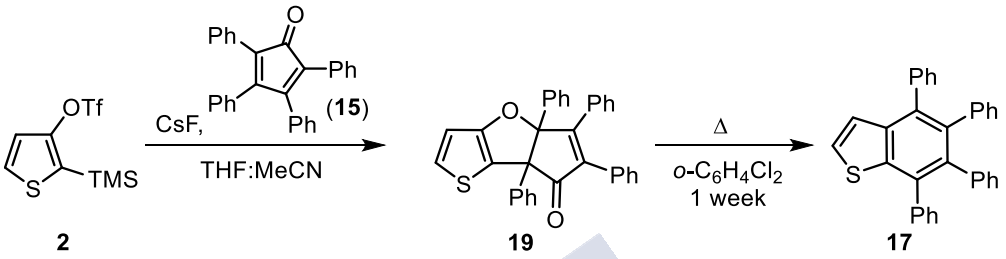


Figure 27. Synthetic intermediate **19** in the reaction between **2** and CsF in presence of tetraphenylcyclopentadienone and its X-ray structure.

2.3.3 Mechanistic studies

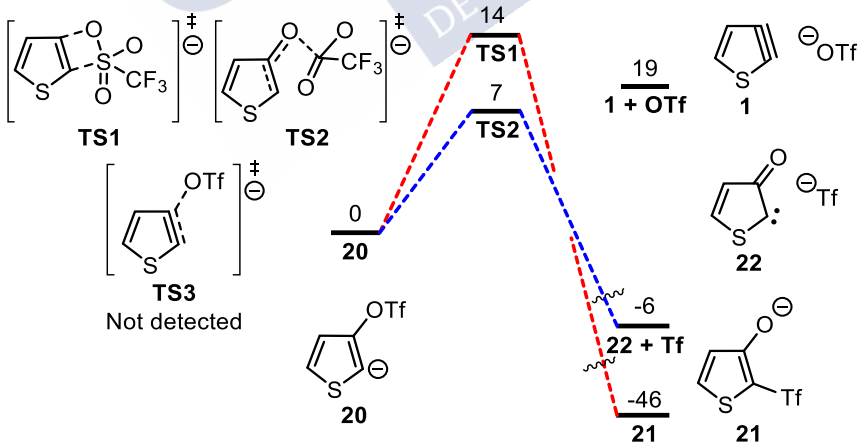
First, in order to demonstrate if **19** is involved in the generation of **17**, we heated the isolated compound in *o*-dichlorobenzene at 180 ºC for one week, obtaining the 3,4,5,6-tetraphenyl-benzothiophene **17** quantitatively. The isolation of compound **19** strongly suggests a non-aryne reaction pathway. So, we decided to study the mechanism in two parts: the formation of **19**, and its evolution into the final product.



Scheme 24. Synthesis of **17** from **2**.

First part of the mechanism

Theoretical calculations,[130] were performed in collaboration with Prof. A. Cobas,[131] to suggest and support plausible reaction pathways. We assumed the generation of anion **20**, from the reaction of **2** with CsF, and evaluated reasonable paths for the evolution of this species (Scheme 25). We found that the formation of the aryne was clearly unfavoured.



Scheme 25. Theoretical calculations on plausible evolution of **20** (ΔG values in Kcal mol^{-1}).

---

[130] **D**ensity **F**unctional **T**heory (DFT) B3LYP/6-31++G(d,p), including a continuum description of the acetonitrile solvent (CPCM).

[131] Theoretical calculations were performed in collaboration with Prof. A. Cobas, Department of Organic Chemistry, University of Santiago de Compostela (USC), Spain.

Then, we considered the possibility of a mechanism involving a thia-Fries rearrangement, which has been observed in many previous attempts of aryne generation,[132] but a relatively high activation barrier, 14 Kcal mol^{-1}, was calculated for this transformation. Finally, we found that the most kinetically favourable mechanism involves the unusual formation of ketocarbene **22**, 7 Kcal mol^{-1} (Scheme 25 and Figure 28). Similar species were detected by Teles and coworkers in the pyrolysis of thiophene-2,3-dicarboxylic acid anhydride.[133]

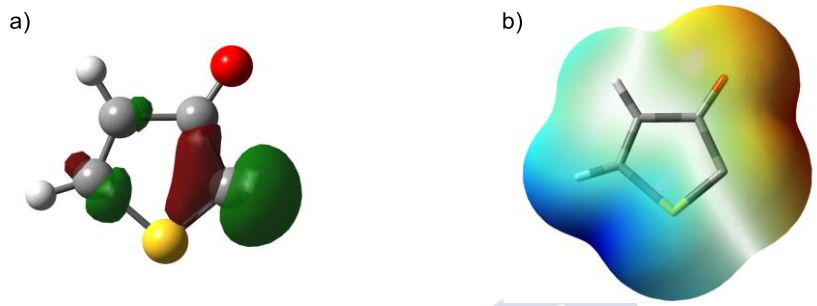
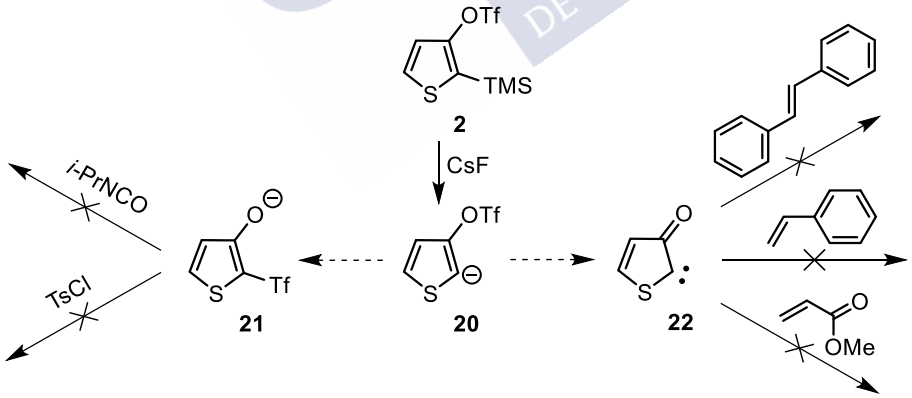


Figure 28. a) Calculated HOMO and b) total electron density map of ketocarbene **22**.

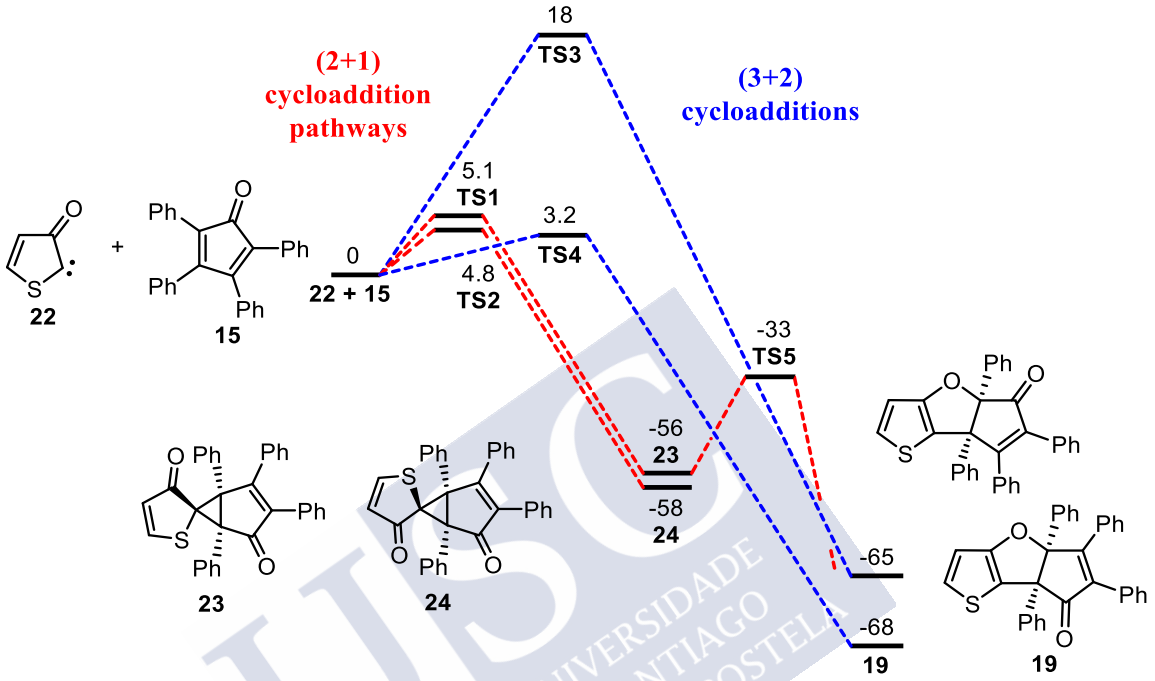
Concurrently to the development of this computational study, we tried to get experimental evidences of the generation of any of these alternative intermediates. Thus, we performed the reaction of **2** in the presence of other different reaction partners, such as isopropyl isocyanate or tosyl chloride, in order to trap any alkoxide **21** derived from a thia-Fries rearrangement, and such as styrene, stilbene or methyl acrylate, with a focus on trapping the hypothetical carbene **22**. However, all attempts resulted unsuccessful.



Scheme 26. Trapping experiments performed.

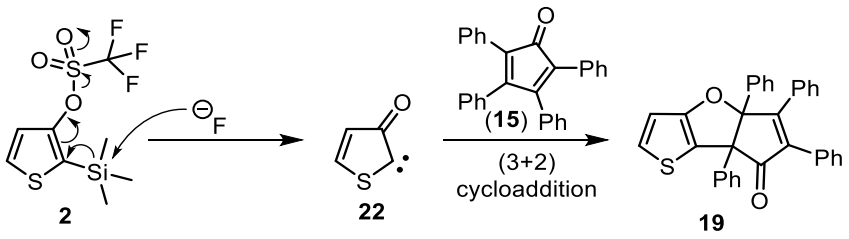
[132] a) A. M. Dyke, D. M. Gill, J. N Harvey, A. J. Hester, G. C. Lloyd-Jones, M. P. Muñoz, I. R. Shepperson *Angew. Chem. Int. Ed.* **2008**, *47*, 5067–5070; b) M. Korb, H. Lang, *Chem. Soc. Rev.* **2019**, *48*, 2829–2882.
[133] J. H. Teles, Jr. B. A. Hess, L. J. Schaad, *Chem. Ber.* **1992**, *125*, 423–431.

Despite the lack of further experimental evidences, we assumed the possible generation of ketocarbene **22** as an alternative to the aryne, and computed its plausible reaction with cyclopentadienone **15**.[134] We found that the (2+1) cycloaddition, with one of the double bonds of the diene, leading to the spirocompound **23** could be accessible, but the very asynchronous (3+2) cycloaddition to afford **19** is more favourable (Scheme 27).



Scheme 27. Theoretical calculations of the cycloaddition reactions between ketocarbene **22** and cyclopentadienone **15** (ΔG values in Kcal mol^{-1}).

Taking into account these results, we proposed that **19** is formed by the mechanistic pathway shown in Scheme 28, although the formation of the spirocompound **23** can not be ruled out.

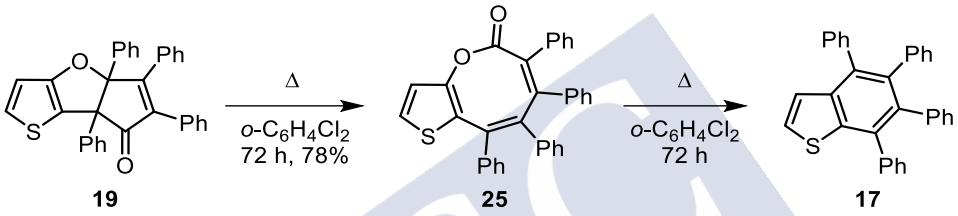


Scheme 28. Mechanistic proposal for the formation of **19**.

[134] DFT B3LYP/6-31++G(d,p), including a continuum description of the acetonitrile solvent.

Second part of the mechanism

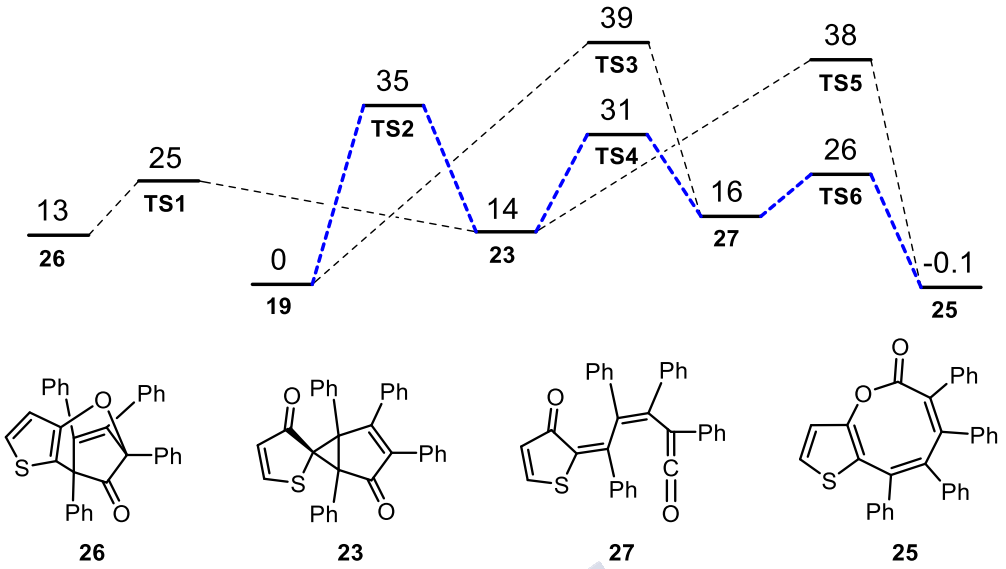
Regarding to the last part of the mechanism, we examined carefully the reaction of **19** to afford the final product (**17**). As aforementioned, this reaction occurs quantitatively after one week, thus we followed the reaction along the time and observed the appearance of a new intermediate compound, which could be isolated after 72 hours of reaction, in a 78% yield. Subsequently, we confirmed the transformation of this newly isolated compound into benzothiophene **17** after heating for additional 72 hours. This intermediate was tentatively identified as **25**, by NMR (22 aromatic protons, one of them with the characteristic coupling constant of *ortho* positions on thiophene, $J_{H\text{-}H}$ = 4.7 Hz), IR (a sharp peak at 1728 cm^{-1}) and mass spectra (m/z = 482), although its characterisation remains ambiguous.



Scheme 29. Study of the second part of the mechanism. Isolation of reaction intermediate **25** and corroboration of its transformation into **17**.

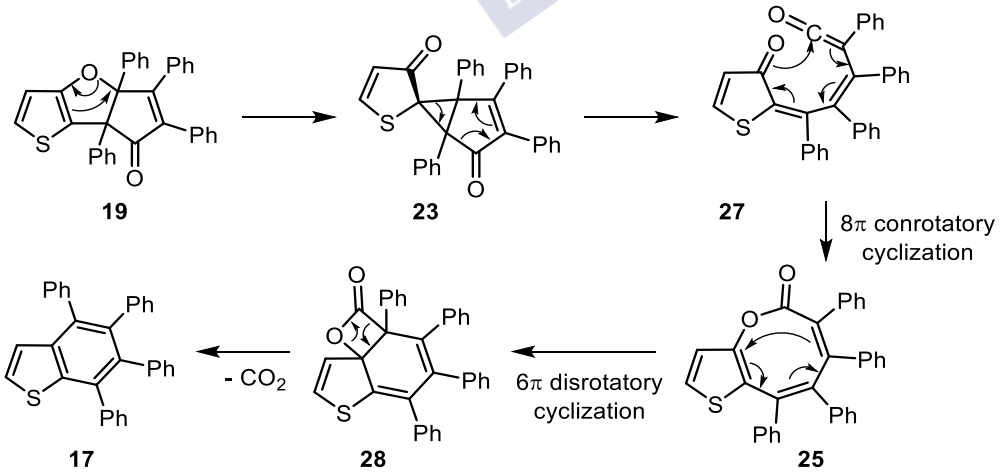
We also evaluated by theoretical calculations the evolution of **19**,[135] and found that the products **23** and **19**, resulting from the (2+1) and (3+2) cycloaddition reactions respectively, and the intermediate **26**, are interconnected (Scheme 30). Apparently, the most favourable reaction pathway evolves from **19** to the ketene **27**. This compound would suffer an intramolecular cyclisation (8π conrotatory) to afford the most stable intermediate, the lactone **25**. Zwitterionic pathways and other alternatives were studied and resulted disfavourable.

[135] DFT-B3LYP/6-31++G(d,p).



Scheme 30. Theoretical calculations on the formation of **25** (ΔG values in Kcal mol^{-1}).

The formation of benzothiophene **17** from the proposed 8-membered lactone **25** could be explained as a result of a thermal 6π-disrotatory perycyclic reaction to afford tricycle **28**, followed by irreversible decarboxylation to yield **17**. This kind of tandem process has been observed for similar compounds.[136] Thus, on the basis of experimental data and theoretical calculations, the mechanism outlined in Scheme 31 could be proposed for the transformation of the isolated (and unambiguously characterised) intermediate compound **19** into the final product, benzothiophene **17**.

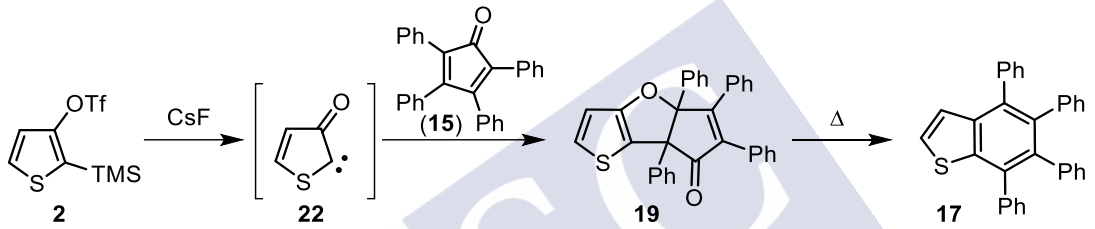


Scheme 31. Mechanistic proposal for the formation of **17**.

[136] a) D. Ramaiah, S. Rajadurai, P. K. Das, M. V. George, *J. Org. Chem.* **1987**, *52*, 1082–1089; b) A. Izuoka, S. Miya, T. Sugawara, *Tetrahedron Lett.* **1988**, *29*, 5673–5676.

2.4 Conclusions

To conclude, we synthesised 2-(trimethylsilyl)-3-thiophenyl triflate (**2**) as a potential precursor of 2-thiophyne (**1**). The ability of this triflate to actually generate 2-thiophyne under mild reaction conditions was studied by means of a trapping experiment with 2,3,4,5-tetraphenylcyclopentadienone. A careful study of the reaction mechanism, including the isolation and characterisation of intermediate compounds and DFT theoretical calculations, led to the proposal of a reaction pathway involving the generation of ketocarbene **22**, instead of the targeted hetaryne. Furthermore, a plausible mechanism for the overall transformation into benzothiophene **17**, involving the formation of unexpected intermediates such as the cyclopenta[*b*]thieno[2,3-*d*]furan-7-one **19**, has been proposed



Scheme 32. Mechanism concluded to explain the formation of **17** from the compound **2**.

Remarkably, even having a potentially "*suitable precursor*" and obtaining a reaction product which could be initially considered as a "*strong evidence*" to support the generation of 2-thiophyne, the mystery around this elusive hetaryne remains unresolved.

3 1,7-Naphthodiyne

3.1 Background information

Bisaryne intermediates were postulated for the first time in 1959, however they did not become synthetically useful until the decade of eighties, when some of them served as platforms to obtain PAHs (see Chapter 1, section 1.2.4). The reactions reported so far involving bisarynes are often low-yielding processes, and thus, the selection of appropriate precursors for their generation has proven to be crucial for success. Currently, both possible benzodiyne synthons, 1,4-benzodiyne[93] and 1,3-benzodiyne,[137] are known and their bis(trimethylsilyl)aryl bistriflate precursors have been described. In the case of naphthalene, four out of the five possible bisarynes were published (Figure 29) prior to this work.

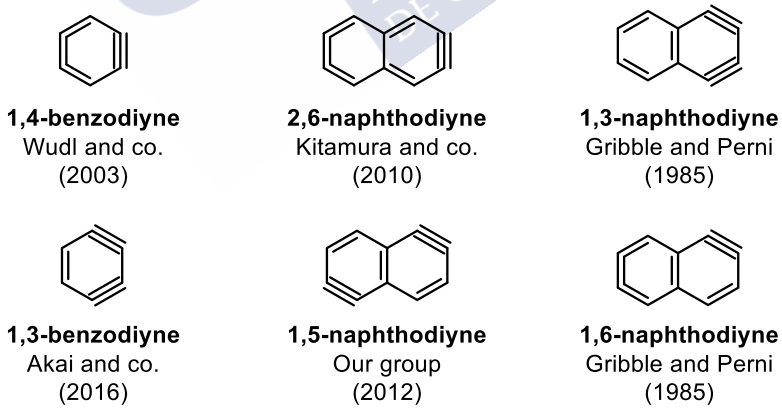
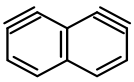


Figure 29. Bisarynes in benzene and naphthalene reported prior to this work.

[93] H. M. Duong, M. Bendikov, D. Steiger, Q. Zhang, G. Sonmez, J. Yamada, F. Wudl, *Org. Lett.* **2003**, *5*, 4433–4436.
[137] T. Ikawa, S. Masuda, A. Takagi, S. Akai, *Chem. Sci.* **2016**, *7*, 5206–5211.

However, only 2,6-naphthodiyne[138] and 1,5-naphthodiyne[139] had suitable TMS/OTf precursors, while 1,3-naphthodiyne and 1,6-naphthodiyne,[140] were generated from *o*-Br/OTs arenes under strongly basic conditions, by treatment with phenyl lithium (Figure 29).

Thus, at the time of starting this PhD work, the only unknown bisaryne synthon derived from naphthalene was 1,7-naphthodiyne (Figure 30). In fact, we only could find one article mentioning this species as a model compound to study the presence of dehydrogenated PAHs in interstellar matter.[141]



1,7-naphthodiyne

Figure 30. 1,7-naphthodiyne; the last bisaryne in naphthalene.

1,7-Naphthodiyne synthon could be highly interesting as a novel building block to synthesise V-shaped arenes, a family of compounds scarcely studied, in comparison with the linear[103] or helical topologies,[142] in spite of the interesting potential applications attributed to semiconductors with bent-shaped π-electron cores and other V-shaped arene derivatives.[143]

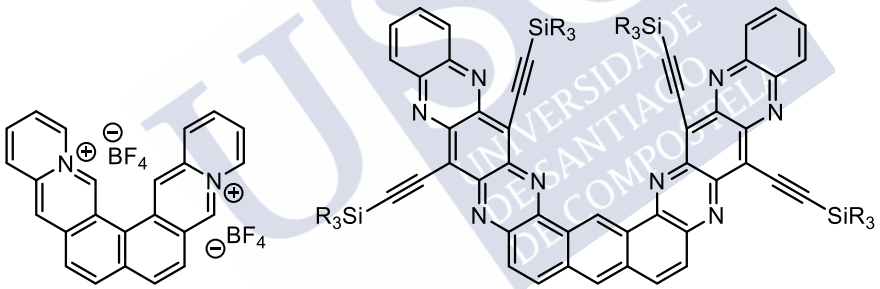


Figure 31. Examples of V-shaped arenes derivatives.

---

[138] C. Kitamura, Y. Abe, T. Ohara, A. Yoneda, T. Kawase, T. Kobayashi, H. Naito, T. Komatsu, *Chem. A Eur. J.* **2010**, *16*, 890–898.
[139] D. Rodríguez-Lojo, A. Cobas, D. Peña, D. Pérez, E. Guitián, *Org. Lett.* **2012**, *14*, 1363–1365.
[140] G. W. Gribble, R. B. Perni, K. D. Onan, *J. Org. Chem.* **1985**, *50*, 2934–2939.
[141] F. Pauzat, D. Talbi, Y. Ellinger, *Astron. Astrophys.* **1995**, *293*, 263–277.
[103] a) For perphenyltetracene see: Y. Xiao, J. T. Mague, R. H. Schmehl, F. M. Haque, R. A. Pascal, Jr., *Angew. Chem. Int. Ed.* **2019**, *58*, 2831–2833; b) For dodecacene see: F. Eisenhut, T. Kühne, F. García, S. Fernández, E. Guitián, D. Pérez, G. Trinquier, G. Cuniberti, C. Joachim, D. Peña, F. Moresco, *ACS Nano* **2020**, *14*, 1011–1017.
[142] a) Y. Shen, C. F. Chen, *Chem. Rev.* **2012**, *112*, 1463–1535; b) A. Robert, G. Naulet, H. Bock, N. Vanthuyme, M. Jean, M. Giorgi, Y. Carissan, C. Aroulanda, A. Scalabre, E. Pouget, F. Durola, Y. Coquerel, *Chem. Eur. J.* **2019**, *25*, 14364–14369; c) C. M. Cruz, S. Castro-Fernández, E. Maçôas, J. M. Cuerva, A. G. Campaña, *Angew. Chem. Int. Ed.* **2018**, *57*, 14782–14786.
[143] a) T. Okamoto, *Polym. J.* **2019**, *51*, 825–833; b) R. Pathak, K. Vandayar, W. A. L. Van Otterlo, J. P. Michael, M. A. Fernandes, C. B. De Koning, *Org. Biomol. Chem.* **2004**, *2*, 3504–3509; c) A. Granzhan, J. W. Bats, H. Ihmels, *Synthesis* **2006**, 1549–1555; d) K. Zhao, G. Long, W. Liu, D. S. Li, W. Gao, Q. Zhang, *J. Org. Chem.* **2020**, *85*, 291–295.

3.2 Objectives

As main goal of this part of the thesis, we targeted the synthesis of a suitable precursor of the unknow 1,7-naphthodiyne synthon, and the study of the reactivity of this novel aryne building block.

This project has an extra point of difficulty, due to the necessity of synthesising a strongly hindered 1,2,7,8-tetrasubstituted naphthalene as bisaryne precursor. However, the idea of completing the family of naphthodiynes, together with the interest of the potential utilisation of this novel bisaryne in the synthesis of V-shaped arenes, were decisive for us to address this challenge.

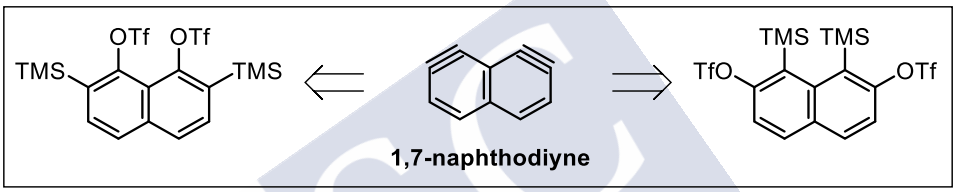


Figure 32. Potential Kobayashi-type precursors of 1,7-naphthodiyne.

3.3 Results and discussion

In principle, different compounds could be adequate precursors of the 1,7-naphthodiyne synthon (**29**). On the basis of our experience in the use of *o*-(trimethylsilyl)aryl triflates as reagents of choice for generating the corresponding arynes efficiently and under mild reaction conditions, we pursued the goal of obtaining a Kobayashi-type precursor for this novel bisaryne, in spite of the difficulty associated to the synthesis of such a highly hindered 1,2,7,8-substituted naphthalene. Therefore, we focused our attention on the design of the synthesis of the adequate bis(trimethylsilyl)naphthalenodiyl bistriflate.

3.3.1 Synthesis of a precursor of 1,7-naphthodiyne

A Kobayashi-type precursor of **29** should contain two sets of trimethylsilyl and triflate groups at positions C(1)/C(2) and C(7)/C(8), respectively. We prioritised the symmetrically substituted isomers, which should involve shorter synthesis. A preliminary retrosynthetic analysis led us to identify the dihydroxynaphthalenes **30** and **31** as suitable starting materials. Both compounds are commercially available, although the 1,8-naphthalenediol is rather unstable, being easily oxidised to afford dimeric and polymeric quinones. In addition, the selective dibromination of compound **30** at positions 1 and 8 had been previously described. So, we decided to start the synthesis from 2,7-naphthalenediol (**30**), thus identifying bistriflate **32** as potential precursors of the targeted 1,7-naphthodiyne (**29**).

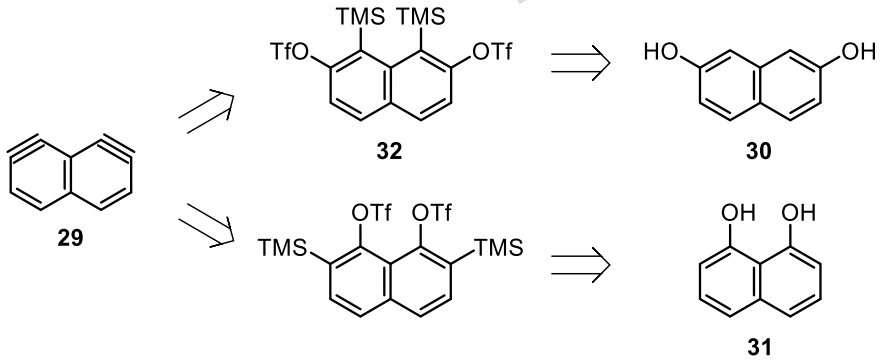
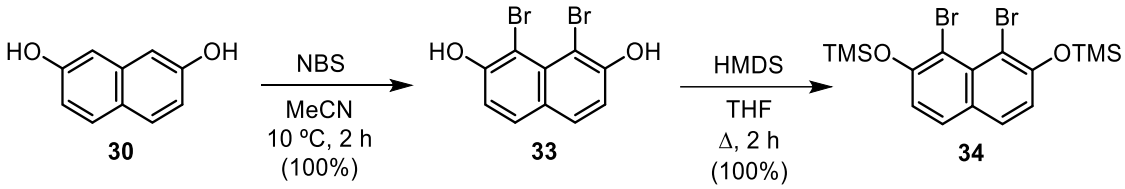


Figure 33. Retrosynthetic analysis of 1,7-naphthodiyne synthon (**29**).

We started the synthesis of **32** as shown in Scheme 33. Regioselective *o*-dibromination of **30** afforded 1,8-dibromo-2,7-naphthalenediol (**33**) in almost quantitative yield after further optimisation of reported procedures (61-74%).[144] Compound **33** decomposes in silica gel, and thus, it was directly used in the next step after a quick filtration. Treatment of 1,8-dibromo-2,7-naphthalenediol (**33**) with HMDS in refluxing THF gave bis(trimethylsilyl)ether **34**, which was used without further purification.



Scheme 33. Synthesis of compound **34**.

The last part of the synthesis, that is, the transformation of **34** into 1,8-bis(trimethylsilyl)naphthalene-2,7-diyl bistriflate (**32**) is quite complex, since it involves several elementary reactions occurring ideally in a single synthetic operation, and since the targeted compound bears a considerable distortion, due to the steric congestion associated to the close proximity of two bulky TMS groups at positions C(1) and C(8), being C(2) and C(7) also substituted.

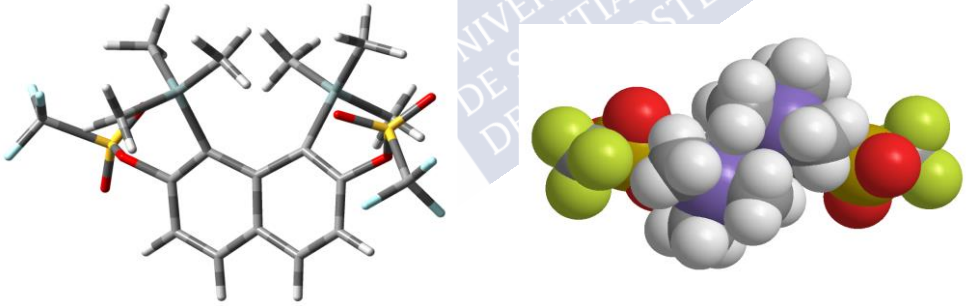


Figure 34. DFT optimised geometry for **32**.[145]

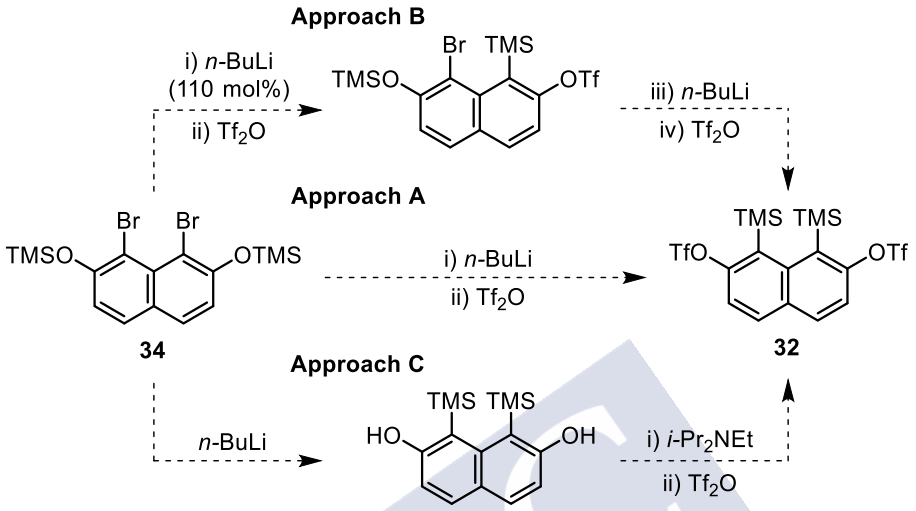
Initially we tried the reaction of compound **34** under our well-established standard conditions for the one-pot transformation of *o*-bromophenols into *o*-(trimethylsilyl)aryl triflates, but using double amounts of both *n*-BuLi and Tf_2O. However, we only detected the formation of products derived from the loss of one and two trimethylsilyl groups (Approach A, Scheme 34). Then, we tried to perform the transformation separately in each the two rings of the

---

[144] a) C. Thirsk, G. E. Hawkes, K. R. Liedl, T. Loerting, R. Nasser, R. G. Pritchard, M. Steele, J. E. Warren, A. Whiting, *J. Chem. Soc., Perkin Trans. 2* **2002**, *9*, 1510–1519; b) K. C. Majumdar, S. Mondal, D. Ghosh, *Tetrahedron Lett.* **2009**, *50*, 4781–4784.

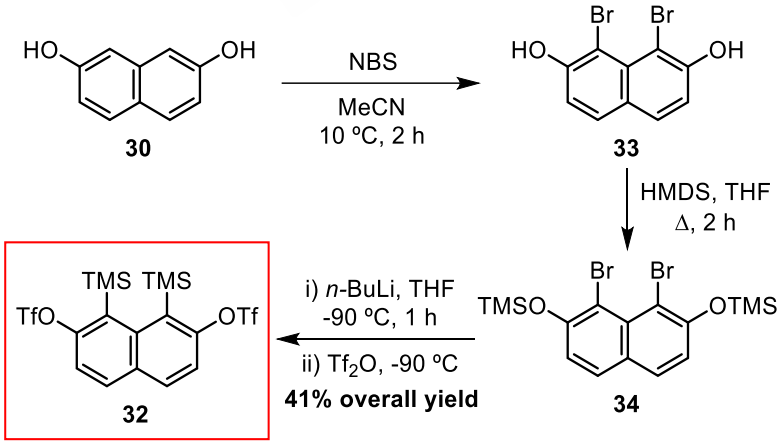
[145] DFT-B3LYP/6-31++G(d,p) in gas phase.

naphthalene moiety (Approach B) to avoid potential troubles related with the generation of doubly charged species, although our efforts were in vain. We also attempted to divide the reaction in two steps; (1) retro-Brook rearrangements, and (2) esterification with triflic anhydride (Approach C), observing again the formation of products with only one TMS group.



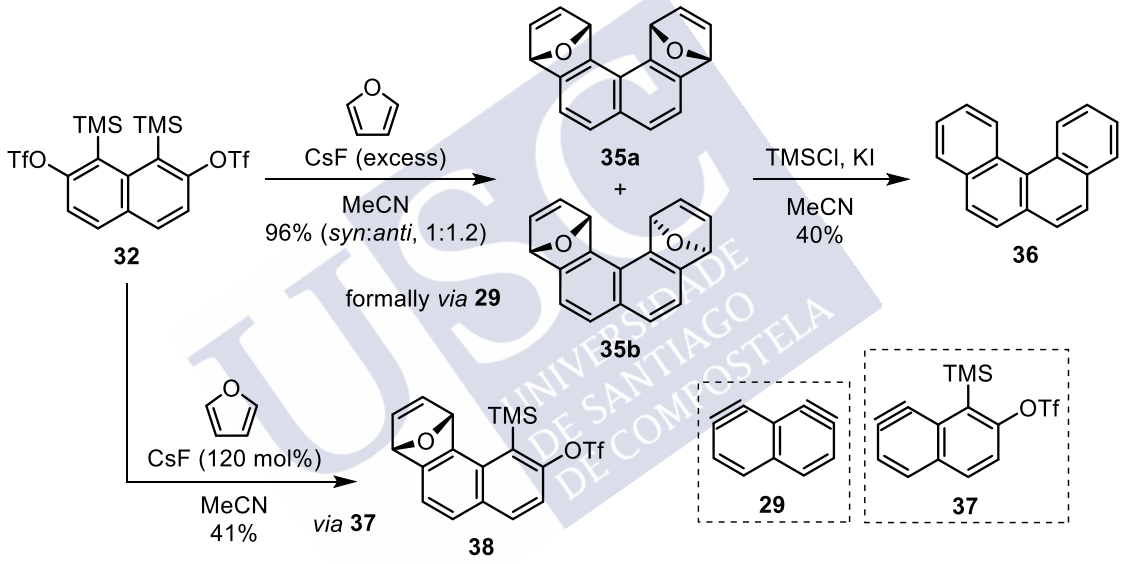
Scheme 34. Attempted approaches to synthesise the potential precursor of 1,7-naphthodiyne **32.**

Finally, we got back to the approach A. After analysing a significative number of reaction conditions (varying temperature, reaction times, etc.), we could isolate bistriflate **32**, initially in low yield (Scheme 34). Might the migration of TMS groups to positions C(1) and C(8) be favoured due to the need for distancing both negative charges, surpassing the barrier caused by steric hindrance. Further optimisation of the reaction conditions allowed us to prepare the potential 1,7-naphthodiyne precursor **32** through a short, three-steps synthesis from commercially available diol **30**, and in 41% overall yield (Scheme 35).



Scheme 35. Synthesis of the 1,7-naphthodiyne precursor **32**.

Once having compound **32** in hands, we evaluated its ability to generate the 1,7-naphthodiyne synthon. Treatment of **32** with excess of CsF in presence of furan, at room temperature and using MeCN as solvent, afforded the mixture of *syn*- and *anti*- adducts (**35**, 1:1.2) in an excellent 96% yield (Scheme 36). We could separate both isomers by column chromatography and found that the major product was the chiral isomer **35b**, as demonstrated by the separation into enantiomers using chiral HPLC. The formation of **35** seems to be the result of two sequential (4+2) cycloaddition reactions, which demonstrates the ability of **32** as a formal precursor of 1,7-naphthodiyne (**29**). Treatment of diastereoisomers **35** with TMSCl and KI, allowed deoxygenation to obtain benzo[*c*]phenanthrene (**36**) in 40% yield. We also generated selectively one single aryne (**37**) from **32**, by adding 120 mol% of CsF, to afford the new aryne precursor **38** in a 41% yield (Scheme 36).



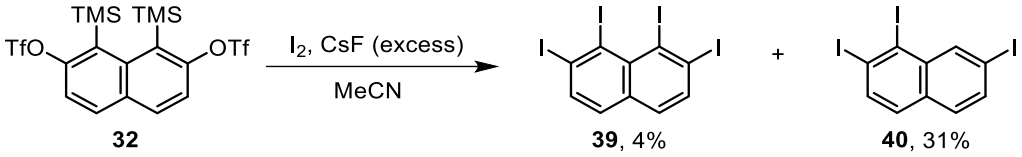
Scheme 36. Trapping experiments with furan.

With these results we concluded that **32** is an efficient precursor of the 1,7-naphthodiyne synthon (**29**). Furthermore, the possibility of generating independently both unsaturations allows us to envisage increased versatility for this bisaryne precursor.

3.3.2 Study of reactivity

Once proved the efficiency of bistriflate **32** as precursor of the naphthodiyine synthon **29** (and also of the functionalysed 1-naphtalyne **38**), we tackled a preliminary study of the participation of these novel arynes in different reactions.

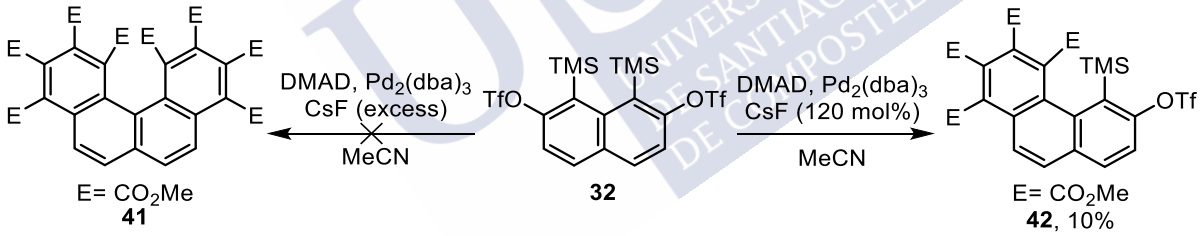
As an example of the participation of this new bisaryne in σ-bond insertion reactions,[146] we used the iodination protocol developed in our research group for the synthesis of *o*-diiodoarenes.[139] The reaction of **32** with CsF in presence of iodine afforded the expected product **39**, although in poor yield. The major product isolated in this reaction was **40**, which could be formed by protonation of the corresponding anionic intermediate (Scheme 37).



32 **39**, 4% **40**, 31%

Scheme 37. Formal I-I σ-bond insertion of 1,7-naphthodiyne synthon (**29**).

Then, we studied the participation of the novel aryne platform in (2+2+2) palladium-catalysed cocyclisations. When we essayed the reaction of **32** with excess of CsF in presence of a catalytic amount of palladium and DMAD, the formation of compound **41** was not detected. Then, we performed the reaction generating selectively one single aryne. We could isolate the expected product **42** in a 10% yield (Scheme 38). The low yield obtained in this reaction is probably due to the steric hindrance, which is in even higher in the double approach attempted before.

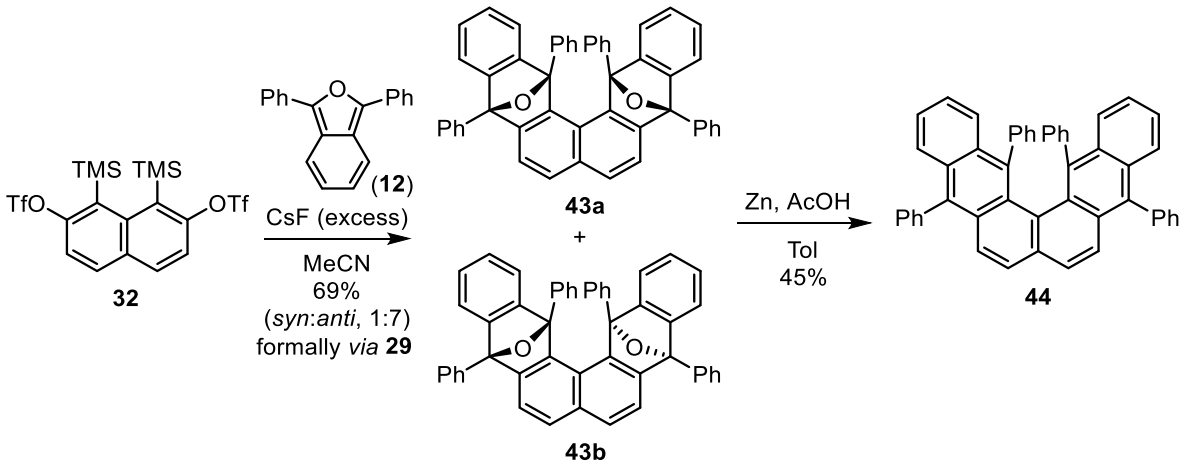


Scheme 38. Study of (2+2+2) palladium-catalysed cocyclisations with DMAD.

Based on these results, we decided to focus our study on the (4+2) cycloaddition reactions, which had already been successfully probed in the trapping experiments with furan. We studied the reaction of **29** with 1,3-diphenylisobenzofuran (**12**), anthracene (**13**) and tetraphenylcyclopentadienone (**15**). Thus, reacting the precursor **32** in presence of 1,3-diphenylisobenzofuran (**12**) under aryne forming conditions, the double Diels-Alder reaction afforded **43** in 69% yield as the 1:7 mixture of *syn*- and *anti*- isomers respectively (Scheme 39).

---

[146] D. Peña, D. Pérez, E. Guitián, *Angew. Chem. Int. Ed.* **2006**, *45*, 3579–3581.
[136] D. Rodríguez-Lojo, A. Cobas, D. Peña, D. Pérez, E. Guitián, *Org. Lett.* **2012**, *14*, 1363–1365.



Scheme 39. Synthesis of naphthotetraphene **44**.

We separate both isomers by centrifugation and characterised them individually and unequivocally, thanks to the X-ray diffraction analysis of the *anti*- isomer **43b** (Figure 35). In this case the *anti*- isomer was the major product, probably due to the steric hindrance for the second cycloaddition. This result demonstrates the excellent ability of the 1,7-naphthodiyne synthon (**29**) as platform to build strained PAHs.

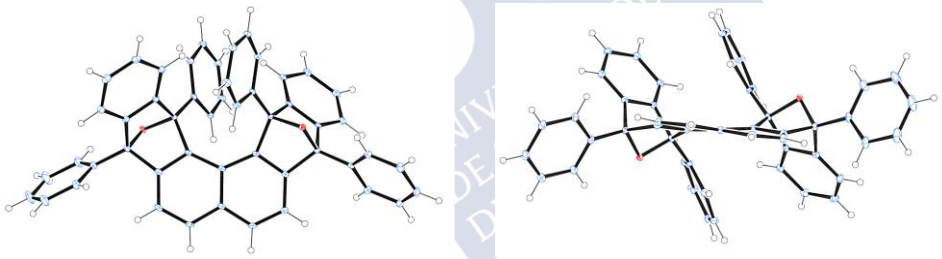


Figure 35. X-ray structure of compound **43b**.

Subsequently, we studied the reduction of the stereoisomers **43** employing metallic zinc in acetic acid, which afforded 5,10,15,16-tetraphenylnaphtho[2,3-*a*]tetraphene (**44**) in a moderate 45% yield (Scheme 39).

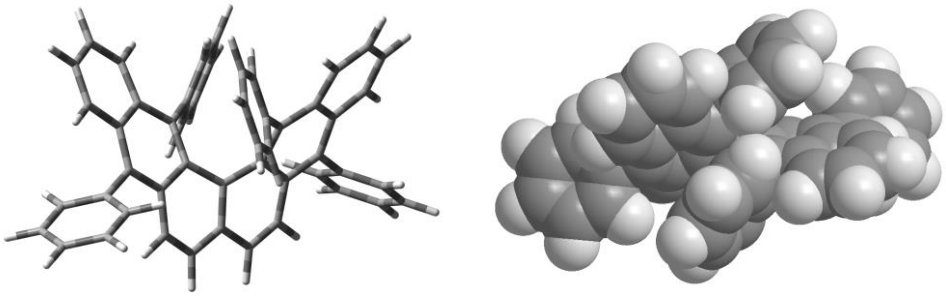
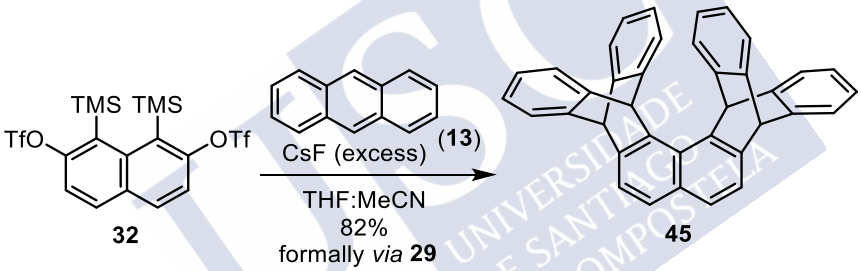


Figure 36. Optimised geometry for **44**.[147]

This compound (**44**) proved to be extremely stable and soluble in many organic solvents, such as hexane or methanol. The computational study of this strained system shown a highly distorted structure, with a dihedral angle of 60° in the internal cove region (Figure 36). Its optoelectronic properties were preliminary studied by UV-vis and fluorescence spectroscopy, showing a HOMO-LUMO gap in the range of organic semiconductors, 2.45 eV. The synthesis of **44** proves the suitability of this approach towards angularly fused polyarene scafolds.



Scheme 40. Synthesis of the iptycene **45**.

We also essayed the (4+2) cycloaddition reactions with other dienes such as anthracene (**13**), which afforded the pentaiptycene **45** in an excellent 82% yield (Scheme 40). This product was also characterised by X-ray diffraction analysis (Figure 37). No products were detected when the reaction was performed with pentacene instead on anthracene.

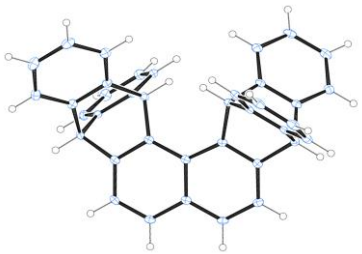
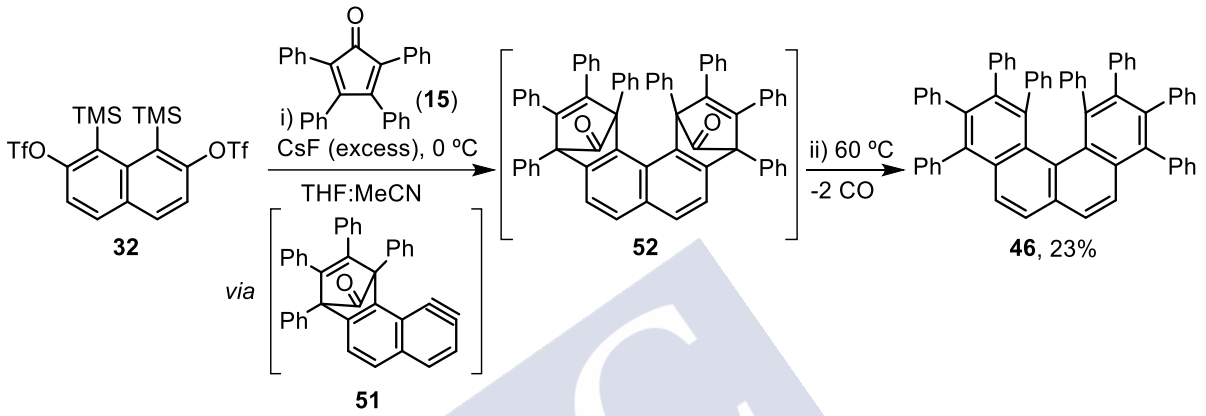


Figure 37. X-ray structure of compound **45**.

[147] DFT-B3LYP/6-31++G(d,p) in gas phase.

On the other hand, cyclopentadienones are great reaction partners in cycloaddition reactions with arynes. Thus, we carried out the reaction of **32** with CsF in presence of 2,3,4,5-tetraphenylcyclopentadienone (**15**), which afforded the expected octaphenylbenzo[*c*]-phenanthrene (**46**) though a double Diels-Alders and cheletropic extrusion of CO, in a 23% yield. This moderate yield is probably due to competing reactions discussed below (see section 3.3.3).



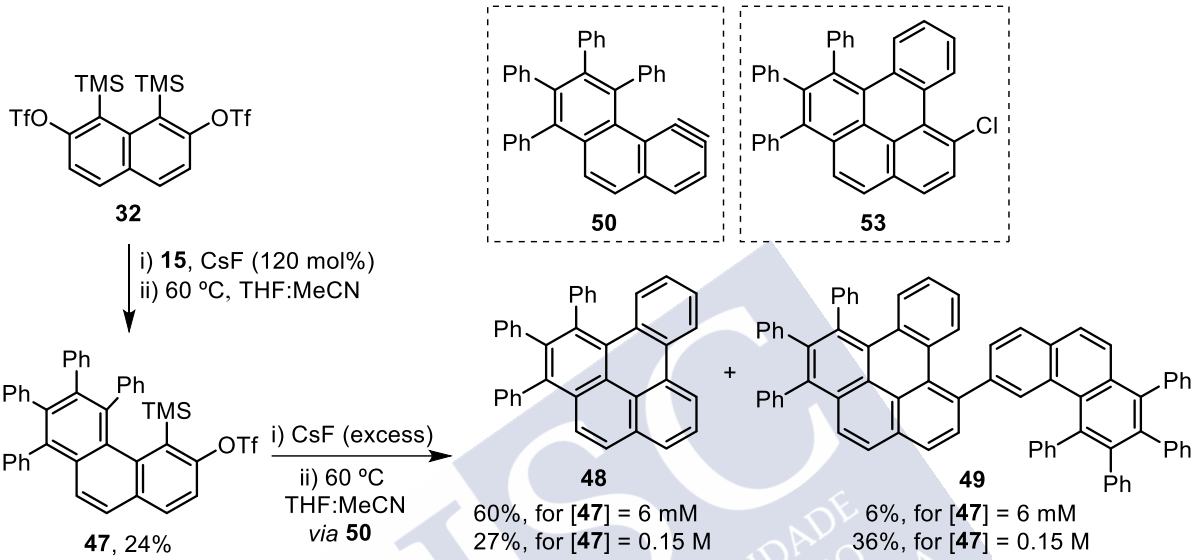
Scheme 41. Synthesis of the benzophenanthrene **46**.

3.3.3 Study of a novel reaction: formal aryne insertion into a C-H bond

Once the formal generation of the 1,7-naphthodiyne synthon (**29**) from **32** was demonstrated, we envisioned the synthesis of new functionalised 3-phenanthryne precursors by selective generation of one single arynic unsaturation from **32** and subsequent (4+2) cycloaddition reaction of the aryne **37** with a suitable partner. Therefore, the reaction of **32** with CsF (120 mol%) in presence of 2,3,4,5-tetraphenylcyclopentadienone (**15**) afforded 4-(trimethylsilyl)-3-phenanthrenyl triflate **47** in a 24% yield (Scheme 42), together with another two side products (in yields below 5%), which were identified by mass spectrometry and NMR spectroscopy as 1,2,3-triphenylbenzo[*e*]pyrene (**48**) and the phenanthryl-substituted derivative **49**. The formation of these products seems to be the result of an unprecedent intramolecular cyclisation through the insertion of the arynic bond of **50** into the C-H bond of the neighbouring phenyl group (Scheme 42).

In order to shed light on the mechanism of this cyclisation, we performed further reactions with **47**. We attempted to obtain the octaphenylbenzo[*c*]phenanthrene (**46**), by reaction between **47** and CsF in presence of the dienone **15**. However, the formation **46** was not detected, but the isolation of compounds **48** and **49** in moderate yields. This evidence suggests that the (4+2) cycloaddition reaction between this hindered aryne **50** and the bulky diene **15** is

prevented. Moreover, it indicates that the formation of **46** (Scheme 41) muss have involved the less hindered aryne **51** and the intermediate **52**. We also studied the behaviour of **47**, under aryne forming conditions, in absence of diene, obtaining **48** (27-60%) and **49** (6-36%) in variable ratios depending on the concentration (Scheme 42). Finally, the isolation of **53**, when the reaction was performed in carbon tetrachloride (CCl_4) instead of in **t**etra**h**ydro**f**uran (THF), suggests a radical mechanism.

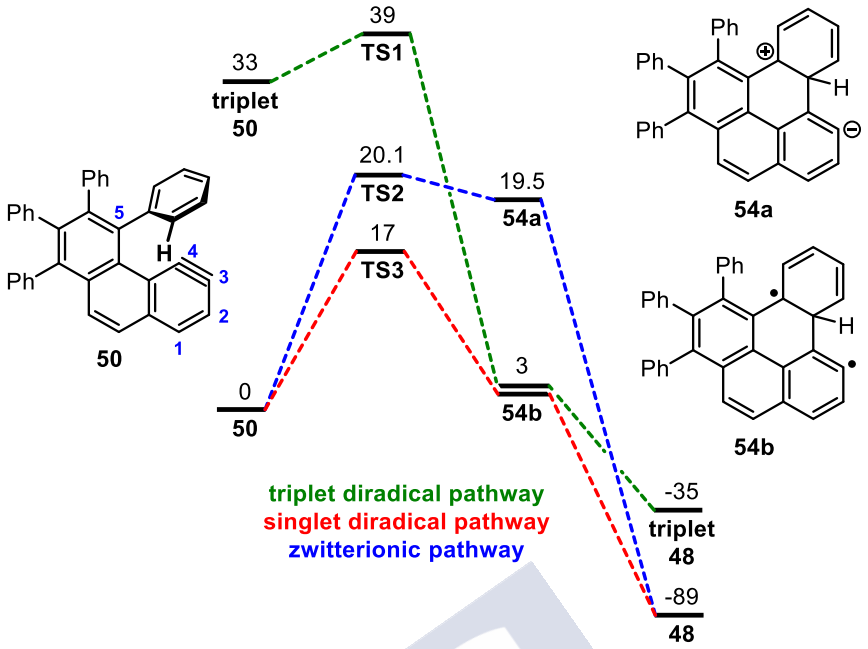


Scheme 42. Study of the reaction of **47** with CsF at different concentrations.

We performed a preliminary computational study by DFT calculations of this novel cyclisation,[148] in collaboration with Prof. A. Cobas.[131] On the one hand, we found that the transition state that leads to the diradical intermediate **54b** (**TS3**), is slightly more stable than the **TS2**, and on the other hand, the singlet diradical **54b** is 16.5 Kcal mol^{-1} more stable than the zwitterion **54a**. Both results indicate a radical cyclisation through singlet diradical **54b**, rather than a polar mechanism.

[148] Geometries were optimised by DFT-B3LYP/6-31G(d), single point calculations by DFT-M062X/6-31G++(d,p) and solvation was computed using CPCM for MeCN.

[131] Theoretical calculations were performed in collaboration with Prof. A. Cobas, Department of Organic Chemistry, University of Santiago de Compostela (USC), Spain.



Scheme 43. Theoretical calculations of the unprecedented cyclisation to the formation of **48** (ΔG values in Kcal mol^{-1}).

The electronic structure of the proposed reaction intermediate was evaluated. In the spin density map of **54b**, both systems can be easily appreciated (Figure 38). One of them, located in the π-cloud of the ring (green), and the other perfectly localised in the sp orbital (blue). The zwitterionic intermediate **54a**, as supported by the calculated electrostatic potential, shown a clearly localised negative charge (red).

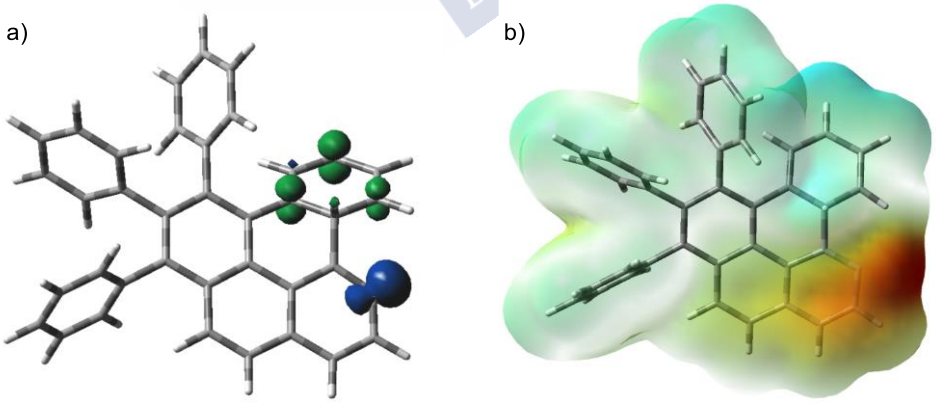
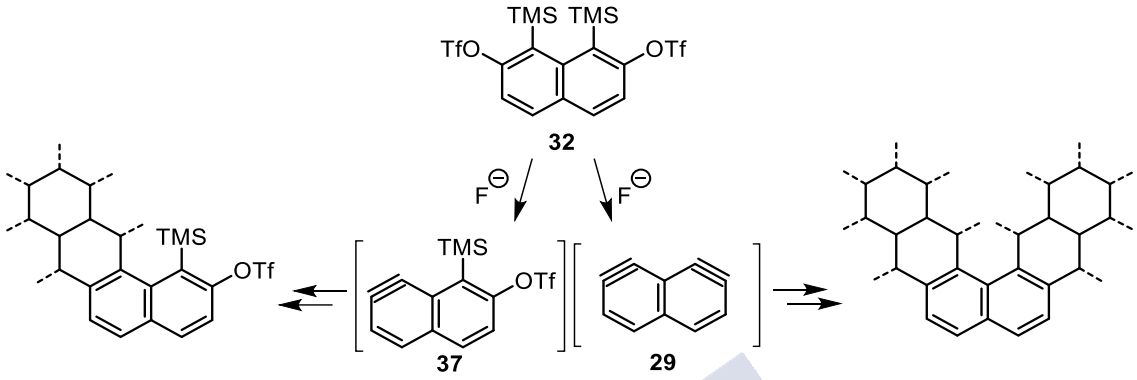


Figure 38. a) Spin density map of **54b**. b) Electron density map of **54a**.

To the best of our knowledge there is no precedent in the literature for an intramolecular arylation reaction as the one described above, involving the intramolecular formal insertion of an aryne into an aryl C–H σ-bond.

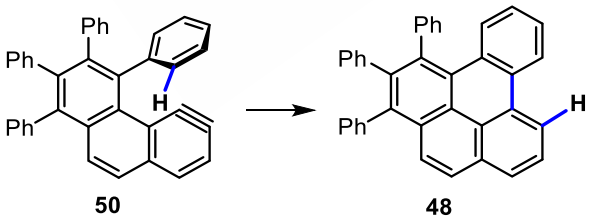
3.4 Conclusions

To summarise, we synthesised 1,8-bis(trimethylsilyl)naphthalene-2,7-diyl bistriflate (**32**), which proved to be an efficient precursor of the novel 1,7-naphthodiyne synthon (**29**).



Scheme 44. Generation and reactivity of one or two arynic unsaturations from 1,8-bis(trimethylsilyl)naphthalene-2,7-diyl bistriflate (**32**).

We have demonstrated its ability to participate in different Diels-Alder reactions, proving its potential as platform towards the synthesis of angular and sterically congested PAHs. Moreover, it was achieved the selective generation and trapping of a single arynic unsaturation from **32**, allowing to obtain the functionalised 3-phenanthryne precursors **38**, **42** and **47**. Furthermore, the generation of one of these arynes, a 5-phenyl substituted 3-phenanthryne (**47**), allowed the serendipitous discovery of a novel intramolecular aryne trapping reaction, involving the formal insertion of the arynes into a C–H σ-bond.



Scheme 45. Mechanistic proposal for insertion of an aryne into a C-H bond.

4 2,6,10-Triphenylenotriyne

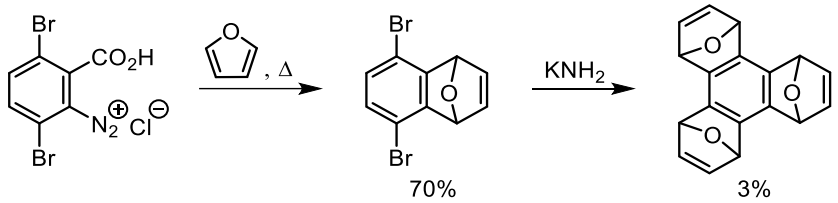
4.1 Background information

As mentioned in previous sections, bisarynes have been significantly studied and exploited in recent years (see sections 1.2 or 3.1). On the contrary, the number of contributions on trisarynes is very scarce, so in this introductory section we will try to cover and debate all the relevant work on this topic. Most of the studies performed refer to 1,3,5-benzotriyne, although approaches to some other trisarynes have been addressed.

4.1.1 1,3,5-Benzotriyne

The first article with a mention to benzotriyne dates from 1966.[85] The authors reported the attempted generation by pyrolysis of acid anhydrides, but their results were inconclusive.

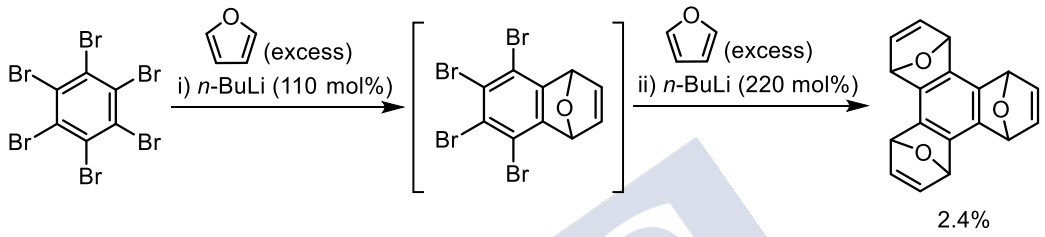
In 1980, Stringer and Wege synthesised for the first time a formal trisadduct of 1,3,5-benzotriyne,[149] albeit the product was obtained in low yield and involving a two steps procedure.



Scheme 46. Synthesis of triepoxytriphenylenes.

[85] E. K. Fields, S. Meyerson, *J. Org. Chem.* **1966**, *31*, 3307–3309.
[149] M. B. Stringer, D. Wege, *Tetrahedron Lett.* **1980**, *21*, 3831–3834.

Almost a decade later, Stoddart and coworkers published the synthesis of the same triepoxytriphenylenes using hexabromobenzene as potential 1,3,5-benzotriyne precursor. The authors reported that the reaction of the hexabromoderivative with three molar equivalents of *n*-butyllithium did not generate the trisaryne equivalent. An alternative two-step procedure first resulted in the isolation of a furan monoadduct, which upon treatment with additional *n*-butyllithium and excess furan , afforded the expected trisadducts in a 2.4% yield (Scheme 47).[150] Few years later (1992), the same group expanded the study about the generation of arynes and polyarynes, but again the lack of efficient precursors resulted in poor yields.[151]



Scheme 47. Improved synthesis of triepoxytriphenylenes.

Despite the low yield, this reaction is interesting, since the minor product (*syn*- adduct) was used to synthesise an impressive molecular cage,[150] and the *anti*- adduct was employed to obtain a novel heptaiptycene (Figure 39).[152] These examples were illustrative of the synthetic potential of trisaryne synthons, and the need of new efficient precursors to be developed.

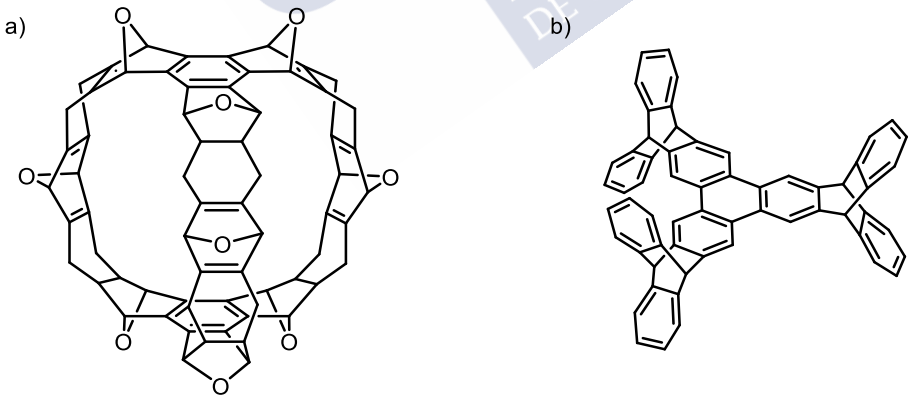


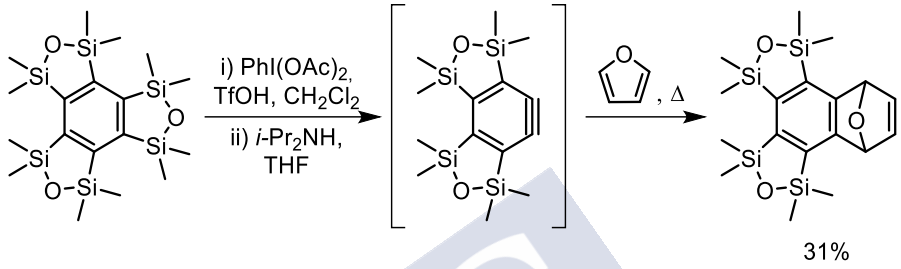
Figure 39. a) Molecular cage synthesised by Stoddart's group. b) Heptaiptycene synthesised by Kohnke's group.

---

[150] B. P. R. Ashton, N. S. Isaacs, F. H. Kohnke, G. S. D. Alcontres, J. F. Stoddart, *Angew. Chem. Int. Ed. Engl.* **1989**, *28*, 1261–1263.
[151] F. Raymo, F. H. Kohnke, F. Cardullo, U. Girreser, J. F. Stoddart, *Tetrahedron* **1992**, *48*, 6827–6838.
[152] F. M. Raymo, M. F. Parisi, F. H. Kohnke, *Tetrahedron Lett.* **1993**, *34*, 5331–5332.

During the late nineties, Adamson and Rees claimed the synthesis of fullerene by using the benzotriyne synthon, but they could not provide solid evidences.[153] The following year, two groups concurrently published the detection of cyclic C_6 carbon clusters, by using **F**ourier **T**ransform **I**nfra**r**ed measurements (FTIR) in an argon matrix.[154]

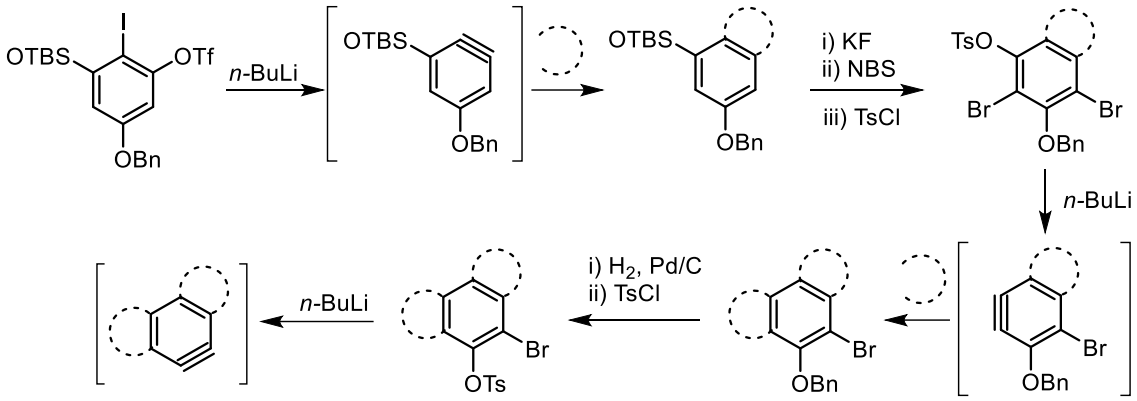
In 2002, Lee and coworkers attempted to obtain an alternative trisaryne precursor from a benzotrisoxadisilole (Scheme 48).[155] Nevertheless, they found that this compound is only able to generate one single aryne.



Scheme 48. Attempted 1,3,5-benzotriyne generation from a benzotrisoxadisilole.

More recently, Suzuki's group published three different strategies for the sequential generation of three arynic unsaturations in a benzene ring,[156] each of them requiring multiple steps. In fact, arene functionalisation and/or functional group interconversions were necessary before the generation of each single aryne. Scheme 49 shows one of these long synthetic protocols.

[153] G. A. Adamson, C. W. Rees, *J. Chem. Soc., Perkin Trans. 1* **1996**, 1535–1543.
[154] a) S. L. Wang, C. M. L. Rittby, W. R. M. Graham, *J. Chem. Phys.* **1997**, *107*, 6032–6037; b) J. D. Persilla-Marquez, J. A. Sheehy, J. D. Mills, P. G. Carrick, C. W. Larson, *Chem. Phys. Lett.* **1997**, *274*, 439–444.
[155] Y. L. Chen, H. K. Zhang, W. Y. Wong, A. W. M. Lee, *Tetrahedron Lett.* **2002**, *43*, 2259–2262.
[156] a) T. Hamura, Y. Ibusuki, H. Uekusa, T. Matsumoto, K. Suzuki, *J. Am. Chem. Soc.* **2006**, *128*, 3534–3535; b) T. Hamura, Y. Ibusuki, H. Uekusa, T. Matsumoto, J. S. Siegel, K. K. Baldridge, K. Suzuki, *J. Am. Chem. Soc.* **2006**, *128*, 10032–10033; c) S. Shinozaki, T. Hamura, Y. Ibusuki, K. Fujii, H. Uekusa, K. Suzuki, *Angew. Chem. Int. Ed.* **2010**, *49*, 3026–3029.



Scheme 49. Generation and trapping of three arynic unsaturations on the benzene core.

4.1.2 Other trisaryne synthons

In 2005, Kunai's group synthesised a compound able to generate three arynic unsaturations in high yield and one single synthetic operation.[157] However, in this molecule each benzyne equivalent is located in an independent aromatic structure, so, despite it was named as a trisaryne, we consider it better described as a molecule with three linked benzynes.

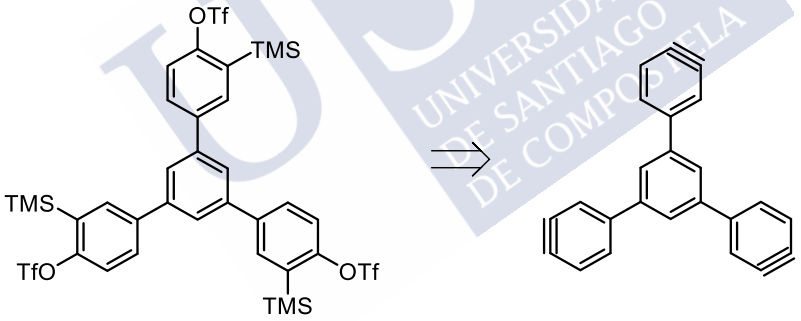
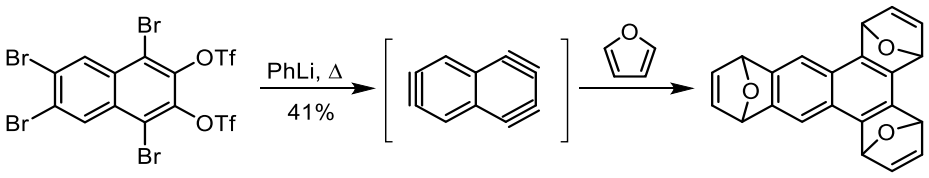


Figure 40. Generation of three benzynes in different (linked) aromatic cores.

Ten years later, Gribble and coworkers synthesised a 1,3,6-naphthotriyne precursor (Scheme 50).[158] They studied its efficiency for generating the corresponding trisaryne synthon by trapping experiments with furan. So, they obtained the expected trisadduct by the triple cycloaddition reaction with furan in a 41% yield. It is important to note that this work was the first and unique example of the one-pot generation of a trisaryne reported to date.

---

[157] J. Ikadai, H. Yoshida, J. Ohshita, A. Kunai, *Chem. Lett.* **2005**, *34*, 56–57.
[158] P. Z. Mannes, E. O. Onyango, G. W. Gribble, *J. Org. Chem.* **2015**, *80*, 11189–11192.



Scheme 50. Generation of 1,3,6-naphthotriyne synthon.

Triphenylene derivatives are important polycyclic aromatic systems in the context of materials chemistry. The triphenylene core is the main structural motif of a broad family of discotic liquid crystals[159] and a useful building block for the construction of porous networks.[160] One of the best synthetic approaches towards triphenylene derivatives is the (2+2+2) palladium-catalysed cyclotrimerisation of arynes.[63] In this context, the development of triphenylene-based polyaryne synthons becomes an interesting goal not yet addressed, at least for chemistry in solution. However, the quick evolution of *on-surface synthesis* in the last years, has provided direct access to novel synthons and new kinds of reactivity and, thus, in 2019, Lin's group synthesised a porous carbon network by heating 2,3,6,7,10,11-hexabromo triphenylene on a silver surface.[161] They postulate the generation of silver complexes of radical 2,6,10-triphenylenotriyne on surface. However, these methods are yet very limited and do not compete with the versatility of organic synthesis in solution.

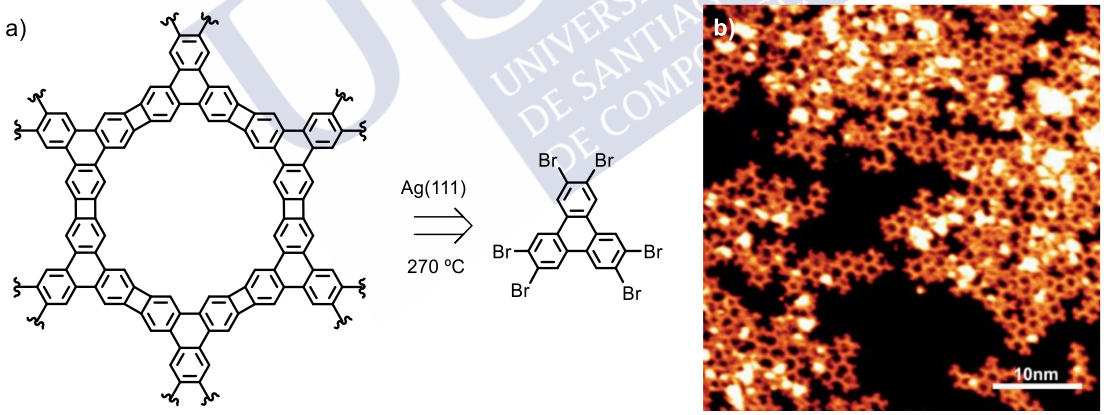


Figure 41. a) O*n surface synthesis* of porous networks. b) STM image of obtained porous networks.

[159] K. Goossens, K. Lava, C. W. Bielawski, K. Binnemans, *Chem. Rev.* **2016**, *116*, 4643–4807.
[160] a) Z. Wang, S. Zhang, Y. Chen, Z. Zhang, S. Ma, *Chem. Soc. Rev.* **2020**, *49*, 708–735; b) S. Das, P. Heasman, T. Ben, S. Qiu, *Chem. Rev.* **2017**, *117*, 1515–1563.
[63] D. Peña, S. Escudero, D. Pérez, E. Guitián, L. Castedo, *Angew. Chem. Int. Ed.* **1998**, *37*, 2659–2661.
[161] R. Zhang, B. Xia, H. Xu, N. Lin, *Angew. Chem. Int. Ed.* **2019**, *58*, 16485–16489.

4.2 Objectives

The purpose of the work described in this chapter is to achieve a suitable trisaryne precursor. Particularly, we became interested in the 2,6,10-triphenylenotriyne synthon, due to its great potential as novel platform to obtain three-fold symmetric nanographenes and other star-shaped PAHs with an extra point of structural complexity.

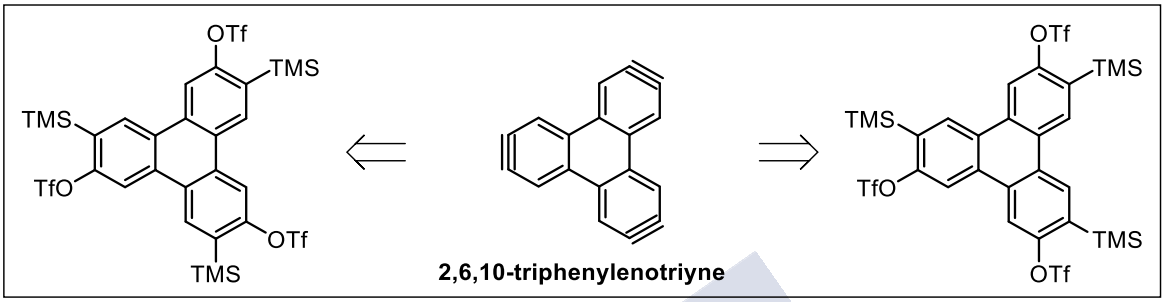


Figure 42. Potential 2,6,10-triphenylenotriyne precursors.

To address this goal, we again relied on the suitability of Kobayashi-type precursors and thus, we selected this kind of tristriflates as the ideal candidates to render the target 2,6,10-triphenylenotriyne synthon.

4.3 Results and discussion

Successful transformations involving arynes are determined by at least two factors: the effective generation of the aryne and the efficiency of the reaction with the arynophile. In reactions involving bisarynes, each process should occur twice, and thus the use of adequate precursors, capable of generating the aryne species in high yields, becomes crucial. We can extend this consideration to the development of an efficient precursor of 2,6,10-triphenylenotriyne and thus, we trusted again in the robust Kobayashi's method for aryne generation and focused our attention on the synthesis of the appropriate tristriflates

4.3.1 Synthesis of precursors of 2,6,10-triphenylenotriyne

According to the arguments discussed above, we selected tris(trimethylsilyl)triphenylenotriyl tristriflates **55** as potentially suitable precursors of 2,6,10-triphenylenotriyne (**56**).

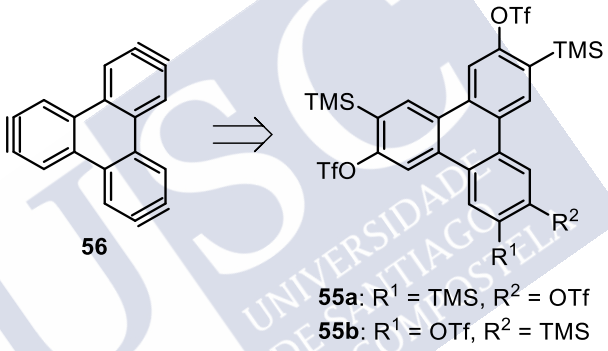
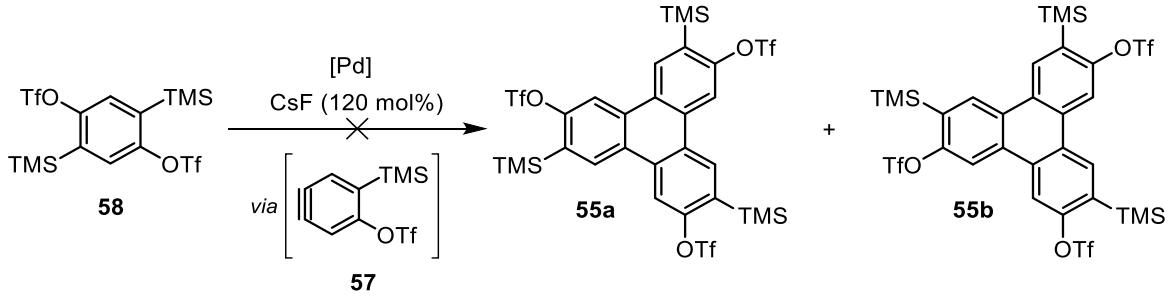


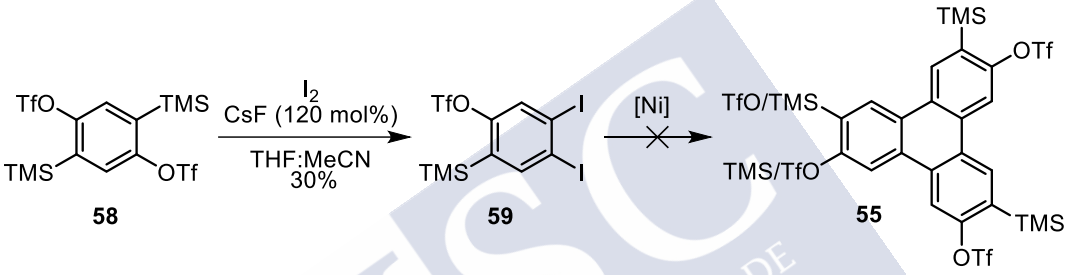
Figure 43. Retrosynthetic analysis of 2,6,10-triphenylenotriyne synthon (**56**).

These triphenylene derivatives could, in principle, be accessed by palladium-catalysed cyclotrimerisation of an adequately functionalised benzyne. Thus, as a first attempt, we essayed the selective generation of **57**, by treatment of **58** with 120 mol% of CsF, in presence of a palladium catalyst, under the general reaction conditions developed in our research group for the cyclotrimerisation of arynes. Other reactions employing **57**, such as (4+2) or (2+2), have been successfully used, however, its participation in metal-catalysed (2+2+2) cycloadditions have not been yet described, probably because this reaction would require coordination of three moieties of this elusive species within the metal coordination sphere. Unsurprisingly, this first attempt resulted unsuccessful, and the desired products **55a** and **55b** were not detected.



Scheme 51. First approach towards the synthesis of **55a** and **55b**.

We also explored another approach through a nickel-promoted coupling from **59** (Scheme 52).[48,139] Thus, we tried similar reaction conditions to those developed by Yamamoto, although, the mixture of the expected products **55** was not observed either.

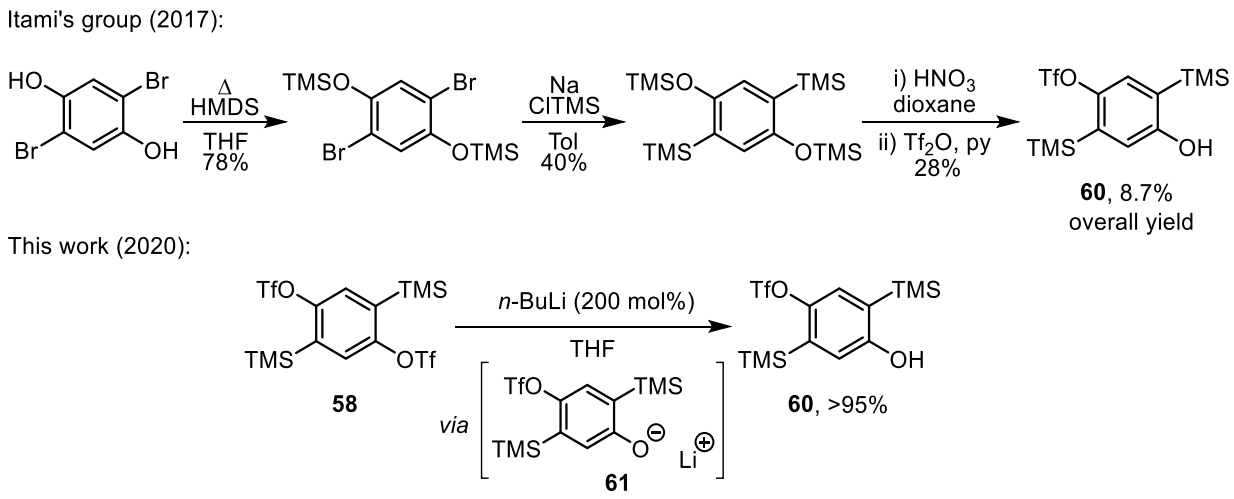


Scheme 52. Attempt of cyclotrimerisation reaction from **59**.

Then, we considered a new approach based on the use of *masked* aryne precursors, such as phenol **60**, which had been synthesised by Itami and coworkers[162,163] through a four-step process in an 8.6% overall yield. Remarkably, we developed an alternative synthesis obtaining **60** in only one step and quantitative yield, by treatment of the commercially available bistriflate **58** with *n*-BuLi (200 mol%, -78 ºC) (Scheme 53). Apparently, the intermediate alkoxide **61** does not react with the excess of organolithium reagent.

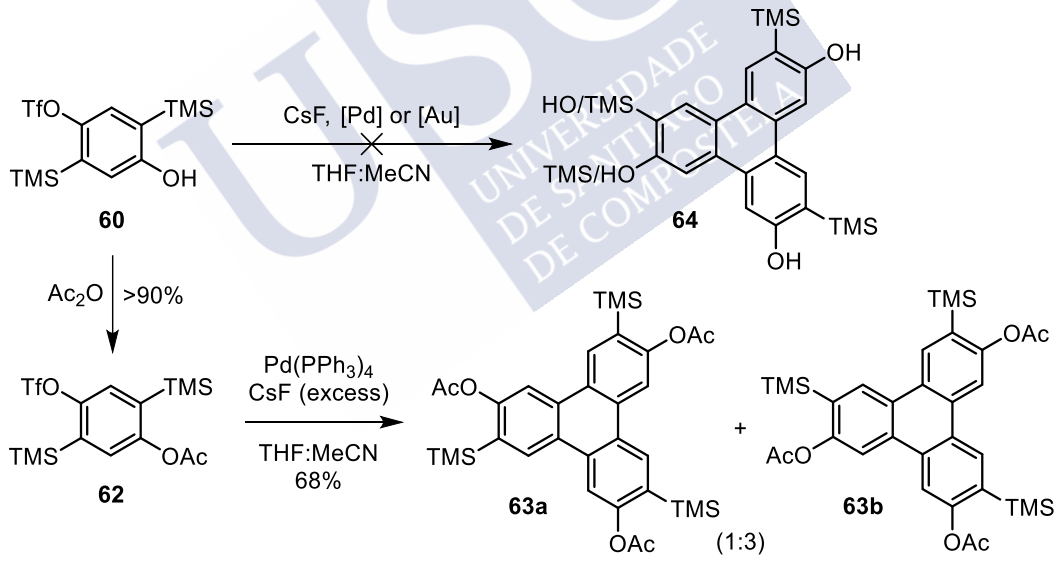
---

[48] N. Pavliček, B. Schuler, S. Collazos, N. Moll, D. Pérez, E. Guitián, G. Meyer, D. Peña, L. Gross, *Nat. Chem.* **2015**, *7*, 623–628.
[139] D. Rodríguez-Lojo, A. Cobas, D. Peña, D. Pérez, E. Guitián, *Org. Lett.* **2012**, *14*, 1363–1365.
[162] S. Suzuki, K. Itami, J. Yamaguchi, *Angew. Chem. Int. Ed.* **2017**, *56*, 15010–15013.
[163] H. Bock, S. Nick, C. Näther, K. Ruppert, *Z. Naturforsch.* **1995**, *50b*, 595–604.



Scheme 53. Syntheses of **60**.

Having phenol **60** in hands, we attempted its participation in (2+2+2) metal-catalysed cyclotrimerisation reactions, employing Pd(0) and Au(I)[164] catalysts, although our efforts were in vain. At this moment, we prepared another second masked aryne precursor, thus, reaction of **60** with acetic anhydride afforded the acetate **62** in 90% yield.[165]



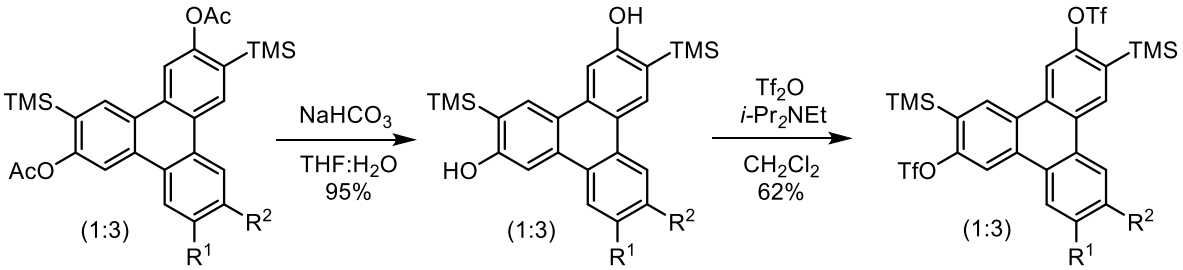
Scheme 54. Attempts of cyclotrimerisation from **60** and **62**.

Then, we prepared acetate **62** as a second masked aryne precursor. Thus, treatment of **60** with acetic anhydride at 110 ºC afforded acetate **62** in a satisfactory 90% yield. Reaction of **62** under aryne forming conditions and in the presence of catalytic amounts of $Pd(PPh_3)_4$ afforded the trimers **63** in a 68% after a short optimisation. They were obtained as the 1:3

---

[164] L. Chen, C. Zhang, C. Wen, K. Zhang, W. Liu, Q. Chen, *Catal. Commun.* **2015**, *65*, 81–84.
[165] S. Collazos PhD Thesis, **2016**, University of Santiago de Compostela, Spain.

mixture, **63a**:**63b**, being the C_3-symmetric isomer (**63a**) the minor product. Even though compounds **63a** and **63b** could be separated and independently characterised, showing easily recognisable ^{1}H NMR spectra, we decided to use the mixture of products to continue the synthesis.



63a: R^1 = TMS, R^2 = OAc
63b: R^1 = OAc, R^2 = TMS

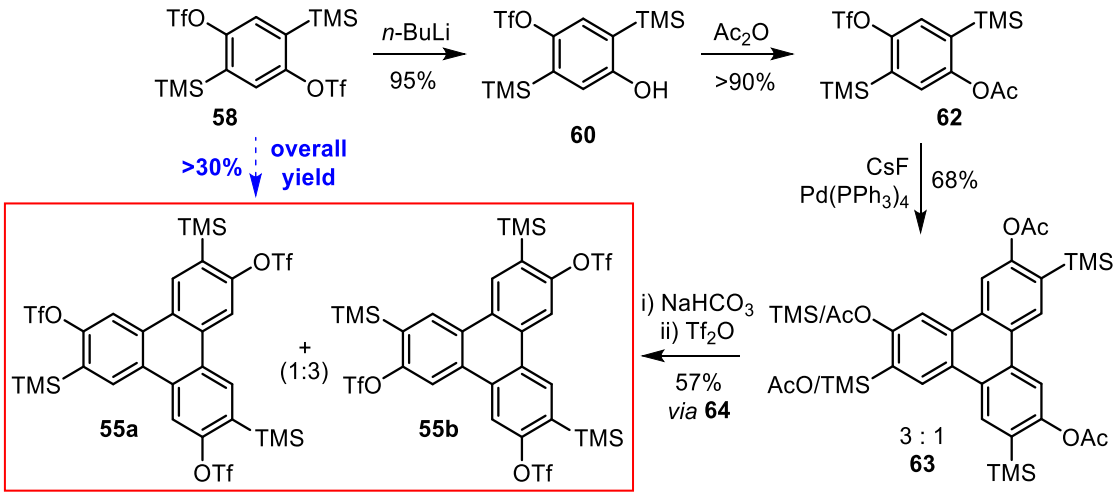
64a: R^1 = TMS, R^2 = OH
64b: R^1 = OH, R^2 = TMS

55a: R^1 = TMS, R^2 = OTf
55b: R^1 = OTf, R^2 = TMS

Scheme 55. Synthesis of potential trisaryne precursors **55**.

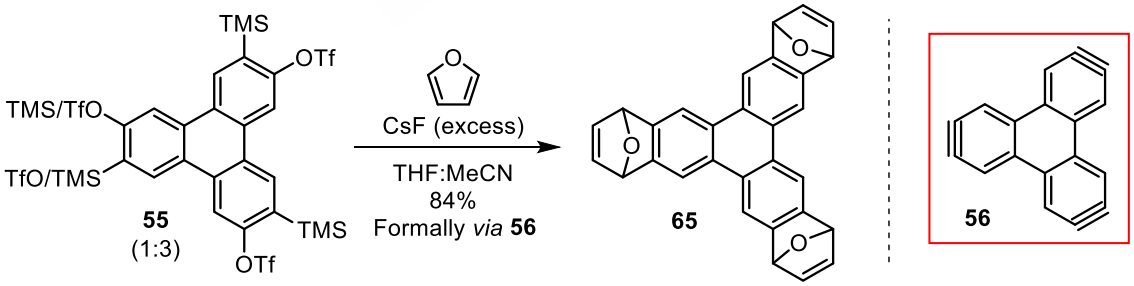
The next step consisted in the development of a deprotection/esterification protocol to convert trisacetates **63** into tristriflates **55**. Successfully the reaction of **63** with an aqueous solution of sodium bicarbonate afforded a mixture of isomers **64** which could be isolated in almost quantitative yield (Scheme 55). These triphenols were subsequently esterified with triflic anhydride in a 62% yield. The targeted potential trisaryne precursors **55a** and **55b** were thus obtained as a 1:3 mixture of isomers (Scheme 55). Both compounds presented very characteristic spectra, for instance **55a** showed ^{1}H NMR with only three singlets, two of them corresponding to the aromatic protons, around 8.5 ppm, and another corresponding to the protons in the TMS group, at 0.5 ppm. In contrast, the ^{1}H NMR of **55b** had nine signals due to the lack of symmetry. These compounds are very stable, allowing their storage for months.

To sum up, considering the commercially available bistriflate **58** as our starting material, we have been able to synthesise the targeted tristriflates **55**, in only five steps and a 34% yield (Scheme 56).



Scheme 56. Synthesis of potential trisaryne precursors **55** from **58**.

Having tristriflates **55**, we aimed to study their ability to generate their corresponding trisaryne synthon. Thereby, we performed the reaction of the mixture of isomers **55** with CsF in presence of furan, using a 1:1 mixture of THF:MeCN as solvent to achieve the solubility of reagents and products, and isolated compounds **65** as a mixture of stereoisomers in an excellent 84% yield. The ^{1}H NMR spectrum showed characteristic signal at 5.92 ppm corresponding to the bridge-head protons and mass spectra (m/z = 426). This result demonstrates the (probably sequential) generation of the three aryne unsaturations on the triphenylene nucleus and validates tristriflates **55** as synthetic equivalent of 2,6,10-triphenylenotriyne (**56**). Remarkably, failed attempts to obtain these adducts **65** have been published by Hamura and coworkers to synthesise star-shaped PAHs.[166] Indeed, both the novel trisaryne synthon and diastereoisomers **65** are interesting building blocks for the synthesis of three-fold symmetric nanographenes and star-shaped PAHs.



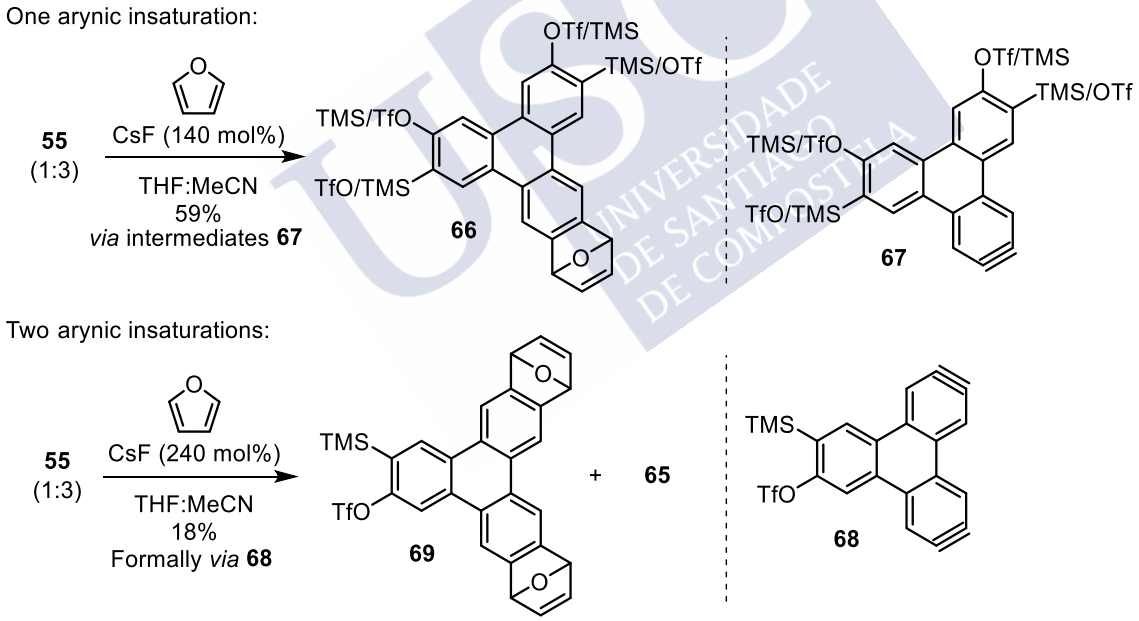
Scheme 57. Trapping experiment of 2,6,10-triphenylenotriyne synthon (**56**) with furan.

Next, we studied the selective generation and trapping of one single (or two) arynic unsaturations independently from **55**, which would broaden the synthetic utility of this

[166] H. Tozawa, T. Kakuda, K. Adachi, T. Hamura *Org. Lett.* **2017**, *19*, 4118–4121.

tristriflates towards triphenelene-based PAHs lacking C_3 Symmetry. By analogy with our work with some bisarynes, we attempted to manage the selectivity of the reaction by controlling accurately the amount of CsF added. Hence, the reaction was performed by adding sequentially THF, furan and MeCN, to a Schlenk tube containing 140 mol% of CsF and **55**, to afford the mixture of isomers **66**, *via* **67**, in a noticeable 59% yield (Scheme 58). The ^{1}H NMR of this mixture of isomers revealed the presence of characteristic signals, such as the corresponding to the vinylic and bridge-head protons, at 7.1 and 6.0 ppm respectively, which resulted diagnostic to confirm the identity of **66**, together with the data obtained by mass spectrometry. Then, we essayed the reaction of **55** with 240 mol% of CsF in presence of furan and obtained the mixture of bisadducts **69**, although in a low 18% yield, being the major product of this reaction the trisadducts **65**, isolated in 50% yield (Scheme 58).

From the best of our knowledge, the results described above constitute the firts example of the generation and trapping of a monoaryne, a bisaryne and a trisaryne from the same precursor compound.



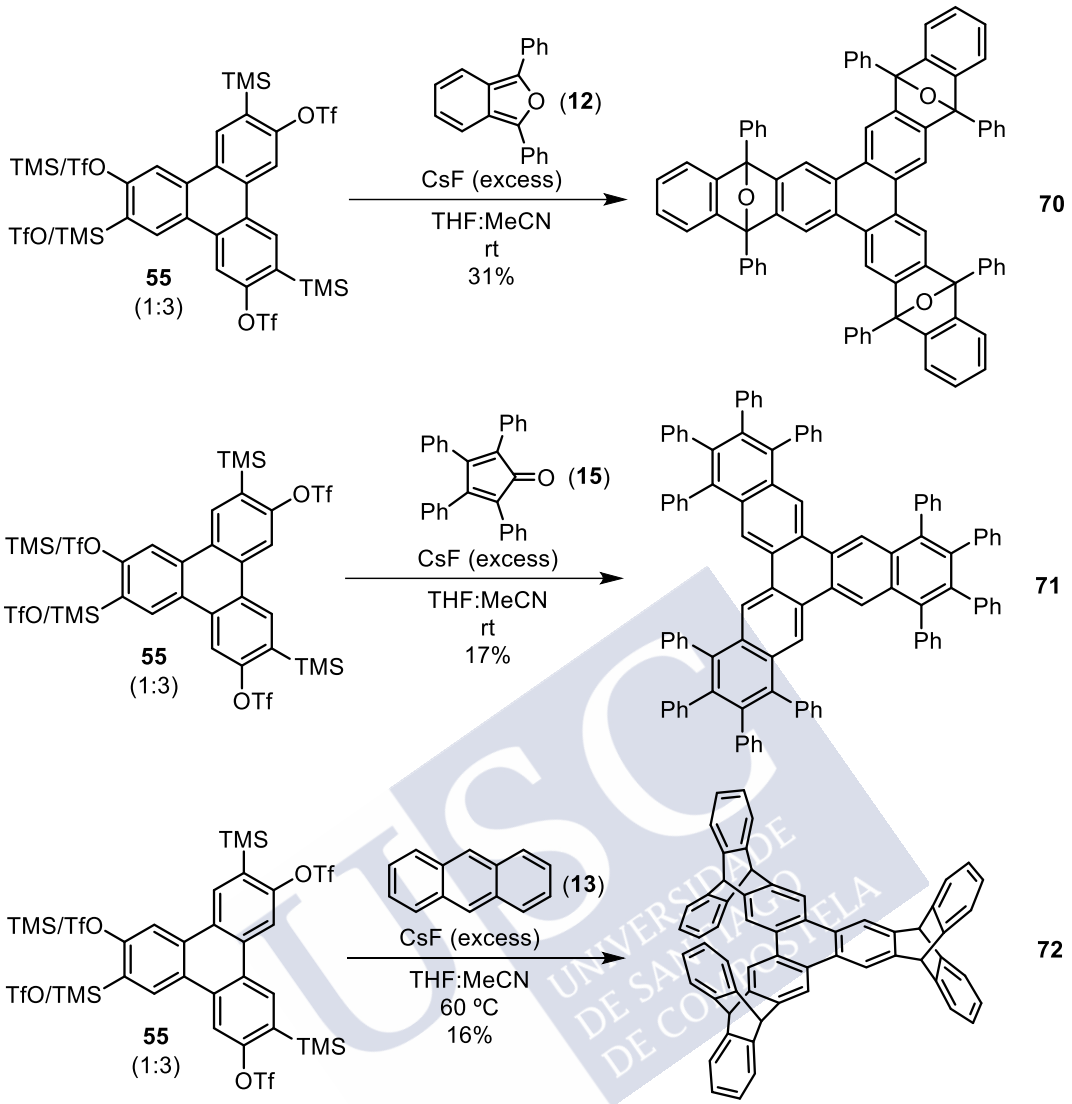
Scheme 58. Generation of one or two arynic unsaturation from **55**.

4.3.2 Study of reactivity with other dienes

Once demonstrated the high efficiency of **55** for generating the 2,6,10-triphenylenotriyne synthon (**56**), we decided to study its reactivity with more complex dienes. As in the previous chapter, we used 1,3-diphenylisobenzofuran (**12**) and tetraphenylcyclopentadienone (**15**), to obtain starphenes, and anthracene (**13**), to synthesise an iptycene derivative. In the first case,

we obtained the expected product **70** as a mixture of stereoisomers in a 31% yield, using **12** as reaction partner. Despite that compounds **70** shown a distinctive signal at 8.5 ppm in the ^{1}H NMR spectrum, corresponding to the protons in the bay regions of the triphenylene core, we could not identify the ratio isomers. The second star-shaped arene, **71**, was obtained by the reaction of **55** with CsF in presence of **15** in a 17% yield, as the result of a triple (4+2) cycloaddition/cheletropic CO extrusion processes (Scheme 59). The spectroscopic data obtained for **71** were coincident with those previously reported by our research group for the same compound. Finally, the synthesis of the heptaiptycene **72** was addressed by reaction of tristiflates **55** with anthracene (**13**) under aryne forming conditions. When the reaction was performed at room temperature, compound 72 was obtained in a low 7% yield. In this experiment, a small amount of undissolved anthracene was observed, so when we carried out the same reaction, but heating at 60 °C, the yield increased up to 16% of isolated heptaiptycene **72** (Scheme 59). The ^{1}H NMR data of this product were identical to those previously published in the literature, containing a characteristic bridge-head proton signal at 5.6 ppm.

USC UNIVERSIDADE DE SANTIAGO DE COMPOSTELA

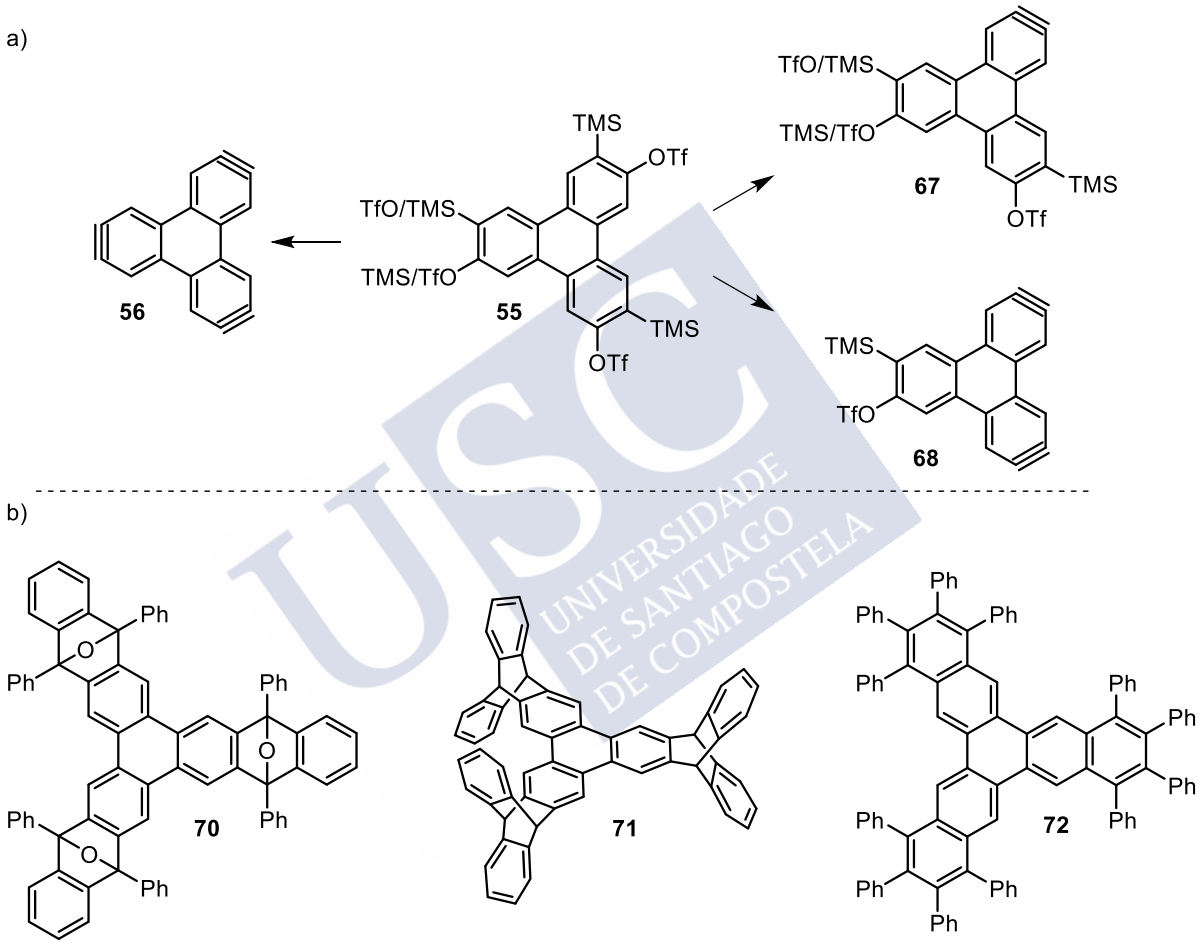


Scheme 59. Reaction of **55** with CsF in presence of different dienes.

It is important to note that these apparently poor results correspond with moderate yield in each cycloaddition, between a 54 and a 67%.

4.4 Conclusions

In summary, we have synthesised the tristriflate precursors **55a** and **55b**, by a novel straightforward method, and demonstrated their high efficiency to generate the 2,6,10-triphenylenotriyne synthon (**56**). Additionally, the selective generation of one, two (less effectively) or three arynic unsaturations from **55** proved the synthetic potential of this species to obtain three-fold symmetric (or not), star-shaped PAHs.



Scheme 60. a) Generation of one, two or three arynic unsaturations and b) compounds synthesised from **55**.

2,6,10-Triphenylenotriyne, **56**, demonstrated a great ability of participating in triple Diels-Alder reactions (e.g. the synthesis of compounds **70**, **71** and **72**). The work included in this chapter, represent the second example of a trisaryne synthon in organic synthesis.

USC
UNIVERSIDADE
DE SANTIAGO
DE COMPOSTELA

5 Aryne-based synthesis of heteroacenes

The work described in this Chapter was performed in collaboration with Ms A. Villamayor.

5.1 Background information

Acenes are a family of PAHs consisting of linearly fused benzene rings, with extremely interesting electronic properties. Pentacene is the reference hole transporting material (*p*-type semiconductor) in OFETs,[167] although other acenes, such as, rubrene (5,6,11,12-tetraphenyltetracene)[168] as well as doped derivatives have been also widely used.[169] However, the variety of *n*-type semiconductor materials for *n*-channel OFETs, is more limited.[170]

Due to their linear fusion of benzenoid rings, unsubstituted acenes can have only one aromatic sextet in their structure, a feature than, according to Clar's model accounts for their low stability, which dramatically decreases with increased number of fused rings. In fact, acenes are rather reactive, affording quinones when exposed to air due to their high HOMO, although in absence of oxygen, they can also evolve towards the corresponding *butterfly dimmer*.[171] The most popular strategies used to avoid their degradation and to obtain stable acenes with tunable properties are discussed below.[104]

[167] H. Klauk, *Chem. Soc. Rev.* **2010**, *39*, 2643–2666.
[168] J. Takeya, M. Yamagishi, Y. Tominari, R. Hirahara, Y. Nakazawa, T. Nishikawa, T. Kawase, T. Shimoda, S. Ogawa, *Appl. Phys. Lett.* **2007**, *90*, 2005–2008.
[169] U. H. F. Bunz, *Acc. Chem. Res.* **2015**, *48*, 1676–1686.
[170] a) L.-L. Chua, J. Zaumseil, J.-F. Chang, E. C. Ou, *Nature* **2005**, *434*, 194–199; b) J. T. E. Quinn, J. Zhu, X. Li, J. Wang, Y. Li, *J. Mater. Chem. C* **2017**, *5*, 8654–8681.
[171] J. E. Anthony, A. G. Jones, *Silylethyne-substituted acenes and heteroacenes*, 105–106, in Organic Electronics II, H. Klauk, Wiley-VCH, **2012**.
[104] M. Müller, L. Ahrens, V. Brosius, J. Freudenberg, U. H. F. Bunz, *J. Mater. Chem. C* **2019**, *7*, 14011–14034.

5.1.1 Substituted acenes

The peripheral substitution of the acene core with bulky groups produces distortion of planarity of the aromatic polycyclic system (*twisted acenes*). This distortion provides increased solubility and processability, and more importantly, the substitution blocks particular positions of the PAHs against photooxidation. Figure 44 shows the examples of a pentacene[172] and a nonacene,[173] which are rather kinetically stable.

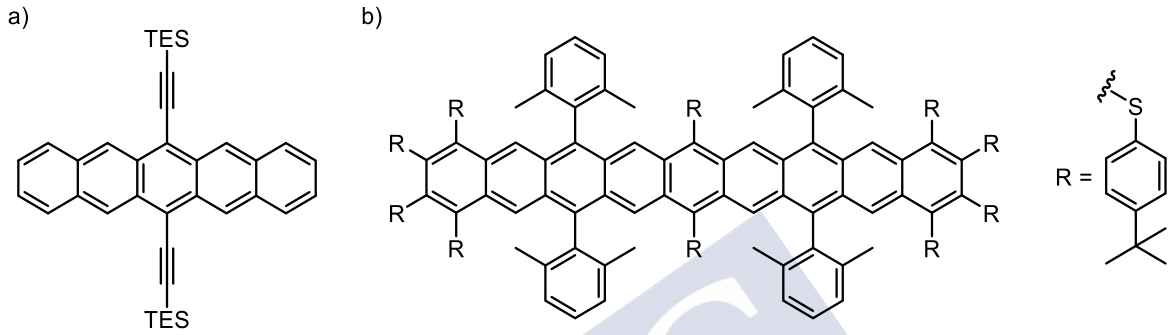


Figure 44. Examples of substituted a) pentacene and b) nonacene.

5.1.2 π-Extended acenes

Another possibility to increase the stability of these compounds, is extending the π-structure. In this way, the number of Clar sextets on their structure is increased. Several examples of large acenes containing pyrene or terminal phenanthrene motives have been published. The next figure shows a decacene containing seven aromatic sextets, instead of exclusively one like their parent analogue.[174]

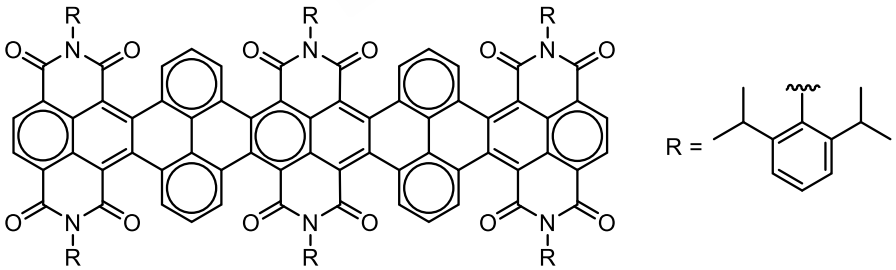


Figure 45. Example of stabilised decacene.

---

[172] J. E. Anthony, D. L. Eaton, S. R. Parkin, *Org. Lett.* **2002**, *4*, 15–18.
[173] I. Kaur, M. Jazdzyk, N. N. Stein, P. Prusevich, G. P. Miller, *J. Am. Chem. Soc.* **2010**, *132*, 1261–1263.
[174] W. Fan, T. Winands, N. L. Doltsinis, Y. Li, Z. Wang, *Angew. Chem. Int. Ed.* **2017**, *56*, 15373–15377.

5.1.3 Heteroatom-containing acenes

Alternatively, the optoelectronic properties of acenes can be modified by the substitution of at least one carbon of their structure by heteroatoms. This approach is generally called *doping* by analogy with the atomic doping strategies in inorganic semiconductors.[175]

N-Doped acenes (or azaacenes) are surely the most studied of this family. They usually have lower HOMO and LUMO energy levels than their isoelectronic acene analogues due to the presence of electronegative nitrogen atoms (Figure 46).[31,176] The synthesis and applications of heteroacenes and heteroarenes in OFETs, OLEDs and bulk heterojunction photovoltaic devices has been recently reviewed.[177] *O*-doped acenes[178] and mixed nitrogen and oxygen-containing derivatives have been less explored,[179] although examples have been provided of promising candidates to design novel semiconductor materials (Figure 46).

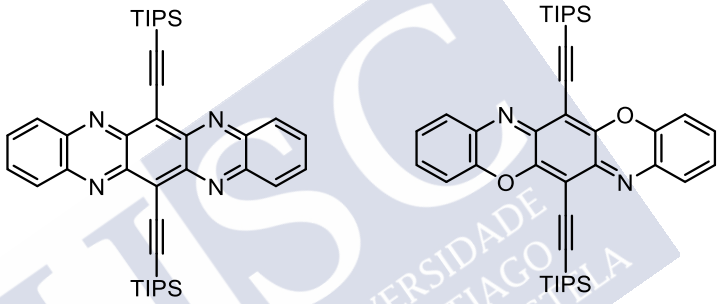


Figure 46. Examples of doped acenes.

The structural diversity of this family can be further expanded introducing different ring sizes. In fact, the presence of nitrogenated or sulphured five member rings in heteroacenes is

[175] X.-Ye Wang, X. Yao, A. Narita, K. Müllen, *Acc. Chem. Res.* **2019**, *52*, 2491–2505.
[31] A. N. Lakshminarayana, C. Chi, *N-Containing Polycyclic Heteroarenes*, 225–226, in *Polycyclic Arenes and Heteroarenes, Q. Miao,* Wiley-VCH, **2016**.
[176] a) Z. Liang, Q. Tang, J. Xu, Q. Miao, *Adv. Mat.* **2011**, *23*, 1535–1539; b)
[177] U. H. F. Bunz, J. Freudenberg, *Acc. Chem. Res.* **2019**, *52*, 1575–1587.
[178] a) Y. Wang, S. Qiu, S. Xie, L. Zhou, Y. Hong, J. Chang, J. Wu, Z. Zeng, *J. Am. Chem. Soc.* **2019**, *141*, 2169–2176; b) S. Dong, T. Y. Gopalakrishna, Y. Han, H. Phan, T. Tao, Y. Ni, G. Liu, C. Chi, *J. Am. Chem. Soc.* **2019**, *141*, 62–66.
[179] a) Y. Nicolas, F. Castet, M. Devynck, P. Tardy, L. Hirsch, C. Labrugère, H. Allouchi, T. Toupance, *Org. Electron.* **2012**, *13*, 1392–1400; b) G. Gruntz, H. Lee, L. Hirsch, F. Castet, T. Toupance, A. L. Briseno, Y. Nicolas, *Adv. Electron. Mater.* **2015**, *1*, 1500072.

common. An extra point of complexity is introduced by mixing different heteroatoms in this subtype of acene derivatives (Figure 47). [180,181]

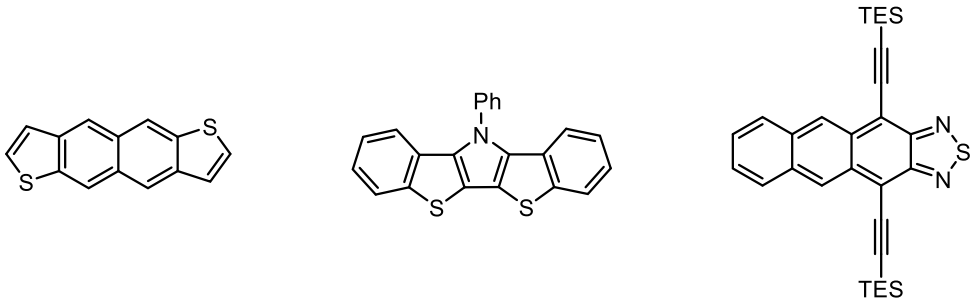


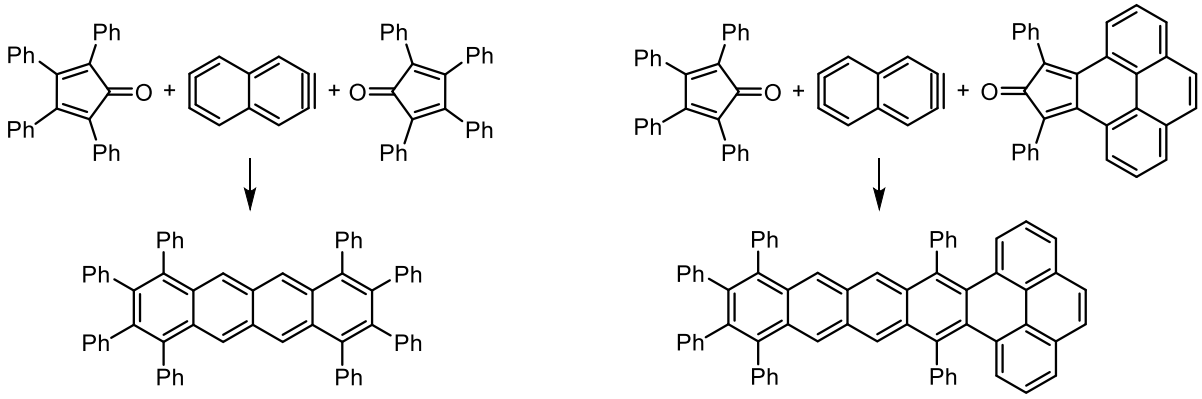
Figure 47. Examples of heteroacenes containing five member rings.

5.1.4 Aryne-mediated synthesis of acenes

Cycloaddition reactions of arynes with appropriate dienes have been extensively applied to the synthesis of a variety of acene derivatives.[96a] Of particular interest, several examples of acenes have been synthesised using bisarynes as privileged synthetic platforms. Thus, taking advantage of their higher stability, substituted and π-extended acenes have been synthesised by reaction of bisarynes with cyclopentadienones.[182,93] Going one step further, the selective generation of each of the two arynic unsaturations from a bisaryne precursor allowed our group to synthesise asymmetric acene derivatives.[183]

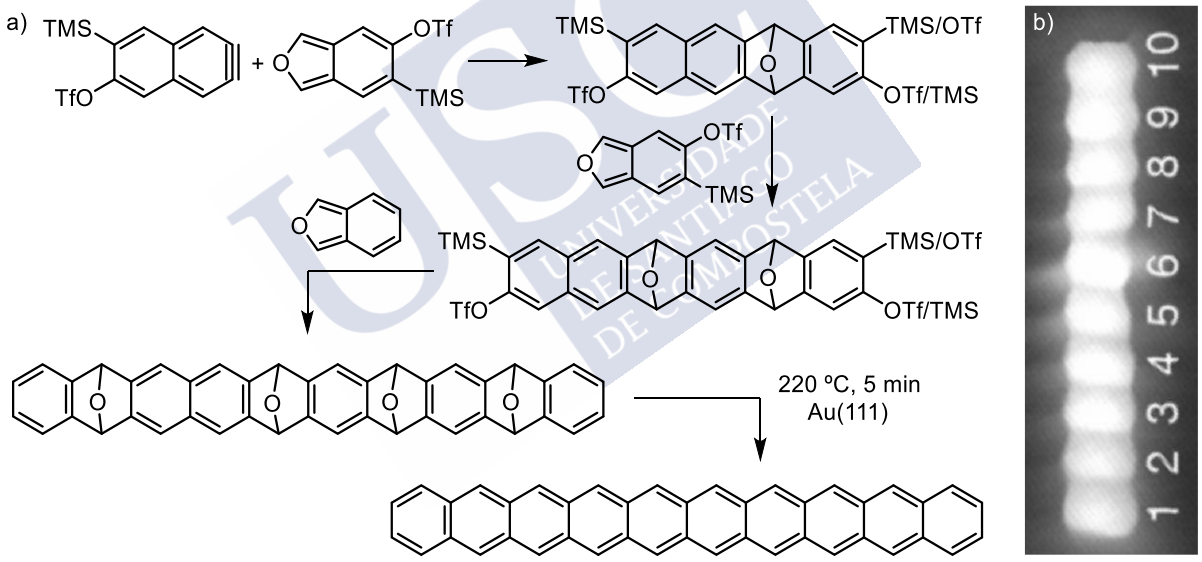
---

[180] W. Mu, S. Sun, J. Zhang, M. Jiao, W. Wang, Y. Liu, X. Sun, L. Jiang, B. Chen, T. Qi, *Org. Electron.* **2018**, *61*, 78–86.
[181] S. Liu, X. Shi, Y. Hu, X. Zhang, W. Sun, Y. Qi, N. Fu, B. Zhao, W. Huang, *Tetrahedron Lett.* **2016**, *57*, 4452–4455.
[96a] D. Pérez, D. Peña, E. Guitian, *Eur. J. Org. Chem.* **2013**, *27*, 5981–6013.
[182] I. I. Schuster, L. Craciun, D. M. Ho, R. A. Pascal Jr., *Tetrahedron* **2002**, *58*, 8875–8882.
[93] H. M. Duong, M. Bendikov, D. Steiger, Q. Zhang, G. Sonmez, J. Yamada, F. Wudl, *Org. Lett.* **2003**, *5*, 4433–4436.
[183] a) D. Rodríguez-Lojo, D. Pérez, D. Peña, E. Guitián, *Chem. Commun.* **2015**, *51*, 5418–5420; b) D. Rodriguez-Lojo PhD thesis, **2014**, University of Santiago de Compostela, Spain.



Scheme 61. Synthesis of symmetric and asymmetric acene derivatives.

On the other hand, unsubstituted long-chain acenes have been obtained by properly designed strategies based on Diels-Alder reactions of aryne and bisaryne building blocks with furanoids, and subsequent deoxygenation of the obtained adducts. Due to its instability, the last steps of their synthesis were performed on-surface.[184]



Scheme 62. a) Synthesis of decacene. b) Constant-height STM image of decacene using a CO-functionalised tip.

In contrast to this proved utility of arynes for the construction of acenes and π-extended derivatives, the application of these reactive species to the synthesis of heteroatom-substituted derivatives (heteroacenes) has been barely explored.[185]

---

[184] J. Krüger, F. García, F. Eisenhut, D. Skidin, J. M. Alonso, E. Guitián, D. Pérez, G. Cuniberti, F. Moresco, D. Peña, *Angew. Chem. Int. Ed.* **2017**, *56*,11945–11948.

[185] a) J. Li, P. Li, J. Wu, J. Gao, W.-W. Xiong, G. Zhang, Y. Zhao, Q. Zhang, *J. Org. Chem.* **2014**, *79*, 4438–4445; b) S. Matsuoka, S. Jung, K. Miyakawa, Y. Chuda, R. Sugimoto, T. Hamura, *Chem. Eur. J.* **2018**, *24*, 18886–18889.

5.2 Objectives

In this context, the objective of this part of the thesis is to expand the application of the synthetic methodologies developed in our laboratory based on bisarynes, to the synthesis of a novel family of heteroacenes. In particular, we became interested in those containing five membered rings as potential *n*-type semiconductors. We aimed to provide a robust methodology based on 1,3-dipolar cycloadditions to obtain triazole and isoxazole derivatives and to perform a preliminary study of their optoelectronic properties.

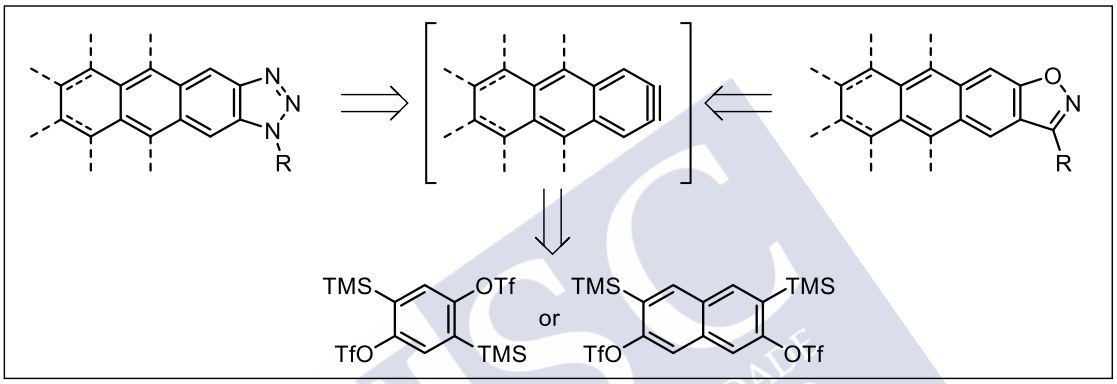


Figure 48. Synthesis of novel heteroacenes by means of aryne chemistry.

5.3 Synthesis of heteroacenes: acenotriazoles and acenoisoxazoles

As synthetic targets of this project we selected heterocyclic analogues of substituted and/or π-extended anthracenes, tetracenes and pentacenes, containing terminal triazole and isoxazole five-membered rings. According to the retrosynthetic analysis shown before (section 5.2), the approach is based in the use of bisaryne precursors as key starting materials (Figure 49), due to their ability to independently generate both arynic unsaturations, so they can react with different arynophiles in each side.

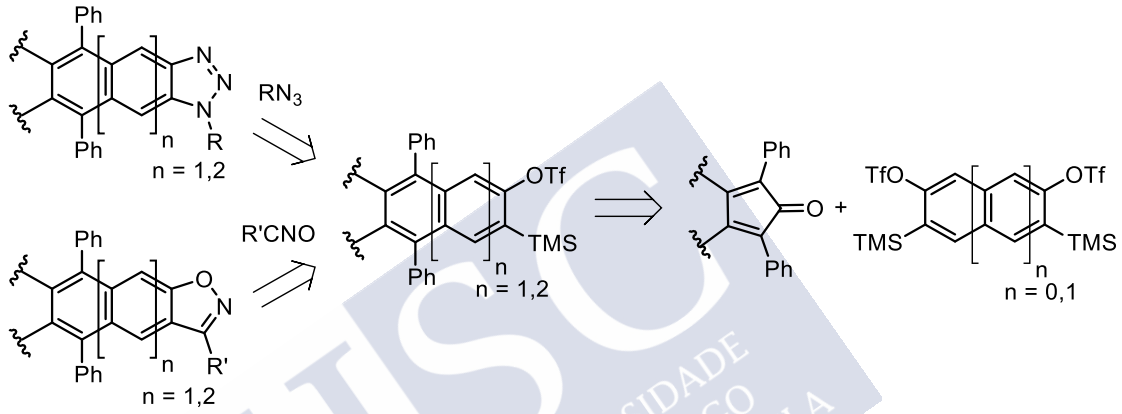


Figure 49. Synthetic approach to acenotriazoles and acenoisoxazoles.

Thus, we envisioned a plausible convergent synthesis of the targeted compounds on the base of two key reactions: (1) selective generation of one of the aryne unsaturations from the bisaryne precursors **58** and **73**, and reaction with an adequate cyclopentadienone (**15**, **76** or **77**) to afford a novel acene-based aryne precursor, using a methodology previously developed in our research group;[186] (2) generation of the second aryne moiety and subsequent 1,3-dipolar cycloaddition with azides and nitrile oxides as reaction partners, to access the targeted heteroacenes.

The first part of the work involved in this chapter involves the preparation of starting materials (Figure 50). We started with the synthesis of bistriflates **58**[93] and **73**,[138] precursors of 1,4-benzodiyne and 2,6-naphthodiyne synthons respectively, following previously reported procedures. Chlorooxime **74** was synthesised according to the protocol published by Larock's

---

[186] D. Rodríguez-Lojo, D. Peña, D. Pérez, E. Guitián, *Synlett* **2015**, *26*, 1633–1637.
[93] H. M. Duong, M. Bendikov, D. Steiger, Q. Zhang, G. Sonmez, J. Yamada, F. Wudl, *Org. Lett.* **2003**, *5*, 4433–4436.
[138] C. Kitamura, Y. Abe, T. Ohara, A. Yoneda, T. Kawase, T. Kobayashi, H. Naito, T. Komatsu, *Chem. A Eur. J.* **2010**, *16*, 890–898.

group in 2010.[187] Benzyl azide (**75**) and tetraphenylcyclopentadienone (**15**) were directly obtained from commercial sources, while cyclopentadienones **76** and **77** were synthesised following a described procedure through a Knoevenagel condensation between 1,3-diphenyl-2-propanone and diones derived from phenanthrene or pyrene.[188]

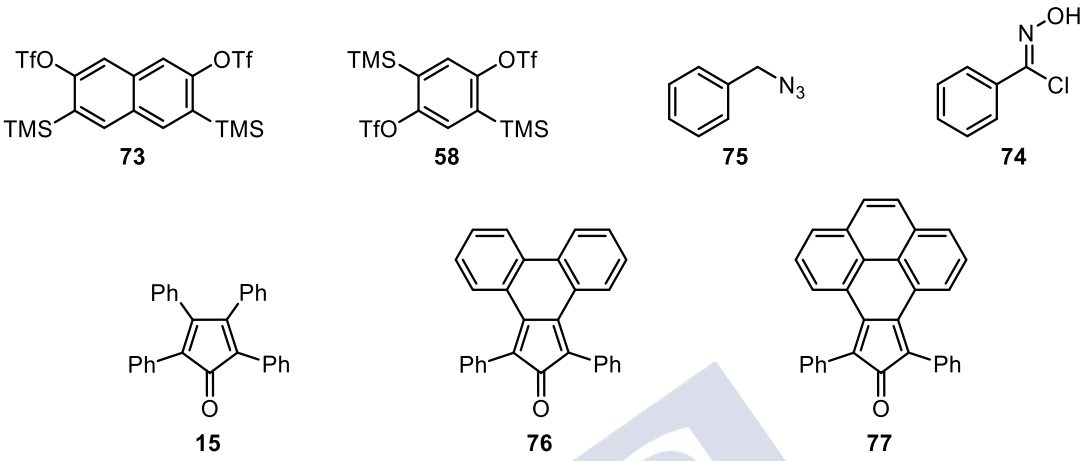
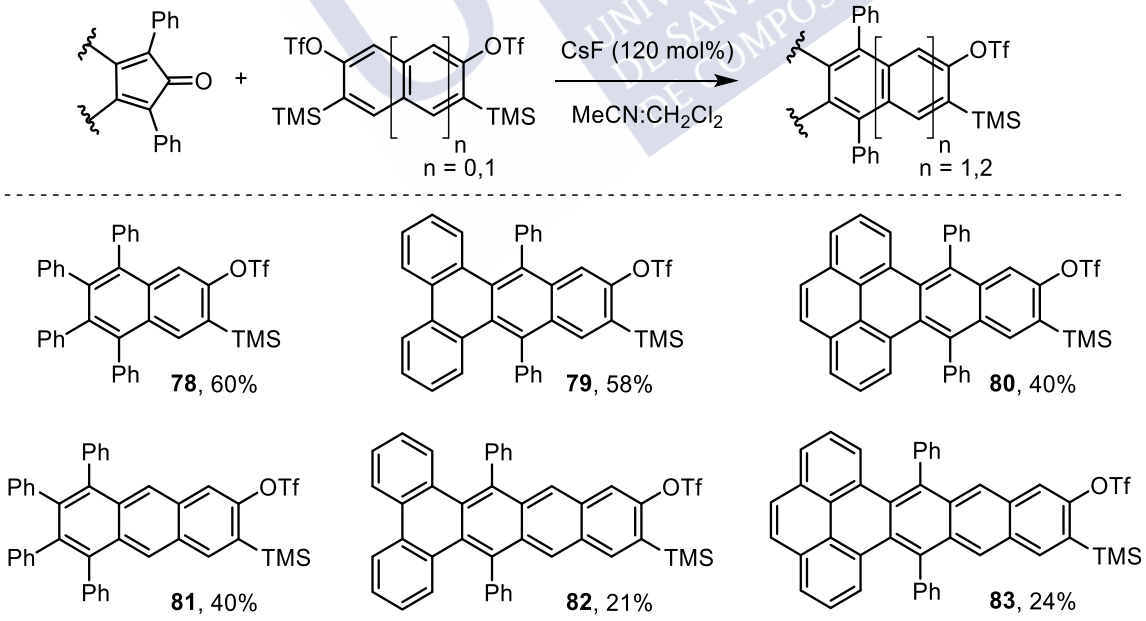


Figure 50. Selected starting materials.

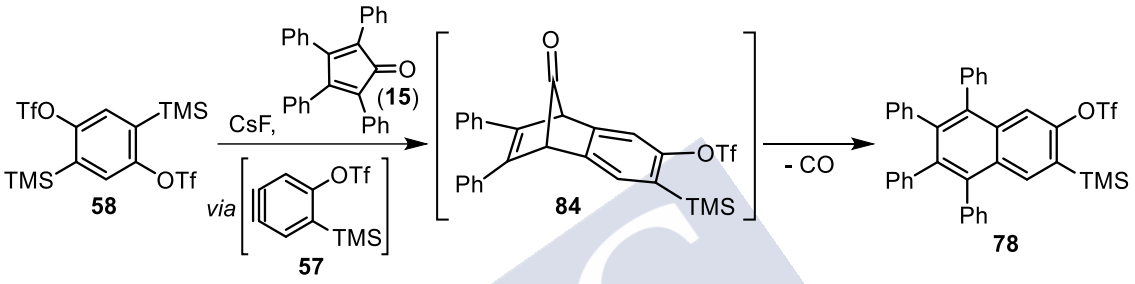
Then, we performed the selective generation of one single aryne unsaturation from **58** and **73**, by reaction with a 120 mol% of CsF in presence of each of the previously mentioned cyclopetadienones, at 50 ºC for 12 hours. We obtained aryne precursor **78** to **83** in reasonable yields, as Rodríguez-Lojo et al. reported before.[186]



Scheme 63. Synthesis of extended acene-based aryne precursors.

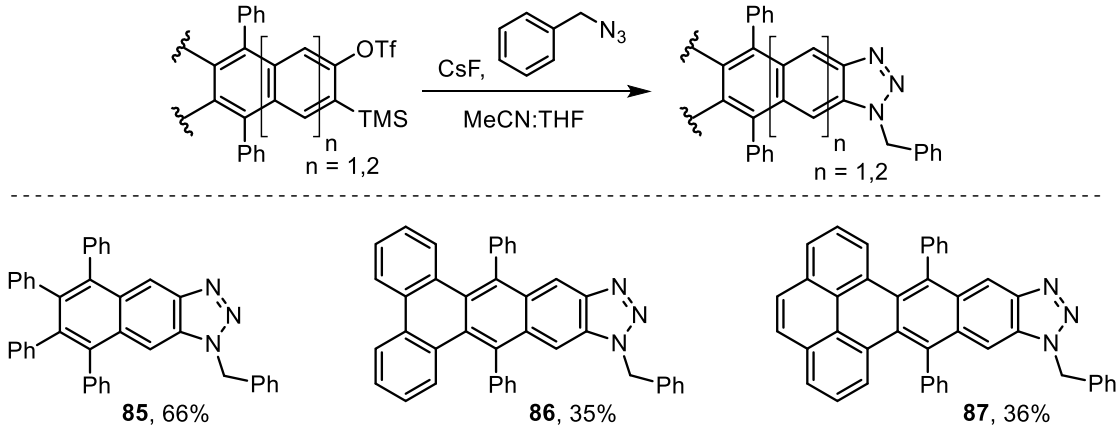
[187] A. V. Dubrovskiy, R. C. Larock, *Org. Lett.* **2010**, *12*, 1180–1183.
[188] R. A. Pascal Jr., W. D. McMillan, D. Van Engen, R. G. Eason, *J. Am. Chem. Soc.* **1987**, *109*, 4660–4665.
[186] D. Rodríguez-Lojo, D. Peña, D. Pérez, E. Guitián, *Synlett* **2015**, *26*, 1633–1637.

The reaction implies the selective generation of one single arynic unsaturation from the corresponding bisaryne precursors, followed by a Diels-Alder reaction with a cyclopentadienone. The intermediate cycloadducts, as **84**, can be detected in some cases, and forced to evolve, through the cheletropic extrusion of CO, by additional heating to obtain the complex aryne precursors required (Scheme 64). The selection of the solvent plays an important role in this reaction, allowing a slow aryne generation and high selectivity, due to the partial precipitation of the products that minimises the possibility of generating the second arynic unsaturation.



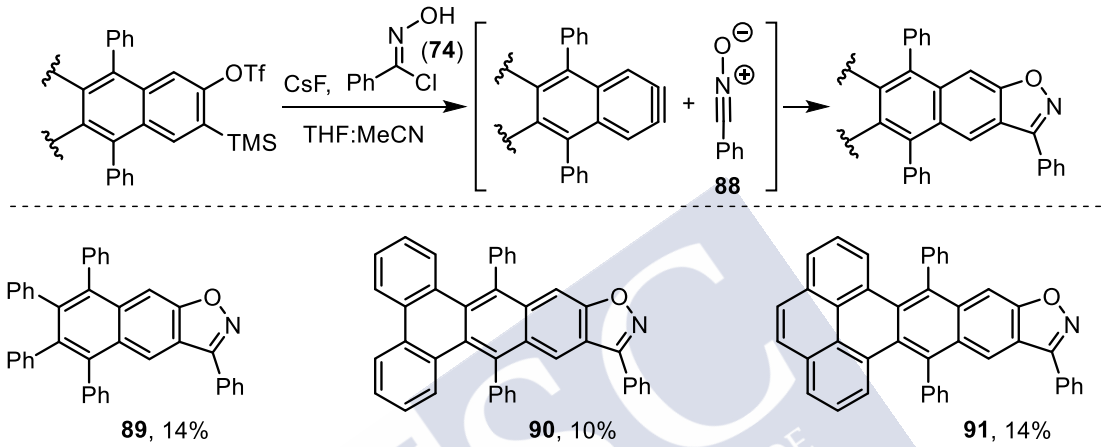
Scheme 64. Synthesis of the complex aryne precursor **78**.

With the aryne precursors shown in Scheme 63 in hands, we studied their reactivity as dipolarophiles in (3+2) cycloaddition reactions with benzyl azide (**75**). First, we used aryne precursors **78**-**80**, obtained from bistriflate **58**. Compounds **85**, **86** and **87** were obtained by reaction with CsF in presence of benzyl azide (**75**) in moderate to good yields (Scheme 65). Triazole derivatives exhibited a characteristic signal in their ^{1}H NMR spectra corresponding to the benzylic protons at 5.9 ppm. Then, we performed the same reaction with precursors **81**, **82** and **83** but, although the expected (3+2)-adducts were detected, their isolation and characterisation could not be achieved, probably due to the expected instability associated to the extension of the linearly-fused system.



Scheme 65. Triazole derivatives synthesised.

Due to the unsuccessful results obtained in the reaction of the arynes derived from **81**-**83** with benzyl azide (**75**), this time we focused on triflates **78**-**80**. Hence, we performed the reaction of the mentioned aryne precursors with CsF in presence of benzonitrile oxide (**88**) at room temperature, to afford the corresponding products **89**, **90** and **91** in low yield (Scheme 66). In this reaction the fluoride ion not only induces the generation of the aryne, attacking the silicon of the trimethylsilyl group, but also is potentially involved in the formation of the benzonitrile oxide (**88**) from the corresponding chlorooxime **74**, acting as a base.



Scheme 66. Isoxazole derivatives synthesised.

The acenoisoxazoles **89**, **90** and **91** can be easily recognised by ^{13}C NMR spectroscopy due to the presence of two peaks, in the range between 155 and 165 ppm, corresponding to the carbon atoms next to the oxygen and nitrogen. Furthermore, compounds **89** and **90** were characterised by X-ray diffraction analysis.

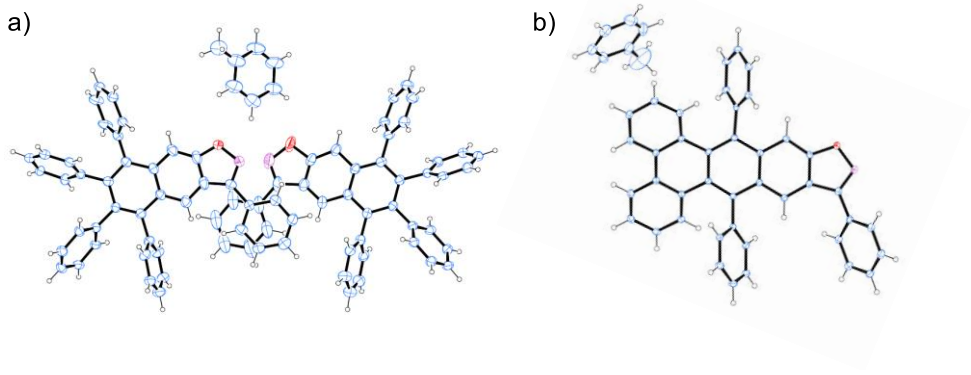


Figure 51. X-ray structure of compounds a) **89** and b) **90**.

5.4 Preliminary study of electronic properties of heteroacenes

Among the most important parameters in order to evaluate the potential behaviour of the novel heteroacenes as organic semiconductors are the energy level of frontier orbitals, HOMO and LUMO, and the energetic difference between them (gap). However, other parameters such as such as the solid state packing or the charge carrier mobility, are also crucial. For instance, pentacene presents a HOMO-LUMO gap around 2.1 eV, and suitable charge mobilities, however, its utilisation in devices is limited due to its instability.

The novel heteroacenes synthesised are very soluble and stable. Their optoelectronic properties, that were preliminary evaluated by UV-vis and fluorescence spectroscopy and **c**yclic **v**oltammetry (CV).

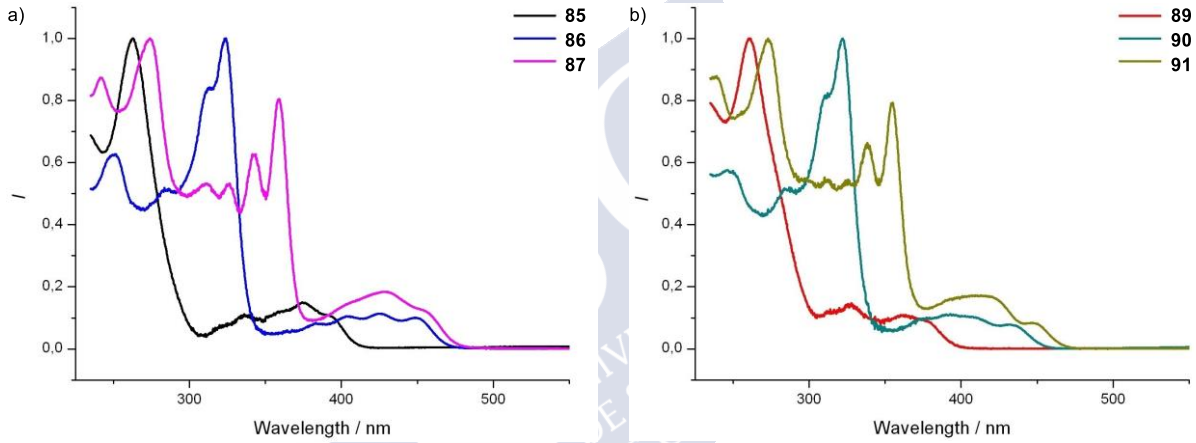


Figure 52. Absorption spectra of a) triazoles **85**, **86** and **87**, and b) isoxazoles **89**, **90** and **91**.

The UV-vis absorption spectra show the most intense band for anthracene derivatives **85** and **89** at 261-263 nm, whereas doped tetracene heterocyclic analogues **86** and **90** show this band at 323 nm. The compounds including five linearly fused rings, **87** and **91**, presented the λ_{max} at 273-274 nm, and second sharp peak around 370 nm. The λ_{onset} corresponds to the less energetic transition and it is normally attributed to the HOMO-LUMO excitation of one electron, and thus, it is possible to use this parameter to estimate the HOMO-LUMO energetic difference (gap_{opt}). While isoxazoles **89**, **90** and **91** presented a λ_{onset} at 401, 455 and 465 nm respectively, triazoles **85**, **86** and **87** shown a slight bathochromic shift around 10 - 20 nm. Based on these values, the optical gap was calculated for the six new heteroacenes, showing values ranging between 3.03 eV and 2.59 eV for the triazole series, and between 3.10 and 2.67 eV for the isoxazoles (Figure 52, Table 1).

Data obtained by fluorescence spectroscopy are also collected in Table 1. Compounds **85** and **89** presented an emission band peak (λ_{Em}) approximately at 430 nm, while **86**, **87**, **90** and **91** have it between 460 and 490 nm (Figure 53).

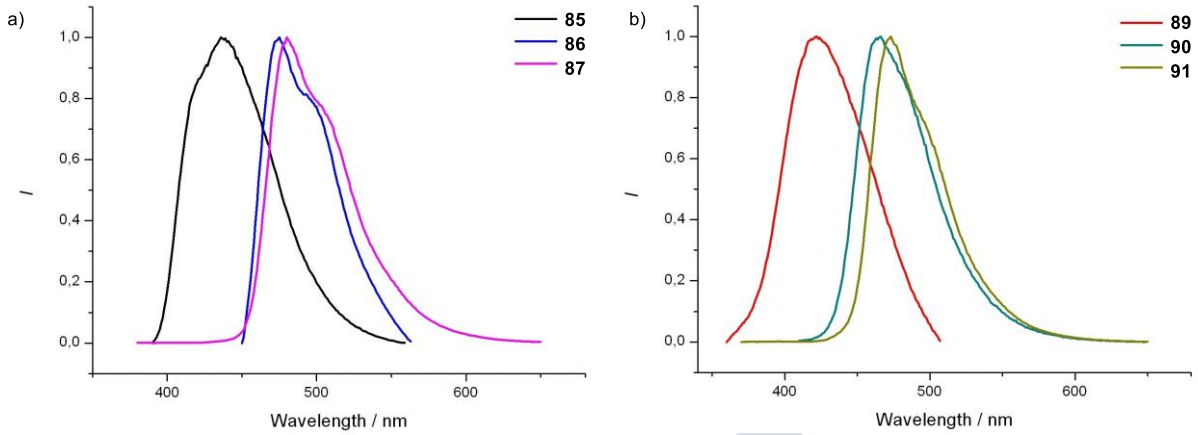
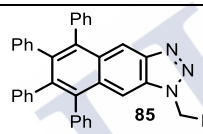
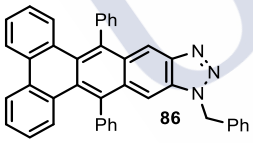
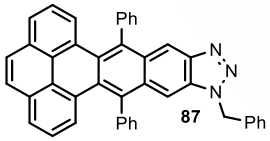
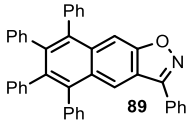
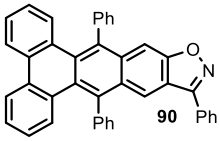
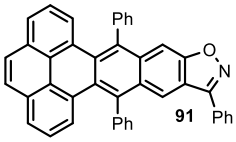


Figure 53. Emission spectra of a) triazoles **85**, **86** and **87**, and b) isoxazoles **89**, **90** and **91**.

Table 1. Spectroscopic data for the absorption and emission of compounds **85** to **87** and **89** to **91** in CH_2Cl_2.

Entry	Product	λ_{max}[a] / nm	λ_{onset}[b] / nm	Gap_{opt}[c] / eV	λ_{Em}[d] / nm
1	 **85**	263	410	3.03	438
2	 **86**	324	475	2.62	482
3	 **87**	274	480	2.59	489
4	 **89**	261	401	3.10	421
5	 **90**	322	455	2.73	462
6	 **91**	273	465	2.67	480

a) λ_{max}, the most intense absorption band. b) λ_{onset}, corresponds to the less energetic transition. c) Gap_{opt}, calculated from the λ_{onset} using Planck's equation. d) λ_{Em}, the most intense emission band.

The electrochemical properties of the newly synthesised heteroacenes were also studied by CV. As a representative example, **Figure 54** shows the cyclic voltammogram corresponding to compound **85**. Reduction and oxidation potentials are recorded in Table 2.

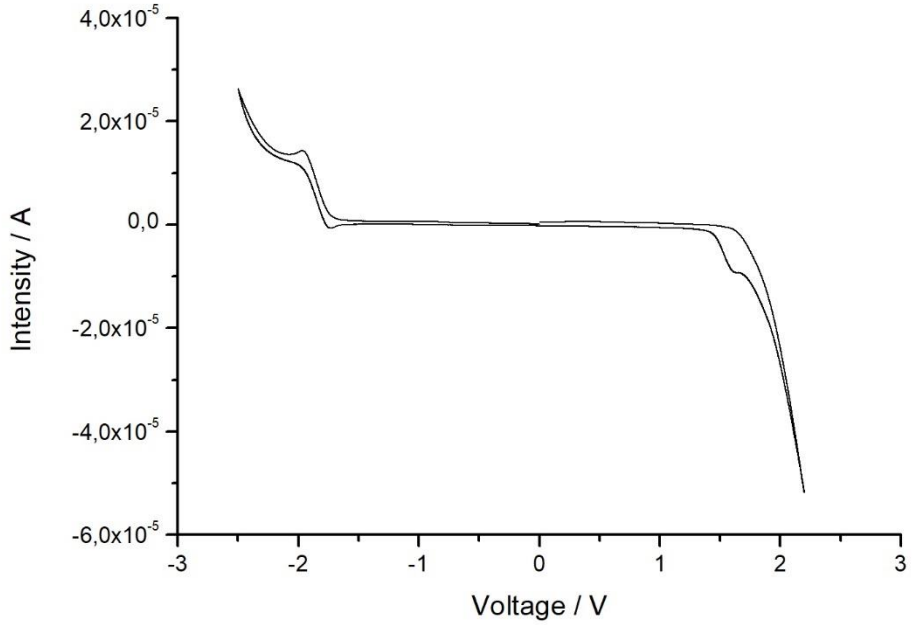
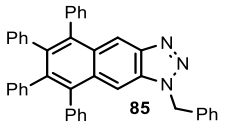
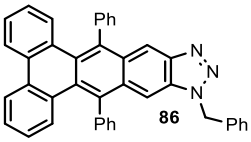
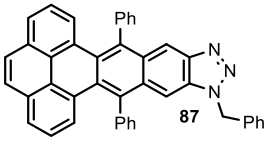
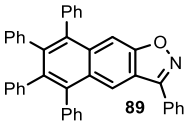
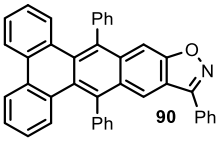
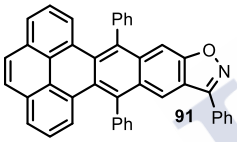


Figure 54. Cyclic voltammogram of compound **85**, measured in Tol:MeCN, 1:5, using *n*-Bu_4NPF_6 (0.1 M) as electrolyte and AgCl/Ag as reference electrode.

HOMO and LUMO values were obtained using ferrocene as internal reference.[189] Obtained values are exposed in Table 2. In Entry 4, the oxidation process was not found, observing only the drift caused by the presence of water at positive values. In this case, we used value obtained for the Gap_{opt} to complete the data (Table 2, placed inside the brackets).

[189] HOMO and LUMO energy levels were calculated from the fisrt Red/Ox potentials, assuming that the energy level for the oxidation of ferrocene (Fc/Fc+) is -4.8 eV (see: E. M. García-Frutos, E. Gutierrez-Puebla, M. A. Monge, R. Ramírez, P. de Andrés, A. de Andrés, R. Ramírez, B. Gómez-Lor, *Org. Electron.* **2009**, *10*, 643–653). This value is obtained from the calculated value -4.6 eV for the standard electrode (E_0), using a **n**ormal **h**ydrogen **e**lectrode (NHE) in vacuum (see: G. Gritzner, J. Kuta, *Pure Appl. Chem.* **1984**, *56*, 461–466), and 0.2 V for the potential of ferrocene against NHE (see: A. J. Bard, L. R. Faulkner, *Electrochemical Methods: Fundamentals and Applications*, p 634, Wiley, **1980**).

Table 2. Data obtained by CV of compounds **85** to **87** and **89** to **91**.

Entry[a]	Product	E_{Ox} / V	E_{Red} / V	E_{HOMO} / eV	E_{LUMO} / eV	Gap_{elec} / eV
1	 **85**	0.94	-2.39	-5.74	-2.41	3.33
2	 **86**	0.82	-2.16	-5.62	-2.64	2.98
3	 **87**	0.85	-2.17	-5.65	-2.63	3.02
4	 **89**	(0.96)	-2.14	(-5.76)	-2.66	(3.10)
5	 **90**	0.79	-2.08	-5.59	-2.72	2.87
6	 **91**	0.96	-2.02	-5.76	-2.78	2.98

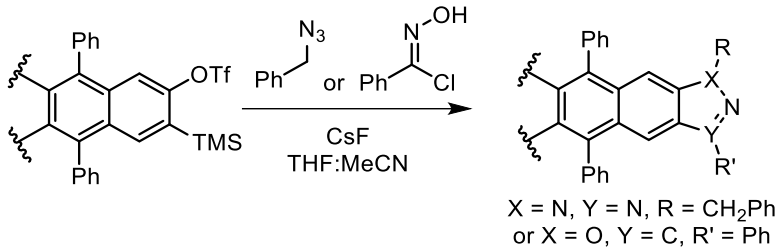
a) Measurements in Tol:MeCN (5:1) solution employing: Bu_4NPF_6 (0.1 M) electrolyte, Ag/Ag^+ electrode and ferrocene (Fc/Fc^+) as internal reference.

These compounds show a *p*-type behaviour, having LUMO energy levels over -3.15 eV,[190] having a potential utility in organic electronics as semiconductor materials. Triazoles **85**, **86** and **87**, and isoxazoles **89**, **90** and **91**, are currently being examined by Ponce's group,[191] with the aim of setting up OFETs and studying their behaviour as charge transport materials.

[190] J. E. Anthony, A. Facchetti, M. Heeney, S. R. Marder, X. Zhan, *Adv. Mater.* **2010**, *22*, 3876–3892.
[191] R. Ponce Ortiz. Department of Physical Chemistry, Faculty of Sciences, University of Malaga, 29071, Malaga, Spain.

5.5 Conclusions

We developed a new strategy to obtain novel *asymmetric* heteroacenes, based in bisaryne chemistry. We controlled sequential generation of each arynic unsaturation and their selective participation in Diels-Alder and 1,3-dipolar cycloadditions.



Scheme 67. Synthesis of heteroacenes by (3+2) cycloadditions.

We synthesised six novel heteroacenes with terminal triazole or isoxazole rings. Studying their electronic properties, we discovered that they present features of *p*-type semiconductors, having a potential use in organic electronics.

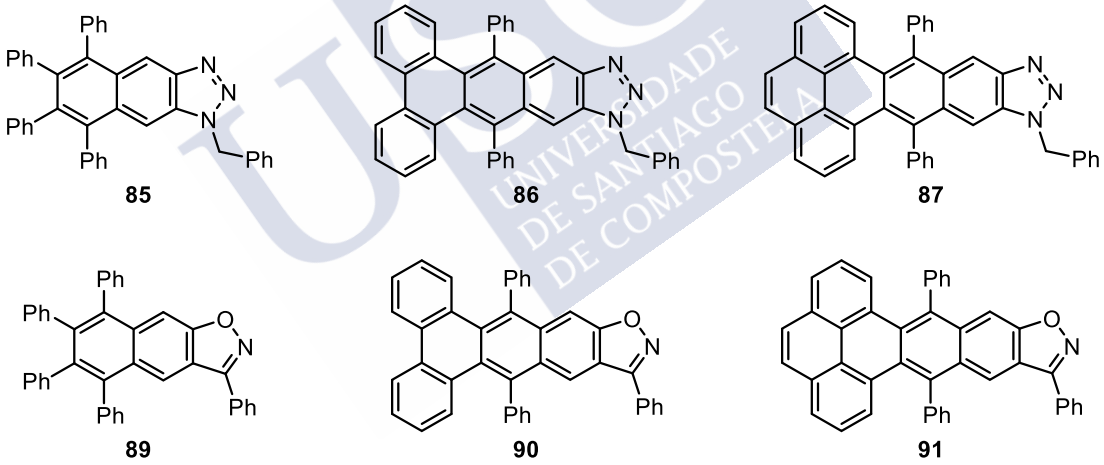


Figure 55. Novel heteroacenes synthesised.

USC
UNIVERSIDADE
DE SANTIAGO
DE COMPOSTELA

6 Kekulene

6.1 Background information

Aromaticity is one of the most interesting phenomena in chemistry.[192] Currently, a definition of this phenomenon refers to an extra stabilisation due to the presence of 4n+2 electrons delocalised in cyclic π-system, and entails consequences in terms of structural and magnetic properties, which can be used as markers of aromatic character. Thus, in presence of an external magnetic field, aromatic compounds undergo a diamagnetic ring current, which induces an opposed magnetic field in the centre of the cyclic system. This feature can be easily observed by NMR, showing a shift of the proton resonances. Regarding to their structure, aromatic molecules show a significant degree of bond length equalisation, that can be measured, for instance, by X-ray diffraction analysis.

6.1.1 Benzene and annulenes

Benzene is the parent aromatic molecule. Since Kekulé proposed its hexagonal structure,[193] several works have targeted its study. Spectroscopic studies[194]and, later, X-ray and neutron diffraction analysis,[195] demonstrated that its structure is a perfect hexagon with D_{6h} symmetry. In ^{1}H NMR, it is observed the expected deshielding of its protons, at 7.16 ppm chemical shift, due to the influence of both magnetic fields, external and induced (Figure 56).

[192] a) P. von R. Schleyer, *Chem. Rev.* **2001**, *101*, 1115–1118, and other articles included in that themed issue; b) N. Martín, L. T. Scott, *Chem. Soc. Rev.* **2015**, *44*, 6397–6400, and other articles included in that themed issue.
[193] a) A. Kekulé, *Bull. Soc. Chim. France* **1865**, *3*, 98–110; b) A. Kekulé, Bull. Acad. Roy. Belg. **1865**, 19, 551–563.
[194] a) R. C. Bailey, C. K. Ingold, H. G. Poole, C. L. Wilson, *J. Chem. Soc.* **1946**, 222–235; b). N. Herzfeld, C. K. Ingold, H. G. Poole, *J. Chem. Soc.* **1946**, 316–333.
[195] O. Ermer, *Angew. Chem. Int. Ed. Engl.* **1987**, *26*, 782–784.

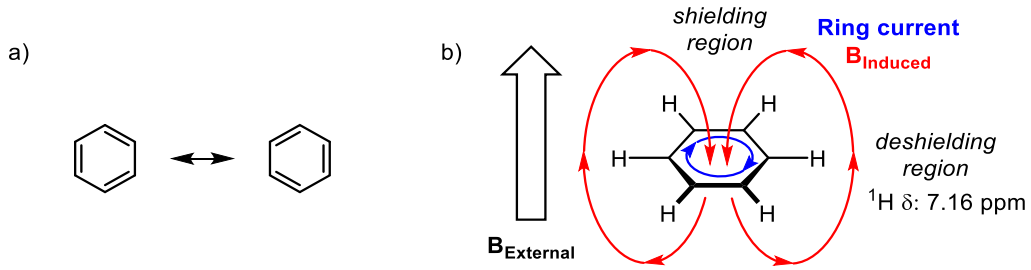


Figure 56. Benzene: a) Resonance structures. b) Diamagnetic anisotropy depiction.

Larger conjugated monocyclic polyenes (annulenes) comprising 4n+2 π-electrons are also aromatic. The study of these species has been conditioned by their limited synthetic availability. A remarkable example was published by Sondheimer, who synthesised the [18]annulene in 1962 (Figure 57).[196] As in the case of benzene, the most stable isomer has a planar, D_{6h} symmetric structure, with a noticeable degree of bond equalisation,[17,197] represented by the resonant structures shown in Figure 57a or by the fully π-delocalised structure depicted below. ^{1}H NMR resonances of hydrogens out of the ring undergo a downfield shift (9.3 ppm), whereas, internal hydrogens are shielded (-3 ppm).[198]

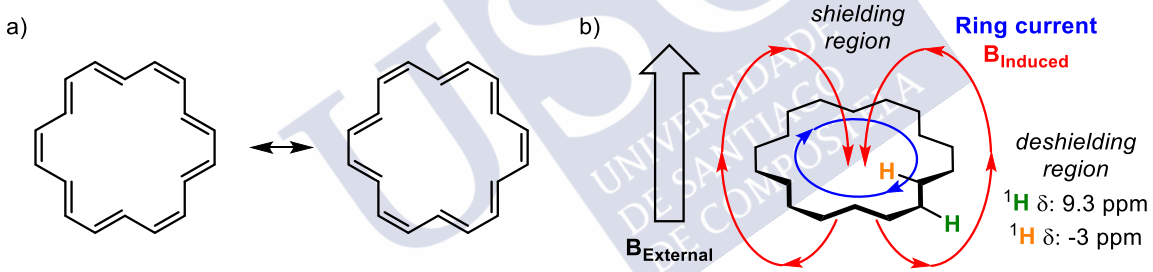


Figure 57. [18]annulene a) Kekule's structure. b) Diamagnetic anisotropy depiction.

6.1.2 Story of kekulene

In 1951, McWeeny studied by means of MO calculations the electronic structure of a series of large aromatic systems with hexagonal symmetry, including a molecule comprised by twelve circularly fused benzenoid rings whose structure could be also analysed as two concentric annulenes bridged by radial single bonds. He suggested that in spite of the large conjugated

---

[196] F. Sondheimer, R. Wolovsky, Y. Amiel. *J. Am. Chem. Soc.* **1962**, *84*, 274–284.
[17] R. Gleiter, G. Haberhauer, *Aromaticity and Other Conjugation Effects,* Wiley-VCH, **2012**.
[197] S. Gorter, E. Rutten-Keulemans, M. Krever, C. Romers, D. W. J. Cruickshank, *Acta Crystallogr. Sect. B* **1995**, *51*, 1036–1045.
[198] J. F. M. Oth, *Pure Appl. Chem.* **1971**, *25*, 573–622.

π-system of this molecule, electrons remain delocalised only into specific benzene rings. By contrast, using the Pauling's approach he concluded the existence of globally delocalised electron currents throughout the whole molecule.[199] Since this early discussion, the electronic structure of this molecule, subsequently named kekulene (see below), has been the object of debate for decades, being of special interest the resonance structures depicted in Figure 58: the Clar structure (left), with the highest possible number of disjointed aromatic π-sextets, and the annulenoid Kekule structure (right), to which superaromatic character could be attributed.[200]

A wonderful summary of the story of kekulene is included in the review published by Buttrick and King.[27]

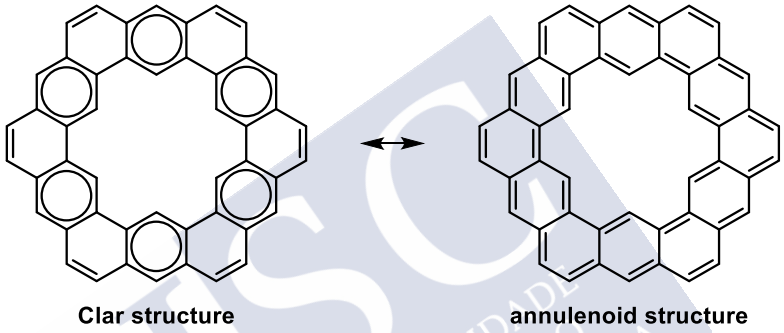


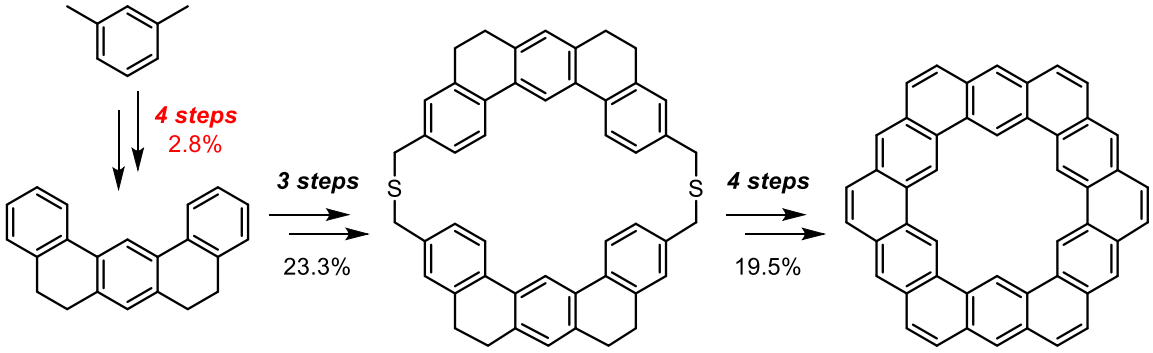
Figure 58. Kekulene structures.

The aforementioned theoretical controversy caught the attention of many scientists and promoted the emergence of several attempts towards the synthesis of kekulene and other cycloarenes, despite the difficulties associated with the synthesis of flat macrocycles.[201] The first unsuccessful approach towards the kekulene was reported in 1965 by Staab, who named this compound in homage to Kekulé due to its resemblance to a super-benzene, at the centennial of Kekulé's benzene formula. Successfully, in 1978, kekulene was synthesised by Diederich and Staab, through a long synthesis in a 0.13% yield as shown in Scheme 68.[202]

---

[199] R. McWeeny, *Proc. Phys. Soc. Sect. A* **1951**, *64*, 921–930.
[200] a) J. Aihara, *J. Am. Chem. Soc.* **1992**, *114*, 865–868; b) H. Jiao, P. R. Schleyer, *Angew. Chem. Int. Ed. Engl.* **1996**, *35*, 2383–2386.
[27] J. C. Buttrick, B. T. King, *Chem. Soc. Rev*. **2017**, *46*, 7−20.
[201] a) F. Vögtle and H. A. Staab, *Chem. Ber.* **1968**, *101*, 2709–2716; b) W. Jenny, R. Paioni, *Chimia* **1968**, *22*, 248–249; c) W. Jenny, R. Paioni *Chimia* **1969**, *23*, 41–42.
[202] a) F. Diederich, H. A. Staab, *Angew. Chem. Int. Ed. Engl.* **1978**, *17*, 372–374; b) H. A. Staab, F. Diederich, *Chem. Ber.* **1983**, *116*, 3487–3503.

This landmark achievement in organic synthesis allowed the experimental study of the structure and some spectroscopic properties of kekulene.[203]



Scheme 68. Diederich and Staab's synthesis of kekulene from *meta*-xylene.[202]

Due to the low solubility of kekulene in common organic solvents, its ^{1}H NMR was achieved in 1,3,5-trichlorobenzene at 215 °C and after about 50,000 scans.[202] They observed three signals in a 2:1:1 intensity ratio and with chemical shifts at 7.9, 8.4 and 10.5 ppm respectively (Figure 59). Moreover, strongly shielding protons, expected for the internal protons in the case of the presence of two annulenoid currents, were not observed, suggesting no global electron delocalisation.

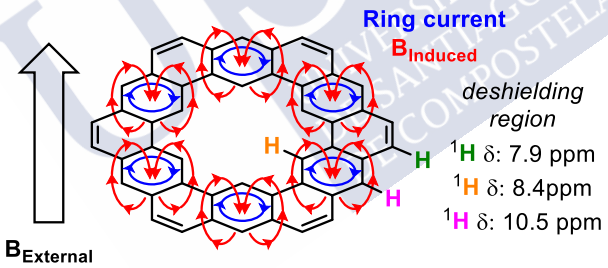


Figure 59. Kekulene chemical shift.

Few years later, the same group reported the X-ray structure of single crystals of kekulene.[203] Its analysis revealed a structure with remarkable bond localisation, with important differences in bond lengths between the two groups of benzene units, being the C-C bonds in the *K*-regions those with shorter bond distances (Figure 60). These experimental evidences are in agreement with the conclusions from MO calculations reported by McWeeny.[199]

[203] H. A. Staab, F. Diederich, C. Krieger, D. Schweitzer, *Chem. Ber.* **1983**, *116*, 3504–3512.

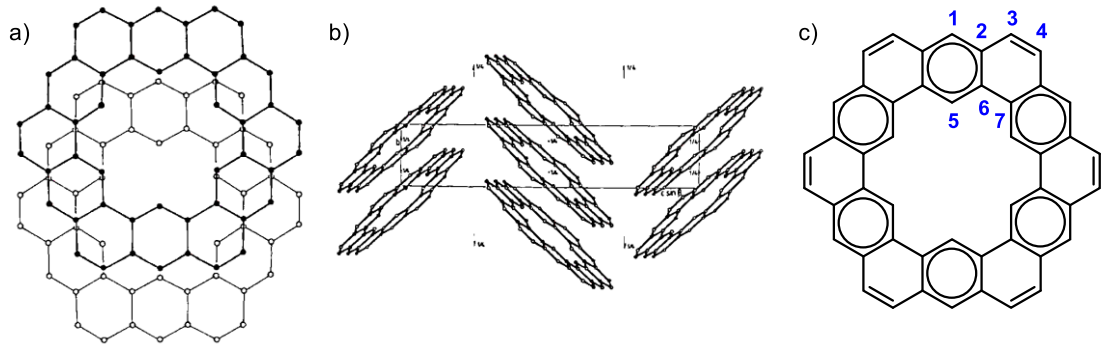


Figure 60. Kekulene X-ray diffraction analysis of kekulene, a) and b) crystal packing, and c) structure including C-C bond distances (in Å); C^1-C^2: 1.40, C^2-C^3: 1.45; C^3-C^4: 1.35; C^2-C^6: 1.42; C^5-C^6: 1.38 and C^6-C^7: 1.45.[203]

It is important to note that these are the only experimental data on kekulene because, apparently, this singular PAH has never been synthesised again since the pioneering work by Diederich and Staab.

6.1.3 Other cycloarenes

Kekulene is the most popular and best studied member of a family of PAHs characterised by the circular arrangement of *cata*-fused benzene rings, named cycloarenes. The synthesis of cycloarenes has been a historical challenge, and it has attracted the efforts of many chemists. Cycloarenes have been used as ideal model to study fundamental scientific questions related with aromaticity. Besides, they have recently caught a renewed attention due to their similarities with graphene pores.[28,204] The number of examples reported of unsubstituted cycloarenes is very limited. They are particularly difficult to synthesise due to their nearly flat

[199] R. McWeeny, *Proc. Phys. Soc. Sect. A* **1951**, *64*, 921–930.
[203] H. A. Staab, F. Diederich, C. Krieger, D. Schweitzer, *Chem. Ber.* **1983**, *116*, 3504–3512.
[28] A. W. Robertson, G.-D. Lee, K. He, C. Gong, Q. Chen, E. Yoon, A. I. Kirkland, J. H. Warner *ACS Nano* **2015**, *9*, 11599−11607.
[204] a) U. Beser, M. Kastler, A. Maghsoumi, M. Wagner, C. Castiglioni, M. Tommasini, A. Narita, X. Feng, K. Müllen, J. *Am. Chem. Soc.* **2016**, *138*, 4322–4325; b) C. Moreno, M. Vilas-Varela, B. Kretz, A. García-Lekue, M. V. Costache, M. Paradinas, M. Panighel, G. Ceballos, S. O. Valenzuela, D. Peña, A. Mugarza, *Science* **2018**, *360*, 199−203.

structure, and thus, extremely low solubility.[205] Substituted analogues have been synthesised taking advantage of their higher solubility (Figure 61).[206]

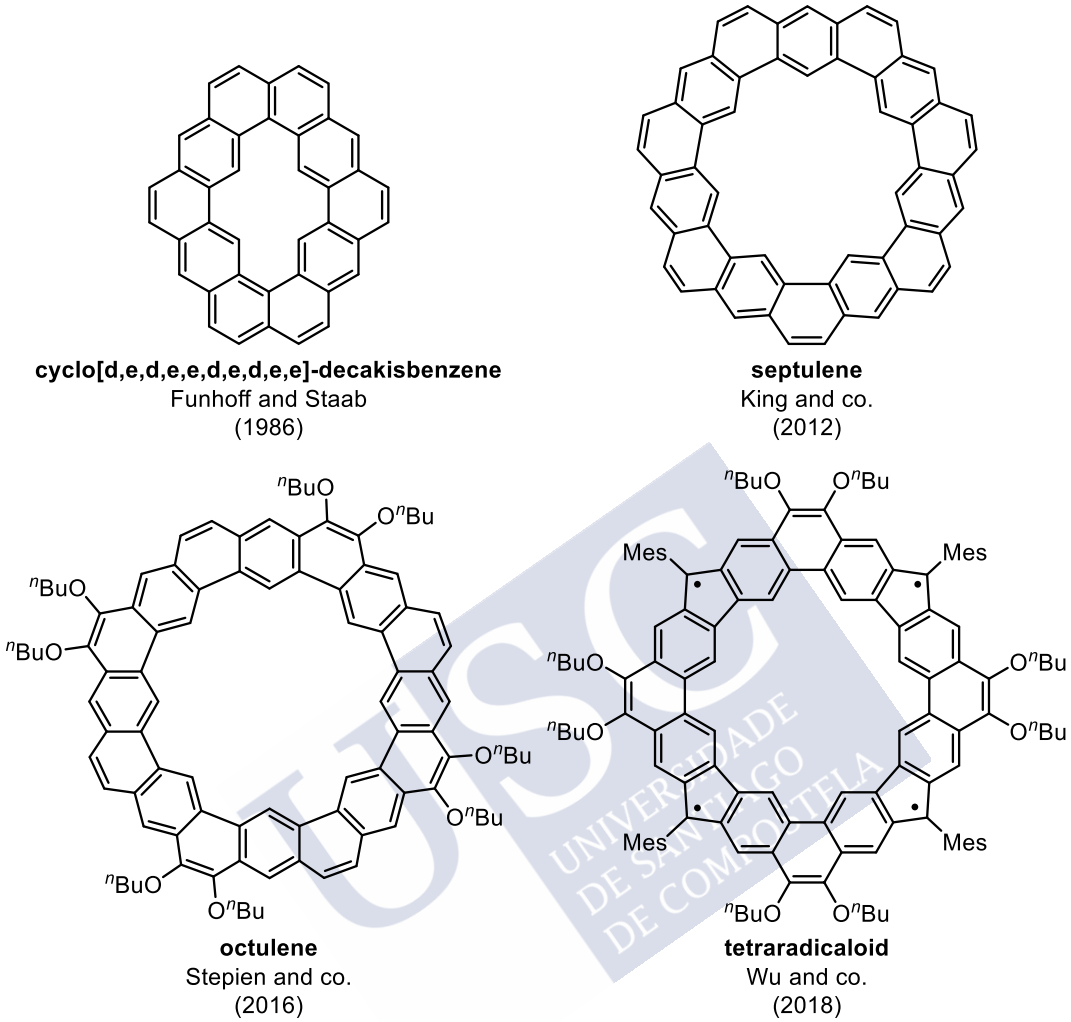


Figure 61. Examples of cycloarenes.

[205] a) D. J. H. Funhoff, H. A. Staab, *Angew. Chem. Int. Ed. Engl.* **1986**, *25*, 742−744; b) B. Kumar, R. L. Viboh, M. C. Bonifacio, W. B. Thompson, J. C. Buttrick, B. C. Westlake, M.-S. Kim, R. W. Zoellner, S. A. Varganov, P. Mörschel, J. Teteruk, M. U. Schmidt, B. T. King, *Angew. Chem. Int. Ed.* **2012**, *51*, 12795−12800.

[206] a) M. A. Majewski, Y. Hong, T. Lis, J. Gregolinski, P. J. Chmielewski, J. Cybinska, D. Kim, M. Stępień, *Angew. Chem. Int. Ed.* **2016**, *55*, 14072−14076; b) X. Lu, T. Y. Gopalakrishna, H. Phan, T. S. Herng, Q. Jiang, C. Liu, G. Li, J. Ding, J. Wu, *Angew. Chem. Int. Ed.* **2018**, *57*, 13052–13056.

6.2 Objectives

This part of the thesis is focused on the study of kekulene from a double perspective:

First, four decades after the first (and only) synthesis of kekulene, we aim to explore new, improved synthesis of this emblematic cycloarene by means of aryne chemistry. In particular, two approaches will be studied, having in common the use of the 1,4-benzodiyne synthon as buiding block. The first retrosynthetic analysis (**A**) envisages a formal four-fold Diels-Alder reaction between 2,7-divinyl-9,10-dihydrophenanthrene and 1,4-benzodiyne as key step of the synthesis. As an alternative, analysis **B** implies the synthesis of 5,6,8,9-tetrahydrobenzo[*m*]tetraphene, a key synthetic intermediate in the route developed by Diederich and Staab, by double cycloaddition reaction of styrene to 1,4-benzodiyne

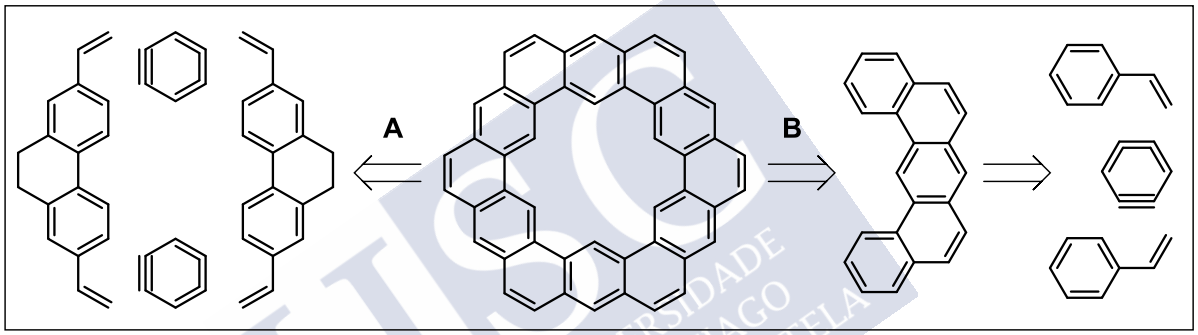


Figure 62. Retrosynthetic analyses of kekulene.

Second, the structural study of kekulene at the single molecular level will be performed in collaboration with the group of Leo Gross (IBM Research, Zurich; ultrahigh-resolution AFM) and with Manuel Melle (CICECO, University of Aveiro; computational calculations).

6.3 Synthesis of kekulene

According to the retrosynthetic analysis A shown above, we proposed a plausible approach to kekulene (**92**) based on the reaction of the 1,4-benzodiyne synthon (**93**) and the divinylarene **94**.

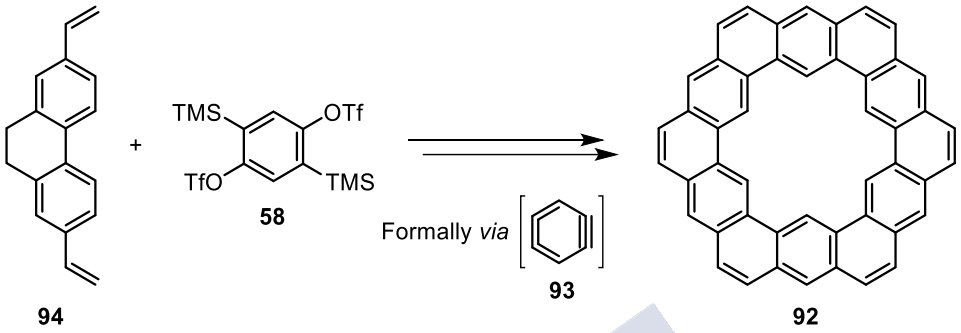
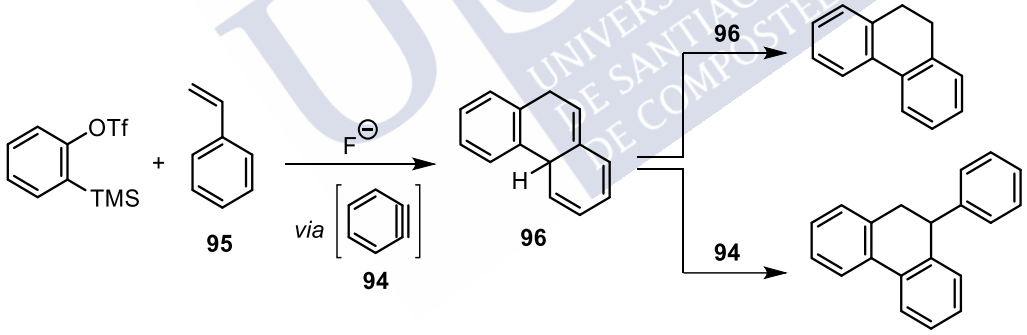


Figure 63. Synthetic approach to kekulene (**92**) by cycloaddition reactions of the 1,4-benzodiyne synthon (**93**).

Synthesis of dihydrophenanthrene derivatives by reactions between styrenes and arynes has been described (Scheme 69),[207] but they are usually complicated by competing processes such as the Alder-ene reaction with a second aryne unit.[208]



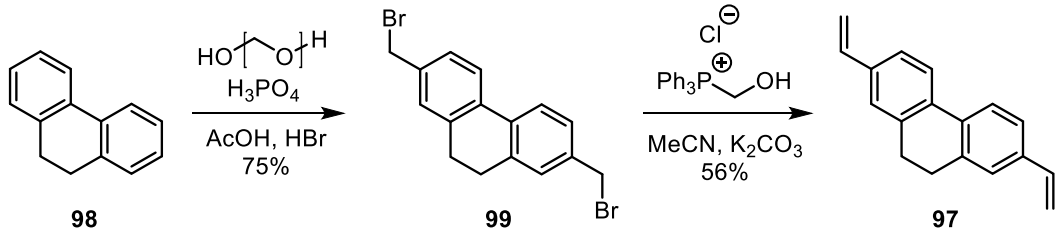
Scheme 69. Reaction between benzyne (**94**) and styrene (**95**).

For the generation of the 1,4-benzodiyne precursor **58**, which is currently commercially available, we choose the efficient and mild procedure reported by Wudl.[93] For the synthesis of the divinyl derivative **97** a first selective double bromomethylation of 9,10-dihydrophenanthrene

---

[207] R. Harrison, H. Heaney, G. Mason, J. M. Sketchley, *J. Chem. Soc.* **1969**, 1684–1689.
[208] a) W. L. Dining, *Tetrahedron Lett.* **1966**, 939–941; b) S. S. Bhojgude, A. Bhunia, R. G. Gonnade, A. T. Biju, *Org. Lett.* **2014**, *16*, 676–679; c) Z. Chen, X. Han, J.-H. Liang, J. Yin, G.-A. Yu, S.-H. Liu, *Chinese Chem. Lett.* **2014**, *25*, 1535–1539; d) S. S. Bhojgude, A. Bhunia, A. T. Biju, *Acc. Chem. Res.* **2016**, *49*, 1658–1670.
[93] H. M. Duong, M. Bendikov, D. Steiger, Q. Zhang, G. Sonmez, J. Yamada, F. Wudl, *Org. Lett.* **2003**, *5*, 4433–4436.

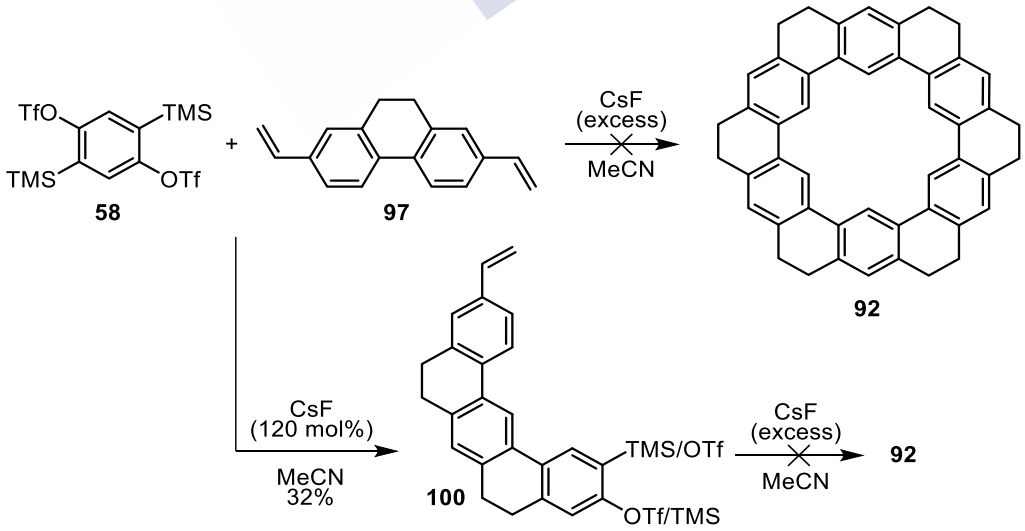
(**98**) afforded **99** in a 75% yield. Subsequently, a Wittig olefination, with *in situ* generated formaldehyde,[209] afforded the targeted compound in a 56% yield. Divinyl derivative **97** tends to polymerise in the presence of oxygen when it is in solution, nevertheless, the pure compound is manageable.



Scheme 70. Synthesis of compound **97**.

With **58** and **97** in hand, we tried to obtain **92** in one step, through the reaction of the 1,4-benzodiyne precursor **58** with CsF in presence of **97**. Analysing the reaction crude we observed the consumption of the aryne precursor **58** and partial recovery of the bisdiene **97**, however, the expected product was not detected (Scheme 71). In a second attempt, we performed the reaction sequentially, thus, generation of one single aryne from **58** in presence of **97** afforded **100** in a 32% yield. Other expected products, such as those derived from the feasible Alder-ene reaction, were not detected.

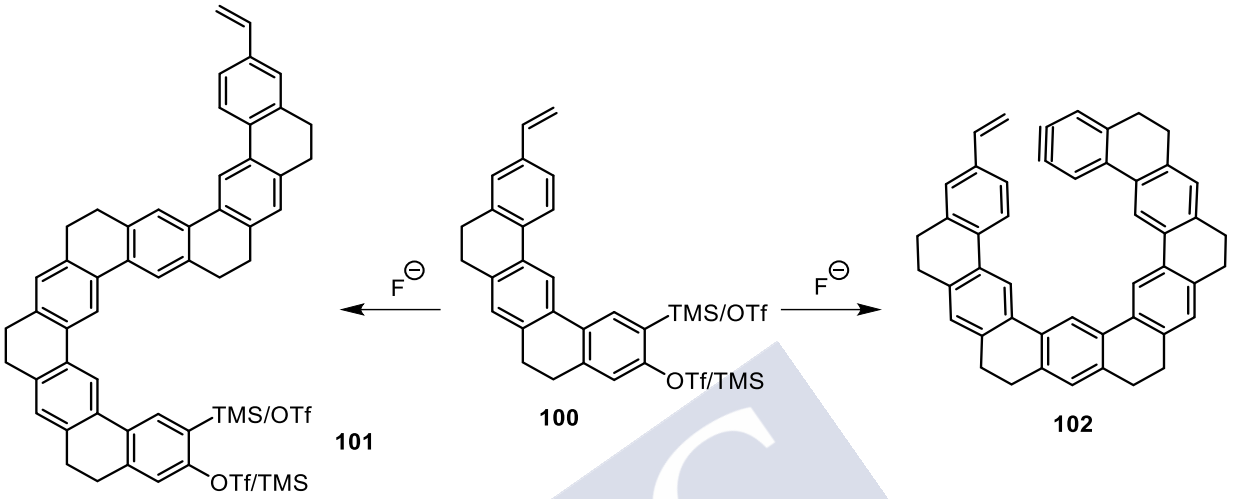
Subsequently, we tried the dimerisation of **100**, and thus, we essayed its reaction with CsF. Although, the aryne precursor **100** was consumed, the formation of **92** was not observed either.



Scheme 71. Synthetic attempts towards **92**.

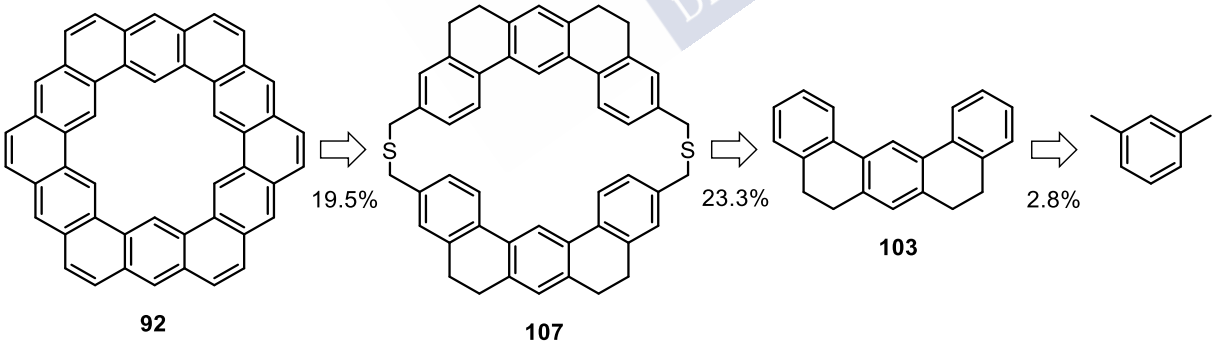
[209] W. Huang, J. Xu, *Synth. Commun.* **2015**, *45*, 1777–1782.

The detection of peaks with m/z concordant with the mass of dimers lead us to think about two plausible reasons of the failure of this strategy: a strong *anti*- selectivity of the first Diels-Alder reaction to afford compound **101**, or that intermediate **102** is not flexible enough to achieve the needed geometry for the second intramolecular cycloaddition.



Scheme 72. Plausible intermediates of these approaches.

At this point, we reviewed the original synthesis performed by Diederich and Staab (Scheme 73),[202] and realised that the main weakness of their otherwise superb synthetic route,[210] is the access to the specific intermediate **103**, which was obtained in four steps and a 2.8% overall yield (Scheme 73).[202]



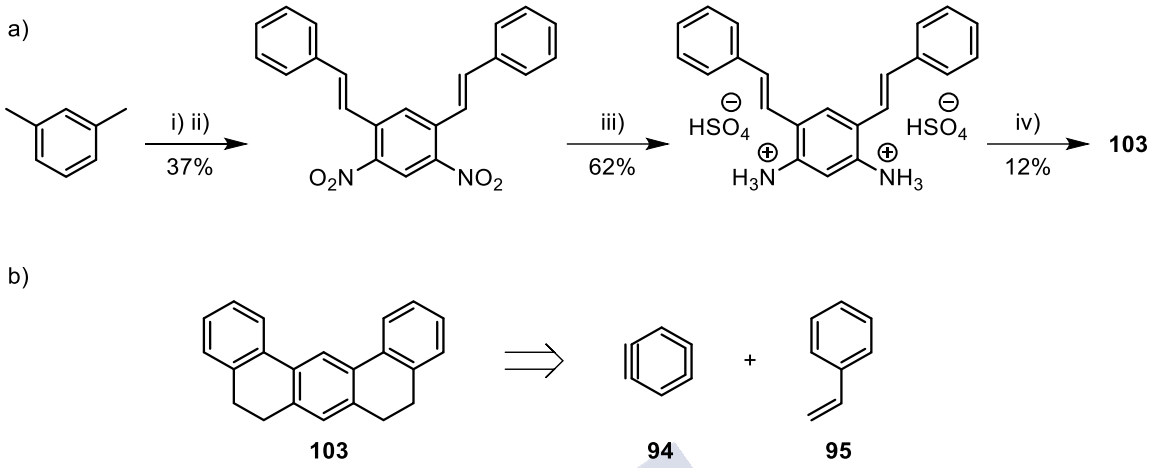
Scheme 73. Retrosynthetic scheme of kekulene (**92**) by Diederich and Staab.

In addition, some of the transformations involved harsh reaction conditions, such as a double nitration with high volumes of hot fuming nitric acid, or a reduction step under 90 atm

---

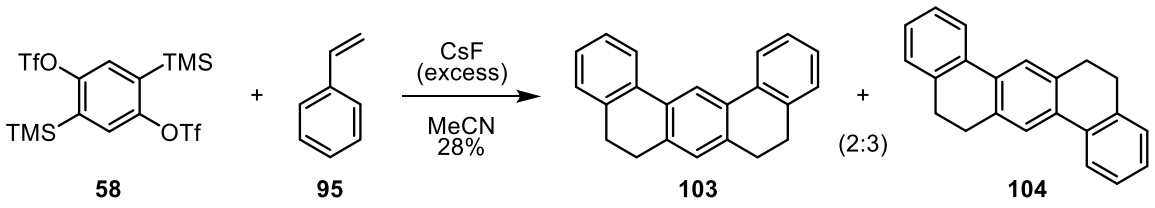
[202] a) F. Diederich, H. A. Staab, *Angew. Chem. Int. Ed. Engl.* **1978**, *17*, 372–374; b) H. A. Staab, F. Diederich, *Chem. Ber.* **1983**, *116*, 3487–3503.
[210] H. Miyoshi, S. Nobusue, A. Shimizu, Y. Tobe, *Chem. Soc. Rev.* **2015**, *44*, 6560–6577.

of H_2 (Scheme 74a). As an alternative, we envisioned a very suitable strategy towards the synthesis of **103** in one step using the 1,4-benzodiyne synthon (Scheme 74b).



Scheme 74. a) Staab and Diederich's synthesis of **103**. Reaction conditions: (i) HNO_3 (c), Δ; (ii) PhCHO, piperidine; (iii) H_2, 90 atm, 10% Pd/C, Δ; (iv) Cu, H_2SO_4 (c), isoamyl nitrite. b) Retrosynthetic analysis of **103**.

Initially, we performed the reaction in refluxing dioxane, similarly to the conditions reported for the synthesis of non-arylated 9,10-dihydrophenanthrene (**98**) by reaction between benzyne and styrene.[208c,211] Thus, treatment of **58** with CsF in presence of styrene (**95**) afforded the expected mixture of tetrahydrobenzotetraphenes, **103** and **104**, in low yield (<17%, Table 3, Entry 1). When the reaction was performed using TBAF instead of CsF, as fluoride source, or additional 18-crown-6 ether, poorer results were obtained (Entries 2 and 3). The molar ratio was optimised (Entries 4 to 7). Finally, we found that the use of acetonitrile as solvent and larger reaction scale led to better yields (Entries 8 to 10). The best results were obtained by reaction of **58** (19 mmol), with **95** and CsF (in a 1:5:6 molar ratio) in refluxing acetonitrile, yielding the mixture of products **103** and **104** in a reasonable 28% yield (Table 3, Entry 11). The ratio of the products was easily determined by ^{1}H NMR.



Scheme 75. Synthesis of **103** and **104**.

[208c] Z. Chen, X. Han, J.-H. Liang, J. Yin, G.-A. Yu, S.-H. Liu, *Chinese Chem. Lett.* **2014**, *25*, 1535–1539.
[211] R. Harrison, H. Heaney, G. Mason, J. M. Sketchley *J. Chem. Soc.* **1969**, 1684–1689.

Table 3. Optimisation of the reaction between **58** and CsF in presence of styrene (**95**).

Entry[a]	Solvent	Molar ratio (**58**:**95**:CsF)	Scale / g (mmol of **58**)	Yield / % (**103** + **104**)[b]
1	Dioxane	1:5:10	0.1	17
2[c]	Dioxane	1:5:10	0.1	11
3[d]	Dioxane	1:5:10	0.1	–
4[e]	ACN	1:5:10	0.1	13
5	ACN	1:5:10	0.1	20
6	ACN	1:2:10	0.1	12
7[f]	ACN	1:25:10	0.1	23
8	ACN	1:5:6	0.1	20
9	ACN	1:5:6	0.75	22
10	ACN	1:5:6	3	26
11	ACN	1:5:6	10	28

a) Typical reaction conditions: reflux, 16 h, [**58**] = 0.05 M. b) Yield of isolated products (≈ 2:3 mixture of **103** and **104**). c) 18-crown-6 (120 mol%) was added. d) TBAF was used as source of fluoride. e) Reaction conducted at rt. f) [**58**] = 0.01 M.

The separation of **103** and **104** was not easy, but it was achieved by consecutive recrystallisations in boiling methanol, as well as by semi-preparative **s**upercritical **f**luid **c**hromatography (SFC), using a Lux@ 5µm *i*-Amylose-1 column (250 x10 mm) (Figure 64).

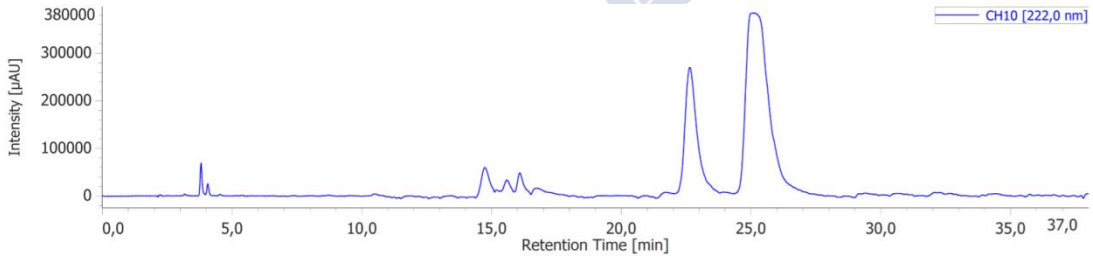
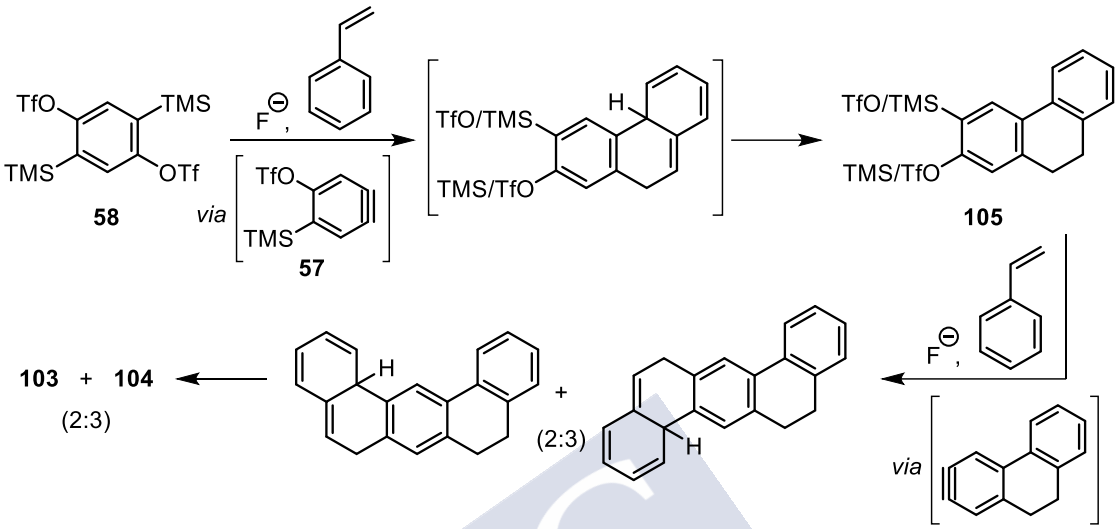


Figure 64. SFC chromatogram of **103** and **104** mixture. Lux@ 5µm *i*-Amylose-1 column (250 x10 mm, 10% MeOH in CO_2, 7 mL flow, 150 Bar, 40 ºC). Retention times: **103**, 22.6 min, and **104**, 25.1 min.

Noticeably, compound **103**, a key intermediate in the synthesis of kekulene, was obtained; in one step from commercially available materials, under mild reaction conditions, and, with a four-fold increased yield, comparing with the original synthesis of **92**.

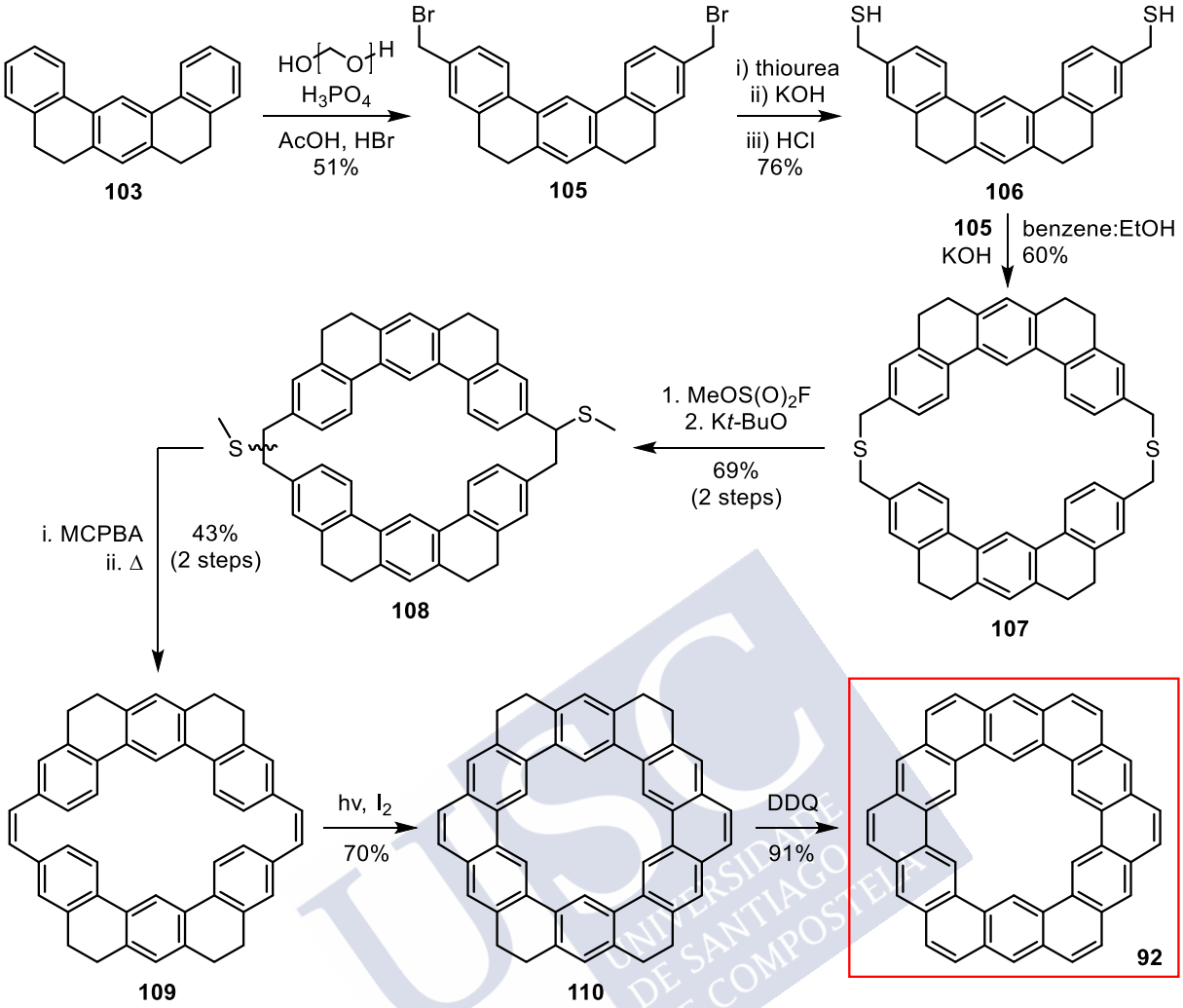
Surprisingly, the unique isolated products from the reaction crude were **103** and **104**, and other products, such as those derived from the Alder-ene reaction, were not observed. We assumed the formation of volatile molecules and insoluble polymers from benzodiyne

precursor **58**. Scheme 76 shows a plausible mechanism for the formation of **103** and **104**, involving two sequential Diels−Alder/H-migration processes, supported by the detection of the aryne precursor **105** in some experiments (Scheme 76).



Scheme 76. Mechanistic proposal for the formation of **103** and **104**.

Having **103** in hand, we tackled the actual synthesis of kekulene (**92**). As a first step, we functionalised positions C(3) and C(11) of the polycyclic system with different (bromo, bromomethyl, vinyl) groups and explored some approaches for dimerisation based in metal catalysed cross-coupling or metathesis reactions, which resulted unsuccessful. Thus, we decided to get back to the synthetic route designed by Diederich and Staab, which was perfectly reproducible in our hands, even though we introduced some minor modifications and performed the reactions under a considerably lower scale. (Scheme 77).



Scheme 77. Diederich and Staab's synthesis of kekulene from **103**.[202]

We started with the selective dimethylbromination of **103**, which allowed to obtain **105** in yields around 60% at 2-3 mmol scale, slightly better than those originally reported. Then, we performed the functional group interconversion, by treatment of **105** with thiourea, to afford **106**. The reaction between **105** and **106** under high dilution conditions, substituting toluene for benzene, led us to obtain the macrocycle **107**. The following methylation of the sulphur atoms of **107**, was achieved in a moderate yield, using methyl trifluoromethanesulphonate instead of methyl fluorosulphonate.[212] The intermediate salt was treated with a bulky base to afford **108** through a Stevens rearrangement. Thereafter, **108** was reacted with *meta*-chloroperbenzoic acid (MCPBA), and subsequently, **109** was obtained by pyrolysis of the intermediate

[212] Currently, methyl fluorosulphonate is not commercially available due to its extreme toxicity.

[202] a) F. Diederich, H. A. Staab, *Angew. Chem. Int. Ed. Engl.* **1978**, *17*, 372–374; b) H. A. Staab, F. Diederich, *Chem. Ber.* **1983**, *116*, 3487–3503.

disulfoxide in a tubular oven under vacuum (<10^{-3} mbar). It was purified by column chromatography eluting with carbon tetrachloride, protecting the solutions from light during the whole process. The ^{1}H NMR spectrum of **109** shown two characteristic singlets at 6.7 and 2.8 ppm corresponding to the olefinic and methylene protons respectively. The double electrocyclic ring closure required to convert **109** into **110** was carried out under irradiation with a catalytic amount of iodine and monitored by TLC. Finally, we performed the dehydrogenation of **110** by treatment with DDQ, to afford the planar and extremely insoluble kekulene (**92**), which precipitate in the reaction media. It was filtered and washed several times with acetate, chloroform, and diethyl ether, and dried under vacuum. The samples obtained of kekulene (**92**) were sent to IBM Research (Zürich) for their study by AFM.

USC UNIVERSIDADE DE SANTIAGO DE COMPOSTELA

6.4 Structural study of kekulene

6.4.1 AFM

Once having kekulene (**92**) in hand, we collaborated with Dr. L. Gross and coworkers[213] in order to study its structure by ultra-high-resolution AFM. This state-of-the-art technique allows to visualise single-molecule images of planar molecules. The sample of kekulene was sublimated on a Cu(111) surface from a silicon wafer by rapid heating,[214] to decrease the expected fragmentation due to its large size and therefore, high sublimation temperature. They found few molecules of kekulene (**92**) and other small and mobile molecules, resulting from fragmentation. The constant-height AFM images of one molecule of kekulene adsorbed on Cu(111) were recorded at different heights using a CO-functionalised tip. Below are shown the kekulene images obtained decreasing the distance between the tip and the sample (Figure 65a-c) and the corresponding Laplace filtered images (Figure 65d−f respectively).

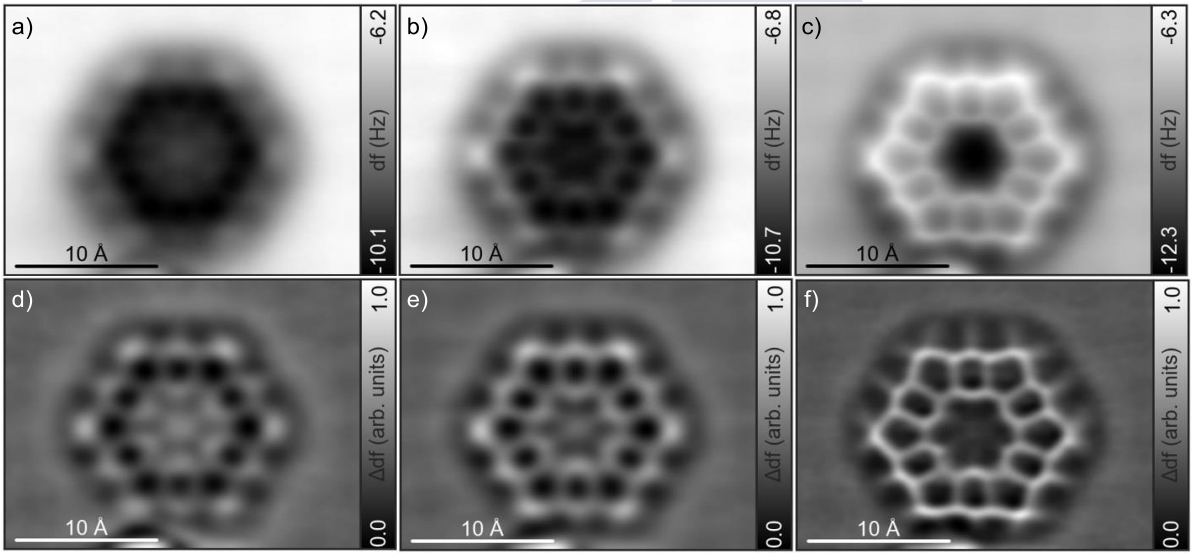


Figure 65. Constant-height AFM images with a CO-functionalised tip of kekulene (**92**) on a Cu(111) surface. We approached the tip by a) z = 1.6 Å, b) 1.9 Å and c) 2.2 Å, with respect to the STM set point of V = 0.1 V, I = 1 pA on the bare Cu(111) surface. Laplace-filtered images are shown in d), e) and f) respectively.

From the AFM images shown above, the molecular structure of kekulene was nicely resolved at the single-molecule level. Furthermore, the analysis of the contrast in these images

---

[213] Z. Majzik, N. Pavliček and L. Gross. *IBM Research* – Zürich. 8803 Rüschlikon (Switzerland).

[214] a) G. Rapenne, L. Grill, T. Zambelli, S. M. Stojkovic, F. Ample, F. Moresco, C. Joachim, *Chem. Phys. Lett.* **2006**, *431*, 219–222; b) B. Schuler, G. Meyer, D. Peña, O. C. Mullins, L. Gross, *J. Am. Chem. Soc.* **2015**, *137*, 9870–9876.

allowed to draw some conclusions about the bond order in these molecules. Despite that resolving the bond-order-related contrast at the periphery of molecules is specially challenging it is possible to compare qualitatively bonds that experience similar background forces.[22b] High bond orders have a brighter appearance at larger tip-sample distances, and shortened aspect, in small heights measurements.[22b] The peripheral C-C bonds, in the *K*-regions of kekulene (**92**), appear as the brightest bonds at moderate tip height (Figure 65b), moreover, the same bonds appear as the shortest bonds at small tip height (Figure 65c). Obtained results denote that these bonds are those with highest bond order in the structure of **92**, in agreement with the data previously acquired by X-ray diffraction analysis.

6.4.2 Calculations

The molecular structure of kekulene was also studied trough the collaboration with Prof. M. Melle-Franco,[215] who computed the kekulene (**92**) in the gas phase and on surface. The gas phase calculations[216] revealed that kekulene possesses a D_{3d} symmetric structure due to the slight distortion caused by steric hindrance between the internal hydrogen atoms. The C-C bond lengths, match perfectly with the experimental results obtained by X-ray diffraction analysis (Figure 66).

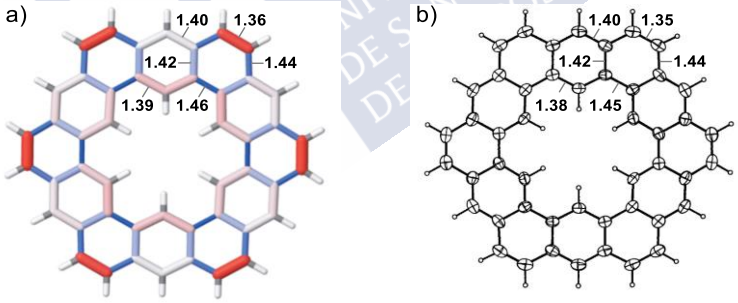


Figure 66. Molecular structure of kekulene (**92**): a) Computed in gas phase; with symmetries of D_{3d}. The colours grade with distance from 1.33 Å (red) to 1.40 Å (white) and to 1.47 Å (blue). b) Experimental data from XRD.

This calculated bonding pattern, which is also reproduced in simulations on the Cu(111) surface, supports once again that the electronic structure of kekulene is best described by the

---

[22b] L. Gross, F. Mohn, N. Moll, B. Schuler, A. Criado, E. Guitián, D. Peña, A. Gourdon, G. Meyer, *Science* **2012**, *337*, 1326–1329.

[215] M. Melle-Franco. *CICECO*, Aveiro Institute of Materials, Department of Chemistry, University of Aveiro, 3810-193 Aveiro, Portugal.

[216] B3LYP-def2-TZVP.

Clar model, with the π electrons delocalised within disjointed aromatic π-sextets, rather than along the whole molecule, as it would be predictable for a hypothetically *superaromatic* Kekulé annulenoid structure. Curiously, kekulene (**92**) has a peculiarly high calculated HOMO-LUMO gap (3.55 eV), similar to the calculated for the much smaller anthracene (3.56 eV).[216]

The calculations of kekulene on the Cu(111) surface are also in agreement with the experimental evidences, supporting the Clar structure as the most representative. Simulations of the AFM images were performed an experimental amplitude of 1 Å and with binding constants between 0.15 and 0.60 Nm^{-1}, and quadrupole, monopole and uncharged tips.[217] The best results (the most similar simulations to the experimental data) were obtained by a d_z^2-like quadrupole tip with $Qd_z^2 = -0.25$ and a bending constant of $k = 0.35$ Nm^{-1}.

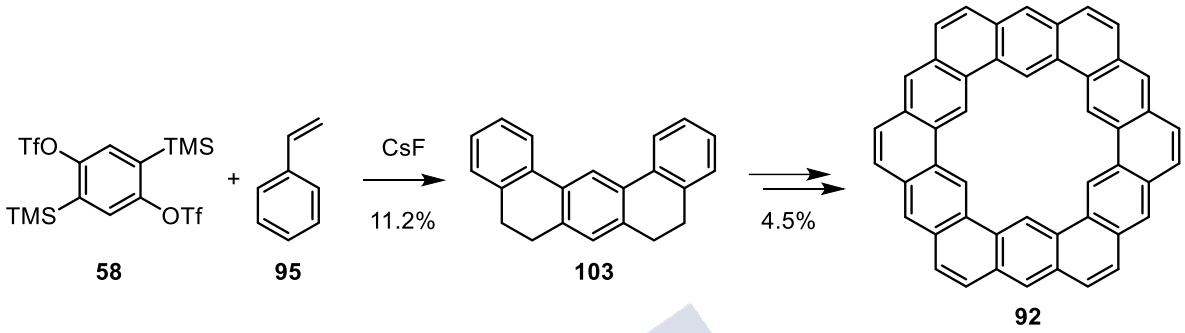
USC UNIVERSIDADE DE SANTIAGO DE COMPOSTELA

[216] B3LYP-def2-TZVP.

[217] **M**olecular **M**echanics (MM) model as implemented in the **P**robe **P**article **M**odel (PPM).

6.5 Conclusions

To conclude, we completed the second synthesis of kekulene (**92**) since the original work performed by Diederich and Staab. We improved it significatively, obtaining the key intermediate **103** in a four-fold increased yield, by means of aryne chemistry.



Scheme 78. Second synthesis of kekulene (**92**).

Additionally, we contributed to the structural study of kekulene at the single-molecular level, in collaboration with Dr. L. Gross and coworkers, and Prof. M. Melle-Franco. High resolution AFM images and theoretical calculations were provided. Both approaches agree with previous experimental evidences and constitute the last support of the Clar structure of kekulene.

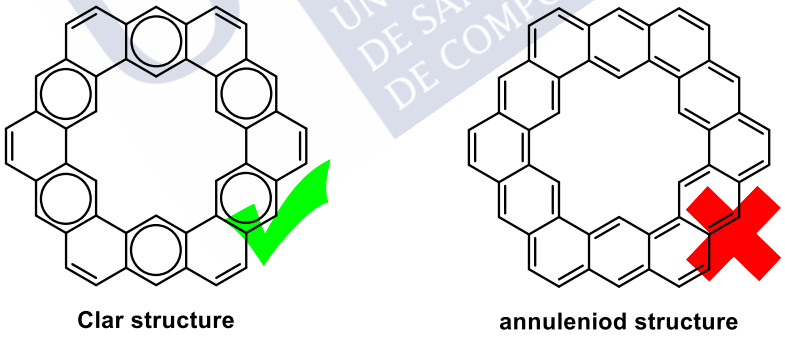


Figure 67. Kekulene's Clar structure.

USC
UNIVERSIDADE
DE SANTIAGO
DE COMPOSTELA

7 Experimental section

7.1 General procedures

All reactions were carried out under argon atmosphere using oven-dried glassware. Manipulation of air-sensitive compounds was carried out using standard Schlenk techniques.

Dry THF, Et_2O, hexane, MeCN, toluene, CH_2Cl_2 and DMF were obtained by an MBraun SPS-800 Solvent Purificarion System. Dioxane was dried by distillation over Na using benzophenone as indicator, 1,2,4-trichlorobenzene was dried by distillation over $CaSO_4$. $CHCl_3$ was dried by distillation over CaH_2. Dry solvents were stored in Schlenk tubes under argon over 4 Å molecular sieves.

Bisarynes precursors 2,5-bis(trimethylsilyl)-1,4-phenylene bis(trifluoro-methanesulfonate) (**58**)[93] and 3,6-bis(trimethylsilyl)naphthalene-2,7-diyl bis(trifluoro-methanesulfonate) (**73**)[138] were synthesised following published procedures. Aryne precursors **85**, **86**, **87**, **89**, **90** and **91** were synthesised following published procedures.[186] Chlorooxime **74**,[187] and cyclopentadienones **76** and **77**,[188] were synthesised following a published procedure. $Pd(PPh_3)_4$ was prepared from $PdCl_2$ following a published procedure.[218] TMSCl, pyridine, *i*-Pr_2NEt, *i*-Pr_2NH, TMEDA, NEt_3 and Tf_2O were dried by distillation from CaH_2. TBAF was dried by heating under vacuum for 3 days (60 - 100 °C) and subsequently dissolved in 1 M stock

[93] H. M. Duong, M. Bendikov, D. Steiger, Q. Zhang, G. Sonmez, J. Yamada, F. Wudl, *Org. Lett.* **2003**, *5*, 4433–4436.
[138] C. Kitamura, Y. Abe, T. Ohara, A. Yoneda, T. Kawase, T. Kobayashi, H. Naito, T. Komatsu, *Chem. A Eur. J.* **2010**, *16*, 890–898.
[186] D. Rodríguez-Lojo, D. Peña, D. Pérez, E. Guitián, *Synlett* **2015**, *26*, 1633–1637.
[187] A. V. Dubrovskiy, R. C. Larock, *Org. Lett.* **2010**, *12*, 1180–1183.
[188] R. A. Pascal Jr., W. D. McMillan, D. Van Engen, R. G. Eason, *J. Am. Chem. Soc.* **1987**, *109*, 4660–4665.
[218] a) L. S. Hegedus, *Palladium in Organic Synthesis* In *Organometallics in Synthesis: A Manual*; M. Schlosser, Ed.; John Wiley & Sons: New York, **1994**; b) M. M. Huq, M. R. Rahman, M. Naher, M. M. R. Khan, M. K. Masud, G. M. G. Hossain, N. Zhu, Y. H. Lo, M. Younus, W. Wong, *J. Inorg. Organomet. Polym.* **2016**, *26*, 1243–1252.

solution. *n*-BuLi was titrated by using diphenyl acetic acid and 1,3-diphenylpropanylidene-tosylhydrazine methods. Finely powdered CsF was dried under vacuum at 100 °C, cooled under argon and stored in a glove-box. Zn was activated following a published procedure.[219] Other commercial reagents were purchased from ABCR GmbH, Sigma-Aldrich or Acros Organics and TCI Chemicals, and were used without further purification unless otherwise noted.

Thin **l**ayer **c**hromatography (TLC) was performed on Merck silica gel 60 F_{254} and chromatograms were visualised with UV light (254 and 365 nm). Column chromatography was performed on Merck silica gel 60 (ASTM 230–400 mesh). Reactions at -78 °C were carried out in a mixture of acetone and dry ice cooling bath and reactions at -100 °C were carried out in a mixture of Et_2O/N_2 cooling bath.

Centrifugation was performed in a Hettich EBA21 centrifuge. Melting points were measured by a Büchi melting point B-450 instrument. **H**igh **p**erformance **l**iquid **c**hromatography (HPLC) was performed with CHIRALPAK IA. Supercritical Fluid Chromatography (SFC) was performed on a JASCO-4000 series apparatus. UV-Vis spectra were measured by a Jasco V-630 spectrometer. Fluorescence in solution was measured in a Fluoromax-2 spectrofluorimeter. Electrochemical measurements were carried out by a C3 Cell Stand Electrochemical Station Instrument, equipped with BAS Epsilon (Bioanalytical Systems, Inc., Lafayette, IN).

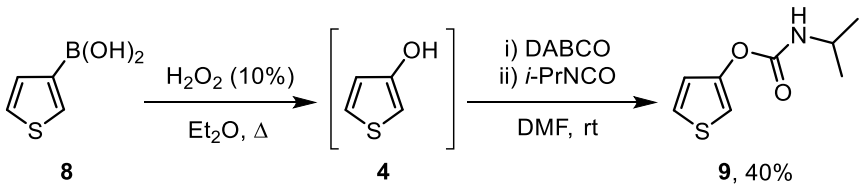
^{1}H, ^{19}F and ^{13}C NMR spectra were recorded at 300, 282 and 75 MHz (Varian Mercury 300 instrument), 400, 376, 101, (Varian Inova 400 instrument), 500, 470 and 125 MHz (Varian Inova 500) or 750, 705 and 188 MHz (Neo 750 instrument) respectively. **L**ow-**r**esolution **m**ass **s**pectra (LRMS) **E**lectron **i**onisation (EI) were obtained at 70 eV on a HP-5988A instrument, while **h**igh-**r**esolution **m**ass s**p**ectra (HRMS) EI were obtained on a Micromass Autospec spectrometer. **A**tmospheric **p**ressure **c**hemical **i**onisation (APCI) HRMS were obtained on a Bruker Microtof. **M**atrix-**a**ssisted **l**aser **d**esorption/**i**onisation (MALDI) - **t**ime-**o**f **f**light (TOF) and **N**anotechnology-**a**ssisted **l**aser **d**esorption/**i**onisation (NALDI) - TOF mass spectra were determined on a Bruker Autoflex instrument.

[219] G. Thanasis, K. Masato, *J. Org. Chem*. **1993**, *58*, 7158–7161.

7.2 Experimental procedures for Chapter 2

7.2.1 Synthesis of 2-(trimethylsilyl)-3-thiophenyl trifluoromethanesulfonate (2)

Synthesis of thiophen-3-yl isopropylcarbamate (9)

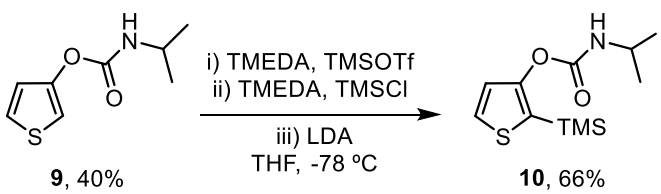


8 **4** **9**, 40%

To an ethereal solution (10 mL) of thiophen-3-ylboronic acid (**8**, 0.50 g, 3.91 mmol), H_2O_2 solution (10% in water, 3.0 mL) was added. The reaction mixture was refluxed for 2 h and the layers were separated. The aqueous layer was extracted with Et_2O (2 x 5 mL). The combined ethereal solutions were washed with NH_4Cl solution (10% in water, 10 mL), water (10 mL), and dried over Na_2SO_4. Most part of the Et_2O was removed by passing an argon flux and heating at 40 °C. The resulting orange ethereal solution of thiophen-3-ol (**4**) was used in the next reaction.

To the obtained thiophen-3-ol (**4**) ethereal solution anhydrous DMF (5.0 mL) and DABCO (0.44 g, 3.9 mmol) were added. The mixture was stirred for 1 h at rt. Isopropyl isocyanate (0.4 ml, 4.0 mmol) was added and solution was stirred for 1 h. Upon completion, it was quenched with water (10 mL) and extracted with EtOAc (3x5 mL). The combined organic layers were dried over Na_2SO_4 and concentrated in vacuo. The crude residue was purified by column chromatography (eluting with CH_2Cl_2) to afford thiophen-3-yl isopropylcarbamate (**9**) as a white solid (294 mg, 40%, m.p.: 87-88 °C). ^{1}H NMR (300 MHz, $CDCl_3$), δ: 7.16 (dd, *J* = 5.1, 3.4 Hz, 1H), 7.00 (dd, *J* = 3.2, 1.2 Hz, 1H), 6.90 (d, *J* = 5.2 Hz, 1H), 5.12 (s, 1H), 3.84 (m, 1H), 1.17 (d, *J* = 6.6 Hz, 6H) ppm. ^{13}C NMR-DEPT (75 MHz, $CDCl_3$), δ: 153.1 (C), 147.7 (C), 123.9 (CH), 121.6 (CH), 109.9 (CH), 43.4 (CH), 22.7 (CH_3) ppm. MS (EI), m/z: 185 (M^+, 100). HRMS (EI), m/z found: 185.0513 (calc. for $C_8H_{11}NO_2S$: 185.0511).

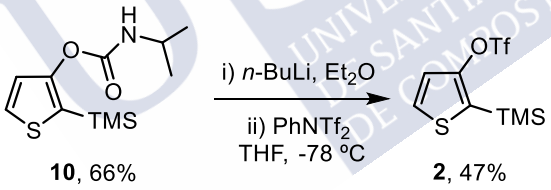
Synthesis of 2-(trimethylsilyl)-3-thiophenyl isopropylcarbamate (10)



9, 40% **10**, 66%

To a solution of carbamate **9** (100 mg, 0.54 mmol) in THF (6.5 mL) at –78 °C, TMEDA (118 µL, 0.81 mmol) was added, followed by TMSOTf (118 µL, 0.65 mmol). After stirring for 5 min, the solution was allowed to warm up to rt (25 min). The mixture was then recooled to –78 °C and TMEDA (0.26 mL, 1.8 mmol) was added, followed by neat TMSCl (82 µL, 0.65 mmol). After 5 min, LDA in THF (1.0 M, 1.35 mmol) was dropwise added (25 min). The mixture was stirred at –78 °C for 2.5 h and quenched with NH_4Cl solution (saturated in water, 5 mL). The layers were separated, and the aqueous layer was extracted with AcOEt (3 x 5 mL). The combined organic layers were dried over Na_2SO_4. Evaporation under reduced pressure afforded the crude product, which was purified by column chromatography (eluting with CH_2Cl_2) to afford **10** as a white solid (92 mg, 66% yield, m.p.: 90 °C). ^{1}H NMR (300 MHz, $CDCl_3$), δ: 7.42 (d, *J* = 4.9 Hz, 1H), 7.00 (d, *J* = 4.9 Hz, 1H), 4.86 (s, 1H), 3.97 – 3.79 (m, 1H), 1.21 (d, *J* = 6.6 Hz, 6H), 0.30 (s, 9H) ppm. ^{13}C NMR-DEPT (75 MHz, $CDCl_3$), δ: 153.5 (C), 153.7 (C), 129.0 (CH), 123.7 (CH), 123.3 (C), 43.4 (CH), 23.1 (CH_3), 0.3 (CH_3) ppm. MS (APCI), m/z: 258 (M^++1, 100). HRMS (APCI), m/z found: 258.0980 (calc. for $C_{11}H_{20}NO_2SSi$: 258.0978).

Synthesis of 2-(trimethylsilyl)-3-thiophenyl trifluoromethanesulfonate (2)



10, 66% **2**, 47%

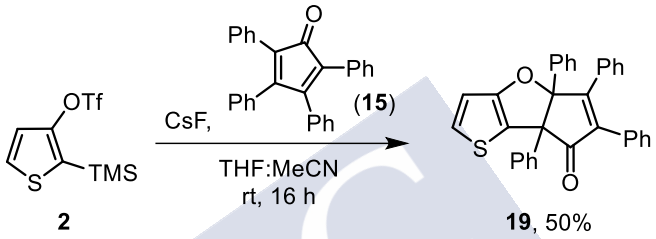
To a solution of silyl carbamate **10** (90 mg, 35 mmol) in THF (4.7 mL) at –78 °C, a solution of *n*-BuLi (2.5 M in hexane, 0.42 mmol) was dropwise added. After stirring for 2 min, Et_2NH (44 µL, 0.42 mmol) was added. 10 min later, $PhNTf_2$ (200 mg, 0.56 mmol) was added in a single portion, and the reaction was stirred additional 25 min at –78 °C. The reaction was then allowed to warm up to rt (25 min). Then, it was quenched wit $NaHCO_3$ solution (saturated in water, 5 mL). H_2O (5 mL) and EtOAc (10 mL) were added. The layers were separated, and the aqueous layer was extracted with EtOAc (2 x 10 mL). The combined organic layers were dried over Na_2SO_4. Evaporation of most part of the solvent under reduced pressure afforded the crude product in AcOEt.[220] The concentrated acetate solution was seeded and purified by column

[220] It is important do not evaporate the crude solution until complete dryness, otherwise the product decomposes. Pure **2** is stable.

chromatography (eluting with hexane) to afford **2** (50 mg, 47% yield) as a colourless oil. ^{1}H NMR (300 MHz, $CDCl_3$), δ: 7.53 (d, *J* = 5.1 Hz, 1H), 7.09 (d, *J* = 5.1 Hz, 1H), 0.39 (s, 9H) ppm. ^{13}C NMR-DEPT (75 MHz, $CDCl_3$), δ: 148.2 (C), 130.7 (CH), 128.1 (C), 121.1 (CH), 118.6 (q, *J* = 320.3 Hz, CF_3), -0.6 (C) ppm. MS (EI), m/z: 304 (M^+, 3), 289 (M^+-15, 13). HRMS (EI), m/z found: 303.9874 (calc. for $C_8H_{11}O_3F_3S_2Si$: 303.9871).

7.2.2 Reactivity of 2-(trimethylsilyl)-3-thiophenyl trifluoromethanesulfonate (2)

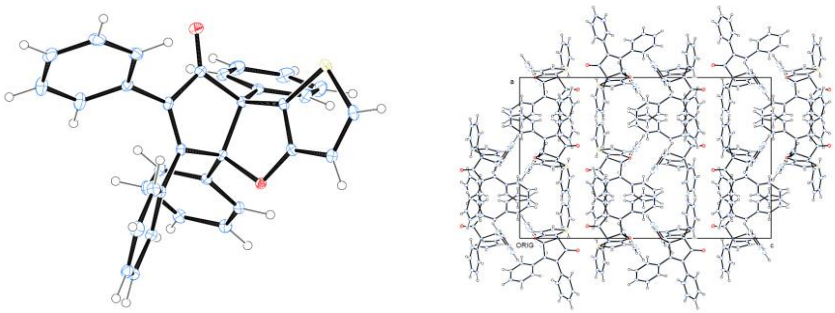
Synthesis of tricycle 19



To a solution of triflate **2** (100 mg, 0.33 mmol) and 2,3,4,5-tetraphenylcyclopentadienone (**15**, 150 mg, 0.39 mmol) in MeCN:THF (1:1, 2 mL) at rt, CsF (300 mg, 1.9 mmol) was added. The mixture was stirred for 16 h. Volatiles were removed under reduced pressure and the residue was purified by column chromatography (eluting with hexane:CH_2Cl_2, 3:2) to afford **19** (80 mg, 50%, m.p.:184-185 °C) as a white solid. ^{1}H NMR (300 MHz, $CDCl_3$), δ: 7.41 (m, 2H), 7.34 (m, 3H), 7.30 (m, 2H), 7.27 (m, 1H), 7.20 – 7.07 (m, 5H), 7.03 – 6.94 (m, 6H), 6.85 (dd, *J* = 6.7, 3.0 Hz, 2H), 6.81 (d, *J* = 5.3 Hz, 1H) ppm. ^{13}C NMR-DEPT (75 MHz, $CDCl_3$), δ: 163.0 (C), 160.4 (C), 142.4 (C), 137.4 (C), 137.1 (C), 133.3 (C), 131.1 (C), 130.4 (CH), 130.3 (CH), 130.0 (CH), 129.3 (CH), 129.3 (CH), 128.6 (C), 128.4 (CH), 128.1 (CH), 127.6 (CH), 127.6 (CH), 127.4 (CH), 127.1 (CH), 126.7 (CH), 118.8 (C), 111.8 (CH), 108.6 (C), 71.2 (C) ppm. IR (ν): 3088, 3058, 3030, 1703, 1445, 1336, 1146, 736, 694 cm^{-1}. MS (EI), m/z: 482 (M^+, 4), 454 (M^+-28, 100). HRMS (EI), m/z found: 482.1343 (calc. for $C_{33}H_{22}O_2S$: 482.1341).

X-Ray structure of 19

The **C**ambridge **C**rystallographic **D**ata **C**entre (CCDC) 1837531 record contains the supplementary crystallographic data for compound **19**. These data can be obtained free of charge from https://www.ccdc.cam.ac.uk/

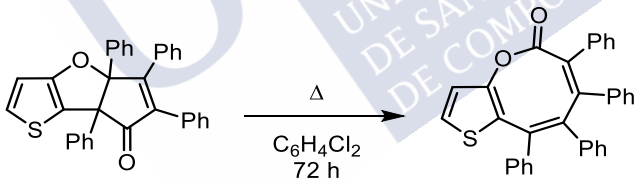


Formula: $C_{33}H_{22}O_2S$

Unit cell parameters: a = 17.0030(6); b = 10.8953(4); c = 25.9401(8)

Space group: P b c a

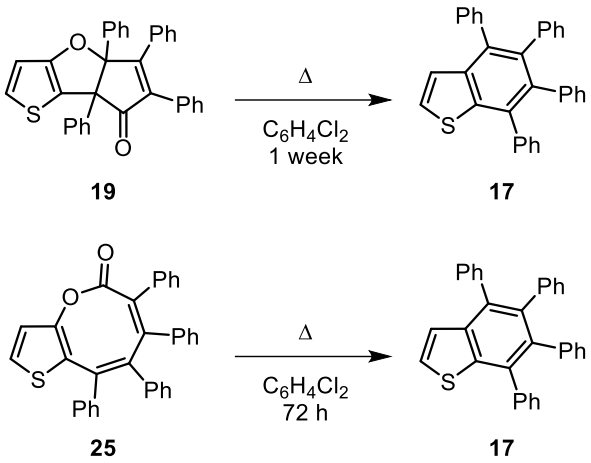
Synthesis of tetraphenyl-5H-thieno[3,2-*b*]oxocin-5-one (25)



19 **25**, 78%

A solution of tricycle **19** (60 mg, 0.12 mmol) in *o*-dichlorobenzene was refluxed (180 °C) for 72 h. The solvent was removed under reduced pressure and the residue was purified by column chromatography (eluting with hexane:CH_2Cl_2, 3:1) to afford **25** (47 mg, 78%, m.p.: 250 °C) as a yellow solid. ^{1}H NMR (300 MHz, $CDCl_3$), δ: 7.27 – 7.15 (m, 7H), 7.10 – 7.02 (m, 4H), 6.86 (d, *J* = 4.7 Hz, 6H), 6.75 m, 4H), 6.37 (d, *J* = 10.6 Hz, 1H) ppm. ^{13}C NMR-DEPT (75 MHz, $CDCl_3$), δ: 163.1 (C), 147.4 (C), 145.4 (CH), 143.6 (C), 142.3 (C), 139.2 (C), 138.7 (C), 138.5 (C), 138.2 (C), 136.8 (C), 135.7 (C), 131.0 (CH), 130.9 (CH), 130.6 (CH), 130.3 (CH), 127.6 (CH), 127.4 (CH), 127.3 (CH), 127.1 (CH), 126.8 (CH), 125.9 (C), 125.8 (C), 123.4 (C) ppm. IR: 3057, 3027, 1728, 1442, 1392, 1249, 1235, 1142, 1099, 731, 695 cm^{-1}. MS (APCI), m/z: 483 (M^++1, 100). HRMS (APCI), m/z found: 483.1411 (calc. for $C_{33}H_{23}O_2S$: 483.1413).

Synthesis of 4,5,6,7-tetraphenylbenzo[*b*]thiophene (17)



A solution of **19** or **25** in *o*-dichlorobenzene was refluxed (180 °C). The conversion of both compounds into **17** was monitored by TLC, observing full conversion after 1 week or 3 days respectively. Spectroscopic data were identical to those described in the literature for this compound.[129] ^{1}H NMR (300 MHz, $CDCl_3$), δ: 7.39 (d, *J* = 5.6 Hz, 1H), 7.33 – 7.19 (m, 10H), 7.16 (d, *J* = 5.5 Hz, 1H), 6.91 – 6.80 (m, 10H) ppm. IR (ν): 3079, 3056, 3025, 1602, 1441, 1417, 1265, 732, 699 cm^{-1}.

7.2.3 Computational details

All the calculations were performed using the Gaussian 09 program package.[221] Geometries of intermediates and transition states were optimised at the density functional level using the B3LYP functional[222] and 6-31G(d) basis set. Frequency calculations were performed at this level to confirm the nature of the stationary points and to obtain the thermal and entropic contribution to the free energy. Single-point calculations were carried out for all optimised gas-

---

[129] A. Bej, A. Chakraborty, A. Sarkar, *RSC Adv.* **2013**, *3*, 15812–15819.

[221] Gaussian 09, Revision **D.01**, M. J. Frisch, G. W. Trucks, H. B. Schlegel, G. E. Scuseria, M. A. Robb, J. R. Cheeseman, G. Scalmani, V. Barone, B. Mennucci, G. A. Petersson, H. Nakatsuji, M. Caricato, X. Li, H. P. Hratchian, A. F. Izmaylov, J. Bloino, G. Zheng, J. L. Sonnenberg, M. Hada, M. Ehara, K. Toyota, R. Fukuda, J. Hasegawa, M. Ishida, T. Nakajima, Y. Honda, O. Kitao, H. Nakai, T. Vreven, J. A. Montgomery, Jr., J. E. Peralta, F. Ogliaro, M. Bearpark, J. J. Heyd, E. Brothers, K. N. Kudin, V. N. Staroverov, R. Kobayashi, J. Normand, K. Raghavachari, A. Rendell, J. C. Burant, S. S. Iyengar, J. Tomasi, M. Cossi, N. Rega, J. M. Millam, M. Klene, J. E. Knox, J. B. Cross, V. Bakken, C. Adamo, J. Jaramillo, R. Gomperts, R. E. Stratmann, O. Yazyev, A. J. Austin, R. Cammi, C. Pomelli, J. W. Ochterski, R. L. Martin, K. Morokuma, V. G. Zakrzewski, G. A. Voth, P. Salvador, J. J. Dannenberg, S. Dapprich, A. D. Daniels, Ö. Farkas, J. B. Foresman, J. V. Ortiz, J. Cioslowski, D. J. Fox, Gaussian, Inc., Wallingford CT, **2009**.

[222] a) A. D. Becke*, J. Chem. Phys.* **1993**, *98*, 5648–5652; b) C. Lee, W. Yang, R. G. Parr, *Phys. Rev. B* **1988**, *37*, 785–789.

phase geometries using the B3LYP functional and the 6-31++G(d,p) basis set. Solvation corrections for acetonitrile of 35.688 were computed using **c**onductor **p**olarizable **c**alculation **m**odel (CPCM).[223]

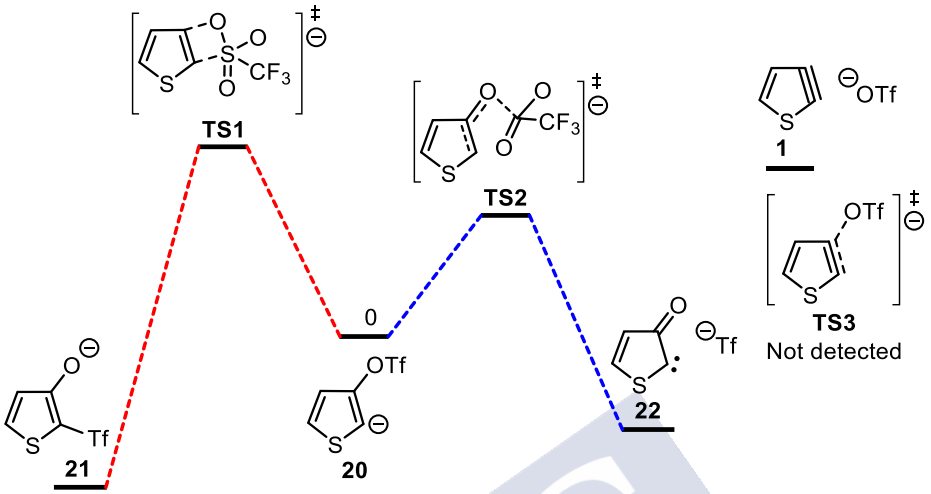


Table 4. Evolution of anion **20**.

Entry[a]	Compound	ΔG / Kcal mol^{-1} (Gas phase)[b]	ΔG / Kcal mol^{-1} (Sol.)[c]
1	**20**	0	0
2	**TS1**	16.8	14
3	**TS2**	8.5	7
4	**1 + OTf**	11.7	19
5	**22 + Tf**	-18.7	-6
6	**21**	-47.5	-46

Geometries optimised by DFT-B3LYP/6-31G(d). b) Single point calculation by DFT-B3LYP/6-31G++(d,p). c) Solvation was computed using CPCM for MeCN.

[223] a) M. Cossi, N. Rega, G. Scalmani, V. Barone, *J. Comp. Chem.* **2003**, *24*, 669–681; b) V. Barone M. Cossi, *J. Phys. Chem. A* **1998**, *102*, 1995–2001.

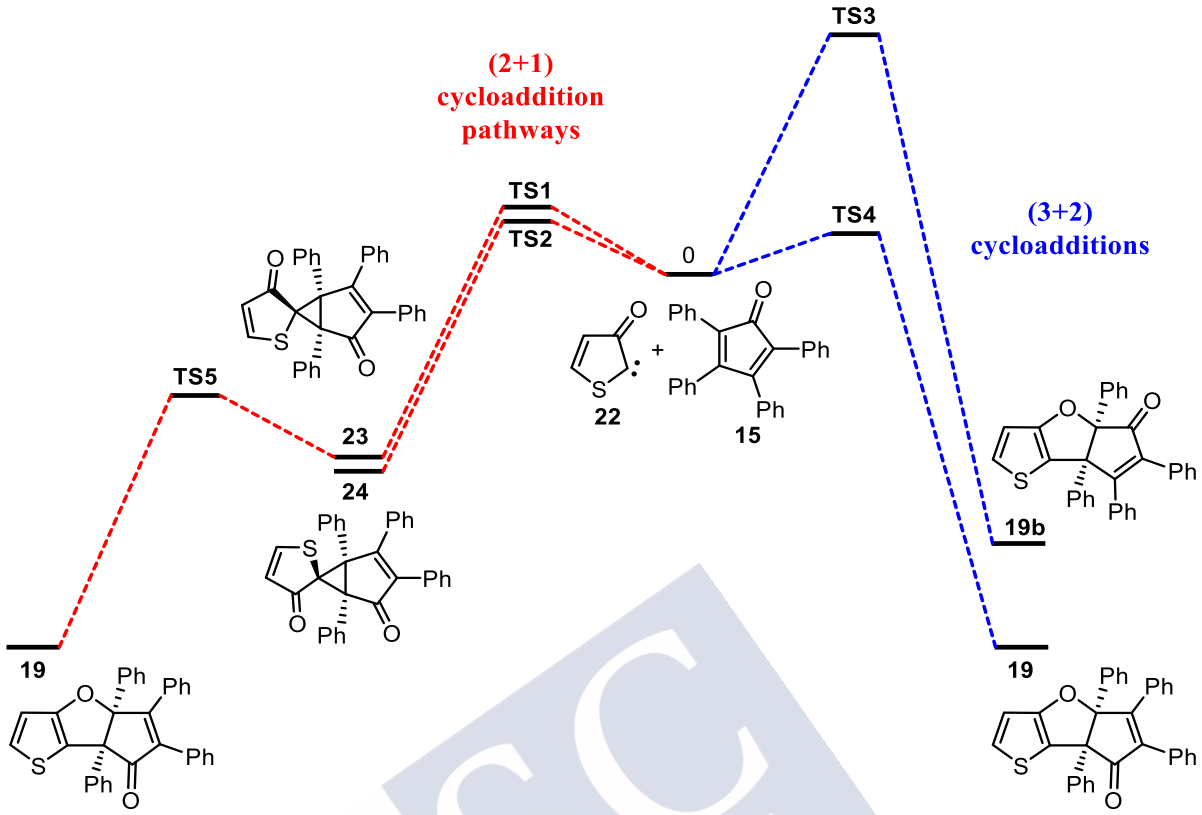


Table 5. Cycloaddition between **22** and **15**.

Entry[a]	Compound	ΔG / Kcal mol^{-1} (Gas phase)[b]	ΔG / Kcal mol^{-1} (Sol.)[c]
1	**22 + 15**	0	0
2	**TS1**	12	5.1
3	**TS2**	13	4.8
4	**TS3**	26	18
5	**TS4**	9.7	3.2
6	**23**	-45	-56
7	**24**	-47	-58
8	**TS5**	-23	-33
9	**19b**	-53	-65
10	**19**	-59	-68

Geometries optimised by DFT-B3LYP/6-31G(d). b) Single point calculation by DFT-B3LYP/6-31G++(d,p). c) Solvation was computed using CPCM for MeCN.

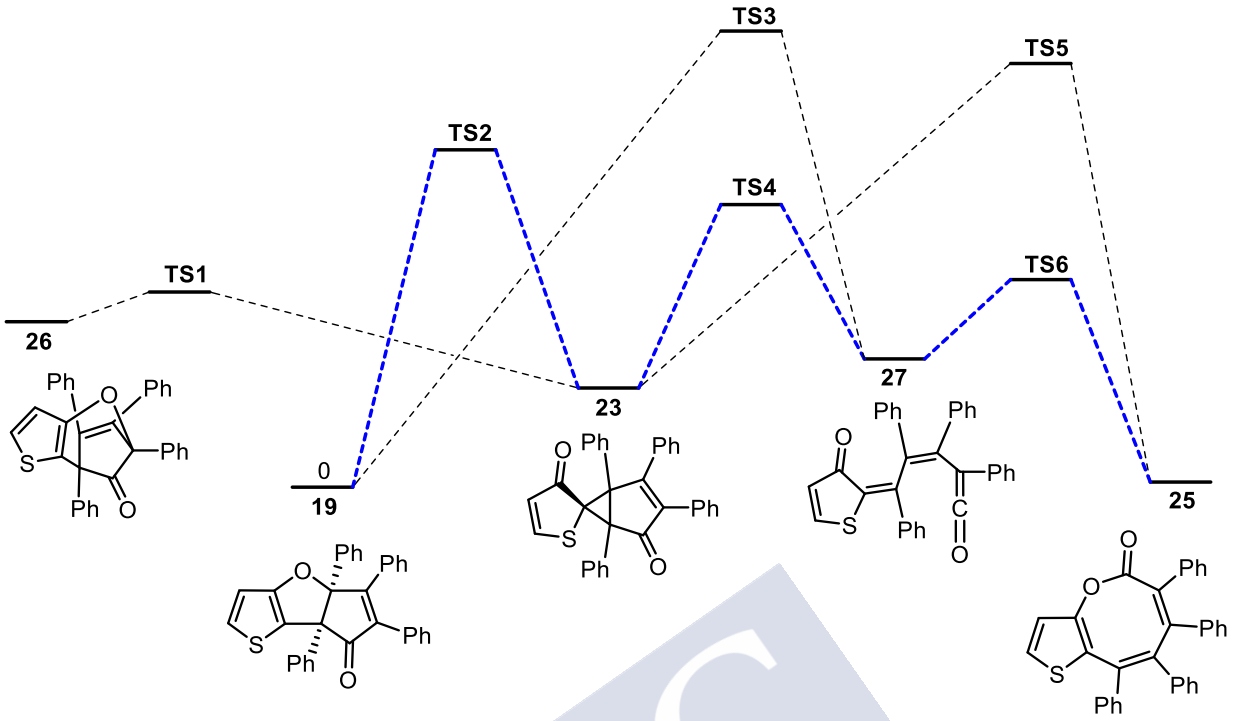


Table 6. Evolution of **19** into **25**.

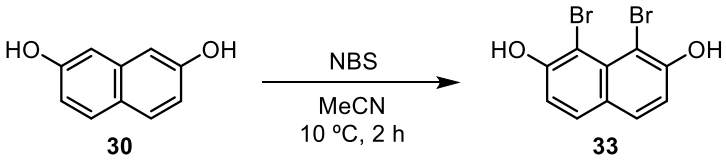
Entry[a]	Compound	ΔG / Kcal mol^{-1} (Gas phase)[b]
1	**26**	13
2	**TS1**	25
3	**19**	0
4	**TS2**	35
5	**23**	14
6	**TS3**	39
7	**TS4**	31
8	**27**	16
9	**TS5**	38
10	**TS6**	26
11	**25**	-0.1

Geometries optimised by DFT-B3LYP/6-31G(d). b) Single point calculation by DFT-B3LYP/6-31G++(d,p).

7.3 Experimental procedures for Chapter 3

7.3.1 Synthesis of 1,8-bis(trimethylsilyl)naphthalene-2,7-diyl bistriflate (32)

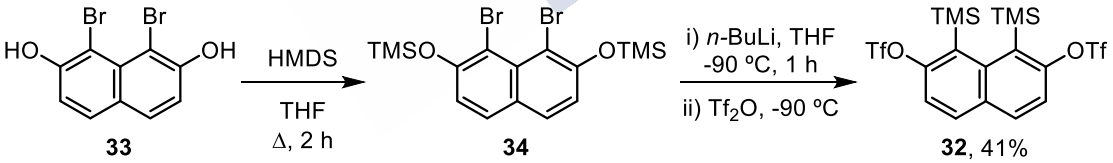
Synthesis of 1,8-dibromonaphthalene-2,7-diol (33)



30 **33**

NBS (1.2 g, 6.7 mmol) was added in portions to a solution of 2,7-naphthalenediol (**30**, 0.5 g, 0.1 M in MeCN) at 10 °C and the mixture was stirred under argon at this temperature for 2 h. The reaction was quenched by adding H_2SO_4 to pH = 1 and the reaction mixture was extracted with CH_2Cl_2 (3 x 100 mL). The solution was quickly filtered through a pad of SiO_2 (CH_2Cl_2) to afford **33** as a brown solid (1 g, >95%),[224] which was used in the next reaction without further purification. Spectroscopic data were coincident with those described in the literature for this compound.[144a] ^{1}H NMR (300 MHz, DMSO), δ: 10.58 (s, 2H), 7.71 (d, *J* = 8.8 Hz, 2H), 7.09 (d, *J* = 8.8 Hz, 2H) ppm.

Synthesis of 1,8-bis(trimethylsilyl)naphthalene-2,7-diyl bistriflate (32)



33 **34** **32**, 41%

A solution of 1,8-dibromonaphthalene-2,7-diol (**33**, 1 g, 3.1 mmol) and HMDS (3.4 mL, 15 mmol) in THF was refluxed for 2 h. Then volatiles (NH_3 and excess HMDS) were removed under reduced pressure. The crude product was dissolved in THF (0.1 M, 22 mL) and cooled to -90 °C. Then, *n*-BuLi solution (2.5 M in hexane, 2.7 mL) was added dropwise and the reaction mixture was stirred at -90 °C for 1 h and allowed to warm up to -80 °C. The reaction mixture was cooled again at -90 °C and Tf_2O (1.3 mL, 7.5 mmol) was dropwise added. The

---

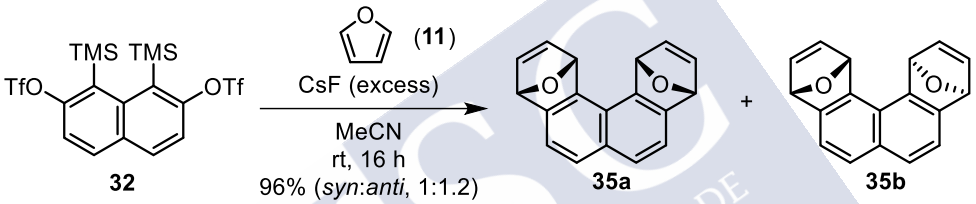
[224] Compound **33** decomposes in silica gel.

[144a] C. Thirsk, G. E. Hawkes, K. R. Liedl, T. Loerting, R. Nasser, R. G. Pritchard, M. Steele, J. E. Warren, A. Whiting, *J. Chem. Soc., Perkin Trans. 2* **2002**, *9*, 1510–1519.

reaction mixture was allowed to warm up to -80 °C and quenched wit $NaHCO_3$ solution (5% in water, 30 mL). After the mixture reached rt, the layers were separated, and the aqueous layer was further extracted with Et_2O (2 x 20 mL).

The combined organic layers were dried over Na_2SO_4 and concentrated in vacuo. The crude residue was purified by column chromatography (eluting with hexane:Et_2O, 39:1) to afford **32** (0.72 g, 41%, m.p.: 72-74 °C) as a white solid. ^{1}H NMR (300 MHz, $CDCl_3$), δ: 7.85 (d, *J* = 8.8 Hz, 2H), 7.36 (d, *J* = 8.8 Hz, 2H), 0.36 (s, 18H; TMS) ppm. ^{13}C NMR-DEPT ($CDCl_3$), δ: 155.3 (C), 143.2 (C), 134.0 (C), 132.4 (CH), 130.1 (C), 118.5 (CH), 118.0 (q, *J*= 320.1 Hz, CF_3), 2.1 (CH_3) ppm. MS (EI), m/z: 553 (M^+-15, 23), 73 (100).

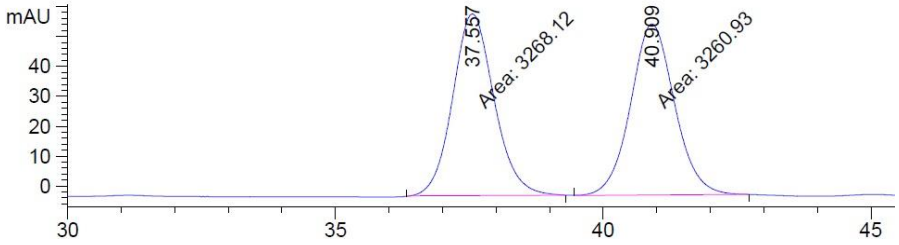
Synthesis of 1,4,9,12-tetrahydro-1,4:9,12-diepoxybenzo[*c*]phenanthrene (35)



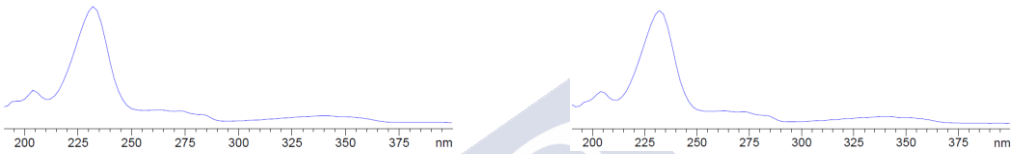
To a solution of furan (**11**, 75 µL, 1.1 mmol) and naphthodiyne precursor **32** (30 mg, 0.05 mmol) in MeCN (0.1 M, 0.5 mL), CsF (64 mg, 0.4 mmol) was added. The mixture was stirred at rt under argon for 16 h. Then, volatiles were removed under reduced pressure and the residue was purified by preparative TLC (eluting with hexane:CH_2Cl_2:Et_2O, 3:2:1) to isolate *syn*-isomer, **35a**, as a white solid (5.6 mg, 42%, m.p.: 142-144 °C), and *anti*-isomer, **35b**, as a yellow solid (7.7 mg, 54%, m.p.: 183-185 °C). Enantiomers of **35b** can be separated by Chiral HPLC (9:1, Hex:*i*-PrOH, 0.5 ml/min).**35a**: ^{1}H NMR (300 MHz, $CDCl_3$), δ: 7.59 (d, *J* = 8.2 Hz, 2H), 7.44 (d, *J* = 7.9 Hz, 2H), 7.19 (dd, *J* = 5.5, 1.8 Hz, 2H), 7.15 (dd, *J* = 5.5, 1.8 Hz, 2H), 6.39 (s, 2H), 5.90 (d, *J* = 1.0 Hz, 2H) ppm. MS (EI), m/z: 260 (M^+, 90), 206 (100). HRMS (EI), m/z found: 260.0837 (calc. for $C_{16}H_{12}O_2$: 260.0837). **35b**: ^{1}H NMR (300 MHz, $CDCl_3$), δ: 7.58 (d, *J* = 8.3 Hz, 2H), 7.44 (d, *J* = 8.0 Hz, 2H), 7.29 (dd, *J* = 5.5, 1.8 Hz, 2H), 7.23 (dd, *J* = 5.5, 1.8 Hz, 2H), 6.25 – 6.18 (m, 2H), 5.90 (d, *J* = 1.8 Hz, 2H) ppm. MS (EI), m/z: 260 (M^+, 90), 206 (100). HRMS (EI), m/z found: 260.0837 (calc. $C_{16}H_{12}O_2$: 260.0837).

Chromatogram of 35b enantiomers

HPLC was performed with CHIRALPAK IA (9:1, Hex:*i*-PrOH, 0.5 ml/min).



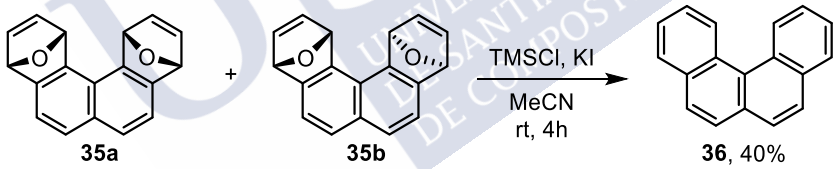
UV-Vis absorption spectra of 35b enantiomers



UV-Vis spectrum at 37.557 min.

UV-Vis spectrum at 40.909 min.

Synthesis of benzo[*c*]phenanthrene (36)

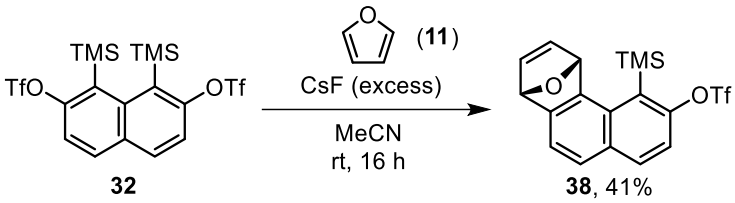


35a **35b** (syn: anti, 1:1.2) **36**, 40%

To a solution of **35** (mixture of isomers, 100 mg, 0.4 mmol) and KI (230 mg 2.2 mmol) in MeCN (3.8 mL), TMSCl (0.2 mL, 2.2 mmol) was dropwise added. The mixture was stirred under argon at rt for 4 h. Then, volatiles were removed under reduced pressure and the residue was purified by column chromatography (eluting with hexane) to isolate benzo[*c*]phenanthrene as a white solid (**36**, 33 mg, 40%). Spectroscopic data were coincident with those described in the literature for this compound.[225] ^{1}H NMR (300 MHz, $CDCl_3$), δ: 9.19 (d, *J* = 8.1 Hz, 2H), 8.06 (d, *J* = 7.8 Hz, 2H), 7.93 (d, *J* = 8.7 Hz, 2H), 7.86 (d, *J* = 8.7 Hz, 2H), 7.75 – 7.64 (m, 4H) ppm.

[225] M. Murai, N. Hosokawa, D. Roy, K. Taka, *Org. Lett.* **2014**, *16*, 4134–4137.

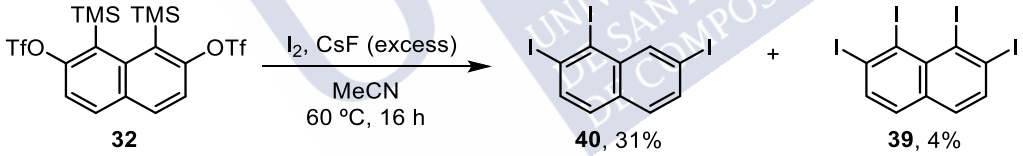
Synthesis of 5-(trimethylsilyl)-1,4-dihydro-1,4-epoxyphenanthren-6-yl trifluoro-methanesulfonate (38)



To a solution of furan (**11**, 75 µL, 1.1 mmol) and naphthodiyne precursor **32** (100 mg, 0.18 mmol) in MeCN (0.1 M, 1.8 mL), CsF (33 mg, 0.22 mmol) was added. The mixture was stirred at rt under argon for 16 h. Then, volatiles were removed under reduced pressure and the residue was purified by column chromatography (eluting with hexane:CH_2Cl_2 gradient) to afford **38** as yellow solid (31 mg, 41%). ^{1}H NMR (300 MHz, $CDCl_3$), δ: 7.93 – 7.84 (m, 1H), 7.71 – 7.62 (m, 1H), 7.61 – 7.53 (m, 1H), 7.24 – 7.08 (m, 3H), 6.57 – 6.49 (s, 1H), 5.94 (s, 1H), 0.65 (s, 9H) ppm.

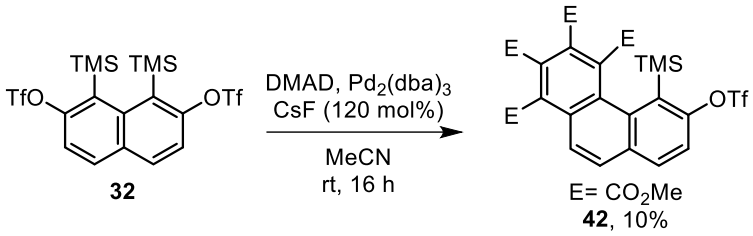
7.3.2 Reactivity of 1,8-bis(trimethylsilyl)naphthalene-2,7-diyl bistriflate (32)

Synthesis of 1,2,7-triiodonaphthalene (40) and 1,2,7,8-tetraiodonaphthalene (39)



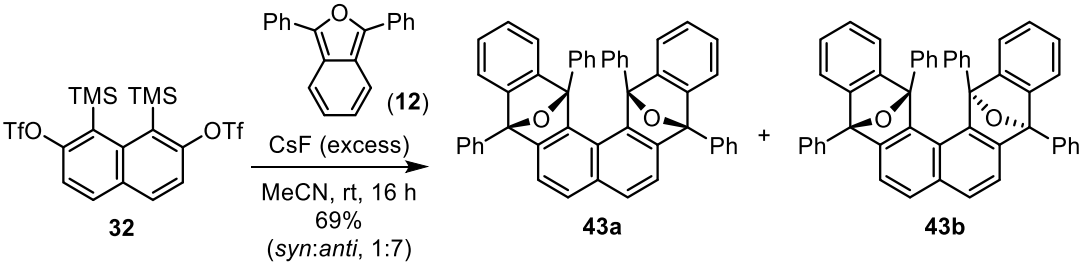
To a solution of iodine (178 mg, 0.7 mmol) and naphthodiyne precursor **32** (100 mg, 0.18 mmol) in MeCN (0.1 M, 1.8 mL), CsF (133 mg, 0.88 mmol) was added. The mixture was stirred at 60 ºC under argon for 16 h. Then, volatiles were removed under reduced pressure and the residue was purified by column chromatography (eluting with hexane) to afford **40** as white solid (28 mg, 31%, m.p.: 155-156 °C) and **39** as white solid (5 mg, 4%, m.p.: 182-183 °C). **40**: ^{1}H NMR (500 MHz, $CDCl_3$), δ: 8.67 (d, *J* = 2.6 Hz, 1H), 7.93 – 7.87 (m, 1H), 7.75 – 7.70 (m, 1H), 7.50 – 7.45 (m, 1H), 7.44 – 7.39 (m, 1H) ppm. ^{13}C NMR-DEPT (126 MHz, $CDCl_3$), δ: 144.2 (CH), 138.3 (C), 136.6 (CH), 135.9 (CH), 131.1 (C), 129.9 (CH), 129.8 (CH), 112.1 (C), 110.5 (C), 95.5 (C) ppm. MS (EI), m/z: 506 (M^+, 100). HRMS (EI), m/z found: 505.7526 (calc. for $C_{10}H_5I_3$: 505.7526). **39**: ^{1}H NMR (500 MHz, $CDCl_3$), δ: 7.93 (d, *J* = 8.5 Hz, 2H), 7.44 (d, *J* = 8.5 Hz, 2H) ppm. ^{13}C NMR-DEPT (126 MHz, $CDCl_3$), δ: 141.4 (C), 136.9 (CH), 132.4 (C), 128.9 (CH), 116.5 (C), 110.8 (C). MS (EI), m/z: 631 (M^+, 100), 504 (M^+-127, 55), 378 (M^+-254, 53). HRMS (EI), m/z found: 631.6474 (calc. for $C_{10}H_4I_4$: 631.6492).

Synthesis of tetramethyl 6-(((trifluoromethyl)sulfonyl)oxy)-5-(trimethylsilyl)phenanthrene-1,2,3,4-tetracarboxylate (42)



To a solution of DMAD (0.17 ml, 1.4 mmol), $Pd_2(dba)_3$ (10 mg, 9.7 µmol) and naphthodiyne precursor **32** (100 mg, 0.18 mmol) in MeCN (0.1 M, 1.8 mL), CsF (33 mg, 0.22 mmol) was added. The mixture was stirred at rt under argon for 16 h. Then, volatiles were removed under reduced pressure and the residue was purified by column chromatography (eluting with CH_2Cl_2:AcOEt, 50:1). Obtained solid was dissolved in Et_2O and precipitated by layering pentane to afford pure **42** as white solid (11 mg, 10%, m.p.: 75-78 ºC). ^{1}H NMR (400 MHz, $CDCl_3$), δ: 7.91 (d, *J* = 8.6 Hz, 1H), 7.76 (d, *J* = 9.1 Hz, 1H), 7.74 (d, *J* = 9.0 Hz, 1H), 7.63 (d, *J* = 8.7 Hz, 1H), 4.02 (s, 3H), 3.92 (s, 6H), 3.62 (s, 3H), 0.04 (s, 9H).ppm. ^{13}C NMR-DEPT (101 MHz, $CDCl_3$), δ: 167.6 (C), 167.4 (C), 167.3 (C), 166.0 (C), 156.4 (C), 135.8 (C), 134.5 (C), 134.5 (C), 133.2 (C), 132.4 (C), 131.6 (C), 131.6 (CH), 130.9 (C), 130.8 (C), 130.0 (CH), 127.4 (C), 123.7 (CH), 121.4 (CH), 53.5 (C), 53.5 (C), 53.5 (C), 53.3 (C), 2.1 (C) ppm. MS (EI), m/z: 481 (M+-150, 40), 648 (M+-15, 11). HRMS (EI), m/z found: 615.0605 (calc. for $C_{25}H_{22}O_{11}F_3SiS$: 615.0604).

Synthesis of 5,10,15,16-tetraphenyl-5,10,15,16-tetrahydro-5,16:10,15-diepoxynaphtho-[2,3-*a*]tetraphene *syn*-isomer (43a) and *anti*-isomer (43b)

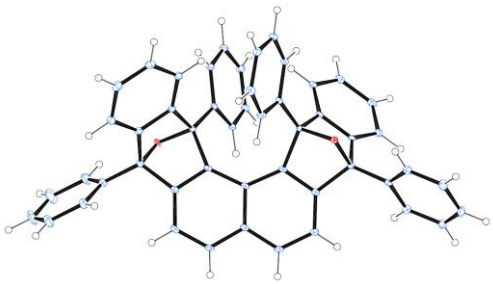


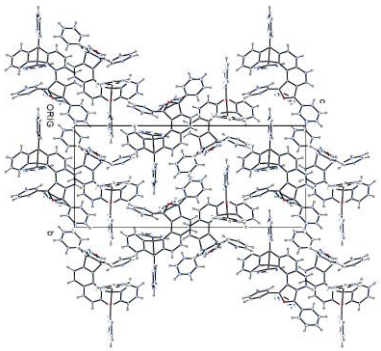
To a solution of 1,3-diphenylisobenzofuran (**12**, 150 mg, 0.6 mmol) and naphthodiyne precursor **32** (100 mg, 0.18 mmol) in MeCN (1.8 mL, 0.1 M), CsF (230 mg, 1.4 mmol) was added. The mixture was stirred at rt under argon for 16 h. Then, volatiles were removed under reduced pressure. The resulting solid residue was centrifuged with water (3 x 10 mL), MeOH

(3 x 10 mL), hexane (3 x 10 mL) and Et_2O (3 x 10 mL) to afford *anti*-isomer, **43b**, as a brown solid (72 mg, 61%, m.p.: 267-269 ºC). The organic ethereal phase was concentrated under reduced pressure to afford *syn*-isomer, **43a**, as a brown solid (10 mg, 8%, m.p.: 273-275 ºC). **43b**: ^{1}H NMR (300 MHz, $CDCl_3$), δ: 7.70 – 7.61 (m, 6 H), 7.54 – 7.44 (m, 6 H), 7.41 (dd, *J* = 8.1, 3.1 Hz, 4 H), 7.36 – 7.23 (m, 8 H), 7.22 – 7.16 (m, 2 H), 6.93 (t, *J* = 7.4 Hz, 2 H), 6.71 (t, *J* = 7.4 Hz, 2 H), 5.89 (d, *J* = 7.2 Hz, 2 H) ppm. ^{13}C NMR-DEPT (75 MHz, $CDCl_3$), δ: 153.6 (C), 151.7 (C), 145.3 (C), 145.3 – 145.2 (C), 145.2 – 145.0 (C), 136.2 (C), 135.5 (C), 132.3 – 131.8 (C), 129.5 (CH), 129.1 (CH), 128.5 (CH), 127.8 (CH), 127.7 (CH), 127.1 (CH), 126.7 (C), 126.1 (CH), 125.8 (CH), 124.0 (CH), 122.5 (CH), 119.3 (CH), 118.0 (CH), 96.5 – 94.3 (C), 90.6 – 88.9 (C), 88.6 (C). MS (EI), m/z: 664 (M^+, 100), 648 (M^+-16, 15). HRMS (EI), m/z found: 664,2404 (calc. for $C_{50}H_{32}O_2$: 664.2402). **43a**: ^{1}H NMR (300 MHz, $CDCl_3$), δ: 7.69 – 7.63 (m, 8 H), 7.53 – 7.45 (m, 8 H), 7.44 – 7.36 (m, 6 H), 7.34 (d, *J* = 7.3 Hz, 4 H), 6.93 (td, *J* = 7.7, 0.7 Hz, 2 H), 6.71 (td, *J* = 7.6, 0.9 Hz, 2 H), 5.90 (d, *J* = 7.2 Hz, 2 H) ppm. ^{13}C NMR-DEPT (75 MHz, $CDCl_3$), δ: 153.7 (C), 151.9 (C), 145.5 (C), 145.3 (C), 136.4 (C), 135.7 (C), 129.7 (CH), 129.3 (CH), 128.6 (CH), 127.8 (CH), 126.3 (CH), 125.9 (CH), 124.2 (CH), 122.7 (CH), 119.5 (CH), 118.2 (CH), 95.3 (C), 88.7 (C). MS (EI), m/z: 664 (M^+, 100), 648 (M^+-16, 15). HRMS (EI), m/z found: 664.2409 (calc. for $C_{50}H_{32}O_2$: 664.2402).

X-Ray structure of 43b

The **C**ambridge **C**rystallographic **D**ata **C**entre (CCDC) 1443038 record contains the supplementary crystallographic data for compound **43b**. These data can be obtained free of charge from https://www.ccdc.cam.ac.uk/



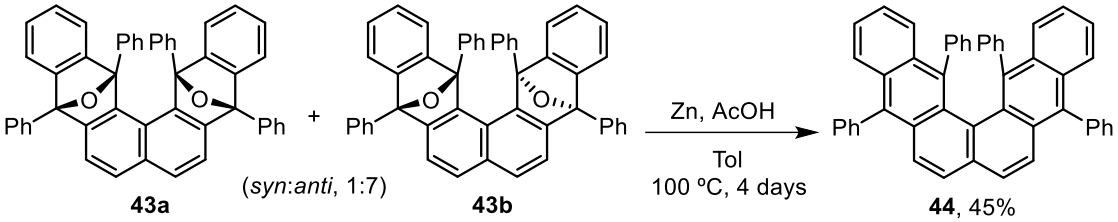


Formula: $C_{50}H_{32}O_2$

Unit cell parameters: a = 8.8161(4); b = 13.0764(6); c = 29.5577(14)

space group: P21/c

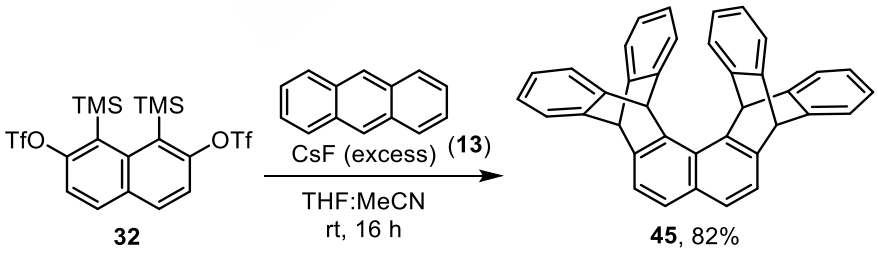
Synthesis of naphtho[2,3-*a*]tetraphene (44)



43a (*syn*:*anti*, 1:7) **43b** **44**, 45%

To a suspension of Zn (50 mg, 0.8 mmol) in AcOH (0.5 mL), a solution of **43** (mixture of isomers, 20 mg, 0.03 mmol) in toluene (10 mL) was added. The mixture was heated at 100 ºC under argon for 4 days. Then, volatiles were removed under reduced pressure and the residue was purified by column chromatography (eluting with hexane: CH_2Cl_2, 4:1) to isolate naphtho[2,3-*a*]tetraphene as a yellow solid (**44**, 8.6 mg, 45%, m.p.: 280-282 ºC). ^{1}H NMR (500 MHz, $CDCl_3$), δ: 8.02 (d, J = 8.2 Hz, 4H), 7.68 – 7.61 (m, 2H), 7.62 – 7.52 (m, 6H), 7.45 – 7.39 (m, 4H), 7.38 – 7.37 (m, 4H), 7.36 – 7.27 (m, 4H), 6.71 (s, 6H), 5.88 (s, 2H) ppm. ^{13}C NMR-DEPT (126 MHz, $CDCl_3$), δ: 140.2 (C), 139.6 (C), 136.1 (C), 133.8 (C), 132.9 (C), 132.1 (CH), 131.8 (CH), 131.6 (C), 131.2 (C), 130.6 (C), 129.5 (C), 129.5 (C), 128.6(CH), 128.5 (CH), 128.1 , 127.8 (CH), 127.3 (CH), 126.4 (CH), 126.1 (CH), 125.6 (CH), 125.5 (CH), 124.7 (CH), 124.5 (CH) ppm. MS (EI), m/z: 632 (M^+, 100). HRMS (EI), m/z found: 632.2504 (calc. for $C_{50}H_{32}$: 632.2504).

Synthesis of 5,10,15,16-tetrahydro-5,16:10,15-bis([1,2]benzeno)naphtho[2,3-*a*]-tetraphene (45)



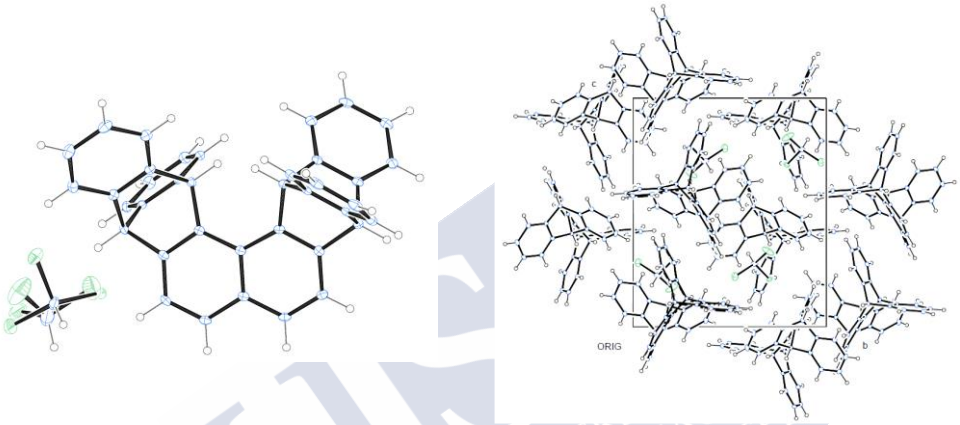
32 **45**, 82%

To a solution of anthracene (**13**, 70 mg, 0.4 mmol) and naphthodiyne precursor **32** (100 mg, 0.18 mmol) in MeCN:THF (1:1, 2 mL), CsF (160 mg, 1.1 mmol) was added. The mixture was stirred at rt under argon for 16 h. Then, volatiles were removed under reduced pressure and the residue was purified by column chromatography (eluting with hexane:CH_2Cl_2, 1:1) to afford **45** (69 mg, 82%, m.p.: 363-365 ºC) as a white solid. ^{1}H NMR (300 MHz, $CDCl_3$), δ: 7.70 (d, *J* = 6.7 Hz, 4H), 7.50 – 7.41 (m, 8H), 7.21 (s, 2H), 7.12 – 7.00 (m, 8H), 5.61 (s, 2H) ppm. ^{13}C

NMR-DEPT (75 MHz, $CDCl_3$), δ: 146.2 (C), 145.4 (C), 141.2 (C), 131.1 (C), 126.8 (CH), 126.5 (C), 125.3 (CH), 125.1 (CH, 123.6 (CH), 123.5 (CH), 122.1 (CH), 55.4 (CH), 53.0 (CH) ppm. MS (EI), m/z: 480 (M^+, 100). HRMS (EI), m/z found: 480.1871 (calc. for $C_{38}H_{24}$: 480.1878)

X-Ray structure of 45

The **C**ambridge **C**rystallographic **D**ata **C**entre (CCDC) 1443039 record contains the supplementary crystallographic data for compound **45**. These data can be obtained free of charge from https://www.ccdc.cam.ac.uk/

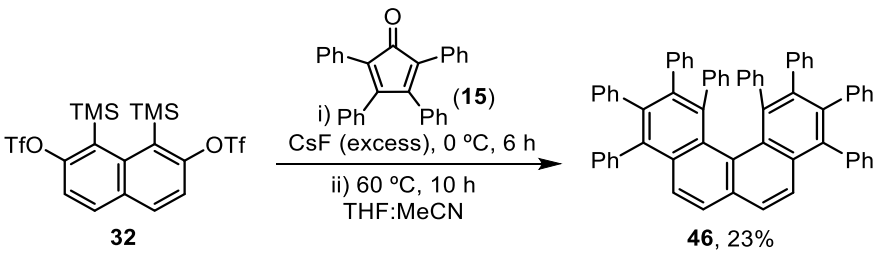


Formula: $C_{38}H_{24}$, $CHCl_3$

Unit cell parameters: a = 14.0105(5); b = 13.0164(5); c = 16.1008(6)

space group: P21/c

Synthesis of 1,2,3,4,9,10,11,12-octaphenylbenzo[*c*]phenanthrene (46)

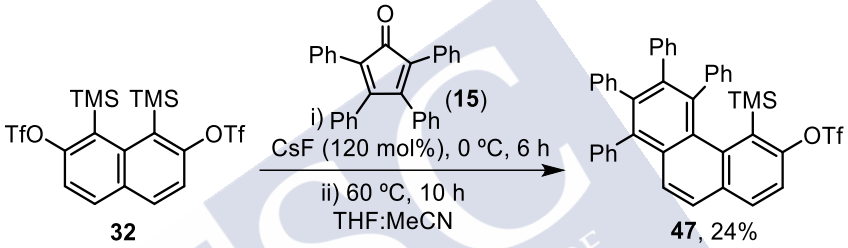


To a solution of naphthodiyne precursor **32** (100 mg, 0.18 mmol) and 2,3,4,5-tetraphenylcyclopentadienone (**15**, 150 mg, 0.4 mmol) in MeCN:THF (1:1, 5 mL) cooled to 0 °C, CsF (160 mg, 1.1 mmol) was added. The mixture was stirred at 0 °C under argon for 6 h. Then, the mixture was heated at 60 °C for 10 h. Volatiles were removed under reduced

pressure and the residue was purified by column chromatography (eluting with CH_2Cl_2) to afford **46** as an orange solid (34 mg, 23%, m.p.: 138-140 °C). ^{1}H NMR (500 MHz, $CDCl_3$), δ: 7.96 (d, *J* = 7.9 Hz, 1H), 7.82 (d, *J* = 8.1 Hz, 1H), 7.52 (d, *J* = 8.9 Hz, 1H), 7.46 – 7.30 (m, 4H), 7.22 – 7.08 (m, 10H), 7.07 – 6.89 (m, 8H), 6.89 – 6.72 (m, 6H), 6.72 – 6.62 (m, 4H), 6.59 – 6.48 (m, 6H), 6.26 (d, *J* = 7.7 Hz, 1H), 6.13 (s, 1H), 5.76 (s, 1H), 5.60 (d, *J* = 7.9 Hz, 1H) ppm. MS (EI), m/z: 836 (M^+, 100). HRMS (EI), m/z found: 836.3475 (calc. for $C_{66}H_{44}$: 836.3443).

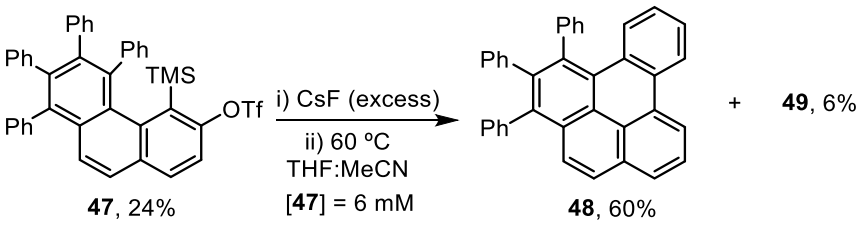
7.3.3 Study of the novel reactivity: formal C-H bond aryne insertion

Synthesis of 5,6,7,8-tetraphenyl-4-(trimethylsilyl)phenanthren-3-yl trifluoromethane-sulfonate (47)



To a solution of cyclopentadienone **15** (60 mg, 0.2 mmol) and naphthodiyne precursor **32** (100 mg, 0.18 mmol) in MeCN:THF (1:1, 5 mL), CsF (33 mg, 0.22 mmol) was added. The reaction mixture was stirred at rt under argon for 6 h. Then, the mixture was heated at 60 °C for 10 h. The solvent was evaporated under reduced pressure and the residue was purified by column chromatography (eluting with hexane:CH_2Cl_2, 3:2) to afford **47** as a white solid (27 mg, 24%, m.p.: 232-233 °C). ^{1}H NMR (500 MHz, $CDCl_3$), 7.76 (d, *J* = 8.7 Hz, 1H), 7.42 (t, *J* = 8.9 Hz, 2H), 7.39 – 7.30 (m, 3H), 7.20 (tt, *J* = 7.3, 1.3 Hz, 1H), 7.16 – 7.09 (m, 1H), 7.05 – 6.90 (m, 11H), 6.87 (tt, *J* = 7.3, 1.4 Hz, 1H), 6.84 – 6.76 (m, 2H), 6.57 (d, *J* = 7.7 Hz, 1H), 6.23 (d, *J* = 7.9 Hz, 1H), -0.11 (s, 9H) ppm. ^{13}C NMR-DEPT (126 MHz, $CDCl_3$), δ: 154.6 (C), 141.0 (C), 140.7 (C), 140.4 (C), 140.3 (C), 139.5 (C), 138.9 (C), 138.9 (C), 137.8 (C), 136.7 (C), 134.7 (C), 134.3 (CH), 132.8 (C), 132.2 (CH), 132.1 (CH), 131.7 (C), 131.5 (CH), 131.1 (CH), 131.2 (CH), 130.9 (C), 130.5 (CH), 130.3 (CH), 127.9 (CH), 127.6 (CH), 127.1 (CH), 127.0 (CH), 126.8 (CH), 126.8 – 126.7 (C), 126.6 (CH), 126.4 (CH), 126.2 (CH), 125.7 (C), 125.6 (CH), 118.3 (CH), 2.3 (CH). MS (EI), m/z: 702 (M^+, 40), 495 (M^+-207, 100). HRMS (EI), m/z found: 702.1850 (calc. for $C_{42}H_{33}O_3F_3SiS$: 702.1872).

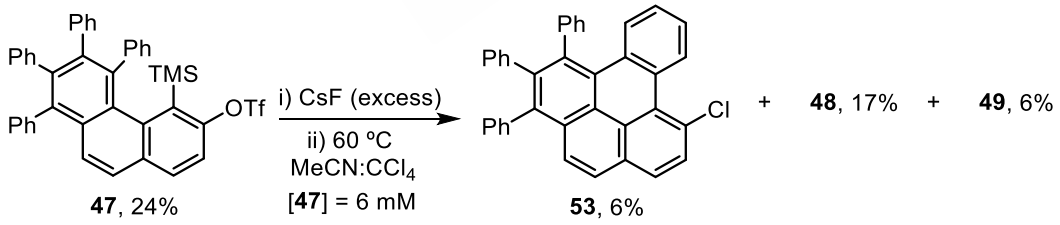
Synthesis of 1,2,3-triphenylbenzo[*e*]pyrene (48)



47, 24% **48**, 60%

To a solution of phenanthryne precursor **47** (20 mg, 0.03 mmol) in MeCN:THF (1:1, 5 mL), CsF (23 mg, 0.15 mmol) was added. The mixture was stirred under argon at 60 °C for 16 h. Then, volatiles were removed under reduced pressure and the residue was purified by column chromatography (eluting with hexane:CH_2Cl_2, 3:2) to afford **48** as a white solid (8.2 mg, 60%, m.p.: 230-231 °C), and **49** (0.82 mg, 6%). Data for **48**: ^{1}H NMR (500 MHz, $CDCl_3$), δ: 8.90 (d, *J* = 7.7 Hz, 1H), 8.78 (d, *J* = 7.8 Hz, 1H), 8.17 (d, *J* = 7.6 Hz, 1H), 8.05 (t, *J* = 7.8 Hz, 1H), 7.93 (d, *J* = 9.2 Hz, 1H), 7.78 (d, *J* = 8.5 Hz, 1H), 7.75 (d, *J* = 9.1 Hz, 1H), 7.58 – 7.48 (m, 1H), 7.27 – 7.23 (m, 2H), 7.22 (d, *J* = 1.7 Hz, 1H), 7.21 (s, 1H), 7.20 – 7.16 (m, 4H), 7.16 – 7.11 (m, 2H), 7.11 – 7.04 (m, 1H), 6.93 (dd, *J* = 4.2, 2.3 Hz, 3H), 6.83 (d, *J* = 3.6 Hz, 1H), 6.81 (d, *J* = 2.4 Hz, 1H) ppm. ^{13}C NMR-DEPT (126 MHz, $CDCl_3$), δ: 143.6 (C), 140.8 (C), 140.7 (C), 140.3 (C), 138.3 (C), 137.3 (C), 132.0 (C), 131.8 (CH), 131.7 (CH), 131.6 (C), 131.4 (CH), 131.0 (C), 130.8 (CH), 130.1 (C), 129.5 (C), 128.3 (CH), 127.7 (C), 127.7 (CH), 127.3 (CH), 126.8 (CH), 126.6 (CH), 126.6 (CH), 126.5 (CH), 126.4 (CH), 126.2 (CH), 125.6 (C), 125.4 (CH), 125.4 (CH), 124.5 (C), 123.5 (CH), 120.3 (CH) ppm. MS (EI), m/z: 480 (M^+, 100). HRMS (EI), m/z found: 480.1860 (calc. $C_{38}H_{24}$: 480.1878).

Synthesis of 8-chloro-1,2,3-triphenylbenzo[*e*]pyrene (53)

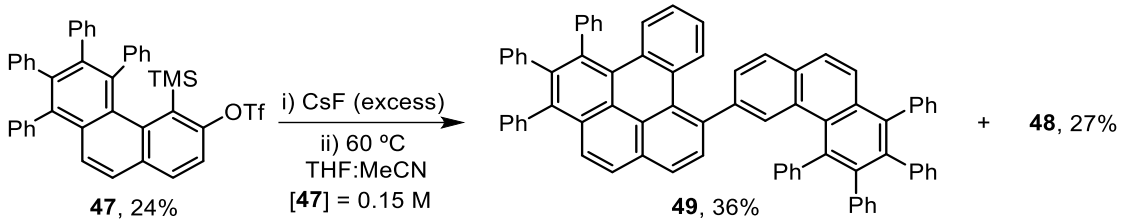


47, 24% **53**, 6%

To a solution of the phenanthryne precursor **47** (20 mg, 0.03 mmol) in MeCN:CCl_4 (4:1, 5 mL), CsF (23 mg, 0.15 mmol) was added. The mixture was stirred under argon at 60 °C for 16 h. Then, volatiles were removed under reduced pressure and the residue was purified by column chromatography (eluting with hexane:CH_2Cl_2, 3:2) to afford **53** (1 mg, 6%) together with **48** (2.4 mg, 17%), and **49** (0.82 mg, 6%). Data for **53**: ^{1}H NMR (500 MHz, $CDCl_3$), δ: 9.42 (d, *J* = 8.2 Hz, 1H), 8.00 (d, *J* = 8.3 Hz, 1H), 7.96 (d, *J* = 8.4 Hz, 1H), 7.82 (d, *J* = 9.1 Hz, 1H), 7.75 (d, *J* = 8.7 Hz, 1H), 7.67 (d, *J* = 9.2 Hz, 1H), 7.40 (t, *J* = 7.2 Hz, 1H), 7.30 – 7.21 (m, 7H), 7.17

– 7.12 (m, 4H), 7.07 (t, *J* = 7.8 Hz, 1H), 6.95 – 6.89 (m, 2H), 6.80 – 6.75 (m, 2H) ppm. MS (EI), m/z: 514 (M^+, 100). HRMS (EI), m/z found: 514.1484 (calc. for $C_{38}H_{23}Cl$: 514.1488).

Synthesis of 1,2,3-triphenyl-8-(5',6',7',8'-tetraphenylphenanthren-3'-yl)benzo[*e*]pyrene (49)



To a solution of the phenanthryne precursor **47** (20 mg, 0.03 mmol) in MeCN:THF (1:1, 0.2 mL) placed in a 1 ml vial, CsF (23 mg, 0.15 mmol) was added. The mixture was stirred under argon at 60 °C for 16 h. Then, volatiles were removed under reduced pressure and the residue was purified by column chromatography (eluting with hexane:CH_2Cl_2, 3:2) to afford **49** as a white solid (4.9 mg, 36%, m.p.: 392-394 °C), and compound **48** (3.7 mg, 27%, characterisation data above). Data for **49**: ^{1}H NMR (400 MHz, $CDCl_3$), δ: 8.40 (s, 1H), 7.97 (d, *J* = 7.8 Hz, 1H), 7.87 (t, *J* = 13.0 Hz, 1H), 7.77 (d, *J* = 7.9 Hz, 1H), 7.72 (d, *J* = 8.9 Hz, 1H), 7.66 (d, *J* = 9.2 Hz, 1H), 7.62 (d, *J* = 7.8 Hz, 4H), 7.55 (d, *J* = 8.3 Hz, 1H), 7.53 – 7.46 (m, 4H), 7.43 (d, *J* = 6.9 Hz, 2H), 7.40 (d, *J* = 8.1 Hz, 2H), 7.35 (d, *J* = 8.1 Hz, 2H), 7.25 – 7.21 (m, 6H), 7.18 (d, *J* = 8.5 Hz, 4H), 7.15 (d, *J* = 7.0 Hz, 4H), 7.10 (d, *J* = 7.9 Hz, 2H), 7.08 – 7.03 (m, 2H), 6.93 (dd, *J* = 19.3, 7.1 Hz, 14H), 6.87 (d, *J* = 8.3 Hz, 2H), 6.82 (d, *J* = 6.9 Hz, 2H), 6.78 (d, *J* = 7.3 Hz, 3H), 6.73 (d, *J* = 6.8 Hz, 3H), 6.45 (d, *J* = 7.6 Hz, 2H).ppm. ^{13}C NMR-DEPT (101 MHz, $CDCl_3$), δ: 143.8 (C), 142.9 (C), 141.0 (C), 140.9 (C), 140.5 (C), 140.5 (C), 140.2 (C), 140.1 (C), 140.0 (C), 139.8 – 139.8 (C), 139.3 – 139.3 (C), 138.4 – 138.4 (C), 138.3 – 138.2 (C), 137.0 (C), 136.0 – 135.9 (C), 132.4 – 132.3 (C), 132.2 – 132.1 (CH), 131.9 – 131.8 (C), 131.8 – 131.7 (C), 131.6 – 131.5 (C), 131.4 (CH), 131.2 (CH), 130.1 (CH), 129.9 (CH), 129.8 (C), 129.3 – 129.2 (CH), 129.1 (CH), 129.1 – 129.0 (C), 128.9 – 128.8 (C), 128.3 (CH), 127.9 (C), 127.7 – 127.4 (C), 127.3 (CH), 126.7 (CH), 126.5 (CH), 126.4 (CH), 126.3 (CH), 126.1 (CH), 125.8 (C), 125.7 (CH), 125.5 (CH), 125.3 (CH), 125.3 – 125.2 (CH), 125.1 (CH), 124.8 (CH), 124.6 (CH). ppm. MS (EI), m/z: 960 (M^+, 100). HRMS (EI), m/z found: 960.3744 (calc. for $C_{76}H_{48}$: 960.3756).

7.3.4 Computational details

All the calculations were performed using the Gaussian 09 program package.[221] Geometries of intermediates and transition states were optimised at the density functional level using the B3LYP functional[222] and 6-31G(d) basis set. Frequency calculations were performed at this level to confirm the nature of the stationary points and to obtain the thermal and entropic contribution to the free energy. Single-point calculations were carried out for all optimised gas-phase geometries using the M062X functional[226] and the 6-31++G(d,p) basis set. Solvation corrections for acetonitrile with a dielectric constant with a dielectric constant of 35.688 were computed using **c**onductor **p**olarizable **c**alculation **m**odel (CPCM).[223]

USC UNIVERSIDADE DE SANTIAGO DE COMPOSTELA

[221] Gaussian 09, Revision **D.01**, M. J. Frisch, G. W. Trucks, H. B. Schlegel, G. E. Scuseria, M. A. Robb, J. R. Cheeseman, G. Scalmani, V. Barone, B. Mennucci, G. A. Petersson, H. Nakatsuji, M. Caricato, X. Li, H. P. Hratchian, A. F. Izmaylov, J. Bloino, G. Zheng, J. L. Sonnenberg, M. Hada, M. Ehara, K. Toyota, R. Fukuda, J. Hasegawa, M. Ishida, T. Nakajima, Y. Honda, O. Kitao, H. Nakai, T. Vreven, J. A. Montgomery, Jr., J. E. Peralta, F. Ogliaro, M. Bearpark, J. J. Heyd, E. Brothers, K. N. Kudin, V. N. Staroverov, R. Kobayashi, J. Normand, K. Raghavachari, A. Rendell, J. C. Burant, S. S. Iyengar, J. Tomasi, M. Cossi, N. Rega, J. M. Millam, M. Klene, J. E. Knox, J. B. Cross, V. Bakken, C. Adamo, J. Jaramillo, R. Gomperts, R. E. Stratmann, O. Yazyev, A. J. Austin, R. Cammi, C. Pomelli, J. W. Ochterski, R. L. Martin, K. Morokuma, V. G. Zakrzewski, G. A. Voth, P. Salvador, J. J. Dannenberg, S. Dapprich, A. D. Daniels, Ö. Farkas, J. B. Foresman, J. V. Ortiz, J. Cioslowski, D. J. Fox, Gaussian, Inc., Wallingford CT, **2009**.

[222] a) A. D. Becke*, J. Chem. Phys.* **1993**, *98*, 5648–5652; b) C. Lee, W. Yang, R. G. Parr, *Phys. Rev. B* **1988**, *37*, 785–789.

[226] Y. Zhao and D. G. Truhlar, *Theor. Chem. Acc.* **2008**, *120*, 215–241.

[223] a) M. Cossi, N. Rega, G. Scalmani, V. Barone, *J. Comp. Chem.* **2003**, *24*, 669–681; b) V. Barone M. Cossi, *J. Phys. Chem. A* **1998**, *102*, 1995–2001.

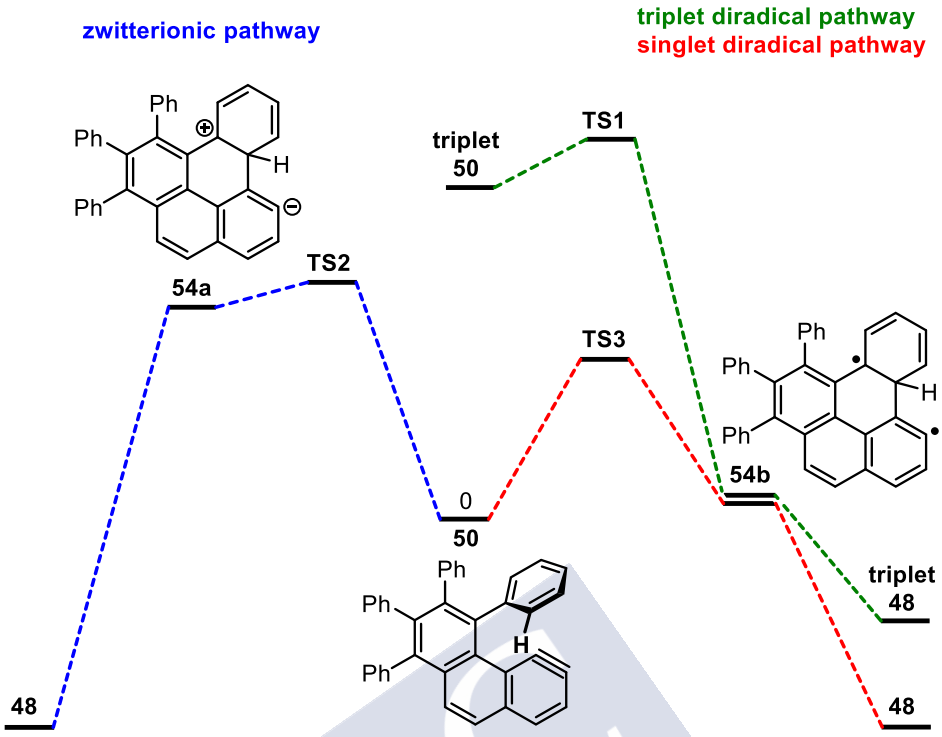


Table 7. Evolution of **50** into **48**.

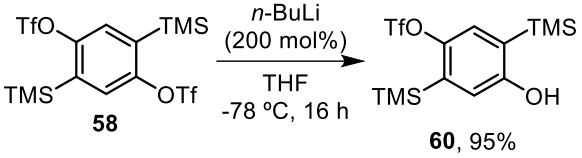
Entry[a]	Compound	ΔG / Kcal mol^{-1} (Sol.)[b]
1	**50**	0
2	**triplet 50 t**	33.4
3	**TS1**	39
4	**TS2**	20.1
5	**TS3**	17
6	**54a**	19.5
7	**triplet 54b**	2.8
8	**singlet 54b**	3.2
9	**triplet 48**	-89
10	**singlet 48**	-35

a) Geometries optimised by DFT-B3LYP/6-31G(d). b) Single point calculation by DFT-M062X/6-31G++(d,p) and solvation was computed using CPCM for MeCN.

7.4 Experimental procedures for Chapter 4

7.4.1 Synthesis of tris(trifluoromethanesulfonate)s 55

Synthesis of 4-hydroxy-2,5-bis(trimethylsilyl)phenyl trifluoromethanesulfonate (60)



To a solution of bistriflate **58**[227] (0.5 g, 100 mol%) in THF (0.3 M, 3.25 mL) at -78 ºC, a solution of *n*-BuLi (2.5 M in hexane, 200 mol%) was dropwise added (10 min). The reaction mixture was allowed to warm up to rt overnight into the cooling bath. Then, volatiles were removed under reduced pressure and the reaction crude was purified by column chromatography (eluting with hexane:CH_2Cl_2, 1:1) to afford **60** as a white solid (354 mg, 95%). Spectroscopic data were coincident with those described in the literature for this compound.[162] ^{1}H NMR (300 MHz, $CDCl_3$), δ: 7.23 (s, 1H), 6.75 (s, 1H), 4.96 (s, 1H), 0.36 (s, 9H), 0.31 (s, 9H) ppm.

Table 8. Optimisation of the reaction between **58** and *n*-BuLi.

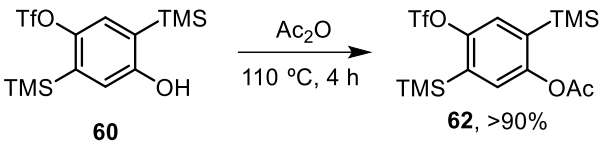
Entry[a]	T / °C	*n*-BuLi / mol%	Scale / g (mmol of **58**)	Yield / %
1	rt	110	0.2	46
2	0	110	0.2	51
3	-20	110	0.2	66
4	-78	110	0.2	85
5	-100	110	0.2	85
6	-100	110	0.2	15
7	-100	140	0.2	90
8	-100	200	0.2	95
9	-78	200	0.5	95
10	-78	200	1	90
11	-78	200	3	30

a) All reactions were carried out using a [**58**] = 0.3 M. Optimisation yields were estimated by ^{1}H NMR directly from the reaction crude.

[227] Currently, bistriflate **58** is commercially available in ABCR and can be synthesise following a described procedure (see ref. 93).

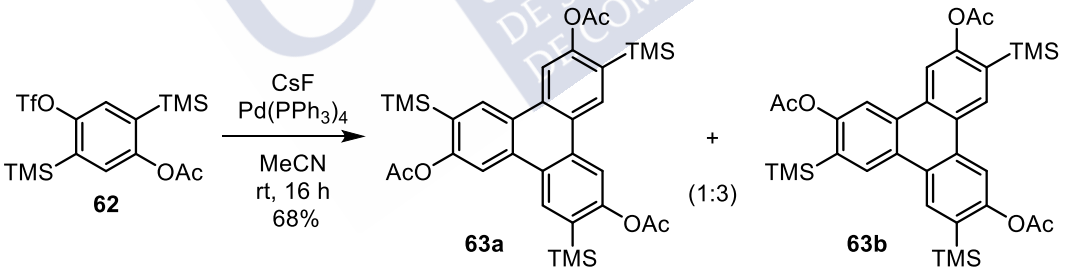
[162] S. Suzuki, K. Itami, J. Yamaguchi, *Angew. Chem. Int. Ed.* **2017**, *56*, 15010–15013.

Synthesis of 4-(((trifluoromethyl)sulfonyl)oxy)-2,5-bis(trimethylsilyl)phenyl acetate (62)



A solution of alcohol **60** (5.7 g, 15 mmol) in Ac_2O (66 mM, 228 mL) was stirred and heated at 110 ºC for 4 h. Then, the mixture was slowly added over $NaHCO_3$ solution (saturated in water, 1 L) and stirred for 2 h at rt. The reaction mixture was extracted with Et_2O (3 x 100 mL) and washed with NaCl solution (saturated in water, 100 mL). The combined organic layers were dried over Na_2SO_4 and filtered. Volatiles were removed under reduced pressure to afford **62** as a brown solid (5.7 g, 90%, m.p.: 57-59 ºC), which was used in the next reaction without further purification. ^{1}H NMR (300 MHz, $CDCl_3$), δ: 7.39 (s, 1H), 7.18 (s, 1H), 2.33 (s, 3H), 0.36 (s, 9H), 0.29 (s, 9H) ppm. ^{19}F NMR (282 MHz, $CDCl_3$), δ: -74.4 ppm. ^{13}C NMR-DEPT (75 MHz, $CDCl_3$), δ: 169.4 (C), 153.9 (C), 152.4 (C), 136.2 (C), 135.7 (C), 130.0 (CH), 125.8 (CH), 21.5 (CH_3), -0.9 (CH_3), -1.22 (CH_3) ppm. MS (APCI), m/z: 429 (M^++1, 100). HRMS (APCI), m/z found: 429.0829 (calc. for $C_{15}H_{24}F_3O_5SSi_2$: 429.0830).

Synthesis of tris(acetate)s 63



To a solution of benzyne precursor **62** (0.2 g, 0.47 mmol) and $Pd(PPh_3)_4$ (54 mg, 47µmol) in MeCN (31 mM, 15 mL), CsF (357 mg, 2.4 mmol) was added. The reaction mixture was stirred at rt for 16 h. then, volatiles were removed under reduced pressure. The reaction crude was purified by column chromathography (eluting with hexane:Et_2O, 1:1) to afford **63a** and **63b** in a 1:3 respectively (159 mg, 66% yield). Both isomers can be partially separated by another column chromatography (eluting with hexane:Et_2O, 4:1). Data for **63b**: white solid, m.p.: 256-257 ºC. ^{1}H NMR (300 MHz, $CDCl_3$), δ: 8.76 (s, 2H), 8.61 (s, 1H), 8.25 (s, 1H), 8.18 (s, 2H), 2.44 (s, 3H), 2.42 (s, 6H), 0.44 (s, 9H), 0.43 (s, 9H), 0.43 (s, 9H) ppm. ^{13}C NMR-DEPT (75 MHz, $CDCl_3$) δ: 169.73 (C), 169.7 (C), 169.6 (C), 155.0 (C), 154.6 (C), 154.5 (C), 132.0 (2C),

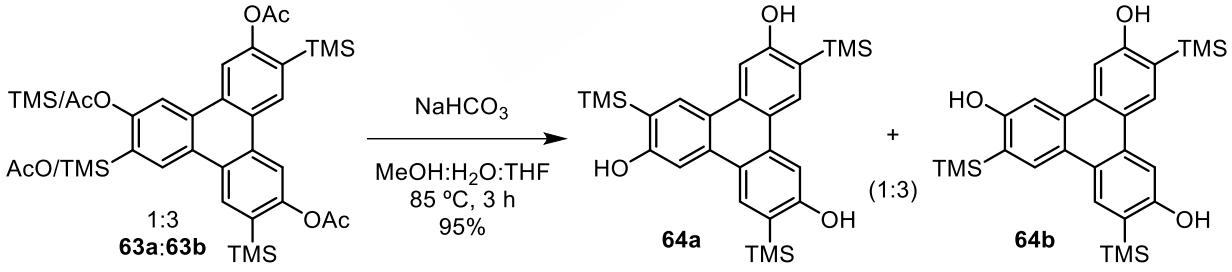
131.6 (CH), 131.3 (2C), 131.2 (C), 130.8 (2CH), 130.7 (C), 127.1 (C), 126.9 (C), 126.6 (C), 116.2 (2CH), 115.6 (CH), 21.8 (CH_3), 21.7 ($2CH_3$), -0.6 (CH_3), -0.8 ($2CH_3$) ppm. MS (APCI), m/z: 619 (M^++1, 100), 618 (M^+, 64). HRMS (APCI), m/z found: 619.2361 (calc. for $C_{33}H_{43}O_6Si_3$: calc: 619.2362). Data for **63a**: white solid, m.p.: 321-322 ºC. ^{1}H NMR (300 MHz, $CDCl_3$), δ: 8.60 (s, 3H), 8.25 (s, 3H), 2.44 (s, 9H), 0.43 (s, 27H) ppm. ^{13}C NMR-DEPT (75 MHz, $CDCl_3$), δ: 169.7 (C), 155.1 (C), 132.3 (C), 131.4 (CH), 131.2 (C), 126.3 (C), 115.6 (CH), 21.8 (CH_3), -0.6 (CH_3) ppm. MS (APCI), m/z: 619 (M^++1, 100), 618 (M^+, 82). HRMS (APCI), m/z found: 619.2359 (calc. for $C_{33}H_{43}O_6Si_3$: 619.2362).

Table 9. Optimisation of **62** cyclotrimerisation.

Entry[a]	Pd catalyst	Scale / g (mmol of **62**)	Yield / %
1	$Pd_2(dba)_3$	0.1	8
2	$Pd(PPh_3)_4$	0.2	68
3	$Pd(PPh_3)_4$	0.5	66
4	$Pd(PPh_3)_4$	1	56
5[b]	$Pd(PPh_3)_4$	0.5	10

a) All reactions were carried out employing: 10 mol%. of [Pd] and 0.08 M concentration. Optimisation yields were isolated.
b) Entry 5 was carry out using commercial $Pd(PPh_3)_4$.

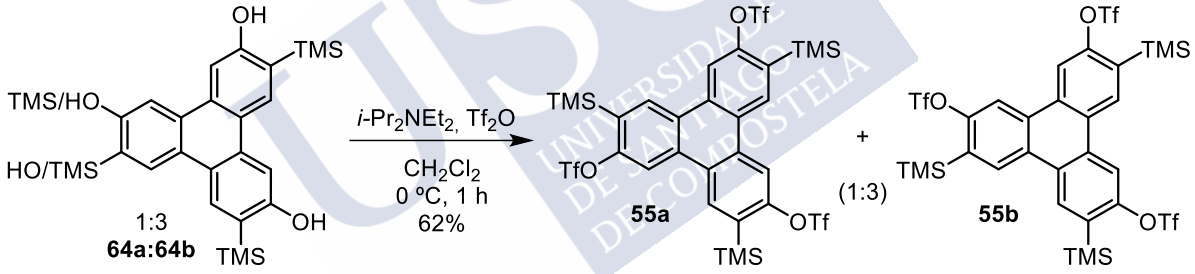
Synthesis of tris(triol)s 64



To a solution of **63a** and **63b** (1:3 respectively, 160 mg, 0.26 mmol) in THF (0.01 M, 26 mL) a 1:1 mixture of $NaHCO_3$ solution (saturated in water, 11 mL) and MeOH (11 mL) was added. The reaction was stirred and refluxed for 3 h. Then, the layers were separated and the aqueous layer was acidify to pH = 1 (by adding HCl in 10% aqueous solution) and extracted with AcOEt (3 x 20 mL). Thereafter, the combined organic layers were dried over $MgSO_4$ and filtered. Volatiles were removed under reduced pressure and the obtained solid was dissolved in

CH_2Cl_2 and dried again over $MgSO_4$. Solvent was removed under reduced pressure to afford **64a** and **64b** (1:3 respectively, 121 mg, 95% yield). Both isomers can be partially separated by column chromatography (eluting with hexane:AcOEt, 9:1). Data for **64b**: white solid, m.p.: 191-192 ºC. ^{1}H NMR (300 MHz, $CDCl_3$), δ: 8.69 – 8.54 (s, 2H), 8.48 (s, 1H), 7.77 (s, 1H), 7.51 (s, 2H), 5.45 (s, 1H), 5.36 (s, 2H), 0.47 (s, 9H), 0.46 (s, 9H), 0.43 (s, 9H) ppm. ^{13}C NMR-DEPT (75 MHz, $CDCl_3$) δ: 159.8 (C), 159.0 (C), 158.7 (C), 132.4 (C), 131.3 (CH), 130.5 (2CH), 127.5 (C), 127.2 (C), 124.6 (C), 124.1 (C), 123.1 (C), 122.6 (C), 108.3 (C), 107.0 (2CH), 106.4 (CH), -0.69 (CH_3) ppm. MS (APCI), m/z: 493 (M^++1, 19). HRMS (APCI), m/z found: 493.2040 (calc. for $C_{27}H_{37}O_3Si_3$: 493.2045). Data for **64a**: white solid, m.p.: 291-292 ºC. ^{1}H NMR (300 MHz, $CDCl_3$), δ: 8.45 (s, 3H), 7.73 (s, 3H), 5.22 (s, 3H), 0.45 (s, 27H) ppm. ^{13}C NMR-DEPT (75 MHz, $CDCl_3$), δ: 160.1 (C), 133.5 (C), 131.3 (CH), 125.4 (C), 121.7 (C), 106.4 (CH), -0.58 (CH_3) ppm. MS (APCI), m/z: 493 (M^++1, 100). HRMS (APCI), m/z found: 493.2044 (calc. for $C_{27}H_{37}O_3Si_3$: 493.2045).

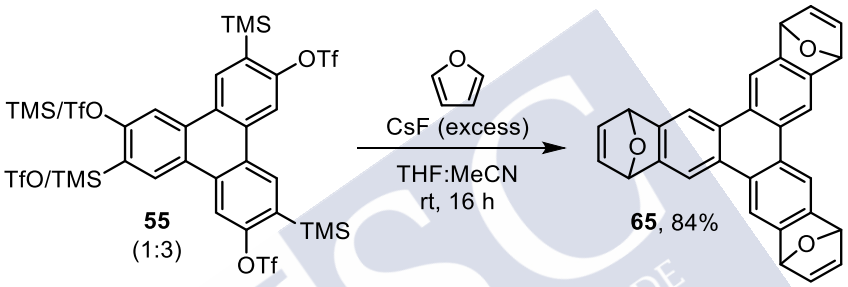
Synthesis of tris(trifluoromethanesulfonate)s 55



To a solution of **64a** and **64b** (1:3 respectively, 80 mg, 0.13 mmol) and *i*-Pr_2NEt in CH_2Cl_2 (0.08 M, 2 mL) at 0 ºC, Tf_2O (0.16 ml, 0.96 mmol) was dropwise added. The reaction mixture was stirred for 1 h at the same temperature. Then, it was quenched with $NaHCO_3$ solution (saturated solution in water, 10 mL) and extracted with CH_2Cl_2 (3 x 5 mL). The combined organic layers were dried over $MgSO_4$ and filtered. Volatiles were removed under reduced pressure. The reaction crude was purified by column chromatography (eluting with Et_2O:hexane, 1:3) to afford **55a** and **55b** (1:3 respectively, 89.5 mg, 62% yield). Both isomers can be partially separated by another column chromatography (eluting with hexane:Et_2O, 39:1). Data for **55b**: white solid, m.p.: 222-223 ºC. ^{1}H NMR (500 MHz, $CDCl_3$), δ: 8.82 (s, 1H), 8.81 (s, 1H), 8.67 (s, 1H), 8.56 (s, 1H), 8.40 (s, 1H), 8.40 (s, 1H), 0.54 (s, 18H), 0.53 (s, 9H) ppm. ^{19}F NMR (471 MHz, $CDCl_3$), δ: -74.07, -74.14, -74.13 ppm. ^{13}C NMR-DEPT (125 MHz, $CDCl_3$), δ: 155.2 (C), 155.0 (C), 155.0 (C), 134.0 (C), 133.9 (C), 133.0 (C), 132.4 (CH), 132.3 (2xCH), 131.9 (C), 131.6 (C), 131.4 (C), 127.9 (C), 127.8 (C), 127.5 (C) , 122.7 – 114.9 (q, J

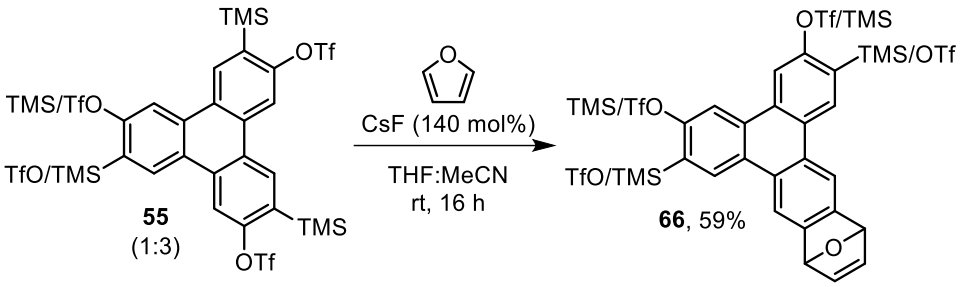
= 320.3 Hz, CF_3), 118.8 (q, J = 320.3 Hz, 2xCF_3), 114.0 (2xCH), 113.8 (CH), -0.8 (CH_3), -0.9 (CH_3) ppm. MS (APCI), m/z: 873 (M^+-15, 95), 888 (M^+, 86) HRMS (APCI), m/z found: 888.0447 (calc. for $C_{30}H_{33}F_9O_9S_3Si_3$: 888.0445). Data for **55a**: white solid, m.p.: 247-249 ºC. ^{1}H NMR (500 MHz, $CDCl_3$), δ: 8.66 (s, 3H), 8.56 (s, 3H), 0.52 (s, 27H) ppm. ^{19}F NMR (471 MHz, $CDCl_3$), δ: -74.1 ppm. ^{13}C NMR-DEPT (125 MHz, $CDCl_3$), δ: 155.4 (C), 133.1 (C), 132.4 (CH), 132.1 (C), 127.3 (C), 118.8 (q, *J* = 320.3 Hz, CF_3), 113.8 (CH), -0.9 (CH_3) ppm. MS (APCI), m/z: 873 (M^+-15, 100), 888 (M^+, 66). HRMS (APCI), m/z found: 888.0449 (calc. for $C_{30}H_{33}F_9O_9S_3Si_3$: 888.0445).

Synthesis of trisadducts 65



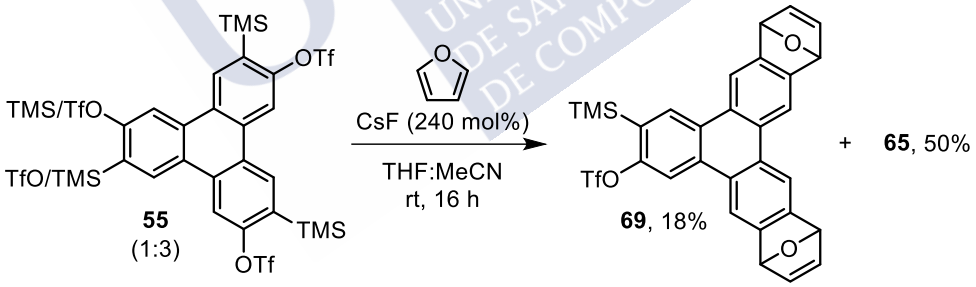
Tristriflates **55** (40 mg, 45 µmol) and CsF (123 mg, 0.81 mmol) were placed in a Schlenk tube under argon atmosphere. Then, THF (1 mL), furan (98 µL, 1.3 mmol) and MeCN (1 mL) were subsequently added. The reaction mixture was stirred at rt for 16 h. Volatiles were removed under reduced pressure. The reaction crude was purified by flash column chromatography (eluting with EtOAc) to afford the mixture of products **65** as a brown solid (16 mg, 84% yield, m.p.: gradual decomposition). ^{1}H NMR (750 MHz, $CDCl_3$), δ: 8.47 – 8.40 (m, 6H), 7.08 – 7.03 (m, 6H), 5.92 (s, 6H) ppm. ^{13}C NMR-DEPT (75 MHz, $CDCl_3$), δ: 146.5 (C), 142.6 (CH), 128.0 (C), 115.0 (CH), 82.5 (CH) ppm. MS (APCI), m/z: 427 (M^++1, 100). HRMS (APCI), m/z found: 427.1329 (calc. for $C_{30}H_{19}O_3$: 427.1329).

Synthesis of monoadducts 66



Triflates **55** (100 mg, 0.11 mmol) and CsF (24 mg, 0.16 mmol) were placed in a Schlenk tube under argon atmosphere. Then, THF (2 mL), furan (25 µL, 0.34 mmol) and MeCN (2 mL) were subsequently added. The reaction mixture was stirred at rt for 16 h. Volatiles were removed under reduced pressure. The reaction crude was purified by flash column chromatography (eluting with a gradient from CH_2Cl_2:hexane, 2:3, to CH_2Cl_2) to afford the mixture of products **66** as a brown solid (49 mg, 59% yield, m.p.: gradual decomposition). ^{1}H NMR (300 MHz, $CDCl_3$), 8.89 – 8.19 (m), 7.16 – 7.04 (m), 5.99 (m), 0.57 – 0.52 (m). MS (APCI), m/z: 735 (M^++1, 100). HRMS (APCI), m/z found: 735.0789 (calc. for $C_{30}H_{29}F_6O_7S_2Si_2$: 735.0792).

Synthesis of bisadducts 69

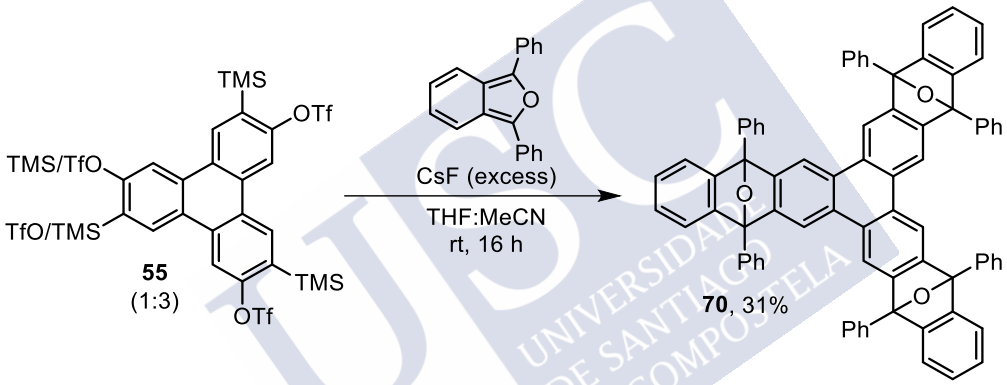


Triflates **55** (100 mg, 0.11 mmol) and CsF (43 mg, 0.28 mmol) were placed in a Schlenk tube under argon atmosphere. Then, THF (2 mL), furan (46 µL, 0.72 mmol) and MeCN (2 mL) were subsequently added. The reaction mixture was stirred at rt for 16 h. Volatiles were removed under reduced pressure. The reaction crude was purified by flash column chromatography (eluting with a gradient from CH_2Cl_2 to AcOEt) to afford the mixture of products **69** (12 mg, 18% yield, m.p.: 213 °C-decomposition) and compounds **65** as a yellow solid (25 mg, 50%). Data for **69**: ^{1}H NMR (500 MHz, $CDCl_3$), δ: 8.74 (s, 1H), 8.73 (s, 1H), 8.50 (s, 1H), 8.49 (s, 1H), 8.46 (s, 1H), 8.45 (s, 2H), 8.44 (s, 1H), 8.43 (d, *J* = 1.6 Hz, 1H), 8.42 (s, 1H), 8.30 (s, 1H), 8.28 (s, 1H), 7.12 – 7.03 (m, 8H), 5.98 (s, 2H), 5.97 (s, 2H), 5.94 (s, 2H), 5.93 (s, 2H), 0.52 (s, 18H)

ppm. ^{19}F NMR (282 MHz, $CDCl_3$), δ: -73.68 ppm. ^{13}C NMR-DEPT (125 MHz, $CDCl_3$), δ: 154.0 (C), 153.9 (C), 148.3 (C), 147.6 (C), 147.2 (C), 147.2 (C), 142.7 (CH), 142.7 (CH), 142.6 (CH), 142.6 (CH), 142.6 (CH), 142.5 (CH), 142.4 (CH), 132.5 (C), 132.2 (CH), 130.7 (C), 128.8 (C), 128.7 (C), 128.6 (C), 128.2 (C), 128.1 (C), 126.8 (C), 126.7 (C), 126.53 (C), 126.5 (C), 118.8 (q, J = 320.1 Hz), 115.1 (CH), 115.1 (CH), 115.1 (CH), 115.0 (CH), 114.9 (CH), 114.8 (CH), 114.8 (CH), 113.2 (CH), 82.5 (CH), 82.5 (CH), 82.4 (CH), 82.4 (CH), -0.5 (CH) ppm. MS (APCI), m/z: 581 (M^++1, 100). HRMS (APCI), m/z found: 581.1065 (calc. for $C_{30}H_{24}F_3O_5SSi$: 581.1060).

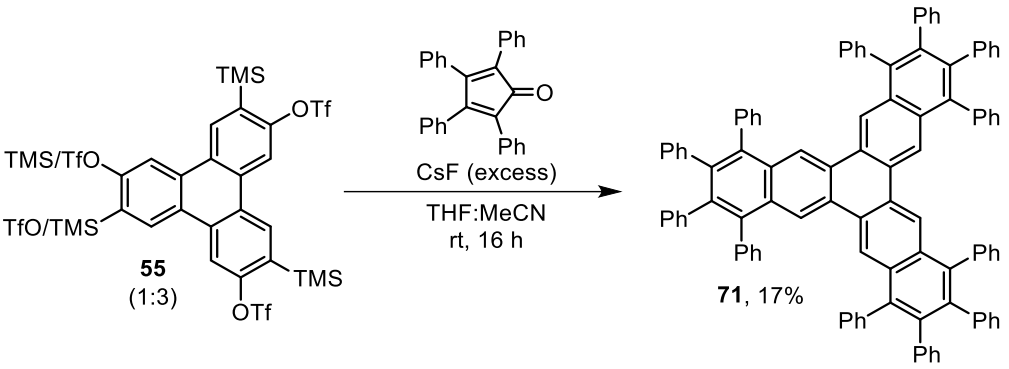
7.4.2 Reactivity of tris(trifluoromethanesulfonate)s 55

Synthesis of compound 70



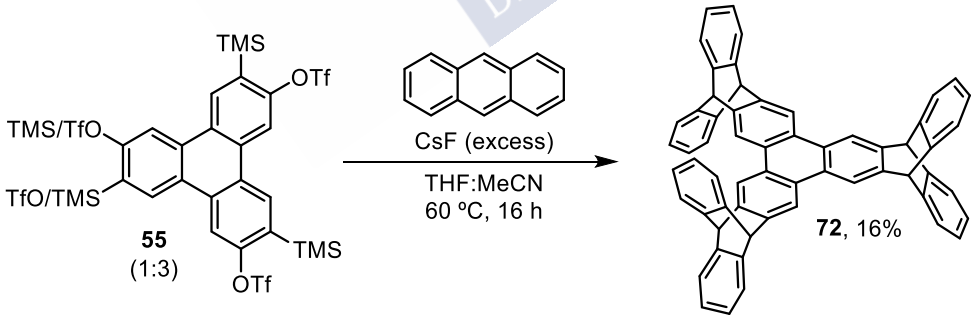
Tristriflates **55** (50 mg, 56 μmol), 1,3-diphenylisobenzofuran (**12**, 55 mg, 0.2 mmol) and CsF (154 mg, 1.0 mmol) were placed in a Schlenk tube under argon atmosphere. Then, THF (2 mL) and MeCN (2 mL) were subsequently added. The reaction mixture was stirred at rt for 16 h. Volatiles were removed under reduced pressure. The reaction crude was purified by flash column chromatography (eluting with a gradient from hexane to CH_2Cl_2) to afford the mixture of products **70** as a white solid (18 mg, 31% yield, m.p.: 214 °C-decomposition). ^{1}H NMR (300 MHz, $CDCl_3$), δ: 8.43 (m, 6H), 8.07 (m, 12H), 7.77 – 7.55 (m, 18H), 7.41 (m, 6H), 7.05 (m, 6H) ppm. ^{13}C NMR-DEPT (75 MHz, $CDCl_3$), δ: 150.0 (C), 149.9 (C), 149.8 (C), 149.7 (C), 148.4 (C), 148.3 (C), 135.3 (C), 135.3 (C), 135.0 (C), 134.9 (C), 128.9 (CH), 128.7 (CH), 128.6 (CH), 128.2 (CH), 128.1 (CH), 128.1 (CH), 127.2 (CH), 127.1 (CH), 126.9 (CH), 126.8 (CH), 126.3 (CH), 126.3 (CH), 120.6 (CH), 120.6 (CH), 120.5 (CH), 115.3 (C), 115.2 (C), 115.0 (C), 90.8 (C), 90.6 (C) ppm. MS (APCI), m/z: 1033 (M^++1, 55), 839 (M^+-194, 100). HRMS (APCI), m/z found: 1033.3679 (calc. for $C_{78}H_{49}O_3$: 1033.3676).

Synthesis of compound 71



Tristriflates **55** (40 mg, 45 µmol), tetraphenylcyclopentadienone (**15**, 62 mg, 0.16 mmol) and CsF (123 mg, 0.8 mmol) were placed in a Schlenk tube under argon atmosphere. Then, THF (1 mL) and MeCN (1 mL) were subsequently added. The reaction mixture was stirred at rt for 16 h. Volatiles were removed under reduced pressure. The reaction crude was purified by flash column chromatography (eluting with a gradient from CH_2Cl_2:hexane, 3:1, to CH_2Cl_2) to afford **71** as a white solid (10 mg, 17% yield, m.p.: >350 °C). Spectroscopic data were coincident with those described in the literature for this compound.[228] ^{1}H NMR (300 MHz, $CDCl_3$), δ: 8.47 (s, 6H), 7.39 – 7.05 (m, 30H), 7.00 – 6.74 (m, 30H) ppm.

Synthesis of heptaiptycene 72



Tristriflates **55** (50 mg, 56 µmol), anthracene (**13**, 36 mg, 0.2 mmol) and CsF (154 mg, 1 mmol) were placed in a Schlenk tube under argon atmosphere. Then, THF (2 mL) and MeCN (2 mL) were subsequently added. The reaction mixture was stirred at 60 °C for 16 h. Volatiles were

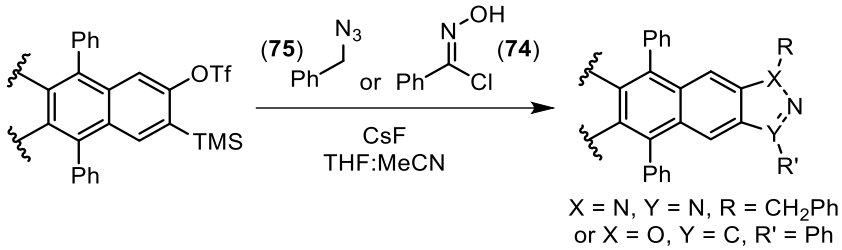
---

[228] R. Zuzak, I. Pozo, M. Engelund, A. Garcia-Lekue, M. Vilas-Varela, J. M. Alonso, M. Szymonski, E. Guitián, D. Pérez, S. Godlewski, D. Peña, *Chem. Sci.* **2019**, *10*, 10143–10148.
[152] F. M. Raymo, M. F. Parisi, F. H. Kohnke, *Tetrahedron Lett.* **1993**, *34*, 5331–5332.

removed under reduced pressure. The reaction crude was purified by flash column chromatography (eluting with a gradient from hexane to Tol) to afford **72** as a white solid (7 mg, 16% yield, m.p.: >350 °C). Spectroscopic data were coincident with those described in the literature for this compound.[152] ^{1}H NMR (300 MHz, $CDCl_3$), δ: 8.56 (s, 6H), 7.51 – 7.40 (m, 12H), 7.06 – 6.97 (m, 12H), 5.62 (s, 6H) ppm.

7.5 Experimental procedures for Chapter 5

7.5.1 General procedure for the synthesis of heteroacenes

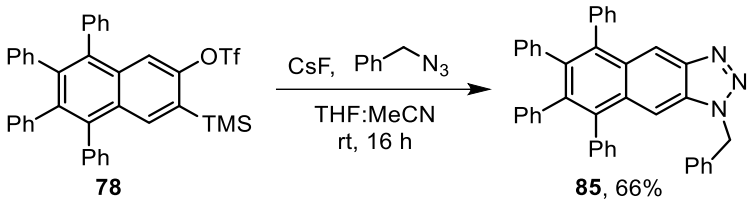


To a solution of the corresponding aryne precursor (50 mg, 1 equiv.) and benzyl azide (**75**) or phenylchlorooxime (**74**) (1.5 equiv.) in MeCN:THF (1:1, 0.05M), CsF (5 equiv.) was added. The reaction mixture was stirred at rt for 16 h. Then, H_2O (10 mL) was added and the aqueous layer was extracted with CH_2Cl_2 (2 x 10 mL). The combined organic layers were dried over Na_2SO_4 and filtered. Volatiles were removed under reduced pressure and the obtained solid was purified by column chromatography to afford the corresponding product.

USC UNIVERSIDADE DE SANTIAGO DE COMPOSTELA

7.5.2 Synthesis of heteroacenes

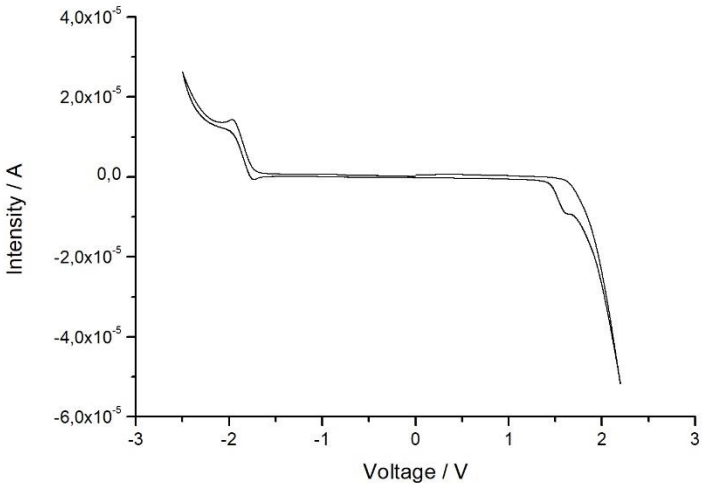
Synthesis of 1-benzyl-5,6,7,8-tetraphenyl-1*H*-naphtho[2,3-*d*][1,2,3]triazole (78)



78 **85**, 66%

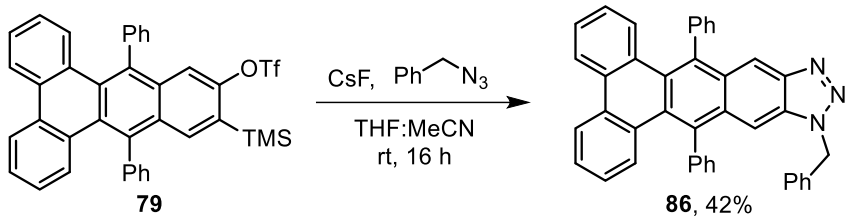
Column chromatography eluting with a gradient from hexane:CH_2Cl_2, 2:1, to CH_2Cl_2:MeOH, 1:9, to afford **85** as a yellow solid (29 mg, 66%, m.p.: 118-119 ºC). ^{1}H NMR (300 MHz, $CDCl_3$), δ: 8.45 (s, 1H), 7.54 (s, 1H), 7.35 – 7.19 (m, 10H), 7.22 – 7.09 (m, 5H), 6.92 – 6.78 (m, 10H), 5.80 (s, 2H) ppm. ^{13}C NMR-DEPT (75 MHz, $CDCl_3$), δ: 139.6 (C), 134.6 (C), 132.5 (C), 131.3 (CH), 131.2 (C), 129.0 (C), 128.5 (C), 128.2 (C), 127.9 (CH), 126.9 (C), 126.8 (CH), 125.6 (CH), 118.0 (C), 105.8 (C), 52.7 (CH_2) ppm. IR (ν): 3057, 3024, 1493, 1441, 1234, 1070, 1027, 740, 697, 556 cm^{-1}. MS (EI), m/z: 563 (M^+, 100), 535 (M^+-28, 12). HRMS (EI), m/z found: 563.2352 (calc. for $C_{41}H_{29}N_3$: 563.2361).

Cyclic voltammogram of 85



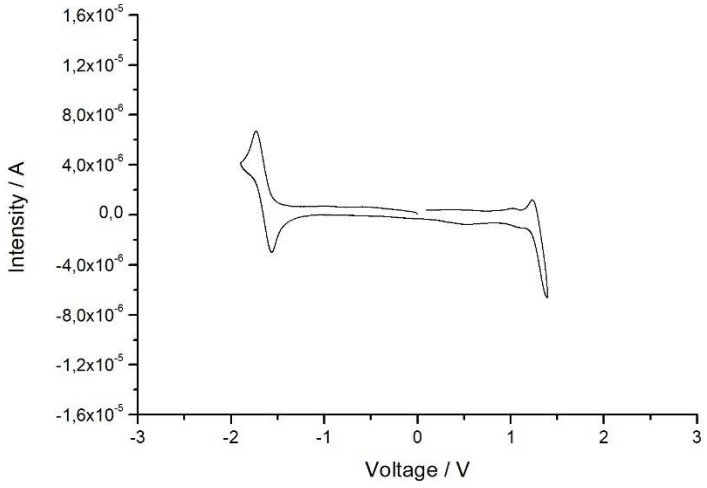
Measured in Tol:MeCN, 1:5, using *n*-Bu_4NPF_6 (0.1 M) as electrolyte and AgCl/Ag as reference electrode.

Synthesis of 11-benzyl-9,15-diphenyl-11*H*-benzo[5,6]tetrapheno[9,10*d*][1,2,3]triazole (86)



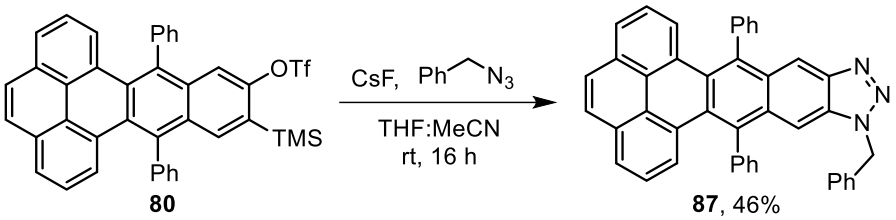
Column chromatography eluting with a gradient from hexane:CH_2Cl_2, 2:1, to CH_2Cl_2:MeOH, 1:9, to afford **86** as an orange solid (18 mg, 42%, m.p.: 261-262 ºC). ^{1}H NMR (300 MHz, $CDCl_3$), δ: 8.74 (s, 1H), 8.18 (d, *J* = 8.0 Hz, 2H), 7.85 (s, 1H), 7.69 – 7.16 (m, 19H), 6.94 (m, *J* = 10.7, 7.7 Hz, 2H), 5.85 (s, 2H) ppm. ^{13}C NMR-DEPT (75 MHz, $CDCl_3$), δ: 141.8 (C),0 141.5 (C), 136.3 (C), 134.9 (C), 132.8 (CH), 132.8 (C), 132.3 (C), 131.3 (C), 130.9 (CH), 130.7 (CH), 130.3 (C), 129.4 (CH), 129.3 (CH), 129.1 (CH), 128.6 (CH), 128.2 (C), 128.1 (CH), 128.0 (CH), 127.5 (CH), 127.3 (CH), 126.3 (CH), 126.1 (CH), 123.6 (CH), 123.5 (C), 117.7 (C), 105.2 (CH), 52.7 (CH_2) ppm. IR (ν): 3051, 2999, 2919, 2850, 1626, 1488, 1440, 1229, 1091, 804, 750, 727, 703, 561 cm^{-1}. MS (EI), m/z: 561 (M^+, 100), 533 (M^+-28, 14). HRMS (EI), m/z found: 561.2209 (calc. for $C_{41}H_{27}N_3$: 561.2205).

Cyclic voltammogram of 86



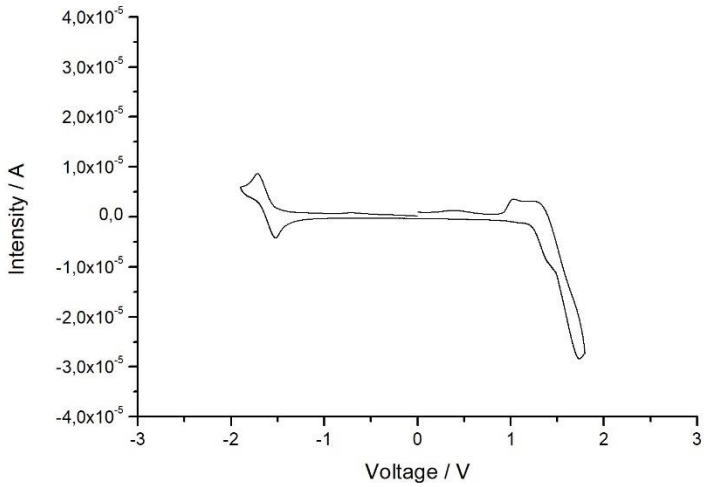
Measured in Tol:MeCN, 1:5, using *n*-Bu_4NPF_6 (0.1 M) as electrolyte and AgCl/Ag as reference electrode.

Synthesis of 11-benzyl-9,15-diphenyl-11*H*-dibenzo[6,7:10,11]tetraceno[2,3-*d*][1,2,3]-triazole (87)



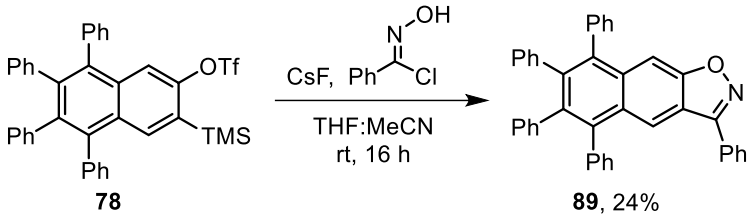
Column chromatography eluting with hexane:CH_2Cl_2, 3:1, to afford **87** as an orange solid (20 mg, 46%, m.p.: 150-151 ºC). ^{1}H NMR (300 MHz,$CDCl_3$), δ: 8.74 (s, 1H), 7.89 – 7.74 (m, 6H), 7.70 (d, *J* = 8.1 Hz, 1H), 7.62 – 7.45 (m, 8H), 7.42 – 7.21 (m, 9H), 5.86 (s, 2H) ppm. ^{13}C NMR-DEPT (75 MHz, $CDCl_3$), δ: 142.3 (C), 142.1 (C), 134.8 (C), 132.6 (CH), 130.9 (C), 130.4 (C), 129.6 (CH), 129.5 (CH), 129.2 (CH), 128.6 (CH), 128.1 (CH), 127.9 (C), 127.0 (CH), 126.9 (CH), 126.5 (C), 126.3 (C), 124.9 (CH), 117.9 (CH), 105.3 (CH), 52.8 (CH_2) ppm. IR (ν): 3049, 2963, 2918, 2851, 1440, 1099, 1074, 832, 749, 703, 547 cm^{-1}. MS (EI), m/z: 585 (M^+, 100), 557 (M^+-28, 12). HRMS (EI), m/z found: 585.2194 (calc. for $C_{43}H_{27}N_3$: 585.2205).

Cyclic voltammogram of 87



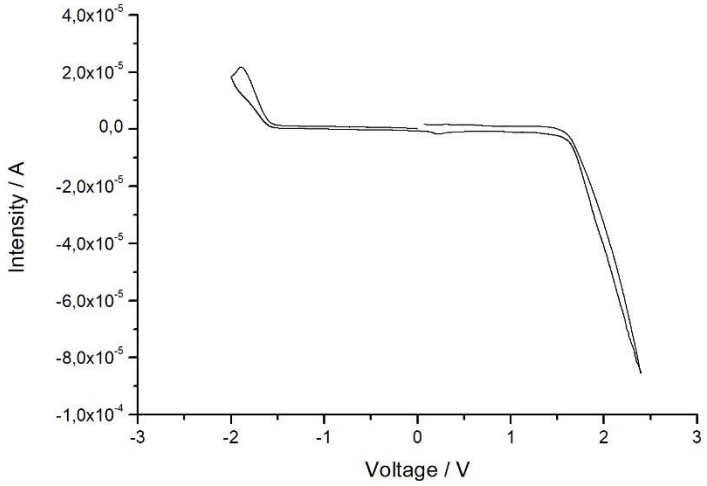
Measured in Tol:MeCN, 1:5, using *n*-Bu_4NPF_6 (0.1 M) as electrolyte and AgCl/Ag as reference electrode.

Synthesis of 3,5,6,7,8-pentaphenylnaphtho[2,3-*d*]isoxazole (89)



Column chromatography eluting with a gradient from hexane:CH_2Cl_2, 1:1, to CH_2Cl_2:MeOH, 2:8, to afford **89** as a white solid (10 mg, 24%, m.p.: 217-218 ºC). ^{1}H NMR (500 MHz, $CDCl_3$), δ: 8.27 (d, *J* = 1.0 Hz, 1H), 7.89 – 7.85 (m, 2H), 7.80 (d, *J* = 1.0 Hz, 1H), 7.48 (m, *J* = 5.1, 2.0 Hz, 3H), 7.32 – 7.21 (m, 10H), 6.89 – 6.83 (m, 10H) ppm. ^{13}C NMR-DEPT (126 MHz, $CDCl_3$), δ: 160.4 (C), 157.4 (C), 141.0 (C), 140.4 (C), 139.5 (C), 139.4 (C), 139.4 (C), 138.4 (C), 138.2 (C), 133.8 (C), 131.4 (CH), 131.4 (CH), 131.2 (CH), 130.5 (CH), 130.1 (C), 129.3 (CH), 129.0 (C), 128.1 (CH), 128.0 (CH), 127.9 (CH), 127.0 (CH), 126.8 (CH), 125.7 (CH), 125.7 (CH), 121.6 (CH), 121.5 (C), 104.9 (CH) ppm. IR (ν): 3058, 3025, 1626, 1493, 1442, 1381, 1073, 1026, 858, 739, 696, 640 cm^{-1}. MS (EI), m/z: 549 (M^+, 100). HRMS (EI), m/z found: 549.2089 (calc. for $C_{41}H_{27}NO$: 549.2093).

Cyclic voltammogram of 89

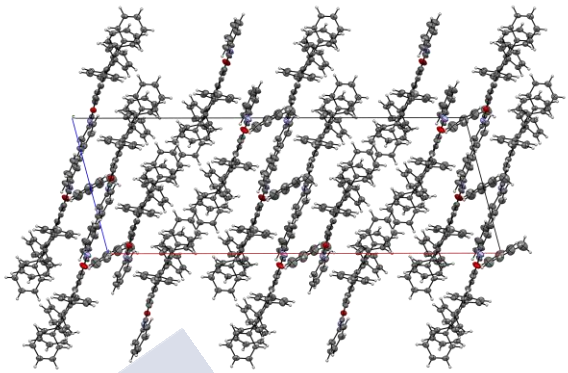


Measured in Tol:MeCN, 1:5, using *n*-Bu_4NPF_6 (0.1 M) as electrolyte and AgCl/Ag as reference electrode.

X-Ray structure of 89

The **C**ambridge **C**rystallographic **D**ata **C**entre (CCDC) 1962803 record contains the supplementary crystallographic data for compound **89**. These data can be obtained free of charge from https://www.ccdc.cam.ac.uk/





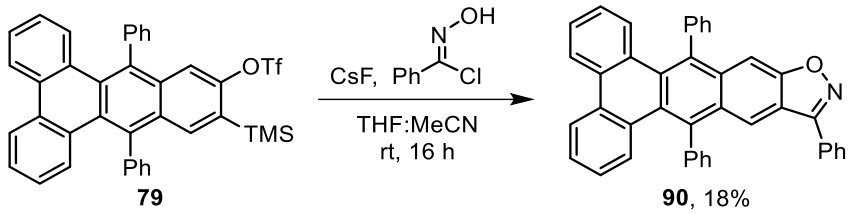
Formula: $C_{86.51}H_{58.90}N_2O_2$

Unit cell parameters: a = 37.0361(15); b = 12.7080(5); c = 13.5304(5)

space group: Cc

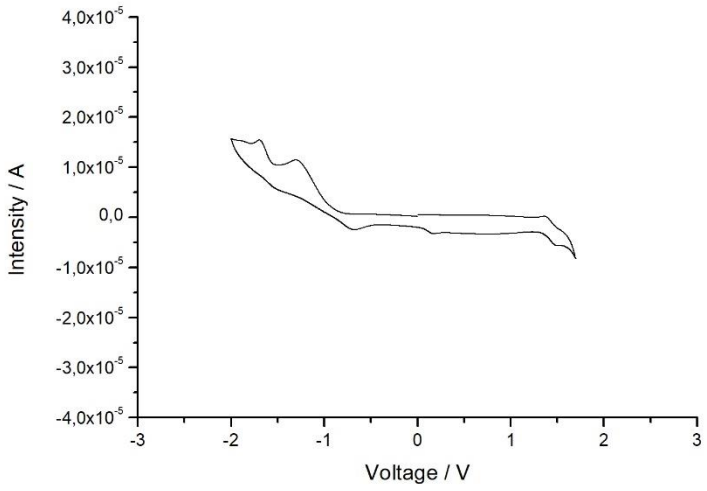
USC UNIVERSIDADE DE SANTIAGO DE COMPOSTELA

Synthesis of 9,13,15-triphenylbenzo[5,6]tetrapheno[9,10-*d*]isoxazole (90)



Column chromatography eluting with a gradient from hexane:CH_2Cl_2, 2:1, to CH_2Cl_2, to afford **90** as a yellow solid (8 mg, 18%, m.p.: 97-98 ºC). ^{1}H NMR (500 MHz,$CDCl_3$), δ: 8.60 (d, *J* = 0.9 Hz, 1H), 8.24 (d, *J* = 8.1, 1.6 Hz, 2H), 8.11 (d, *J* = 0.9 Hz, 1H), 7.96 (m, *J* = 6.6, 2.7, 1.5 Hz, 2H), 7.65 – 7.51 (m, 14H), 7.48 (dd, *J* = 8.4, 1.2 Hz, 1H), 7.36 (m, 2H), 6.99 (m, 2H) ppm. ^{13}C NMR-DEPT (126 MHz, $CDCl_3$), δ: 160.3 (C), 157.5 (C), 141.7 (C), 136.4 (C), 135.1 (C), 133.5 (C), 132.9 (CH), 132.8 (CH), 132.6 (C), 132.2 (C), 131.3 (C), 131.0 (C), 130.9 (CH), 130.6 (CH), 130.6 (CH), 129.9 (C), 129.5 (CH), 129.3 (CH), 128.9 (C), 128.3 (CH), 128.2 (C), 128.2 (CH), 127.6 (CH), 127.2 (CH), 126.2 (CH), 123.6 (CH), 121.7 (C), 121.5 (CH), 104.2 (C) ppm. IR (ν): 3055, 3020, 1624, 1490, 1441, 1349, 860, 806, 753, 727, 702, 647, 568 cm^{-1}. MS (EI), m/z: 547 (M^+, 100). HRMS (EI), m/z found: 547.1943 (calc. for $C_{41}H_{25}NO$: 547.1936).

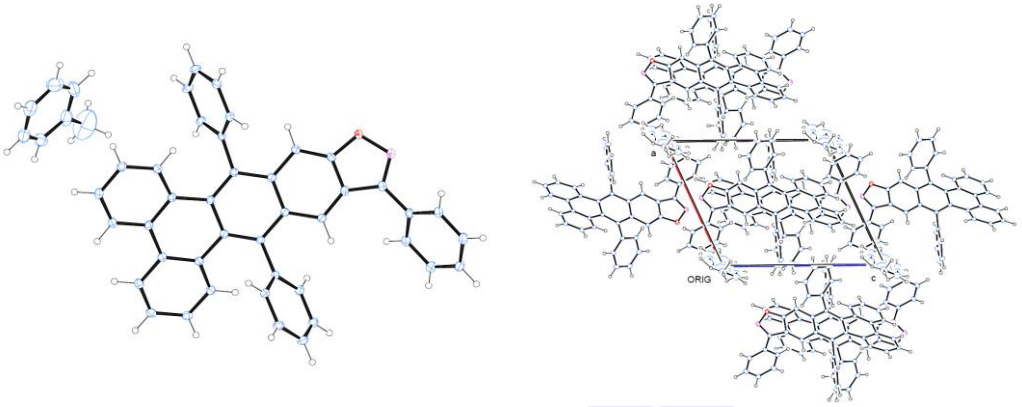
Cyclic voltammogram of 90



Measured in Tol:MeCN, 1:5, using *n*-Bu_4NPF_6 (0.1 M) as electrolyte and AgCl/Ag as reference electrode.

X-Ray structure of 90

The **C**ambridge **C**rystallographic **D**ata **C**entre (CCDC) 1962804 record contains the supplementary crystallographic data for compound **90**. These data can be obtained free of charge from https://www.ccdc.cam.ac.uk/

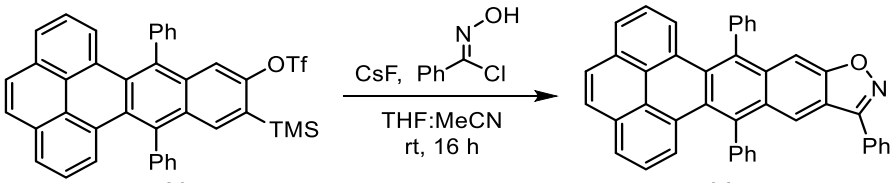


Formula: $2(C_{41}H_{25}NO)\cdot C_7H_8$

Unit cell parameters: a = 11.5524(5); b = 11.8858(5); c = 13.4475(6)

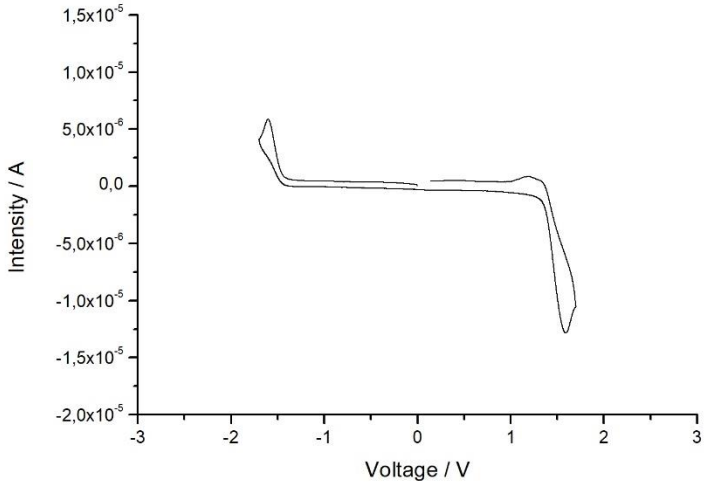
space group: P-1

Synthesis of 9,13,15-triphenyldibenzo[6,7:10,11]tetraceno[2,3-*d*]isoxazole (91)



Column chromatography eluting with a gradient from hexane:CH_2Cl_2, 1:2, to hexane:CH_2Cl_2, 1:3, to afford **91** as a white solid (8 mg, 20%, m.p.: 257-258 ºC). ^{1}H NMR (300 MHz, $CDCl_3$), δ: 8.60 (s, 1H), 8.10 (s, 1H), 7.96 (dd, *J* = 6.6, 3.0 Hz, 2H), 7.90 – 7.77 (m, 5H), 7.65 – 7.50 (m, 14H), 7.34 (td, *J* = 7.9, 3.4 Hz, 2H) ppm. ^{13}C NMR (126 MHz, $CDCl_3$), δ: 160.2 (C), 157.5 (C), 142.2 (C), 137.5 (C), 136.2 (C), 132.6 (CH), 132.5 (CH), 131.1 (C), 130.9 (C), 130.6 (CH), 130.3 (C), 130.1 (C), 129.7 (CH), 129.4 (CH), 129.3 (CH), 128.9 (CH), 128.4 (C), 128.2 (CH), 128.2 (CH), 127.0 (CH), 127.0 (C), 126.7 (CH), 126.2 (CH), 126.1 (C), 125.0 (CH), 121.9 (C), 121.7 (CH), 104.3 (CH) ppm. IR (ν): 3052, 3014, 1526, 1490, 1352, 943, 859, 754, 720, 701, 692, 542 cm^{-1}. MS (EI), m/z: 571 (M^+, 100). HRMS (EI), m/z found: 571.1953 (calc. for $C_{43}H_{25}NO$: 571.1936).

Cyclic voltammogram of 91



Measured in Tol:MeCN, 1:5, using *n*-Bu_4NPF_6 (0.1 M) as electrolyte and AgCl/Ag as reference electrode.

7.5.3 Computational details

All the calculations were performed in collaboration with Prof. A. Cobas[131]using the Gaussian 09 program package.[221] Geometries of final products were optimised at the density functional level using the B3LYP functional[222] and 6-31G(d) basis set. Frequency calculations were performed at this level to confirm the nature of the stationary points and to obtain the thermal and entropic contribution to the free energy.[229]

Time-Dependent DFT Calculations (TD DFT)

Table 10. Wavelengths for HOMO-LUMO transitions.

Entry[a]	Product	λ / nm
1	**85**	390
2	**86**	465
3	**87**	466
4	**89**	381
5	**90**	452
6	**91**	455

a) TD DFT calculations were performed to understand the nature of excited states and the emissions of compounds **85** to **87** and **89** to **91**. The longest wavelength absorption maximum is attributed to HOMO−LUMO transitions.

[131] Theoretical calculations were performed in collaboration with Prof. A. Cobas, Department of Organic Chemistry, University of Santiago de Compostela (USC), Spain.

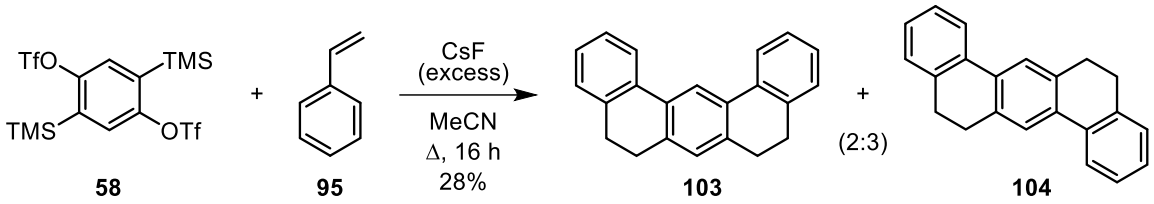
[221] Gaussian 09, Revision **D.01**, M. J. Frisch, G. W. Trucks, H. B. Schlegel, G. E. Scuseria, M. A. Robb, J. R. Cheeseman, G. Scalmani, V. Barone, B. Mennucci, G. A. Petersson, H. Nakatsuji, M. Caricato, X. Li, H. P. Hratchian, A. F. Izmaylov, J. Bloino, G. Zheng, J. L. Sonnenberg, M. Hada, M. Ehara, K. Toyota, R. Fukuda, J. Hasegawa, M. Ishida, T. Nakajima, Y. Honda, O. Kitao, H. Nakai, T. Vreven, J. A. Montgomery, Jr., J. E. Peralta, F. Ogliaro, M. Bearpark, J. J. Heyd, E. Brothers, K. N. Kudin, V. N. Staroverov, R. Kobayashi, J. Normand, K. Raghavachari, A. Rendell, J. C. Burant, S. S. Iyengar, J. Tomasi, M. Cossi, N. Rega, J. M. Millam, M. Klene, J. E. Knox, J. B. Cross, V. Bakken, C. Adamo, J. Jaramillo, R. Gomperts, R. E. Stratmann, O. Yazyev, A. J. Austin, R. Cammi, C. Pomelli, J. W. Ochterski, R. L. Martin, K. Morokuma, V. G. Zakrzewski, G. A. Voth, P. Salvador, J. J. Dannenberg, S. Dapprich, A. D. Daniels, Ö. Farkas, J. B. Foresman, J. V. Ortiz, J. Cioslowski, D. J. Fox, Gaussian, Inc., Wallingford CT, **2009**.

[222] a) A. D. Becke*, J. Chem. Phys.* **1993**, *98*, 5648–5652; b) C. Lee, W. Yang, R. G. Parr, *Phys. Rev. B* **1988**, *37*, 785–789.

[229] The UV-vis absorption spectra were simulated by time-dependent DFT (TD-DFT) calculations at the same level of theory.

7.6 Experimental procedures for Chapter 6

7.6.1 Synthesis of 5,6,8,9-tetrahydrobenzo[*m*]tetraphene (103)



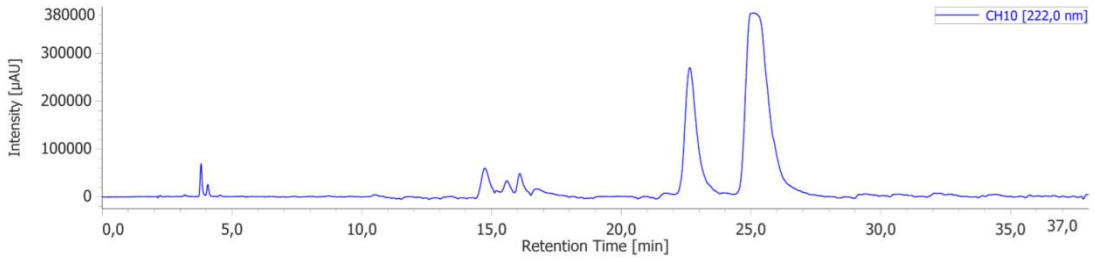
To a solution of **58** and styrene (**95**) in dioxane or MeCN (0.05 M), CsF was added. The reaction mixture was stirred at reflux for 16 h. Then, volatiles were removed under reduced pressure and the obtained solid was purified by column chromatography (eluting with hexane:toluene, 3:1) to afford the mixture of isomers **103** and **104** as a white solid (≈ 2:3 mixture, 1.5 g, 28%). Separation of isomers **103** and **104** was achieved by consecutive recrystallisations in MeOH, although a significant amount of material was lost due to decomposition. Compounds **103** and **104** were also separated by semipreparative SFC.[230] Spectroscopic data were coincident with those described in the literature for these compounds.[202] ^{1}H NMR (300 MHz, $CDCl_3$), δ: 8.13 (s, 1H), 7.85 (s, 1H), 7.50 – 7.15 (m, 6H), 7.10 (s, 1H), 2.86 (s, 8H) ppm..

[230] Details about the SFC are included below.

[202] H. A. Staab, F. Diederich, *Chem. Ber.* **1983**, *116*, 3487–3503.

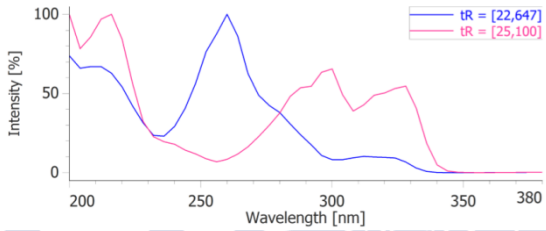
Chromatogram of 103 and 104

SFC was performed with Lux@ 5µm i-Amylose-1 column (250 x 10 mm) (9:1, MeOH: CO_2, 7 ml/min, 150 Bar, 40 ºC).



Retention times: **103**, 22.6 min and **104**, 25.1 min.

UV-Vis spectra of 103 and 104



7.6.2 AFM imaging

AFM imaging of single molecules of kekulene was studied by Z. Majzik, N. Pavliček and L. Gross.[213]

AFM characterisation was performed at a temperature of T = 5K with CO functionalised tips[22,231] and using a qPlus sensor[232] in the frequency modulation mode[233] with a resonance frequency f_0 of about 30 kHz and a quality factor Q of about 100000 at an oscillation amplitude of A = 1 Å. The material was sublimated from a Si wafer[234] onto a Cu(111) substrate, holding the sample at T = 10 K during deposition.

7.6.3 Computational details

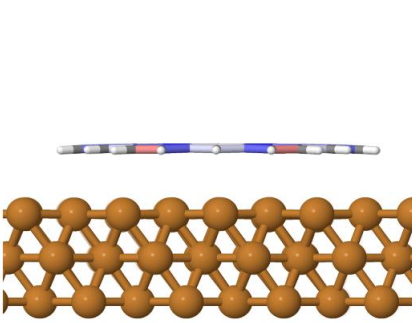
Theoretical calculations of kekulene were performed by M. Melle-Franco.[215]

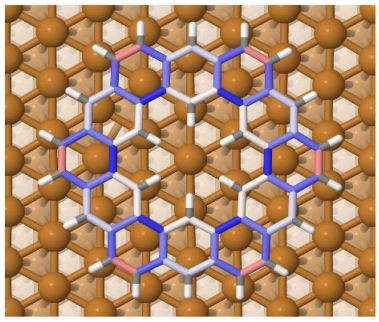
The kekulene molecule was computed in the gas-phase and on the Cu(111) surface. The molecule adsorbed on copper was computed with a QM/MM procedure where the copper surface is modelled by Molecular Mechanics (MM) and it is coupled to the molecule computed at the DFT level via a classical interaction derived empirically to reproduce experimental data.[235] In addition, a model, where charge images induced in the metal are computed classically, QM/MM-CI was also tried.[236] Two different DFT Hamiltonians were used PBE (for the kekulene on surface models) and B3LYP for the vacuum model. While finishing this manuscript, a geometry optimisation with a DFT treatment of kekulene and Cu(111) was also computed yielding similar geometries to the QM/MM-CI. The full DFT model results are still in a preliminary stage but are also mentioned here for completeness. Vacuum calculations were performed with Gaussian 09 with B3LYP and the def2-TVZP Hamiltonian while the kekulene on copper calculations were performed with CP2K 6.1[237] with the PBE Hamiltonian and the

---

[213] Z. Majzik, N. Pavliček and L. Gross. *IBM Research* – Zürich. 8803 Rüschlikon (Switzerland).
[22] a) L. Gross, F. Mohn, N. Moll, P. Liljeroth, G. Meyer, *Science* **2009**, *325*, 1110–1114; b) L. Gross, F. Mohn, N. Moll, B. Schuler, A. Criado, E. Guitián, D. Peña, A. Gourdon, G. Meyer, *Science* **2012**, *337*, 1326–1329.
[231] L. Gross, F. Mohn, N. Moll, G. Meyer, R. Ebel, W. M. Abdel-Mageed, M. Jaspars, *Nat. Chem.* **2010**, *2*, 821–825.
[232] F. J. Giessibl, *Appl. Phys. Lett.* **1998**, *73*, 3956–3958.
[233] T. R. Albrecht, P. Grütter, D. Horne, D. J. Rugar, *Appl. Phys.* **1991**, *69*, 668–673.
[234] B. Schuler, G. Meyer, D. Peña, O. C. Mullins, L. Gross, *J. Am. Chem. Soc.* **2015**, *137*, 9870–9876.
[215] M. Melle-Franco. *CICECO*, Aveiro Institute of Materials, Department of Chemistry, University of Aveiro, 3810-193 Aveiro, Portugal.
[235] S. Rapino, F. Zerbetto, *Langmuir* **2005**, *21*, 2512–2518.
[236] D. Golze, M. Iannuzzi, M.-T. Nguyen, D. Passerone, J. Hutter, *J. Chem. Theor. Comput.* **2013**, *9*, 5086–5097.
[237] J. Hutter, M. Iannuzzi, F. Schiffmann, J. VandeVondele, *Comp. Mol. Sci.* **2014**, *4*, 15–25.

TVZP2 basis set for the kekulene for all models and the DZVP basis set for copper augmented by the D3 classical dispersion correction for the full DFT model.

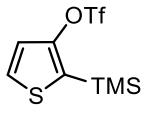




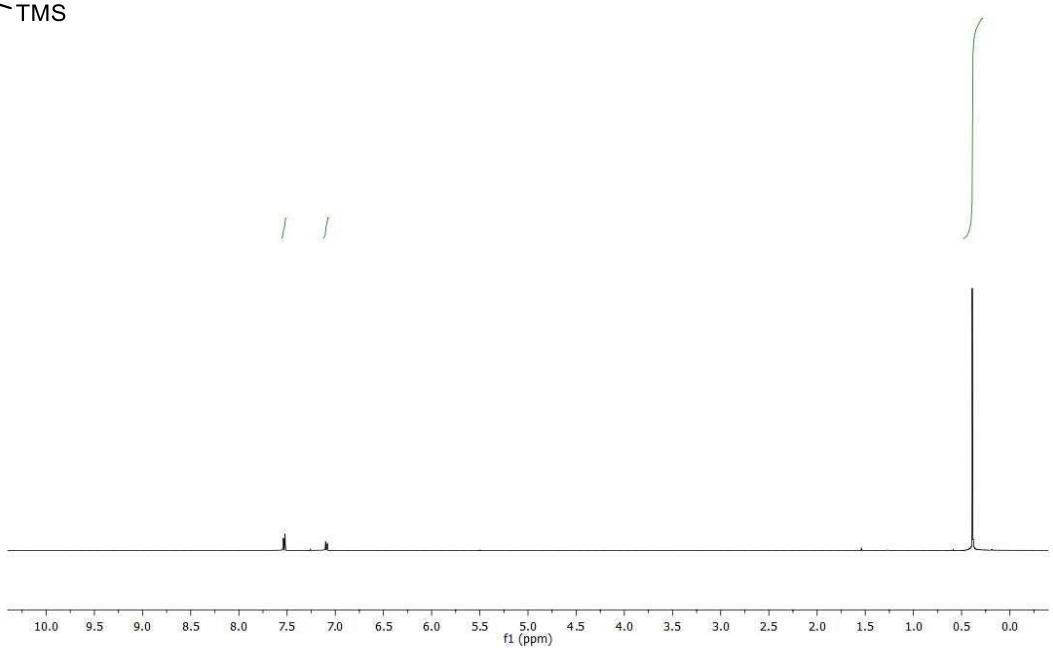
USC UNIVERSIDADE DE SANTIAGO DE COMPOSTELA

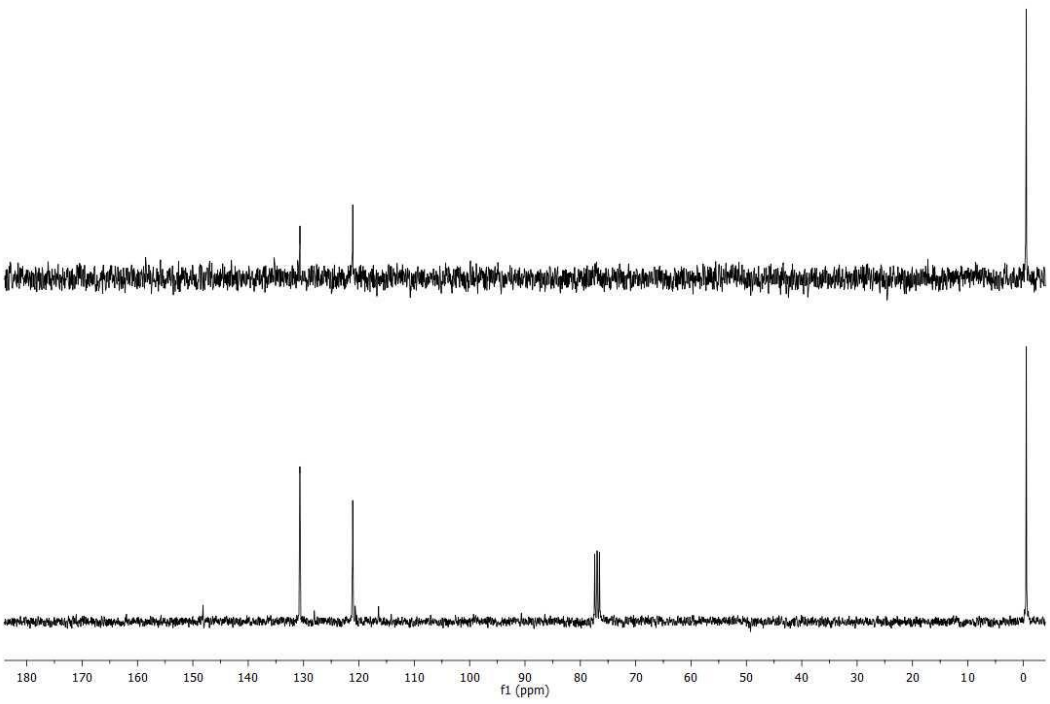
Appendix

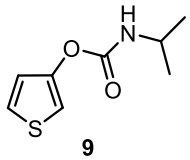
A.1 Selected spectra



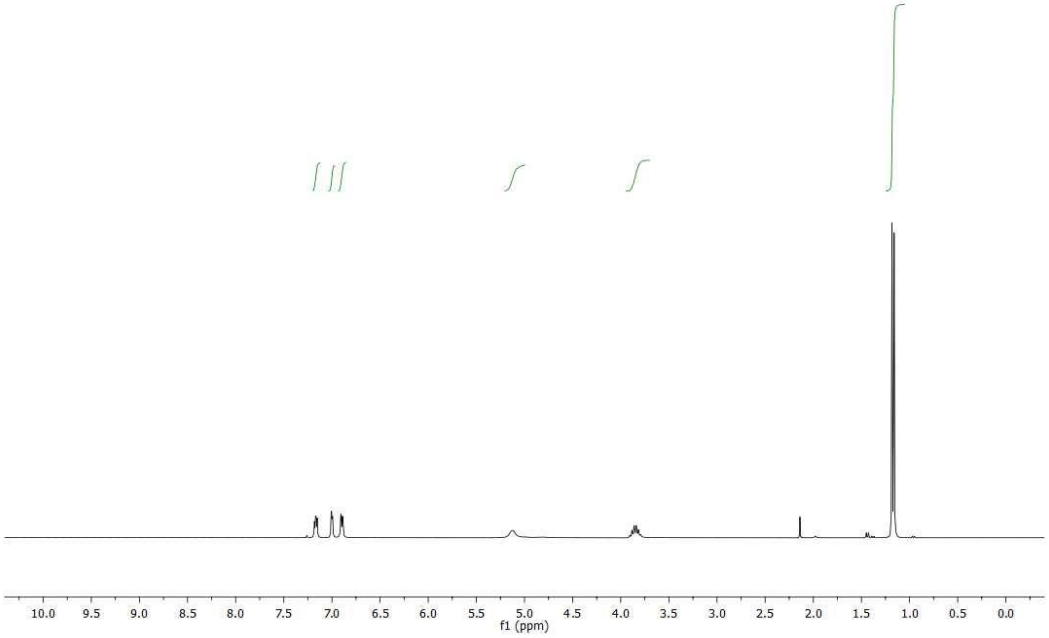
2

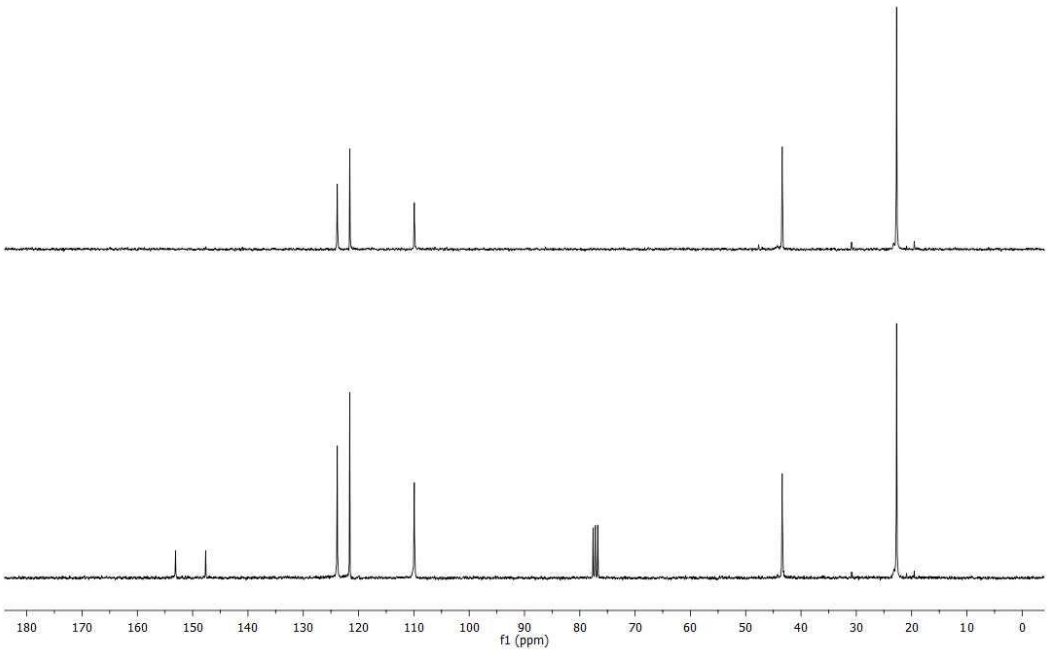


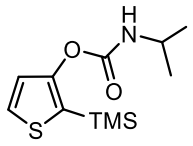




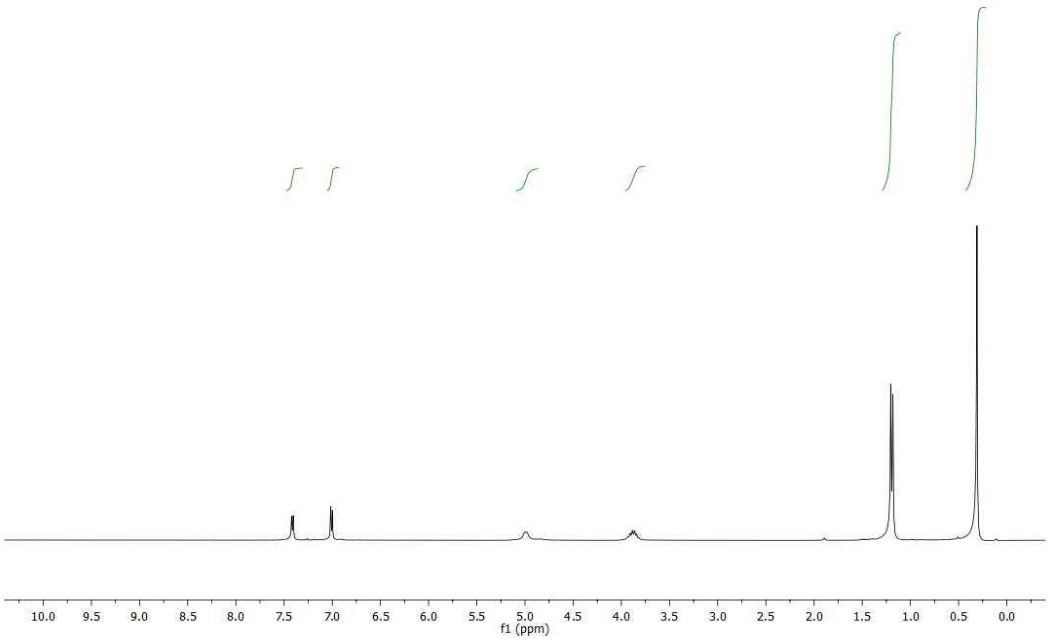
9

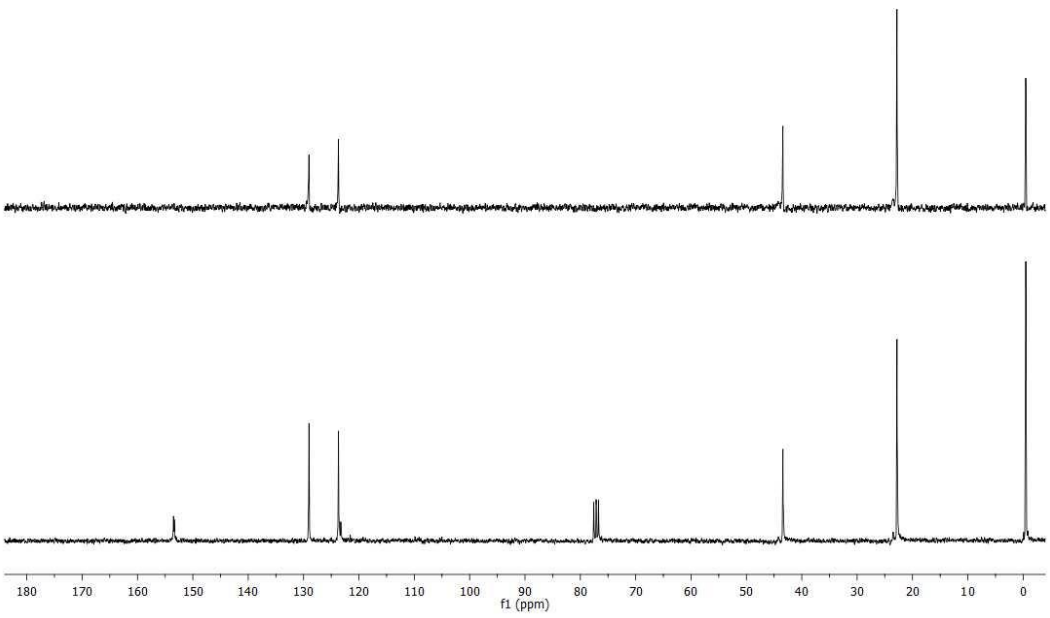

10.0 9.5 9.0 8.5 8.0 7.5 7.0 6.5 6.0 5.5 5.0 4.5 4.0 3.5 3.0 2.5 2.0 1.5 1.0 0.5 0.0
f1 (ppm)

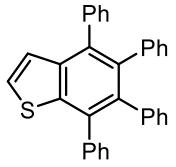

180 170 160 150 140 130 120 110 100 90 80 70 60 50 40 30 20 10 0
f1 (ppm)


H
N
O
O
TMS
S

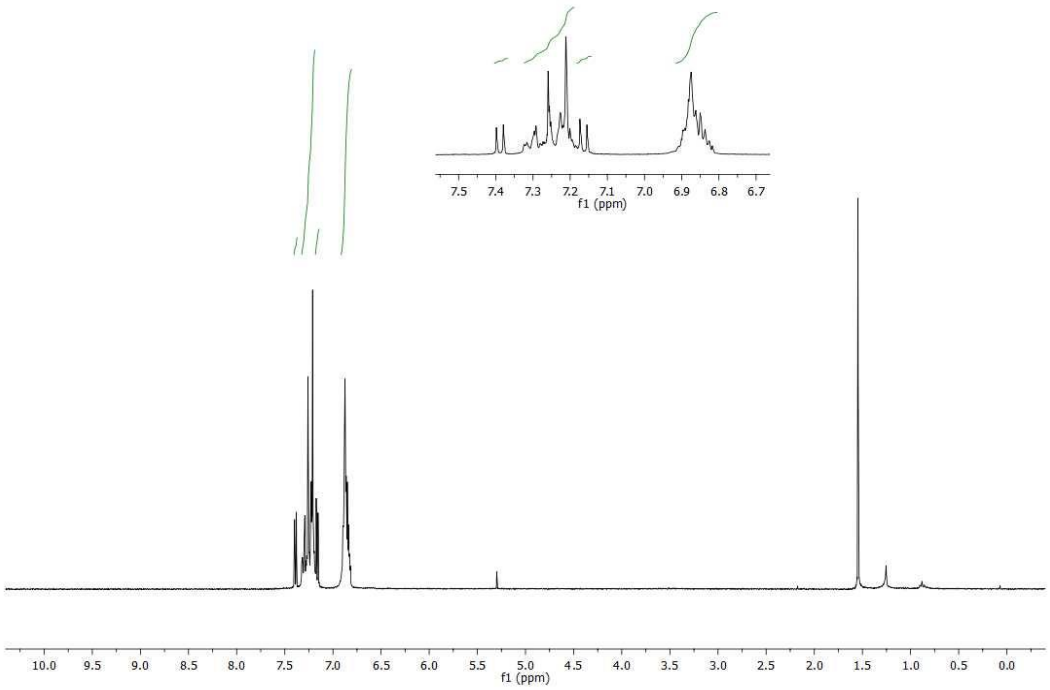
10

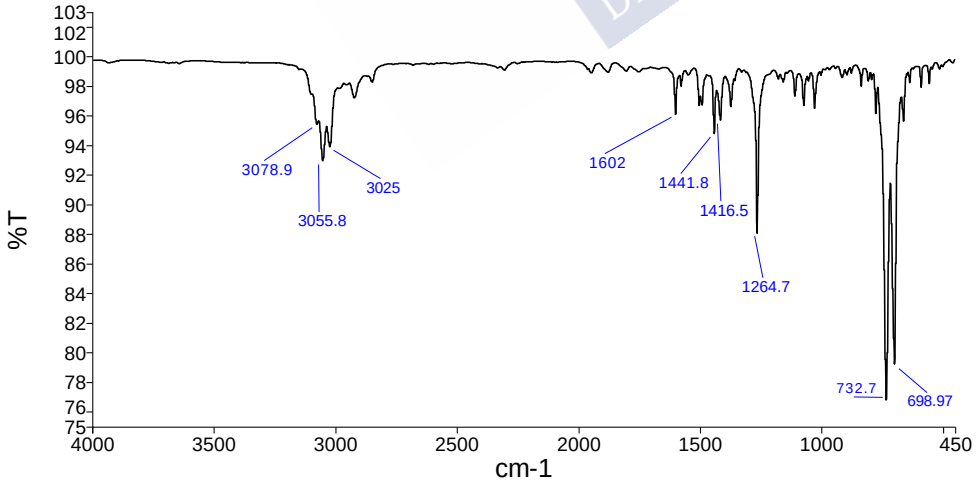

10.0 9.5 9.0 8.5 8.0 7.5 7.0 6.5 6.0 5.5 5.0 4.5 4.0 3.5 3.0 2.5 2.0 1.5 1.0 0.5 0.0
f1 (ppm)

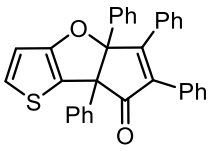

180 170 160 150 140 130 120 110 100 90 80 70 60 50 40 30 20 10 0
f1 (ppm)


Ph
Ph
Ph
Ph
S

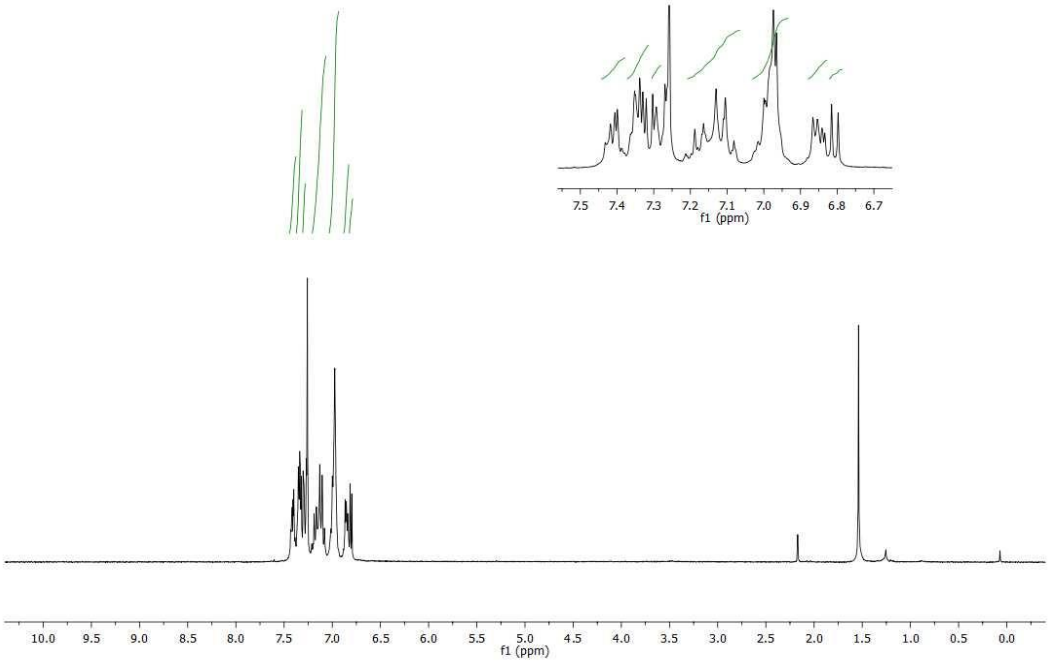
17

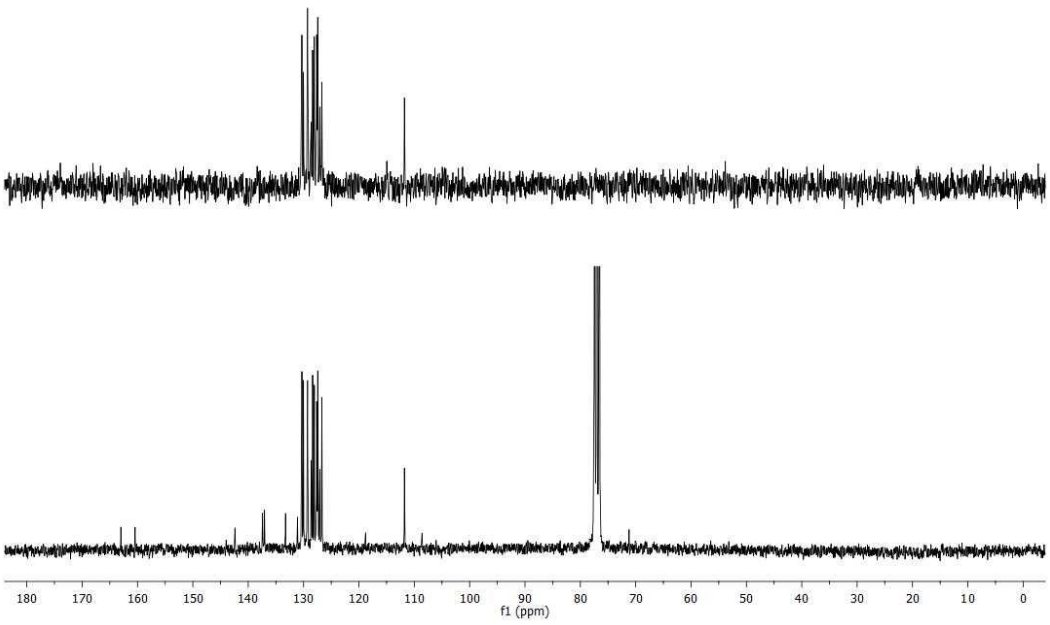

7.5 7.4 7.3 7.2 7.1 7.0 6.9 6.8 6.7
f1 (ppm)
10.0 9.5 9.0 8.5 8.0 7.5 7.0 6.5 6.0 5.5 5.0 4.5 4.0 3.5 3.0 2.5 2.0 1.5 1.0 0.5 0.0
f1 (ppm)

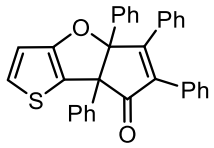

%T
cm-1
3078.9
3055.8
3025
1602
1441.8
1416.5
1264.7
732.7
698.97


Ph
Ph
O
Ph
S
Ph
O

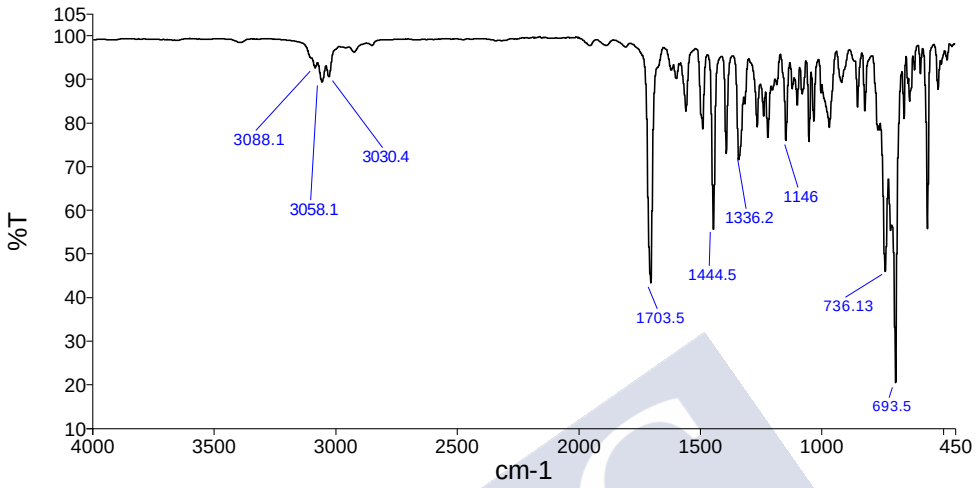
19


7.5 7.4 7.3 7.2 7.1 7.0 6.9 6.8 6.7
f1 (ppm)
10.0 9.5 9.0 8.5 8.0 7.5 7.0 6.5 6.0 5.5 5.0 4.5 4.0 3.5 3.0 2.5 2.0 1.5 1.0 0.5 0.0
f1 (ppm)

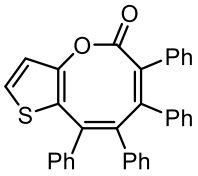

180 170 160 150 140 130 120 110 100 90 80 70 60 50 40 30 20 10 0
f1 (ppm)



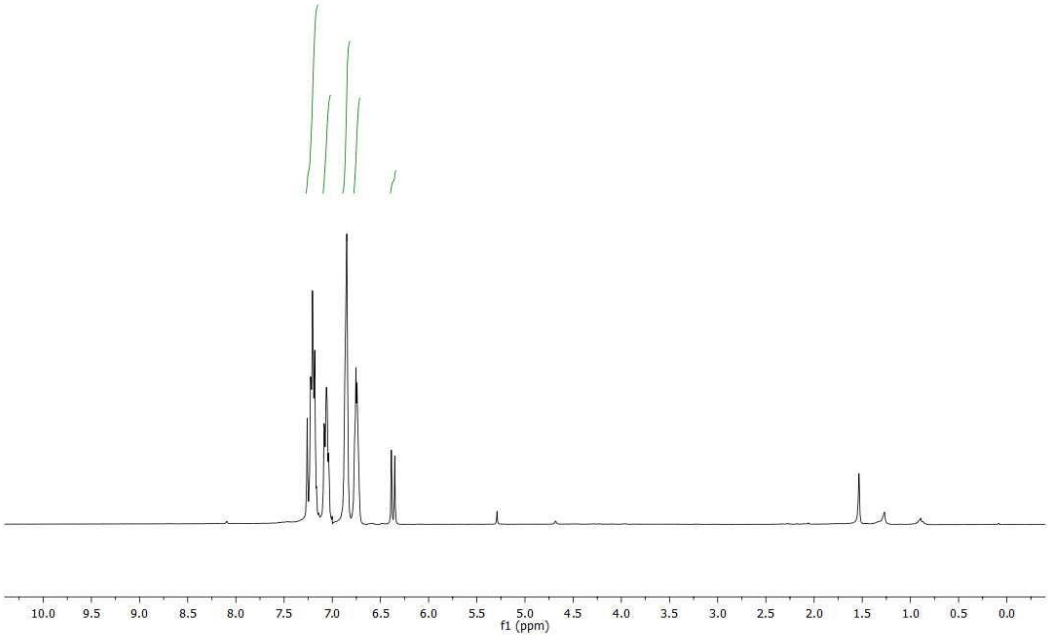
19

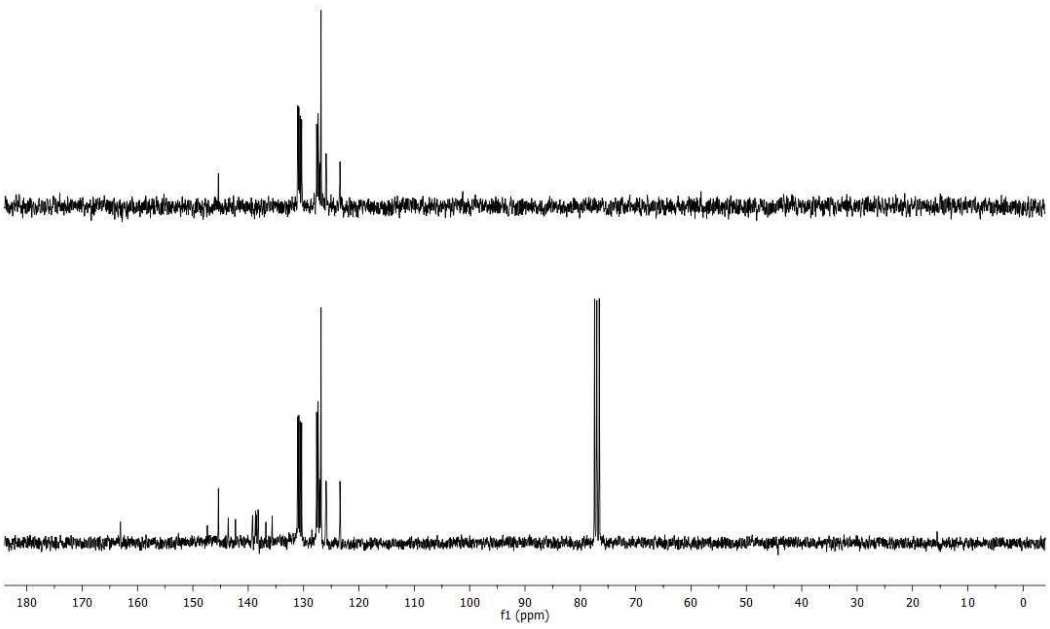


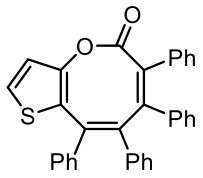
USC UNIVERSIDADE DE SANTIAGO DE COMPOSTELA


O
O
Ph
S
Ph
Ph
Ph

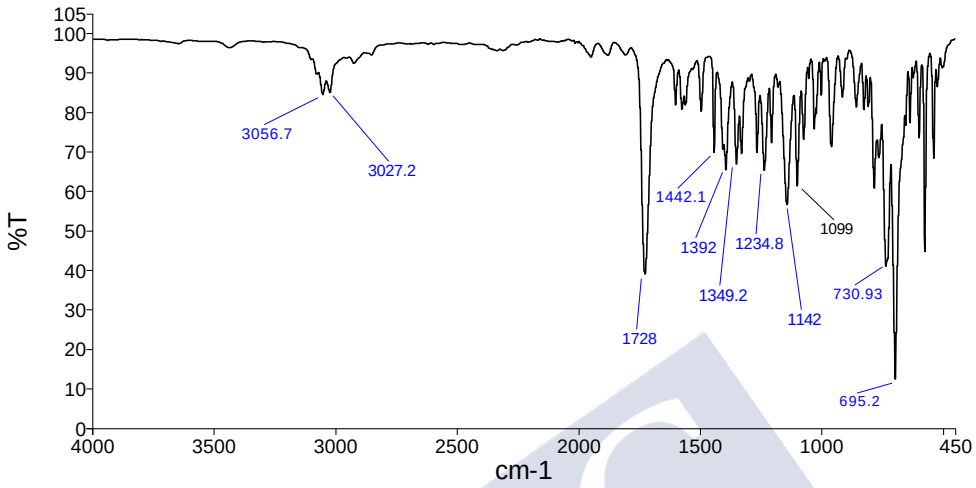
25


10.0 9.5 9.0 8.5 8.0 7.5 7.0 6.5 6.0 5.5 5.0 4.5 4.0 3.5 3.0 2.5 2.0 1.5 1.0 0.5 0.0
f1 (ppm)

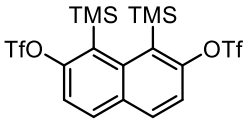

180 170 160 150 140 130 120 110 100 90 80 70 60 50 40 30 20 10 0
f1 (ppm)



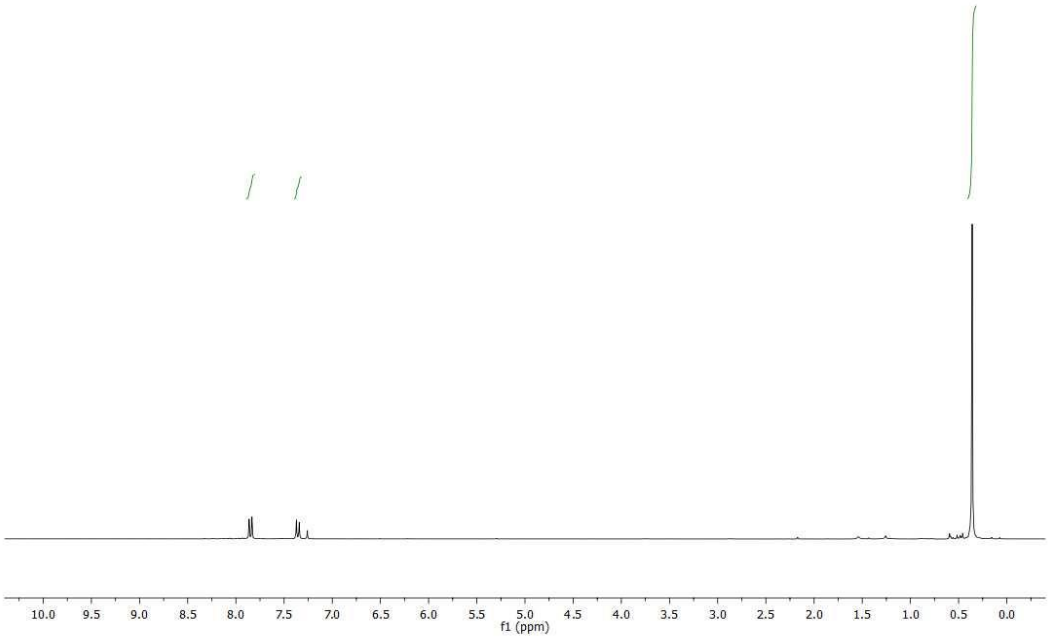
25

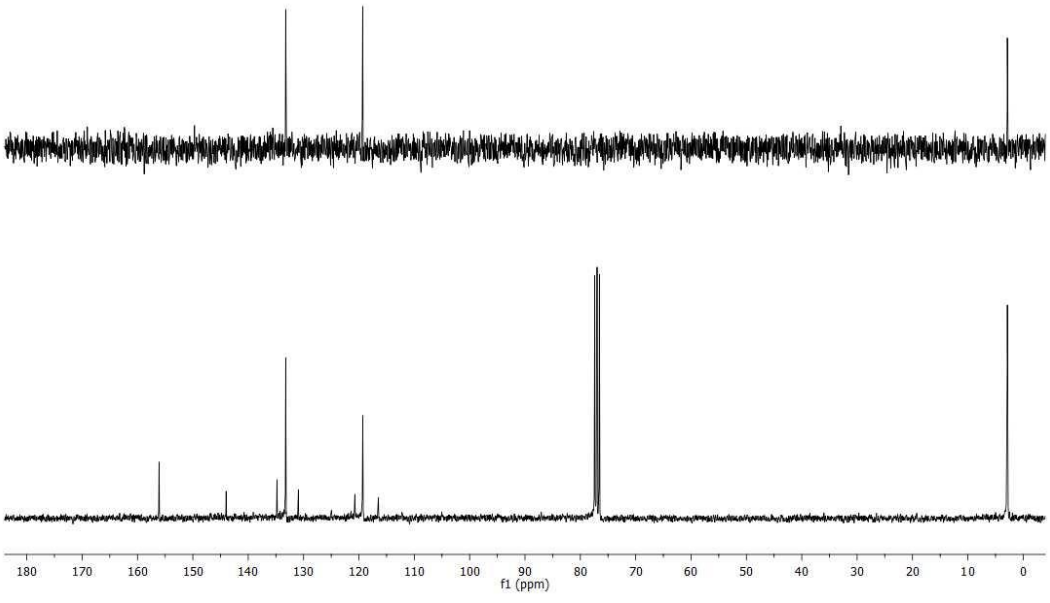


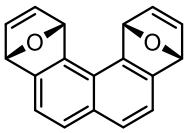
USC UNIVERSIDADE DE SANTIAGO DE COMPOSTELA


TMS TMS
TfO
OTf

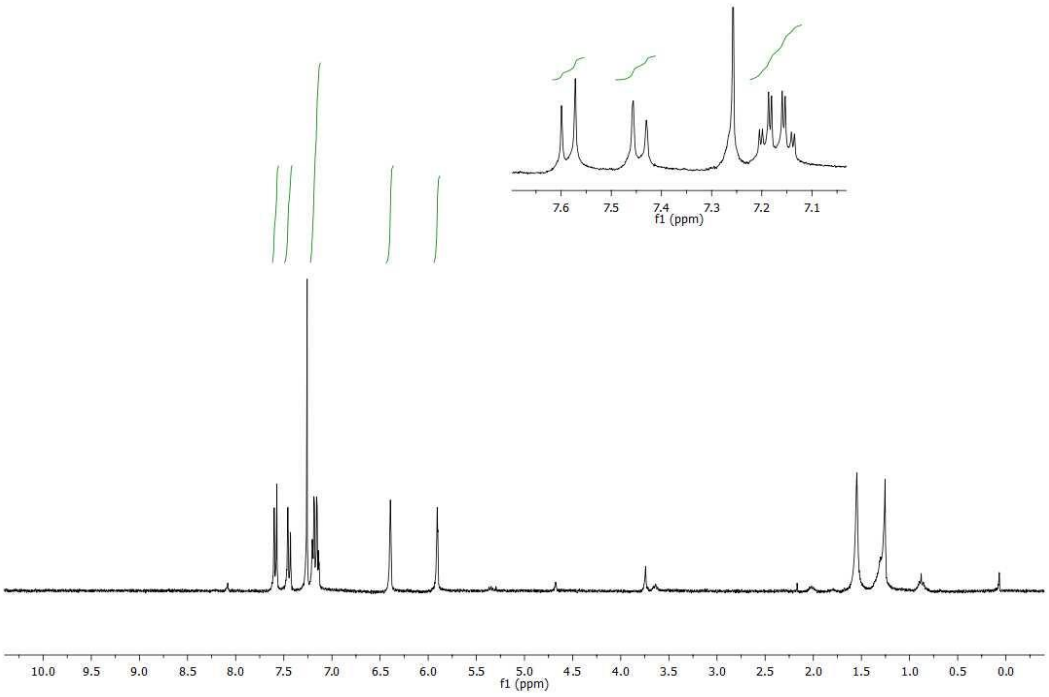
32

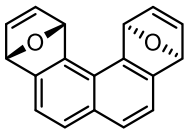

10.0 9.5 9.0 8.5 8.0 7.5 7.0 6.5 6.0 5.5 5.0 4.5 4.0 3.5 3.0 2.5 2.0 1.5 1.0 0.5 0.0
f1 (ppm)


180 170 160 150 140 130 120 110 100 90 80 70 60 50 40 30 20 10 0
f1 (ppm)

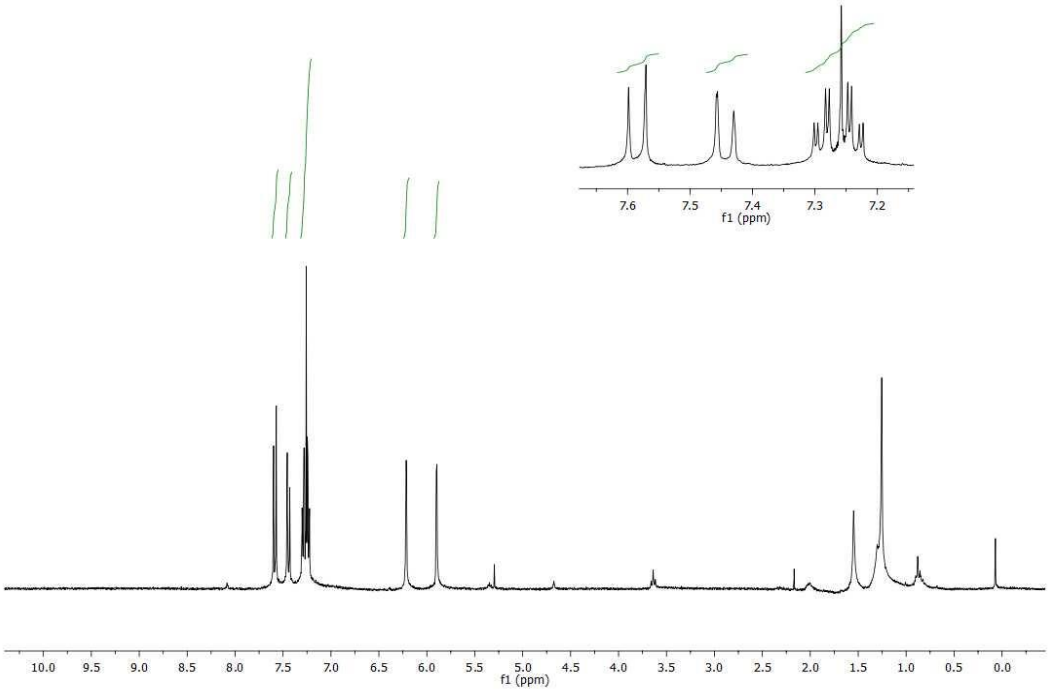


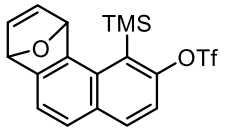
35a


7.6
7.5
7.4
7.3
7.2
7.1
f1 (ppm)
10.0
9.5
9.0
8.5
8.0
7.5
7.0
6.5
6.0
5.5
5.0
4.5
4.0
3.5
3.0
2.5
2.0
1.5
1.0
0.5
0.0
f1 (ppm)

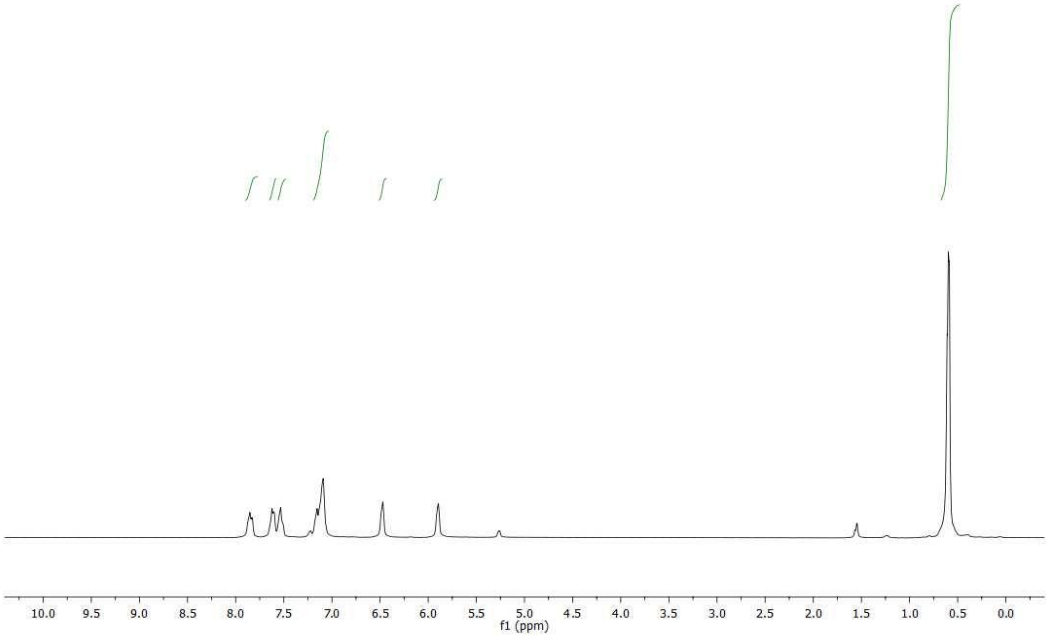


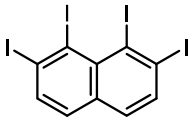
35b


7.6
7.5
7.4
7.3
7.2
f1 (ppm)
10.0
9.5
9.0
8.5
8.0
7.5
7.0
6.5
6.0
5.5
5.0
4.5
4.0
3.5
3.0
2.5
2.0
1.5
1.0
0.5
0.0
f1 (ppm)

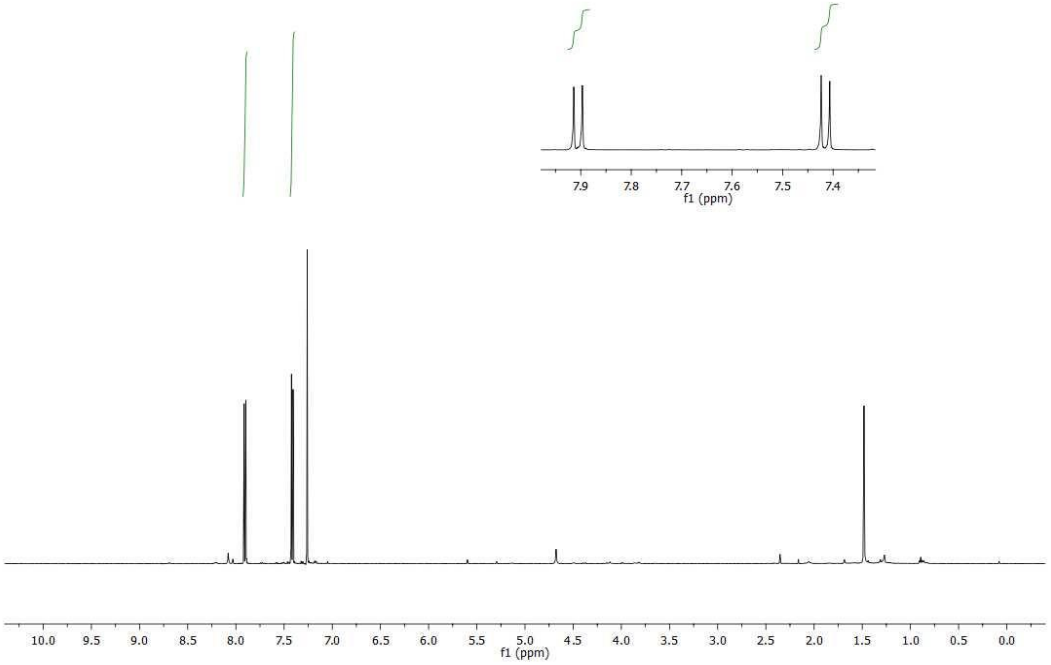

TMS
O
OTf

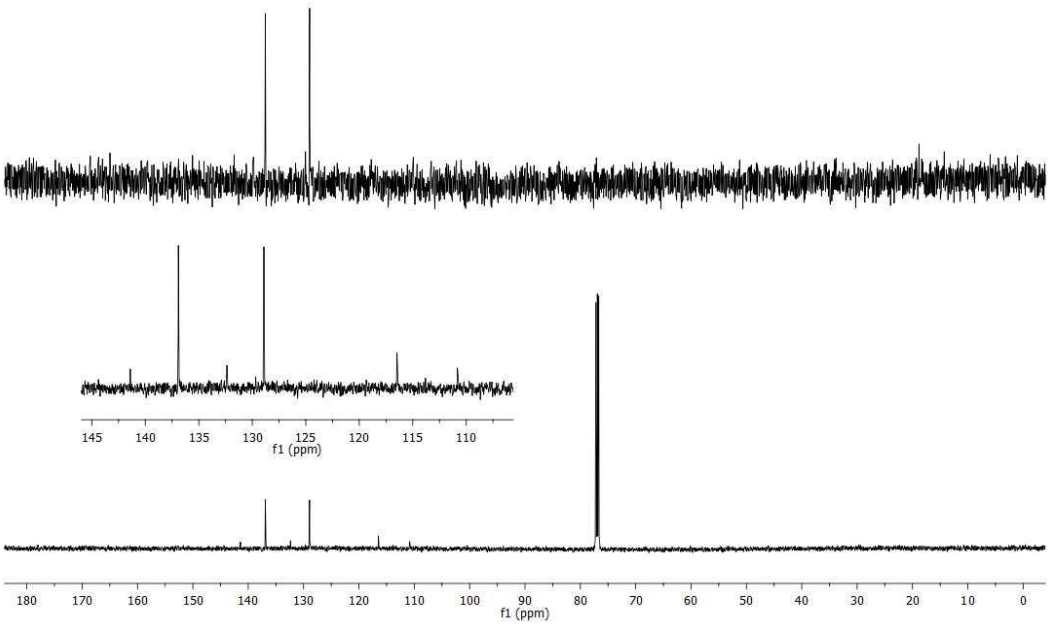
38

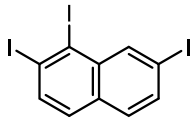

10.0
9.5
9.0
8.5
8.0
7.5
7.0
6.5
6.0
5.5
5.0
4.5
4.0
3.5
3.0
2.5
2.0
1.5
1.0
0.5
0.0
f1 (ppm)



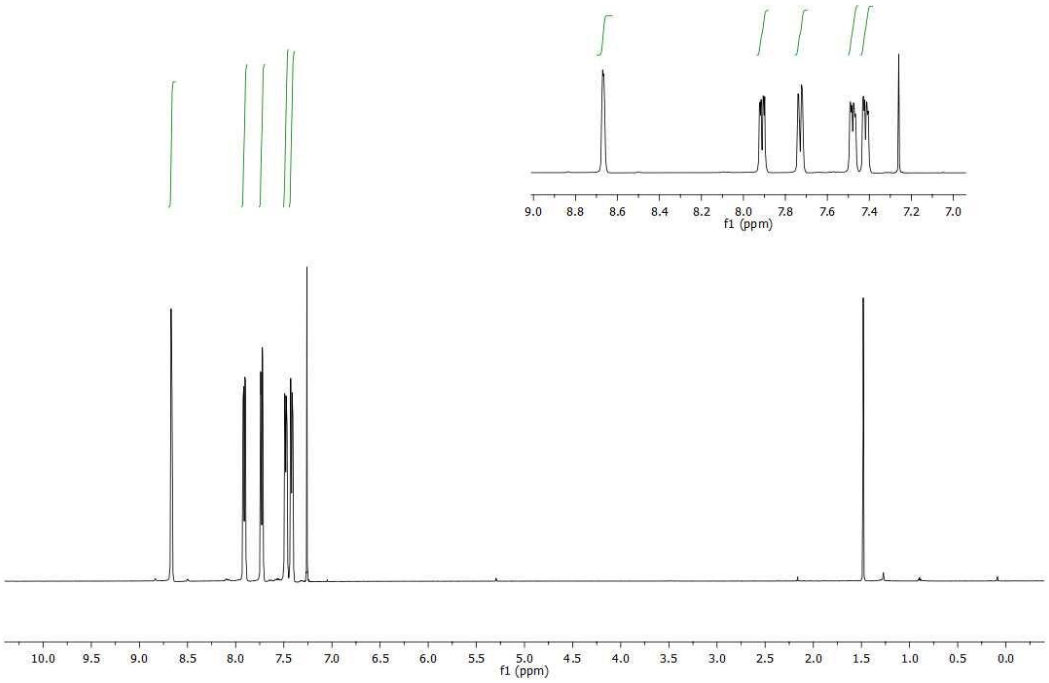
39

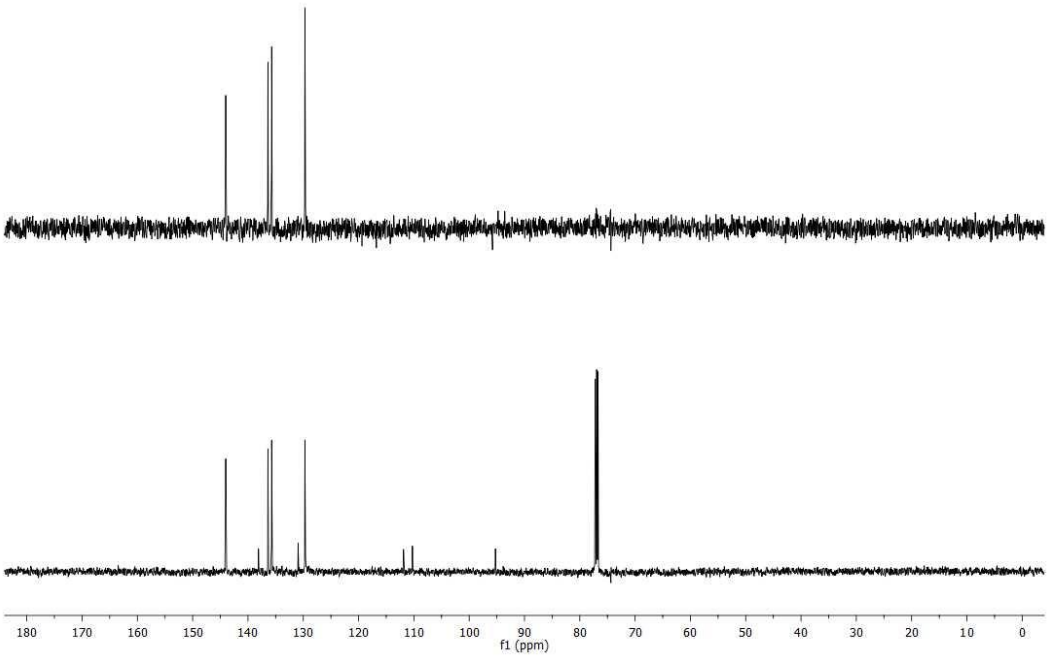

7.9
7.8
7.7
7.6
7.5
7.4
f1 (ppm)
10.0
9.5
9.0
8.5
8.0
7.5
7.0
6.5
6.0
5.5
5.0
4.5
4.0
3.5
3.0
2.5
2.0
1.5
1.0
0.5
0.0
f1 (ppm)

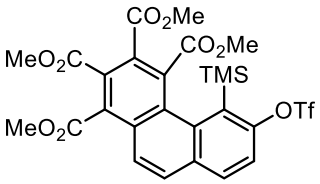

145
140
135
130
125
120
115
110
f1 (ppm)
180
170
160
150
140
130
120
110
100
90
80
70
60
50
40
30
20
10
0
f1 (ppm)



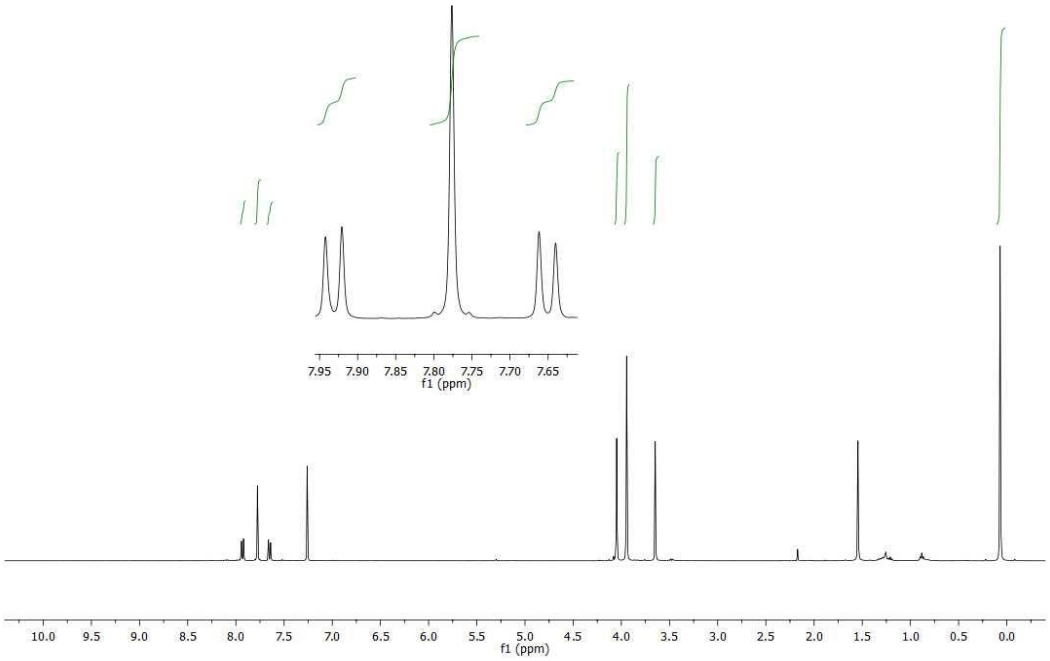
40


9.0 8.8 8.6 8.4 8.2 8.0 7.8 7.6 7.4 7.2 7.0
f1 (ppm)
10.0 9.5 9.0 8.5 8.0 7.5 7.0 6.5 6.0 5.5 5.0 4.5 4.0 3.5 3.0 2.5 2.0 1.5 1.0 0.5 0.0
f1 (ppm)

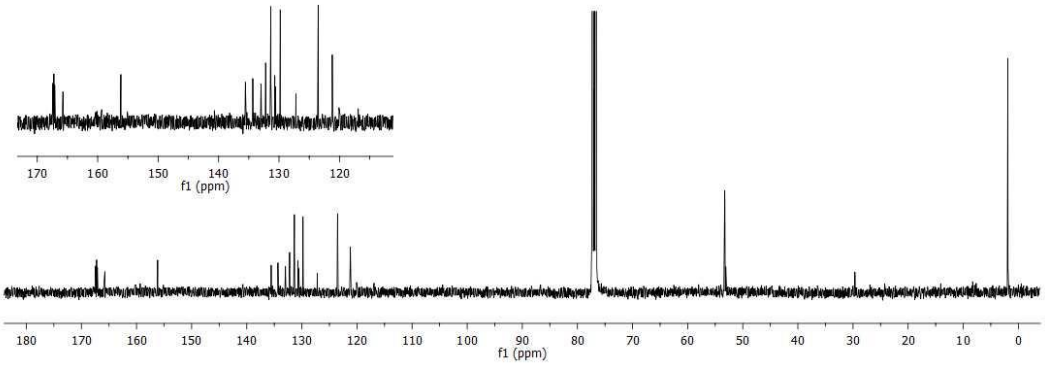

180 170 160 150 140 130 120 110 100 90 80 70 60 50 40 30 20 10 0
f1 (ppm)

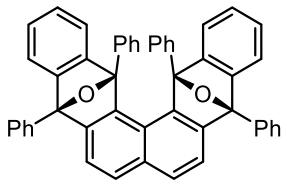

CO2Me
CO2Me
MeO2C
TMS
OTf
MeO2C

42

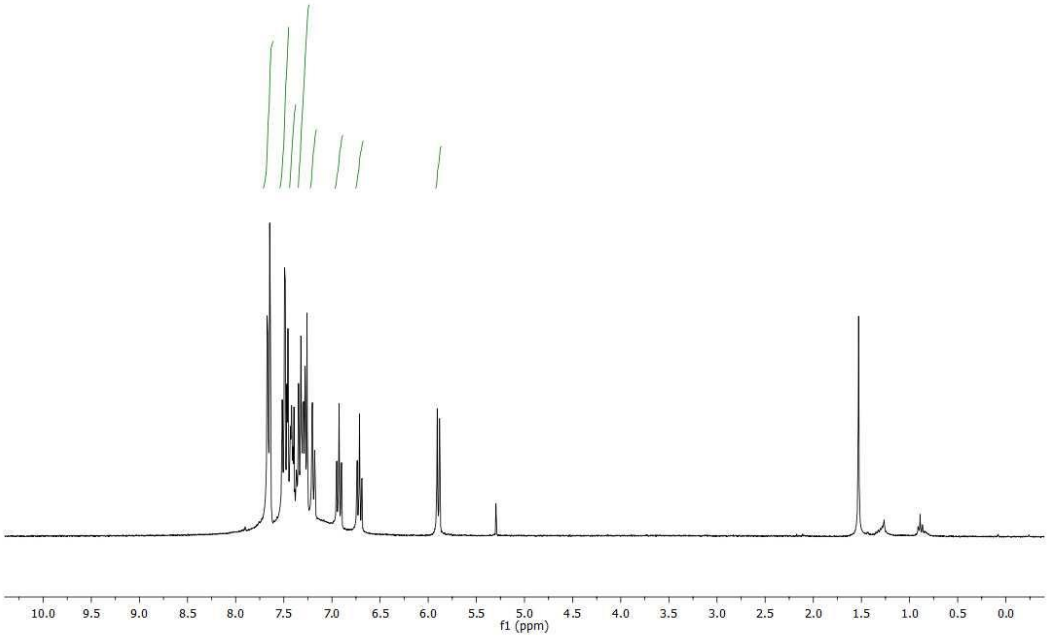

7.95 7.90 7.85 7.80 7.75 7.70 7.65
f1 (ppm)
10.0 9.5 9.0 8.5 8.0 7.5 7.0 6.5 6.0 5.5 5.0 4.5 4.0 3.5 3.0 2.5 2.0 1.5 1.0 0.5 0.0
f1 (ppm)

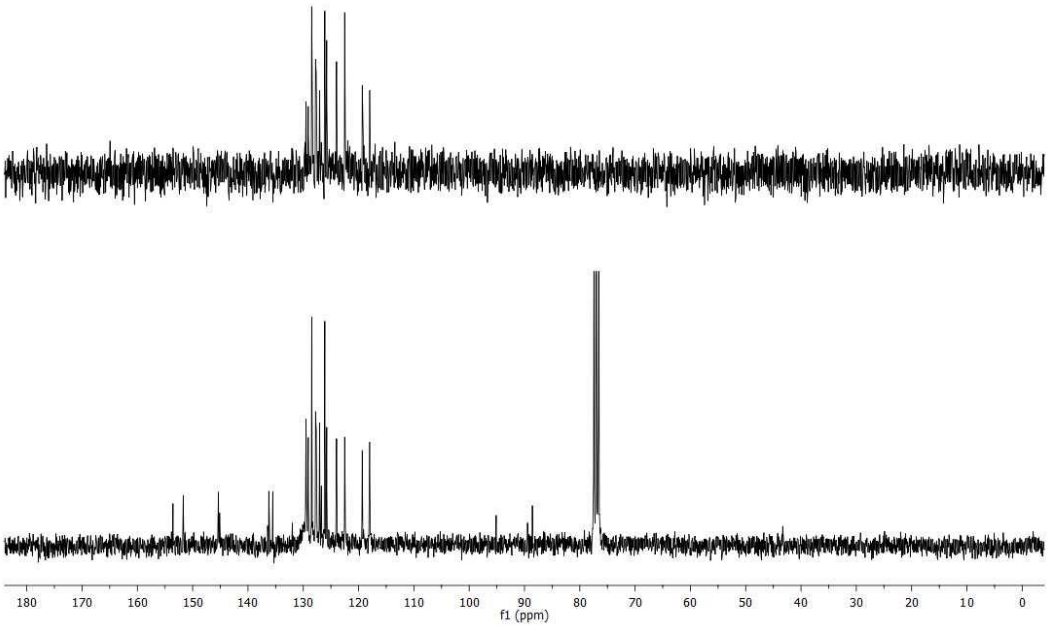


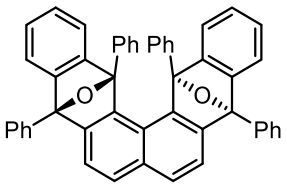

170 160 150 140 130 120
f1 (ppm)
180 170 160 150 140 130 120 110 100 90 80 70 60 50 40 30 20 10 0
f1 (ppm)


Ph Ph
O
O
Ph
Ph

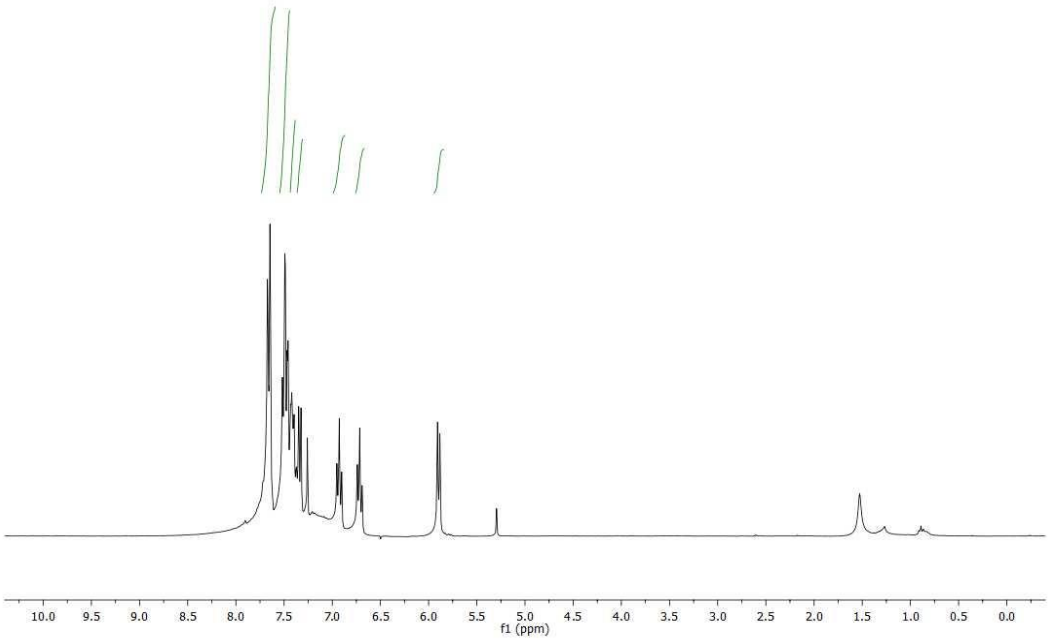
43a

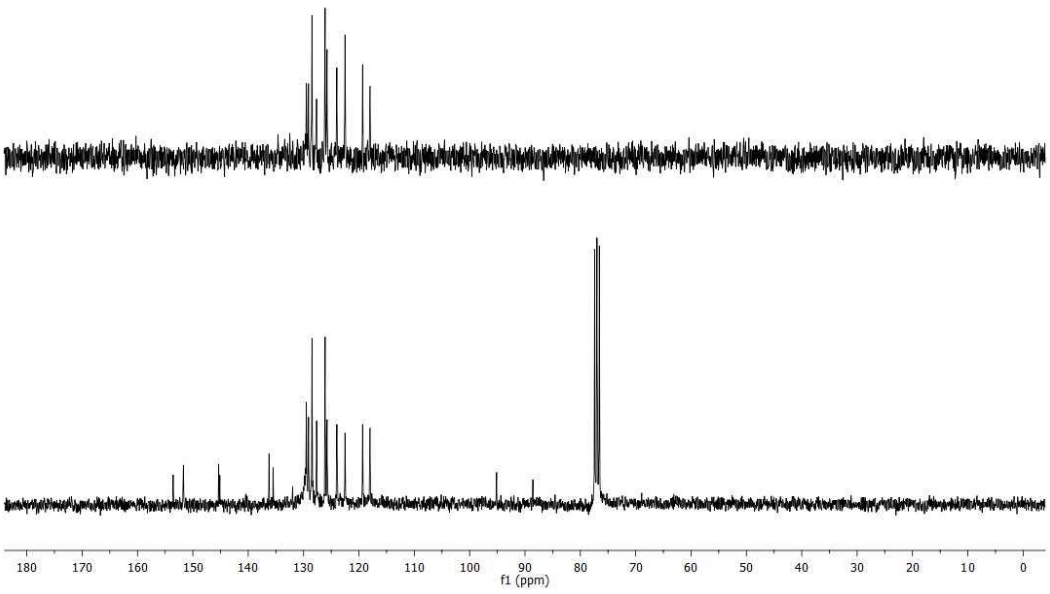

10.0 9.5 9.0 8.5 8.0 7.5 7.0 6.5 6.0 5.5 5.0 4.5 4.0 3.5 3.0 2.5 2.0 1.5 1.0 0.5 0.0
f1 (ppm)

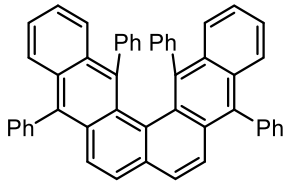

180 170 160 150 140 130 120 110 100 90 80 70 60 50 40 30 20 10 0
f1 (ppm)


Ph Ph
O
O
Ph
Ph

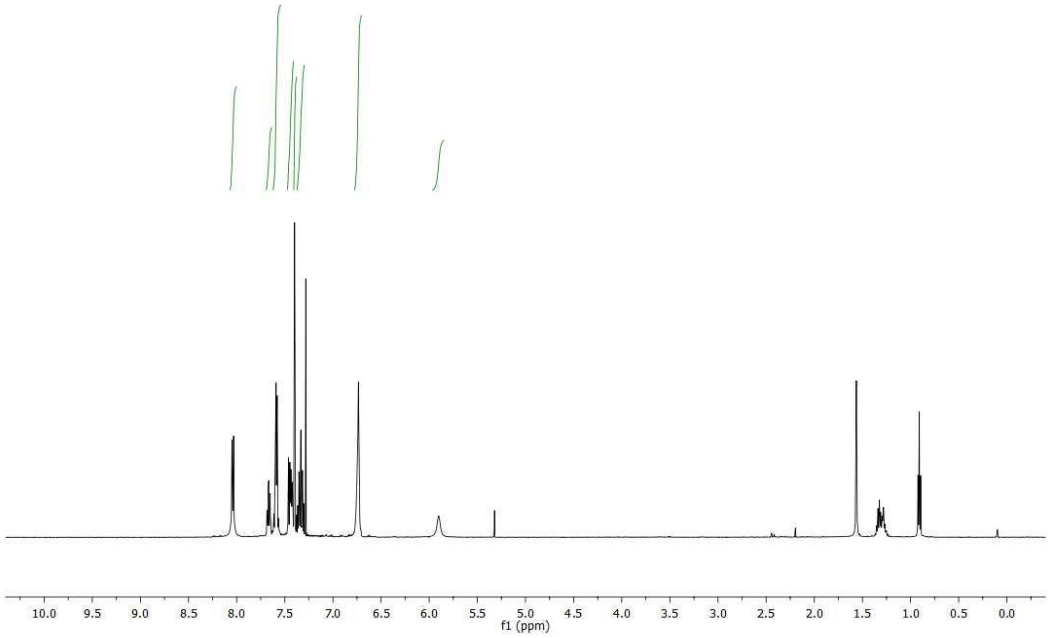
43b

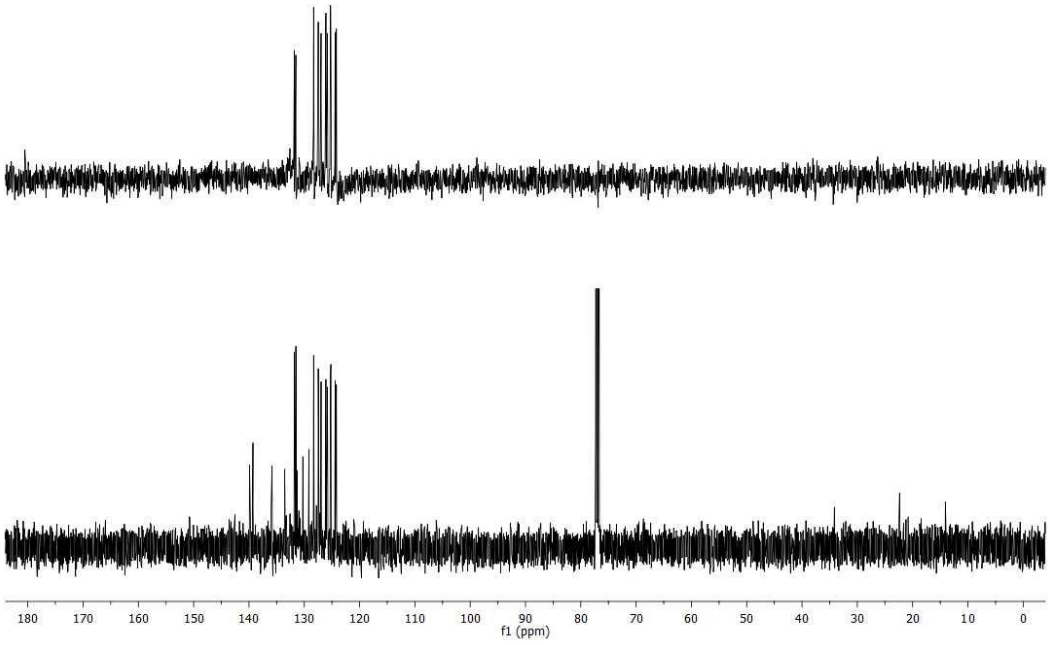

10.0 9.5 9.0 8.5 8.0 7.5 7.0 6.5 6.0 5.5 5.0 4.5 4.0 3.5 3.0 2.5 2.0 1.5 1.0 0.5 0.0
f1 (ppm)

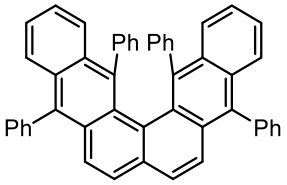

180 170 160 150 140 130 120 110 100 90 80 70 60 50 40 30 20 10 0
f1 (ppm)


Ph Ph
Ph
Ph

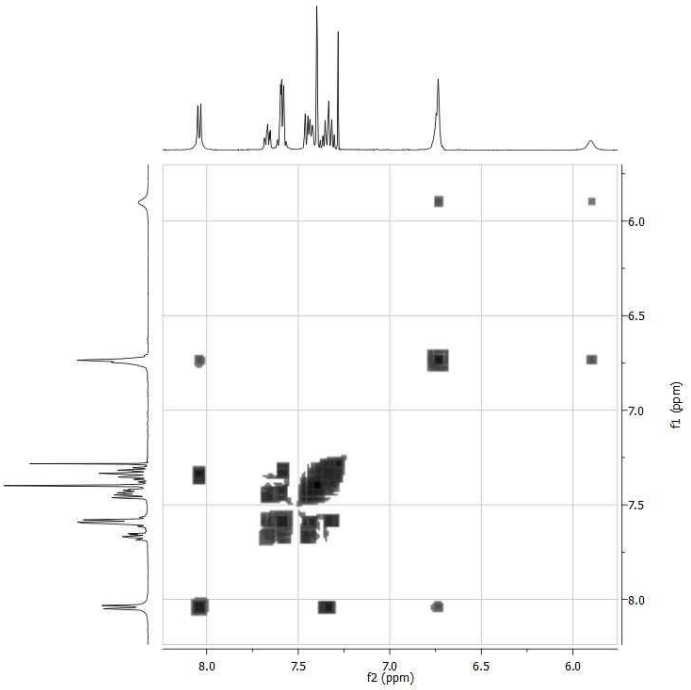
44

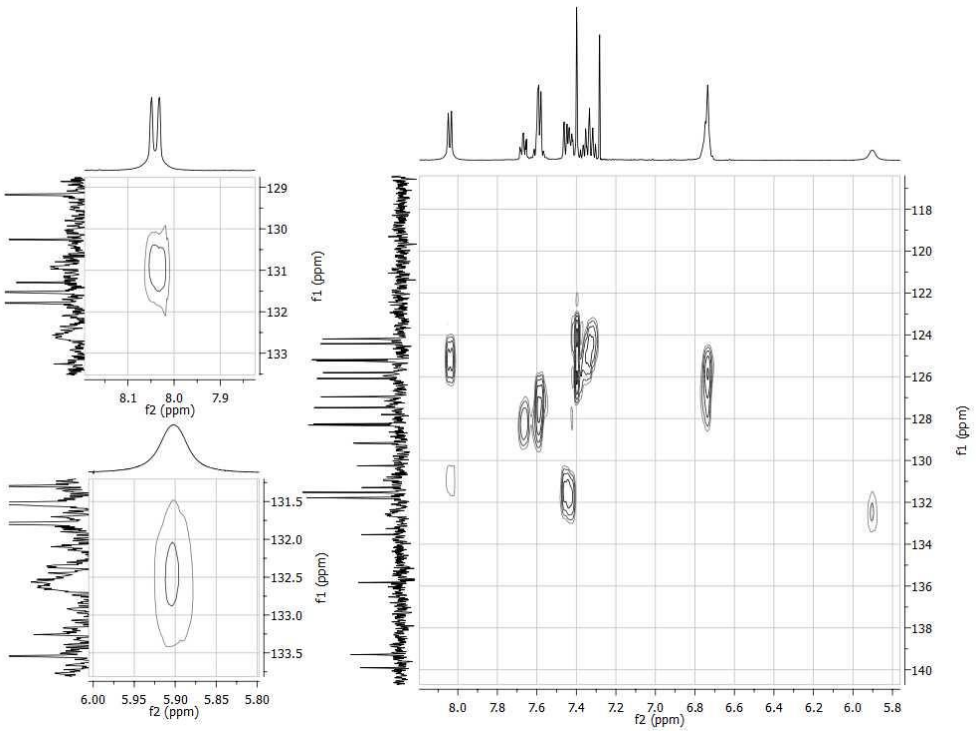

10.0 9.5 9.0 8.5 8.0 7.5 7.0 6.5 6.0 5.5 5.0 4.5 4.0 3.5 3.0 2.5 2.0 1.5 1.0 0.5 0.0
f1 (ppm)

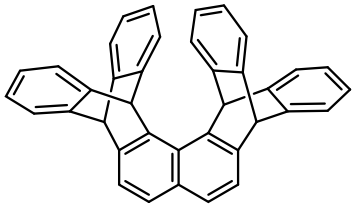

180 170 160 150 140 130 120 110 100 90 80 70 60 50 40 30 20 10 0
f1 (ppm)



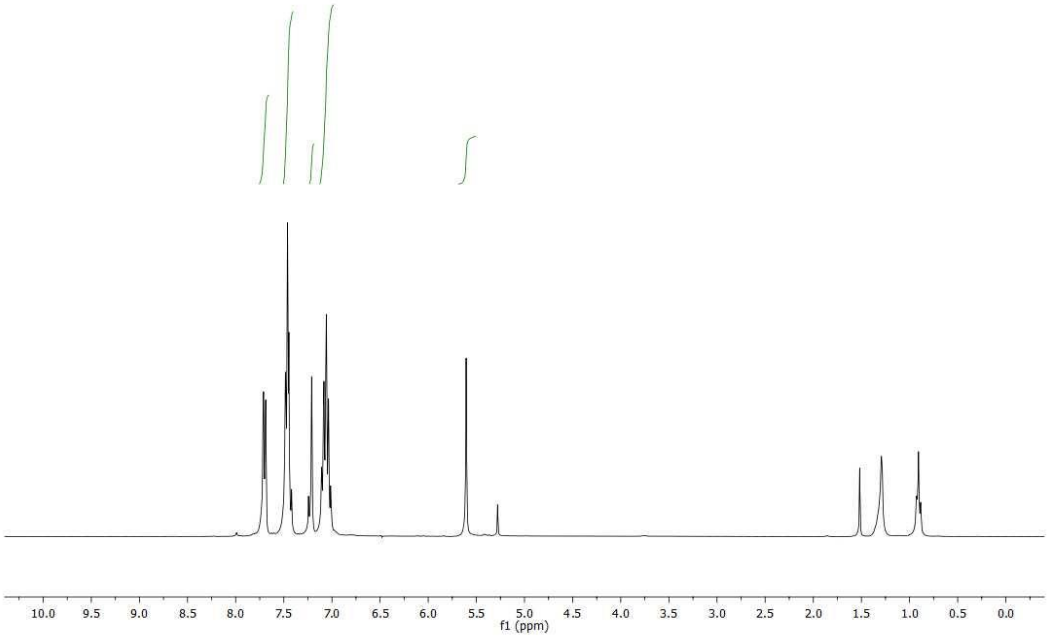
44

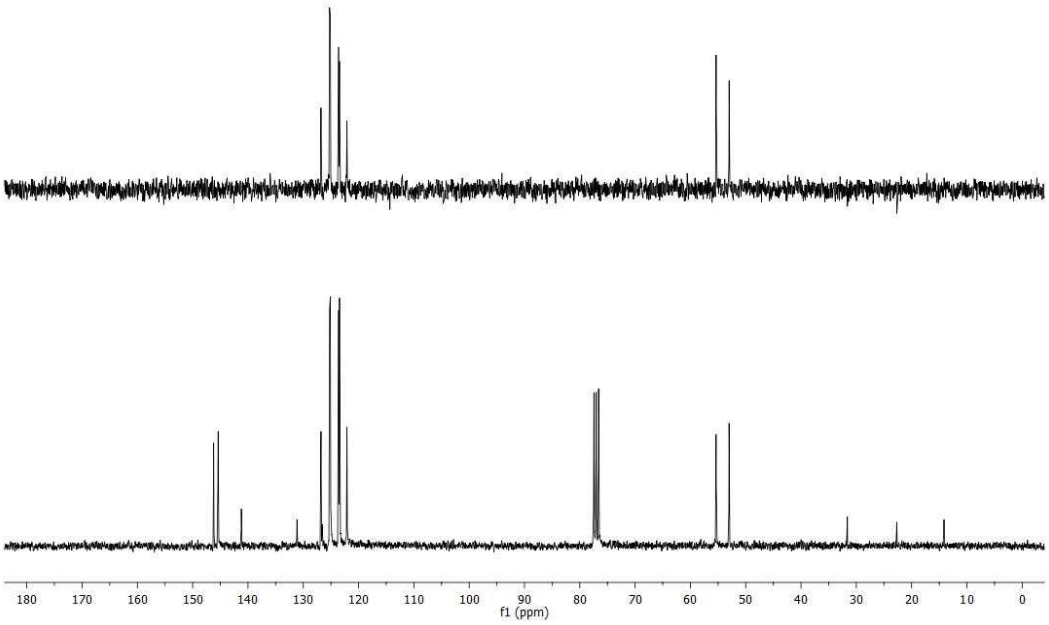


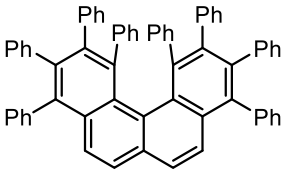




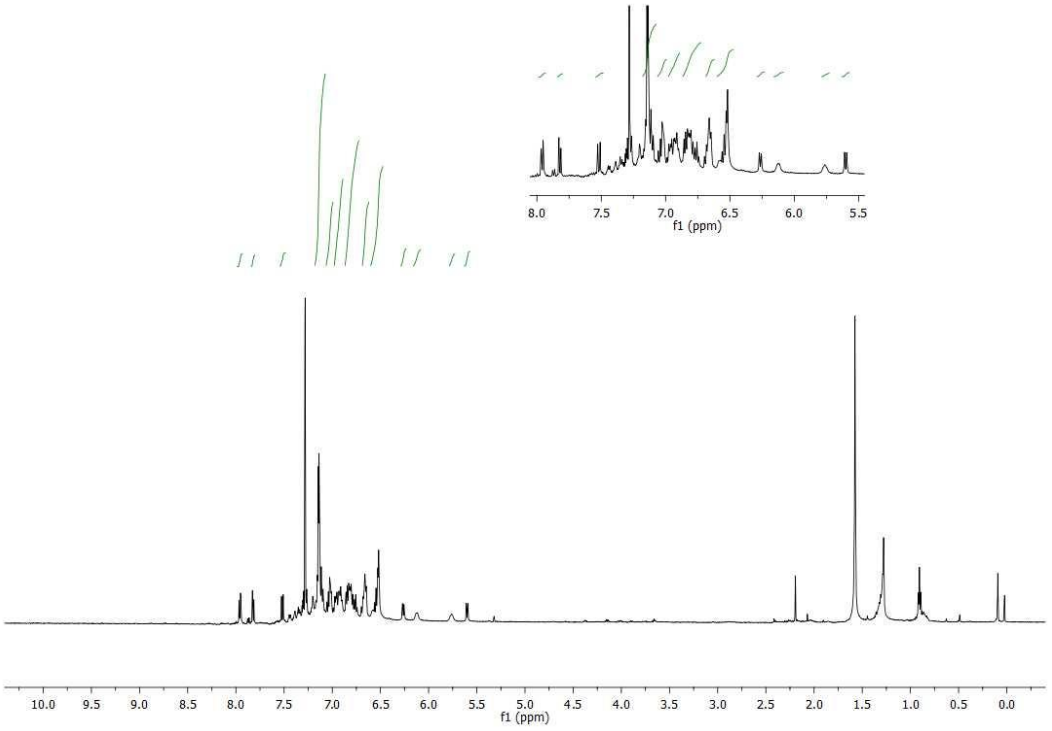
45

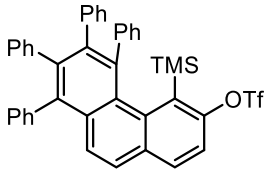

10.0 9.5 9.0 8.5 8.0 7.5 7.0 6.5 6.0 5.5 5.0 4.5 4.0 3.5 3.0 2.5 2.0 1.5 1.0 0.5 0.0
f1 (ppm)


180 170 160 150 140 130 120 110 100 90 80 70 60 50 40 30 20 10 0
f1 (ppm)

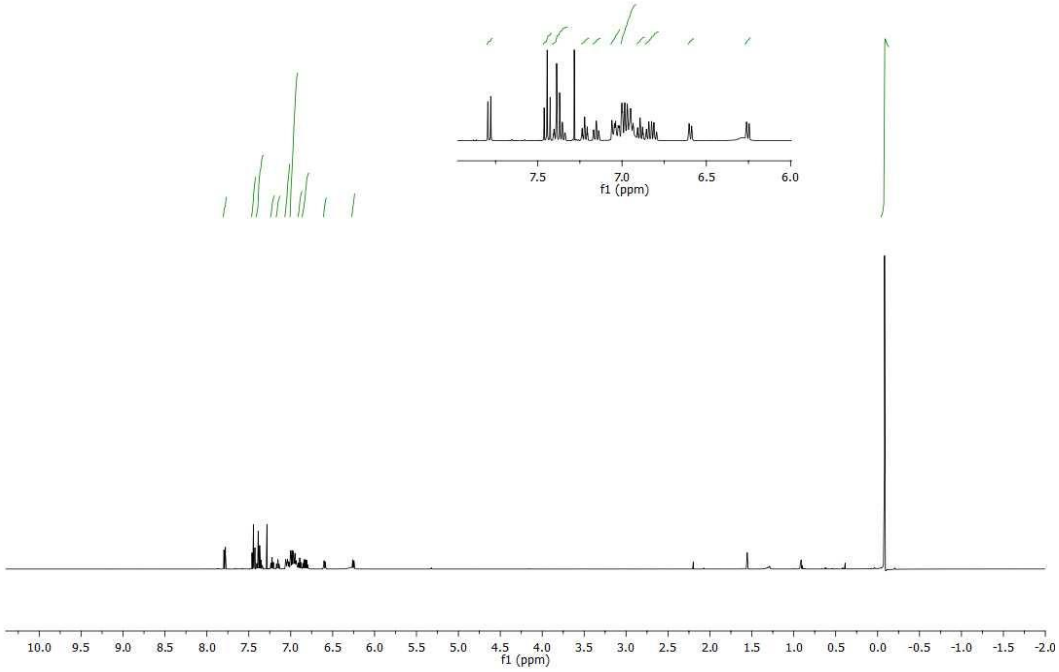

Ph
Ph
Ph
Ph
Ph
Ph
Ph
Ph

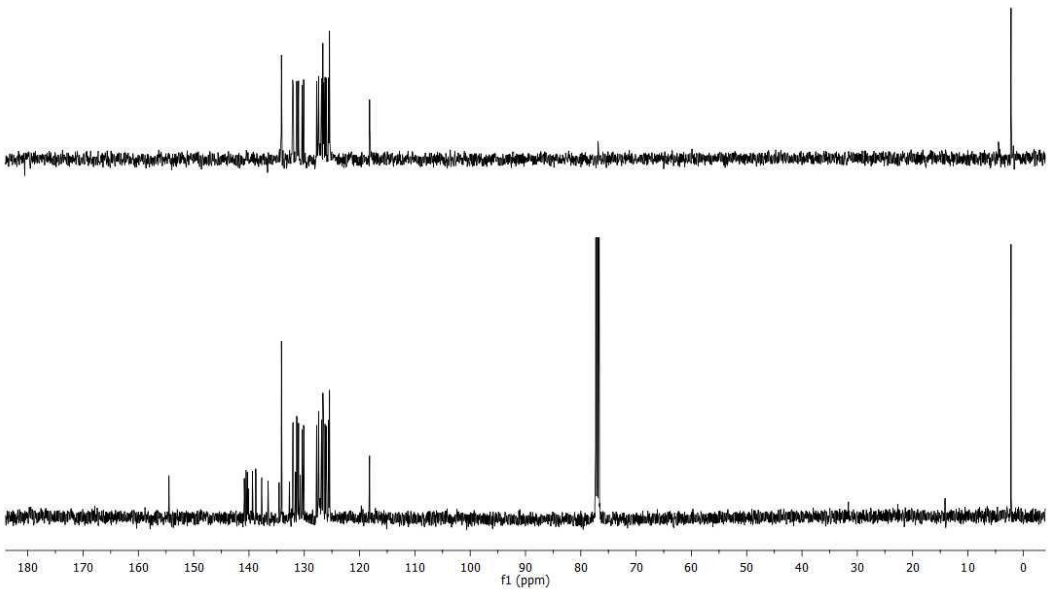
46

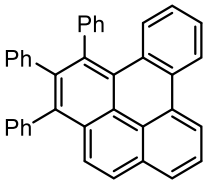

8.0
7.5
7.0
6.5
6.0
5.5
f1 (ppm)
10.0
9.5
9.0
8.5
8.0
7.5
7.0
6.5
6.0
5.5
5.0
4.5
4.0
3.5
3.0
2.5
2.0
1.5
1.0
0.5
0.0
f1 (ppm)


Ph
Ph
Ph
TMS
OTf
Ph

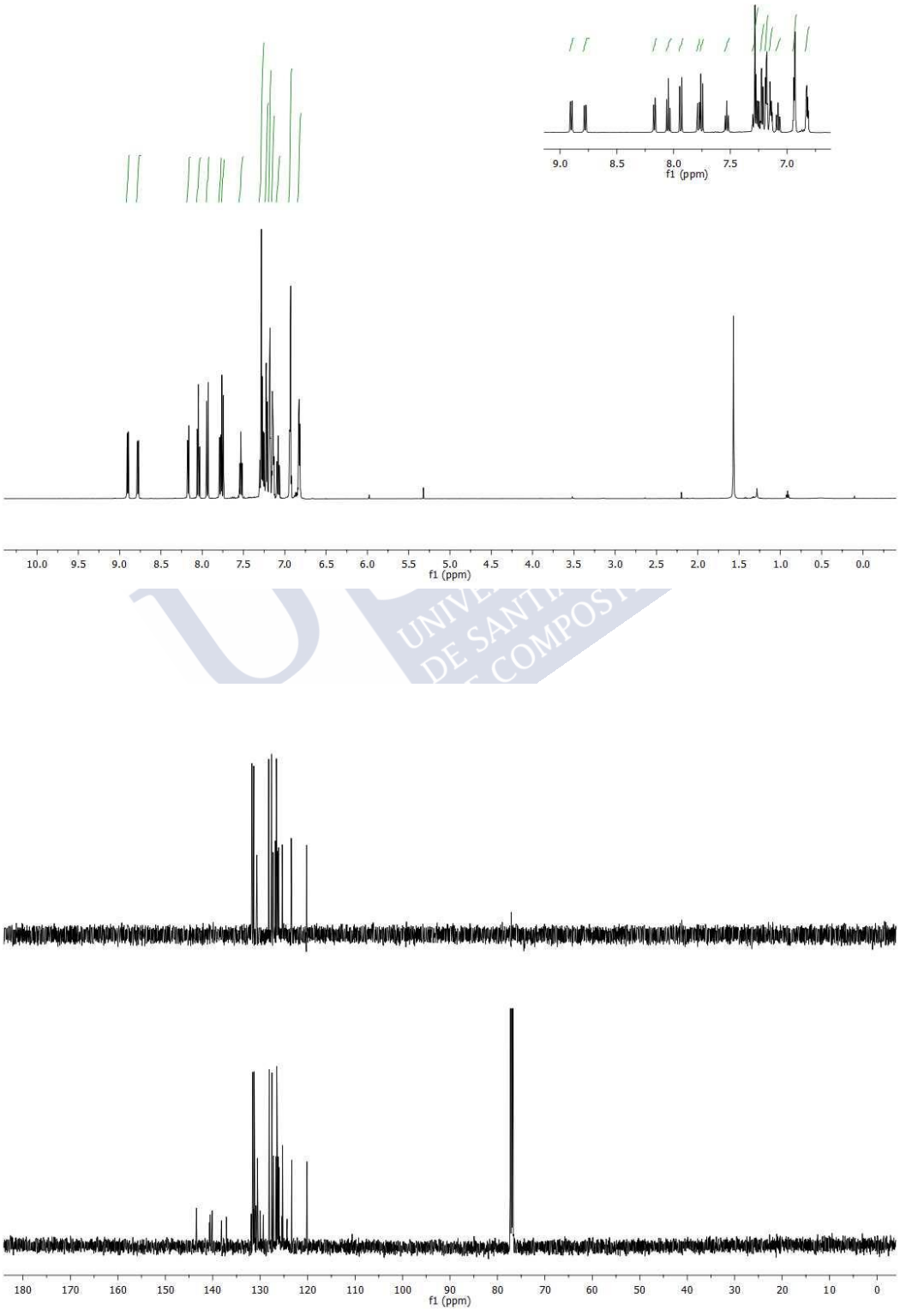
47

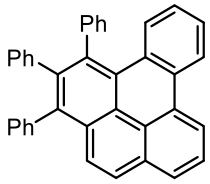

7.5
7.0
6.5
6.0
f1 (ppm)
10.0 9.5 9.0 8.5 8.0 7.5 7.0 6.5 6.0 5.5 5.0 4.5 4.0 3.5 3.0 2.5 2.0 1.5 1.0 0.5 0.0 -0.5 -1.0 -1.5 -2.0
f1 (ppm)


180 170 160 150 140 130 120 110 100 90 80 70 60 50 40 30 20 10 0
f1 (ppm)

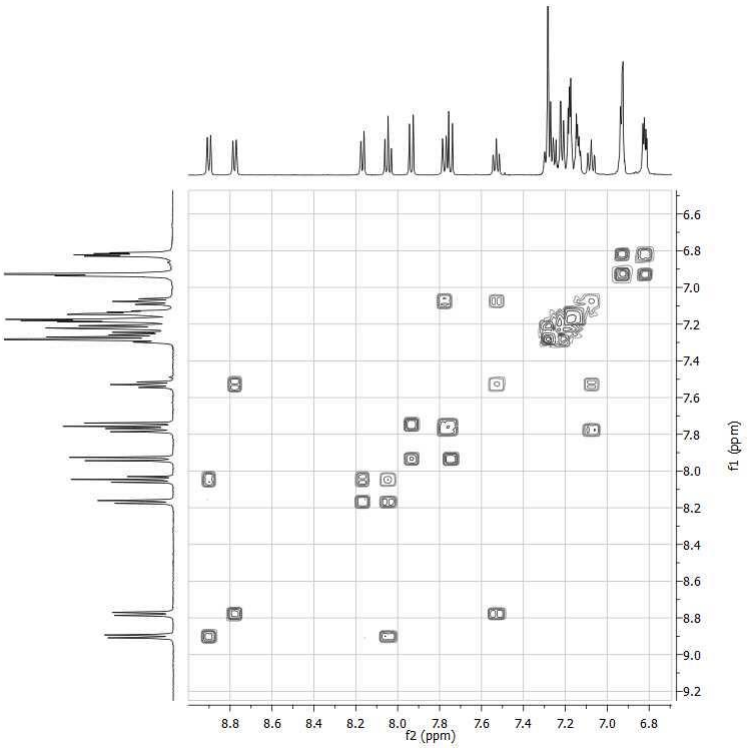

Ph
Ph
Ph

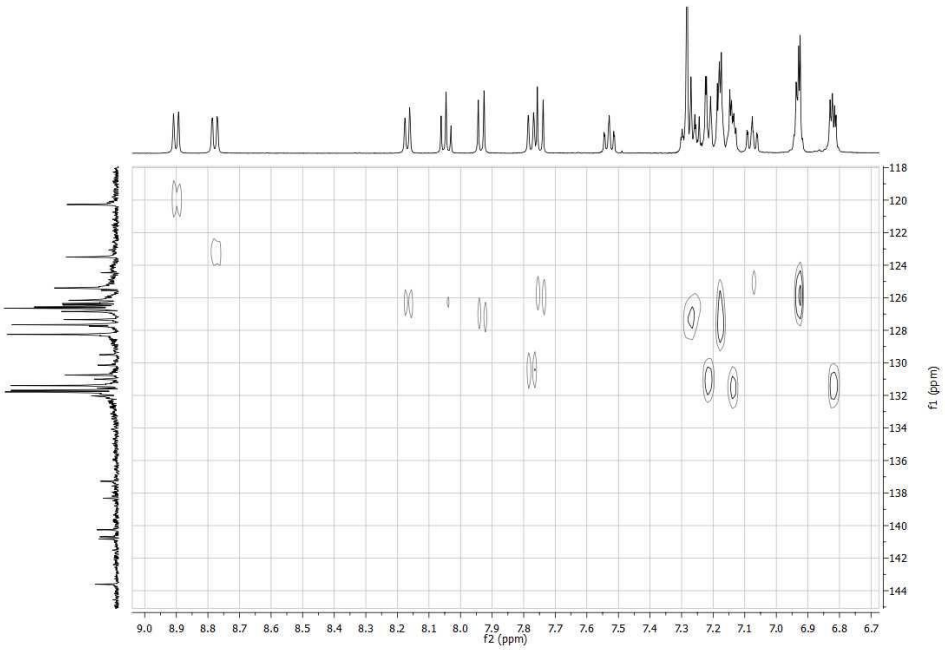
48

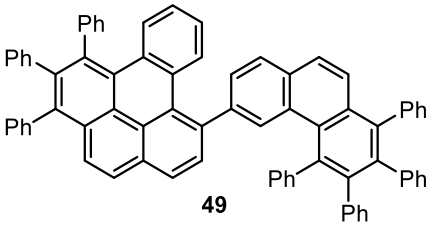

9.0
8.5
8.0
7.5
7.0
f1 (ppm)
10.0
9.5
9.0
8.5
8.0
7.5
7.0
6.5
6.0
5.5
5.0
4.5
4.0
3.5
3.0
2.5
2.0
1.5
1.0
0.5
0.0
f1 (ppm)
180
170
160
150
140
130
120
110
100
90
80
70
60
50
40
30
20
10
0
f1 (ppm)



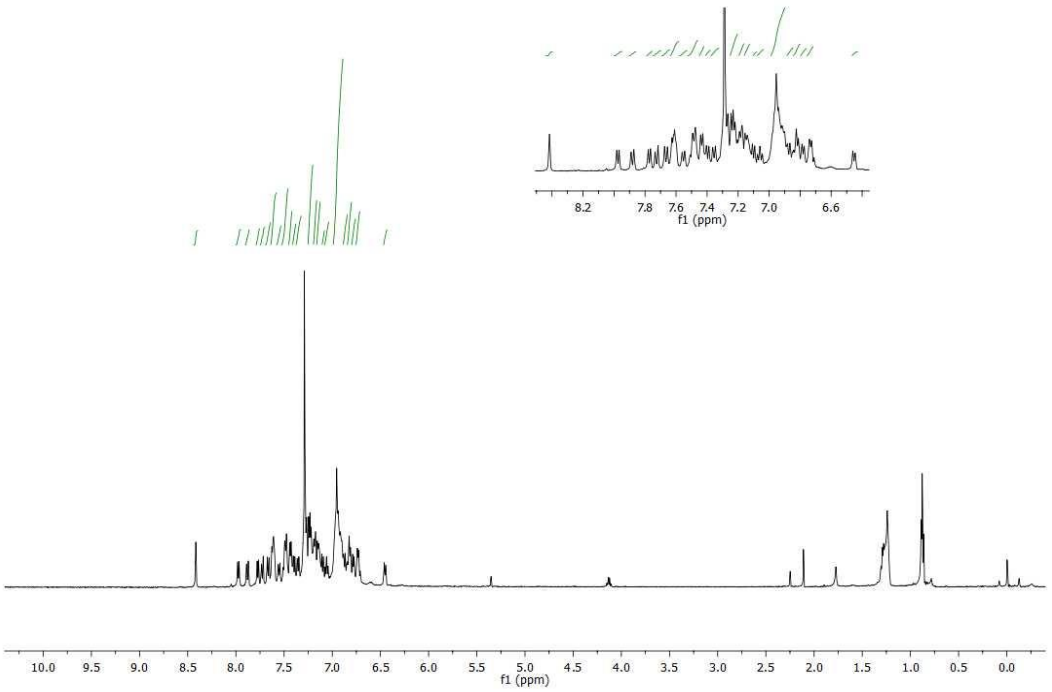
48

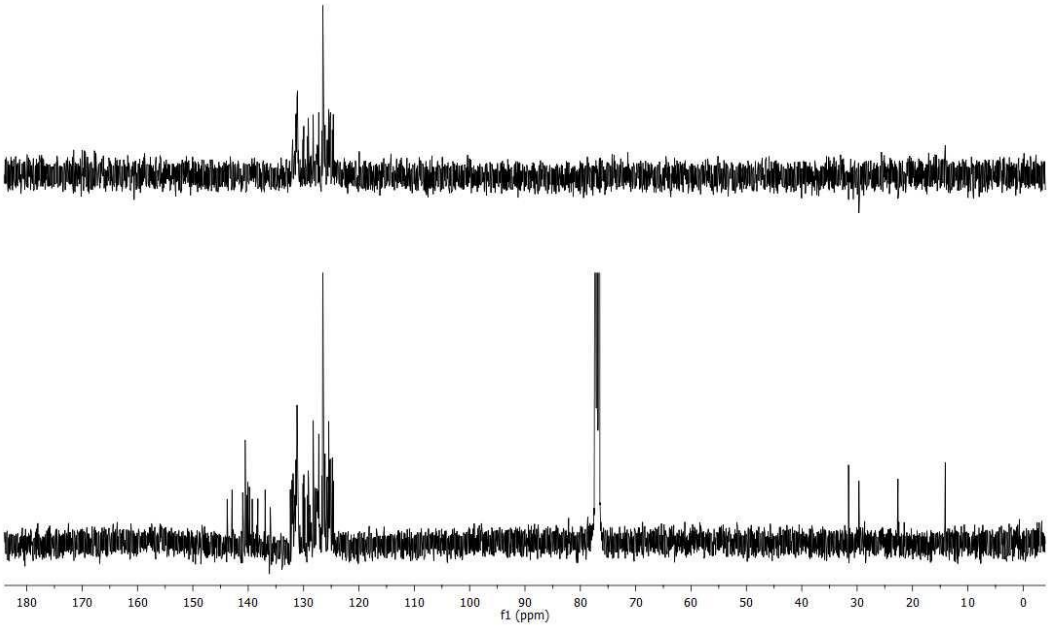


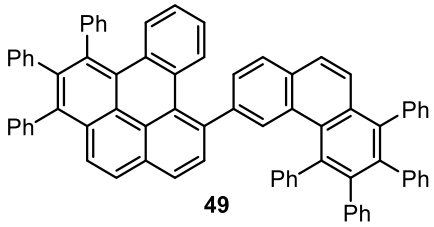



Ph
Ph
Ph
Ph
Ph
Ph

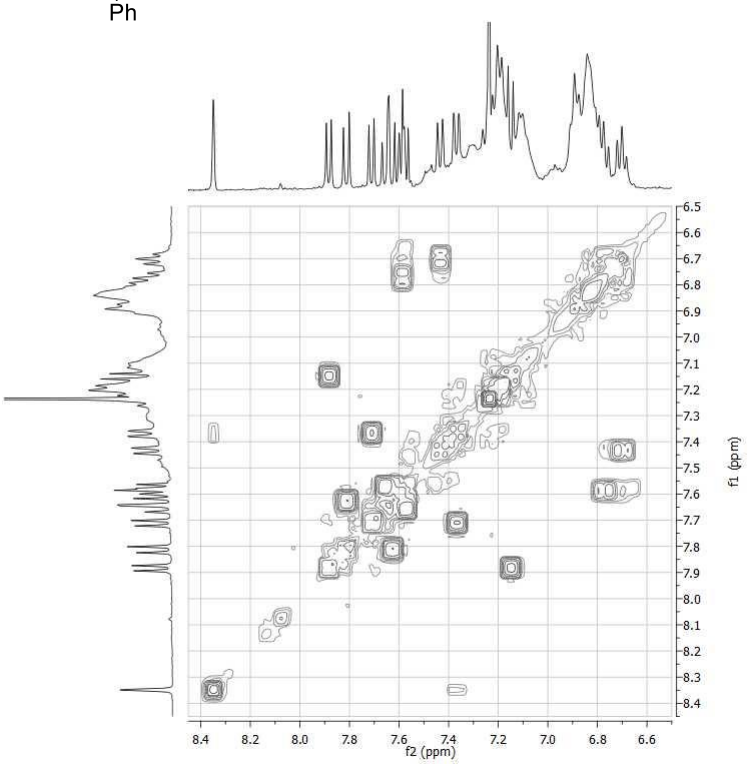
49

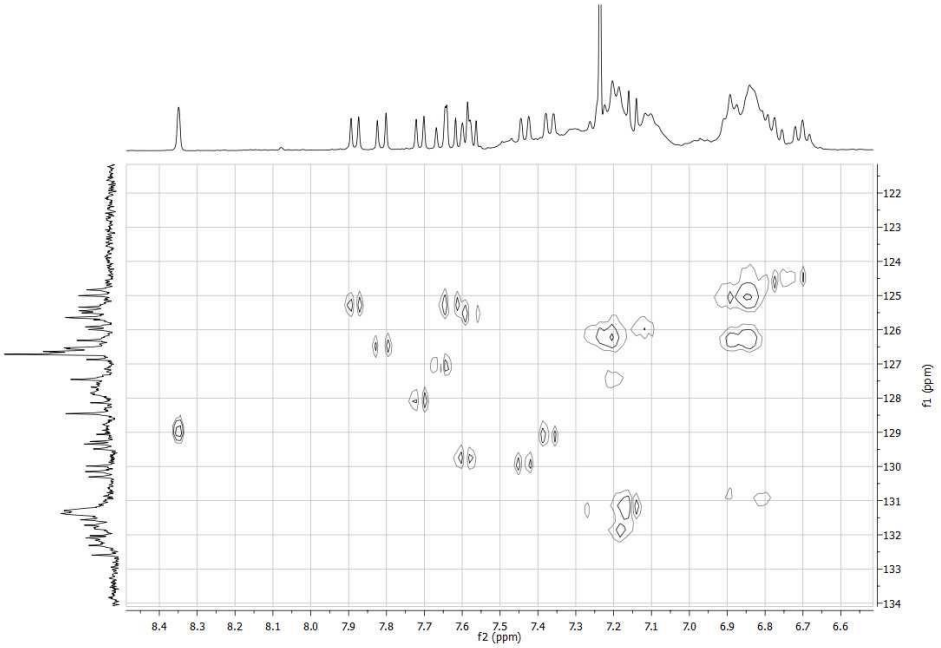

8.2
7.8
7.6
7.4
7.2
7.0
6.6
f1 (ppm)
10.0
9.5
9.0
8.5
8.0
7.5
7.0
6.5
6.0
5.5
5.0
4.5
4.0
3.5
3.0
2.5
2.0
1.5
1.0
0.5
0.0
f1 (ppm)

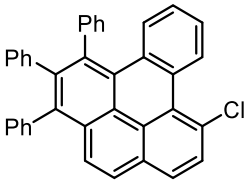

180
170
160
150
140
130
120
110
100
90
80
70
60
50
40
30
20
10
0
f1 (ppm)



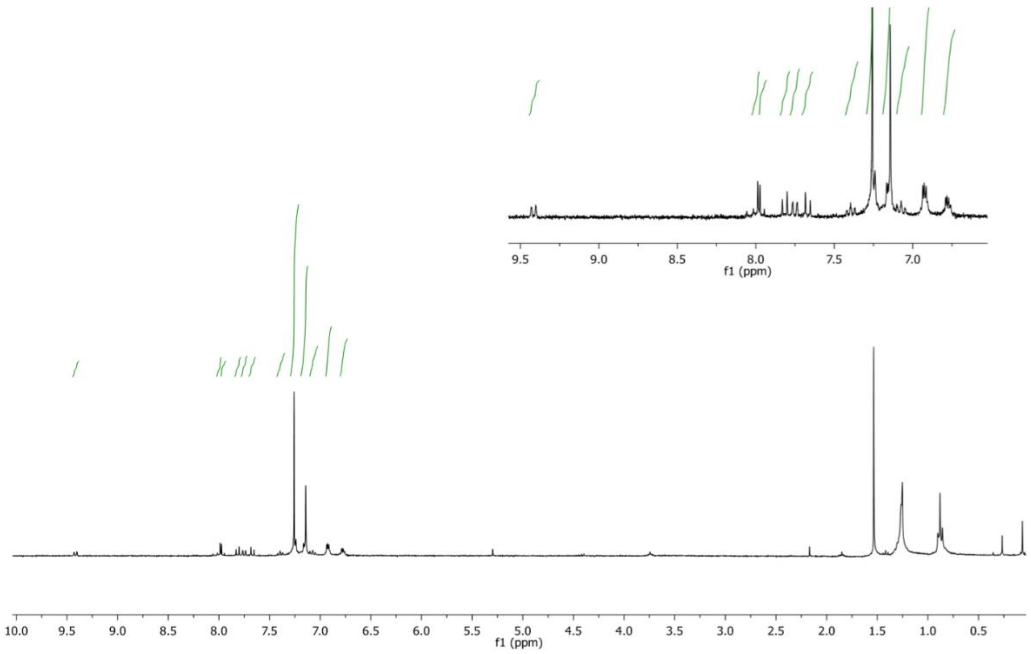
49

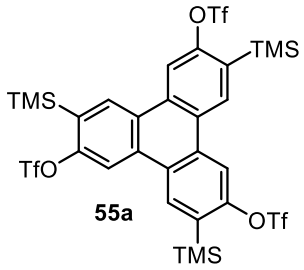




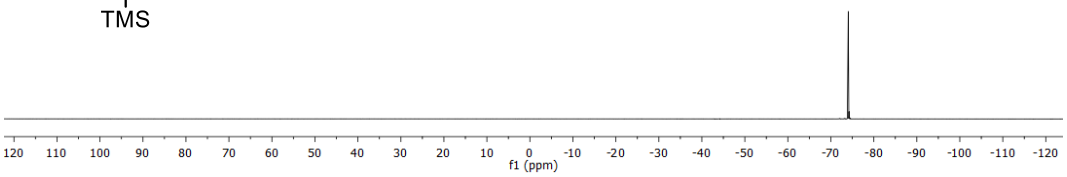

Ph
Ph
Ph
Cl

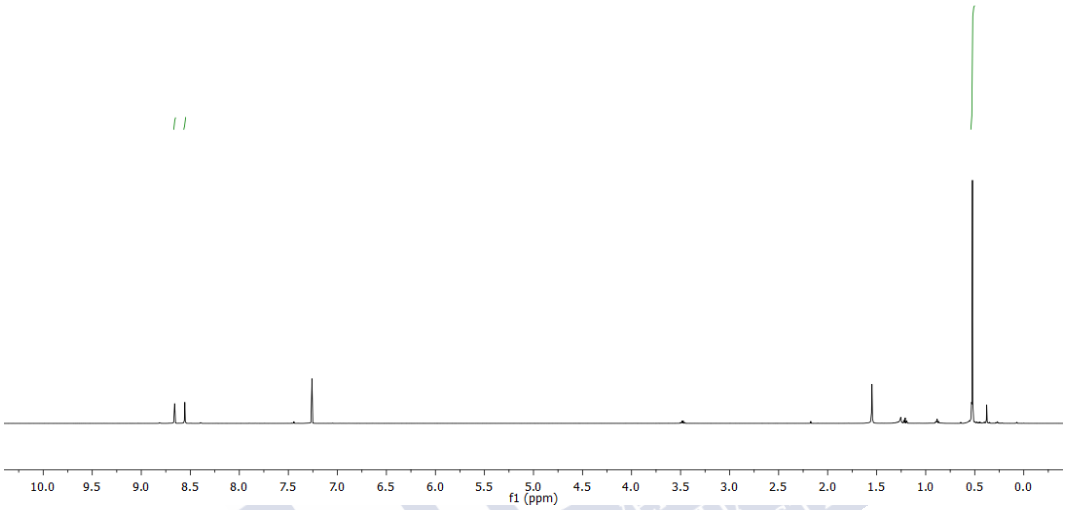
53

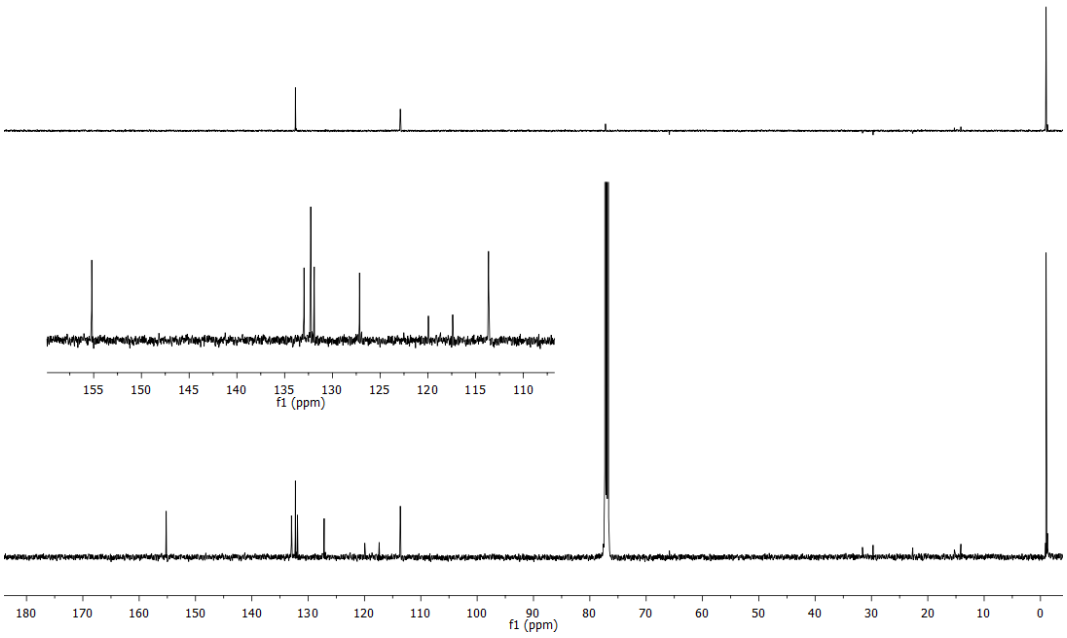

9.5
9.0
8.5
8.0
7.5
7.0
f1 (ppm)
10.0
9.5
9.0
8.5
8.0
7.5
7.0
6.5
6.0
5.5
5.0
4.5
4.0
3.5
3.0
2.5
2.0
1.5
1.0
0.5
f1 (ppm)

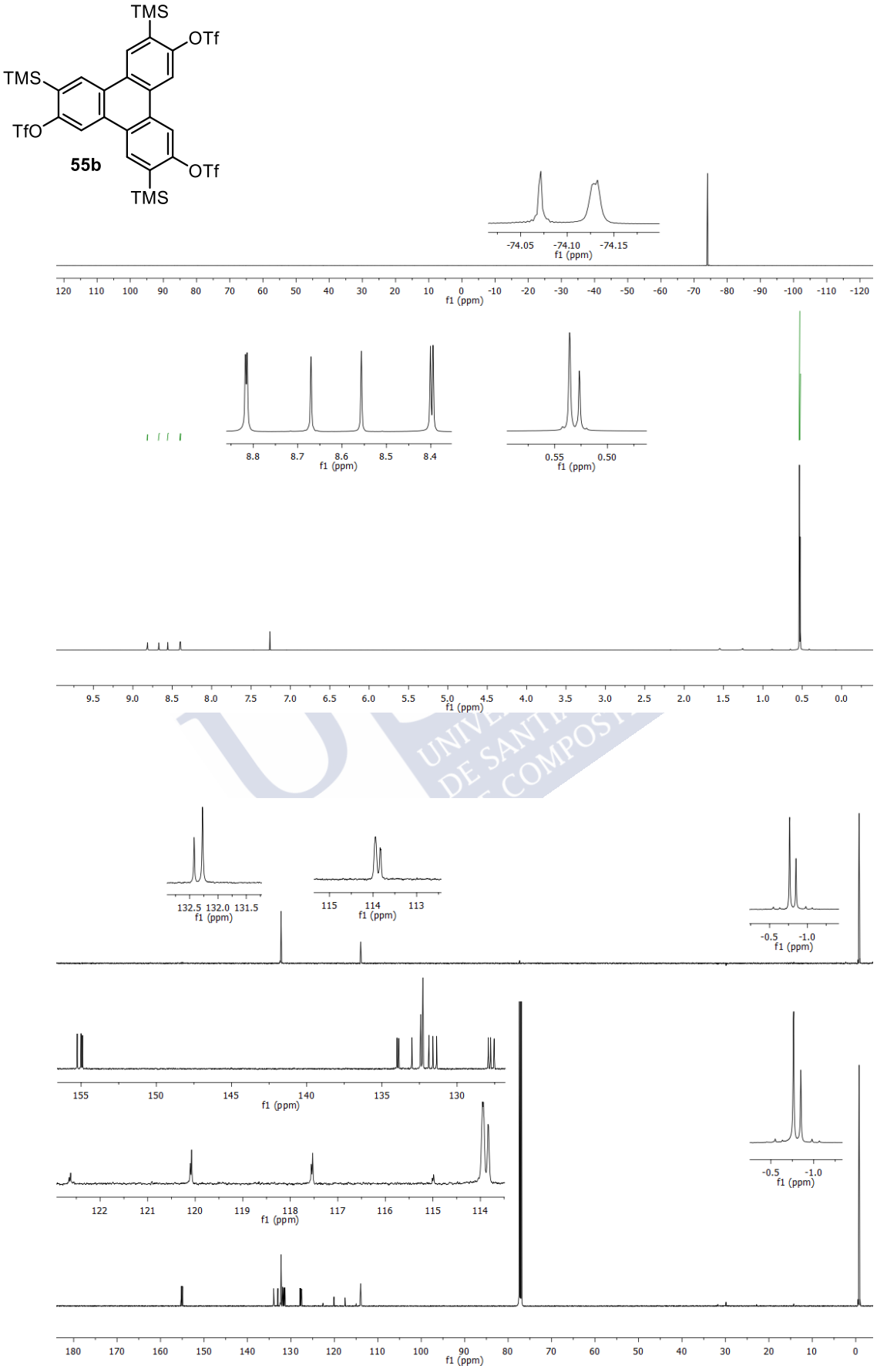


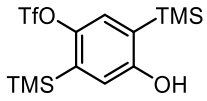
55a



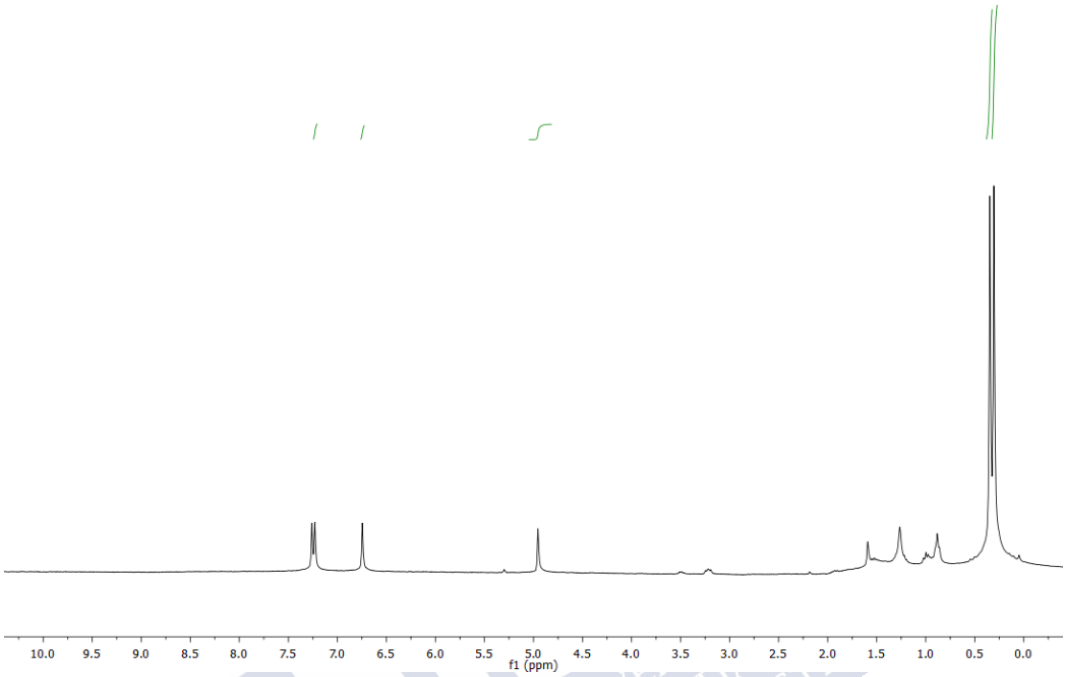


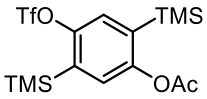



TMS
OTf
TMS
TfO
55b
OTf
TMS
f1 (ppm)

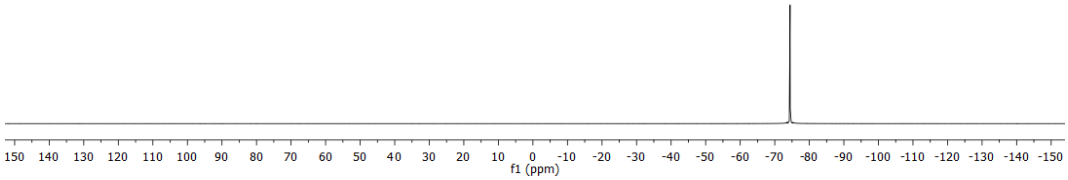

TfO
TMS
TMS
OH

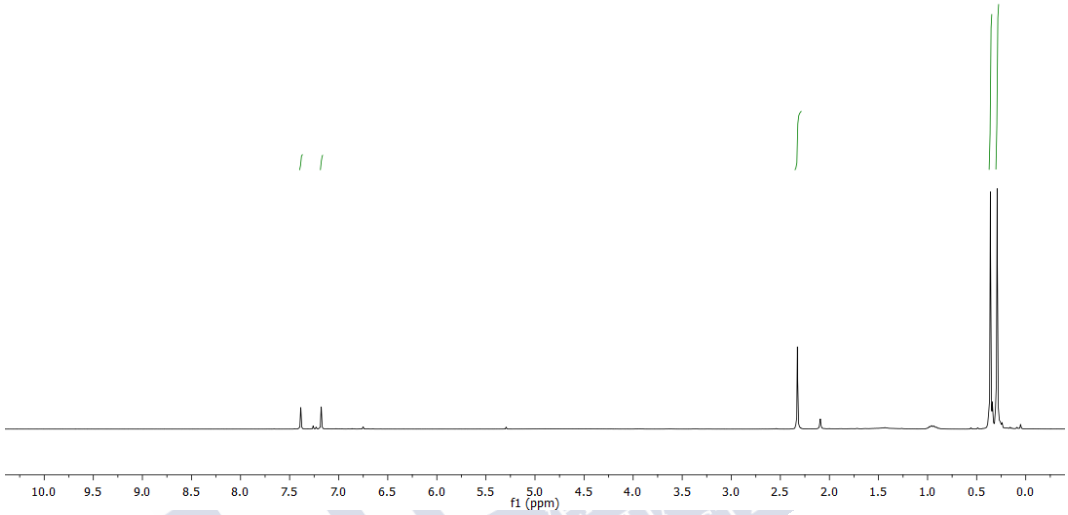
60

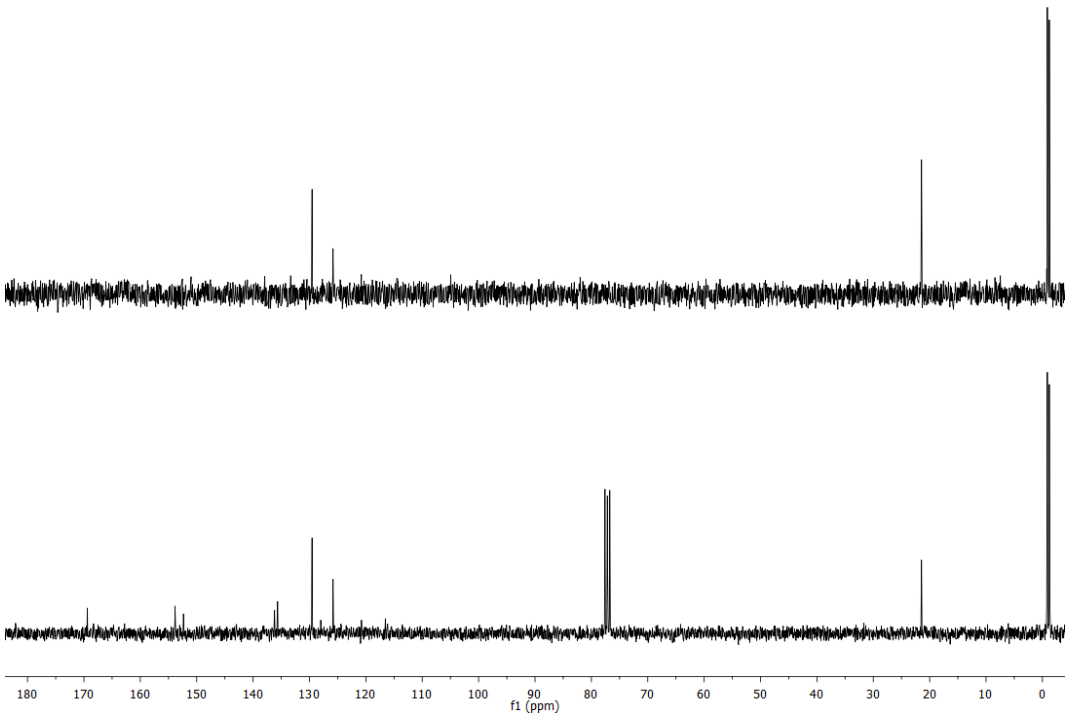

10.0
9.5
9.0
8.5
8.0
7.5
7.0
6.5
6.0
5.5
5.0
4.5
4.0
3.5
3.0
2.5
2.0
1.5
1.0
0.5
0.0
f1 (ppm)

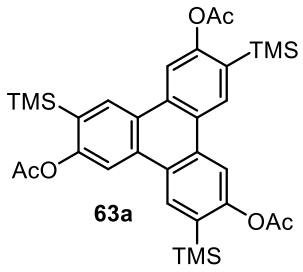

TfO
TMS
TMS
OAc

62

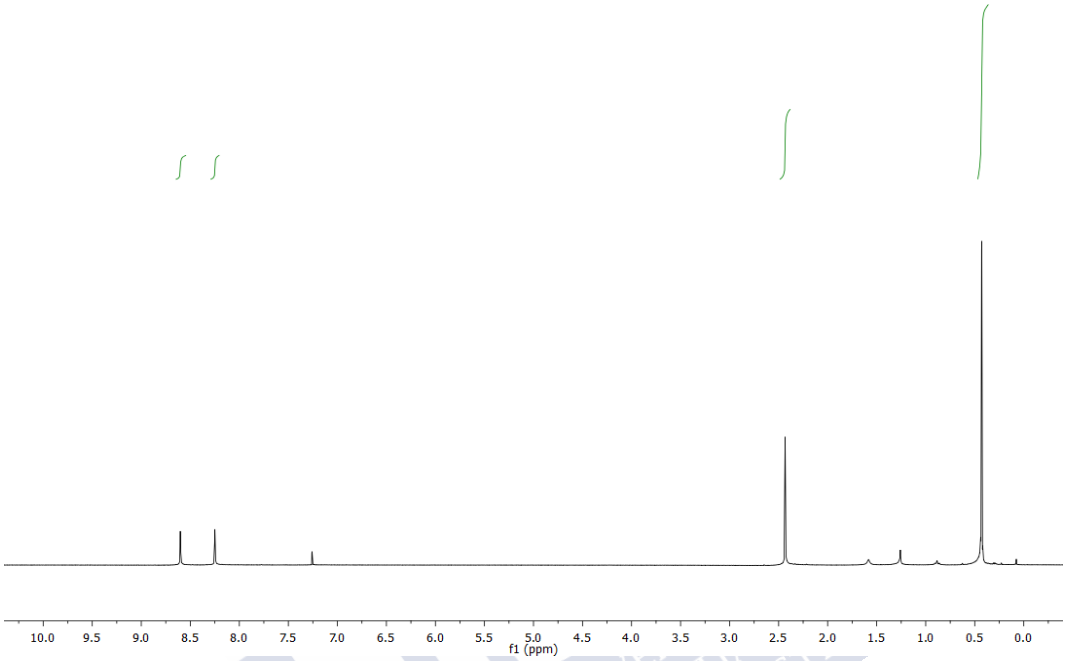

150 140 130 120 110 100 90 80 70 60 50 40 30 20 10 0 -10 -20 -30 -40 -50 -60 -70 -80 -90 -100 -110 -120 -130 -140 -150
f1 (ppm)

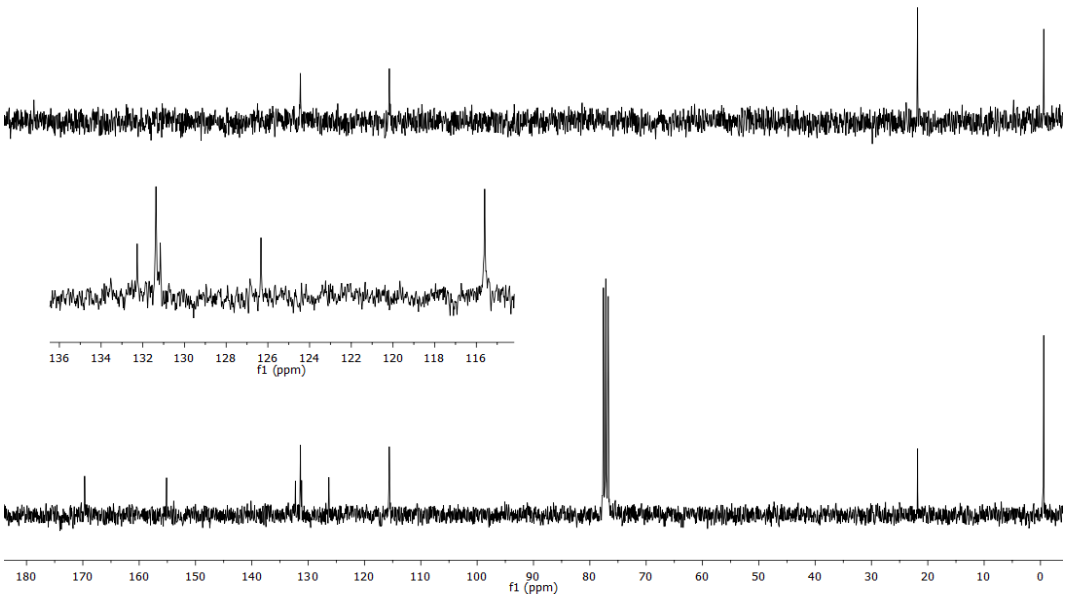

10.0 9.5 9.0 8.5 8.0 7.5 7.0 6.5 6.0 5.5 5.0 4.5 4.0 3.5 3.0 2.5 2.0 1.5 1.0 0.5 0.0
f1 (ppm)

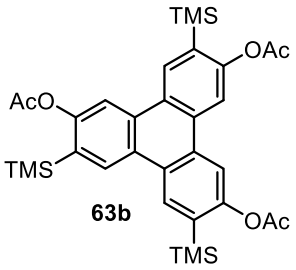

180 170 160 150 140 130 120 110 100 90 80 70 60 50 40 30 20 10 0
f1 (ppm)


OAc
TMS
TMS
AcO
OAc
TMS

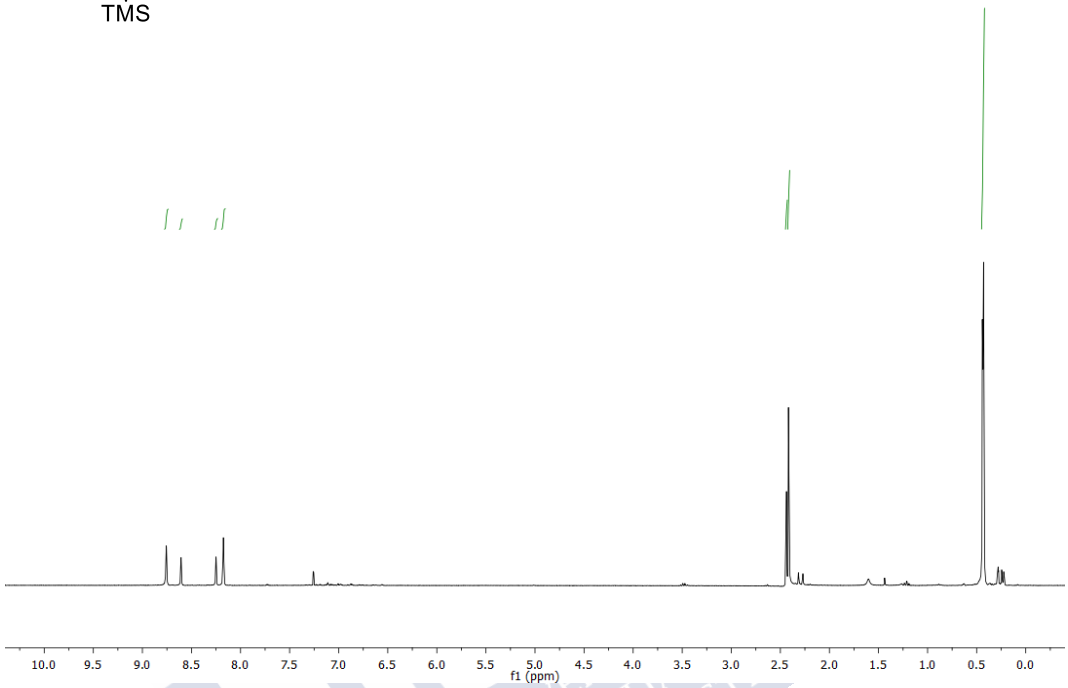
63a

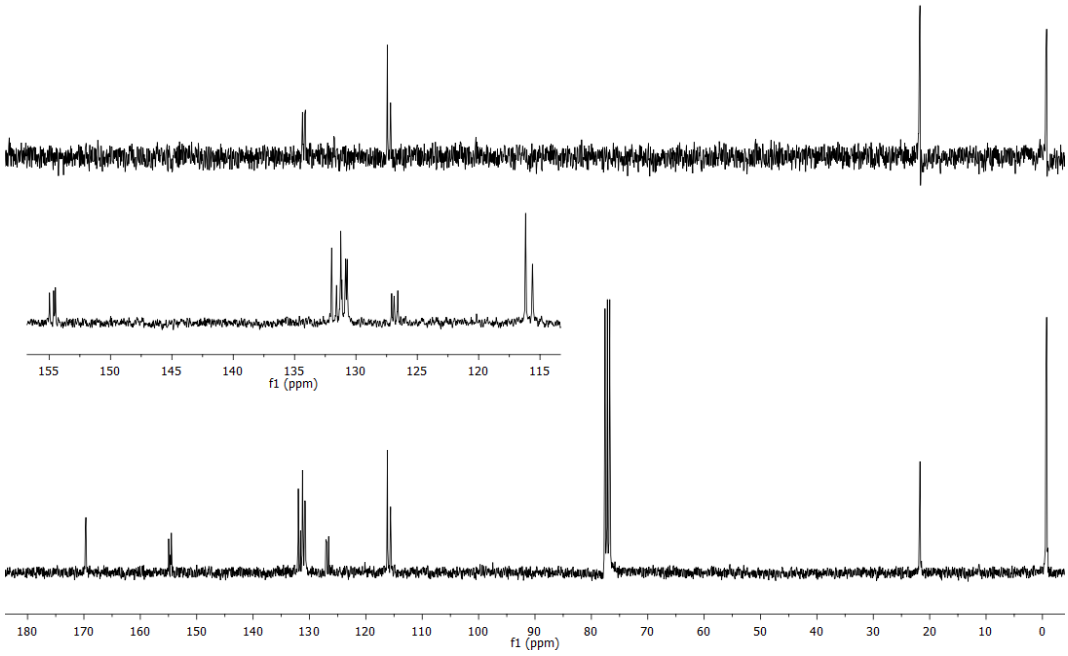

10.0 9.5 9.0 8.5 8.0 7.5 7.0 6.5 6.0 5.5 5.0 4.5 4.0 3.5 3.0 2.5 2.0 1.5 1.0 0.5 0.0
f1 (ppm)

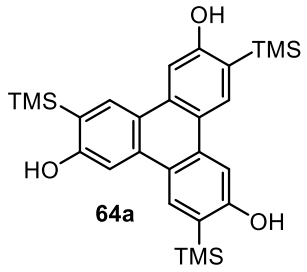

136 134 132 130 128 126 124 122 120 118 116
f1 (ppm)
180 170 160 150 140 130 120 110 100 90 80 70 60 50 40 30 20 10 0
f1 (ppm)


TMS
OAc
AcO
TMS
OAc
TMS

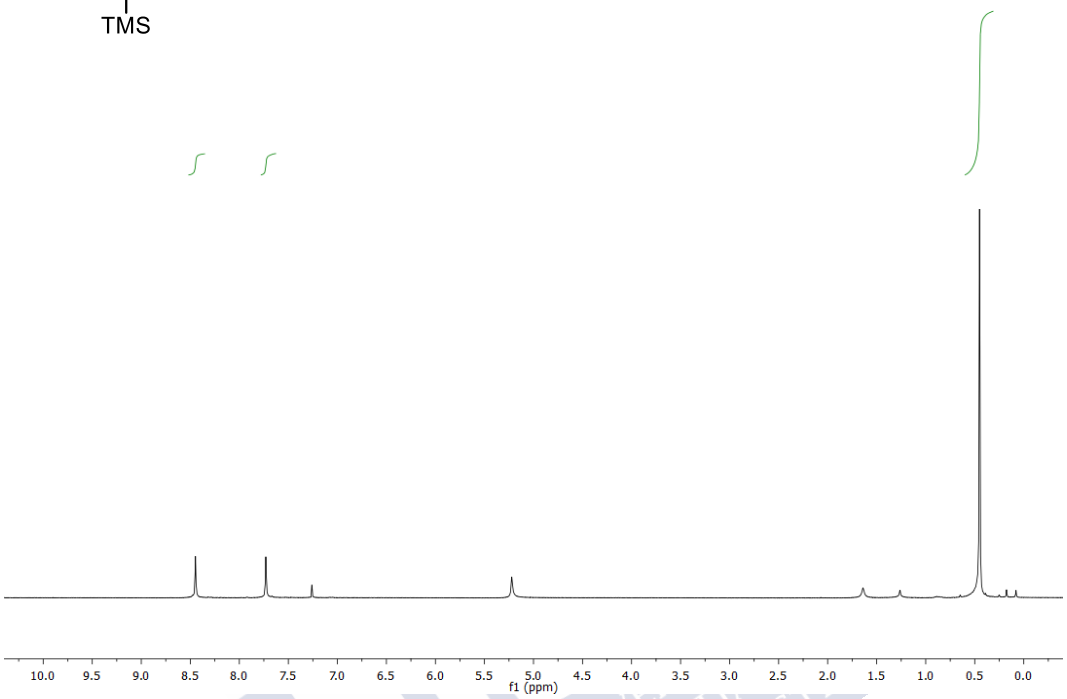
63b

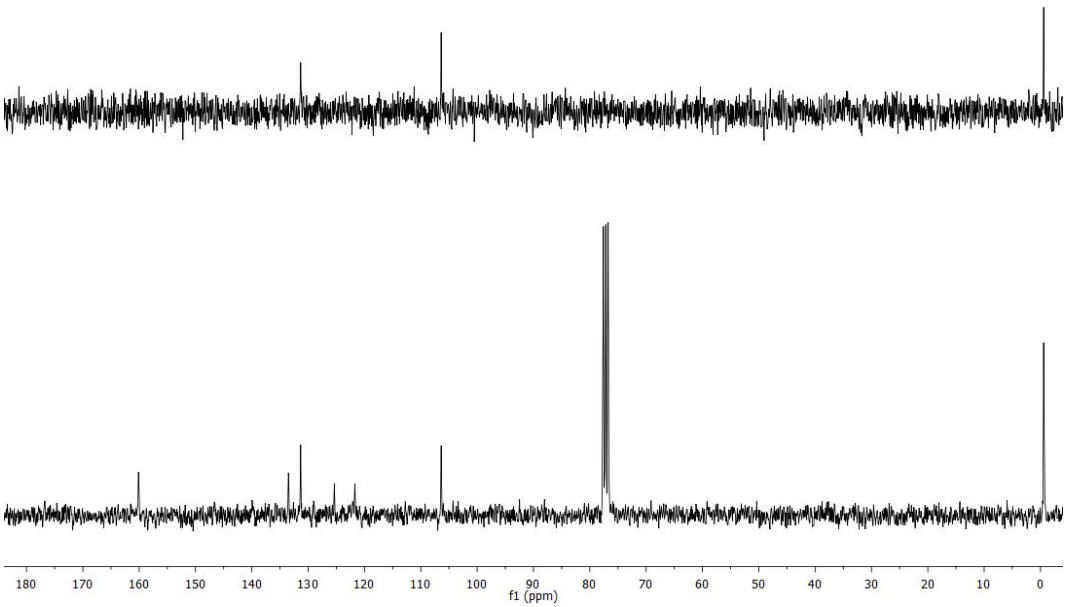

10.0 9.5 9.0 8.5 8.0 7.5 7.0 6.5 6.0 5.5 5.0 4.5 4.0 3.5 3.0 2.5 2.0 1.5 1.0 0.5 0.0
f1 (ppm)

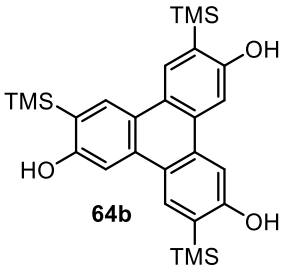

155 150 145 140 135 130 125 120 115
f1 (ppm)
180 170 160 150 140 130 120 110 100 90 80 70 60 50 40 30 20 10 0
f1 (ppm)


OH
TMS
TMS
HO
OH
TMS

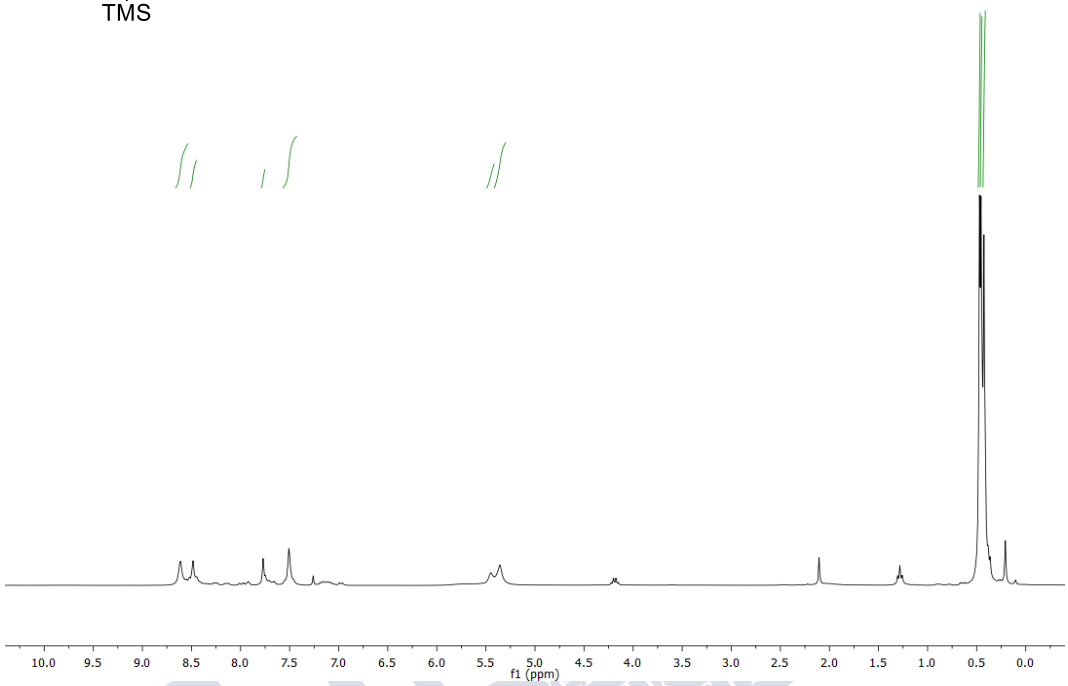
64a

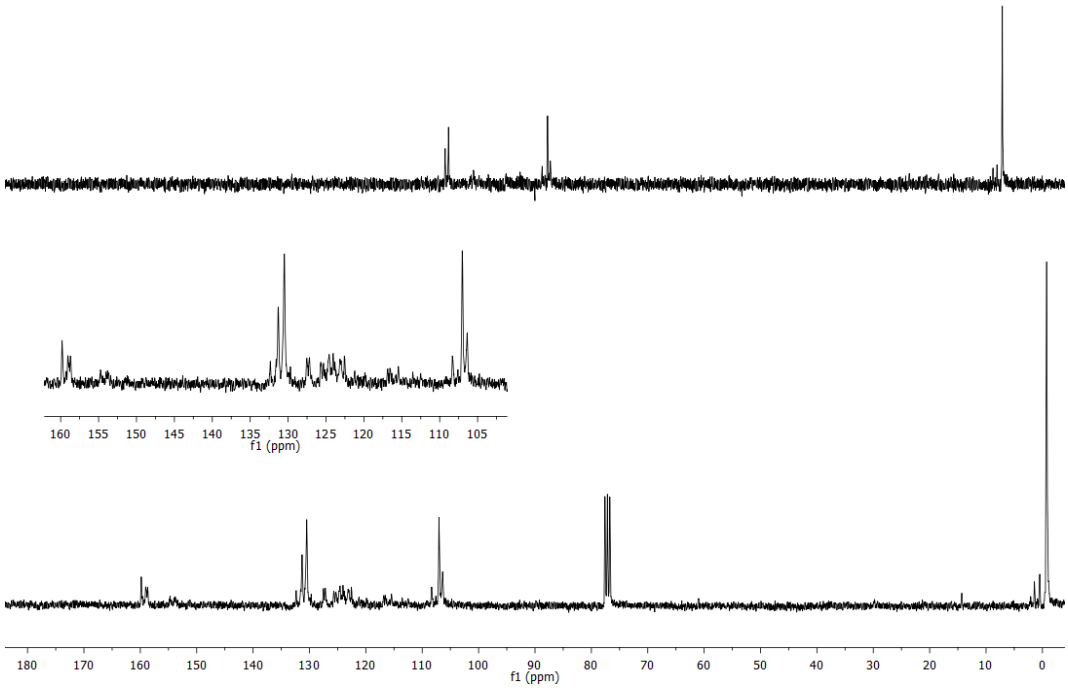

10.0 9.5 9.0 8.5 8.0 7.5 7.0 6.5 6.0 5.5 5.0 4.5 4.0 3.5 3.0 2.5 2.0 1.5 1.0 0.5 0.0
f1 (ppm)

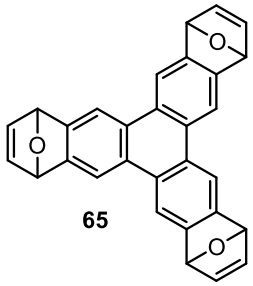

180 170 160 150 140 130 120 110 100 90 80 70 60 50 40 30 20 10 0
f1 (ppm)


TMS
OH
TMS
HO
OH
TMS

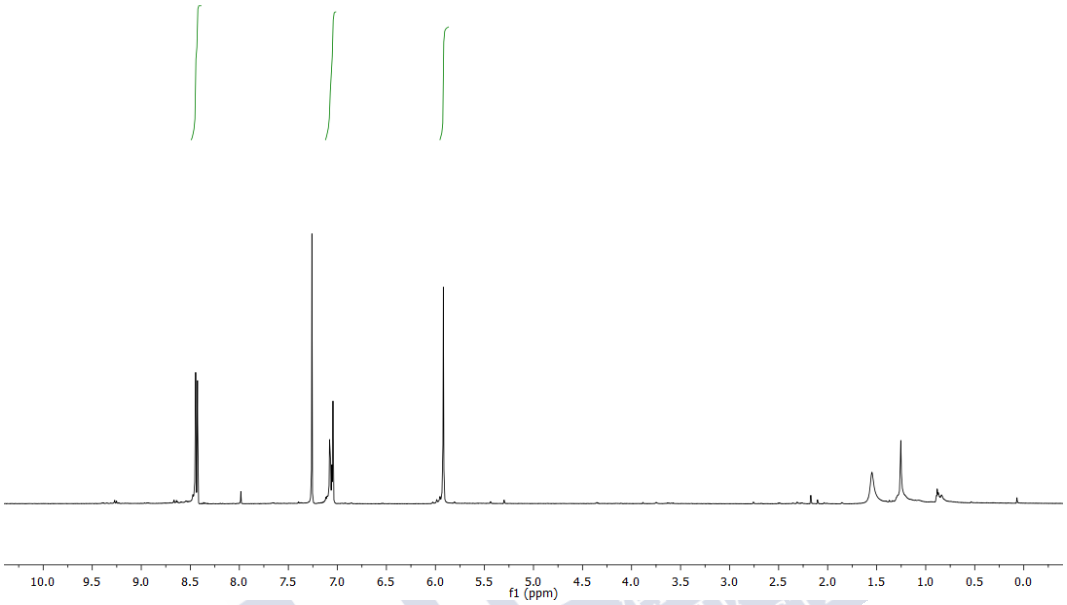
64b

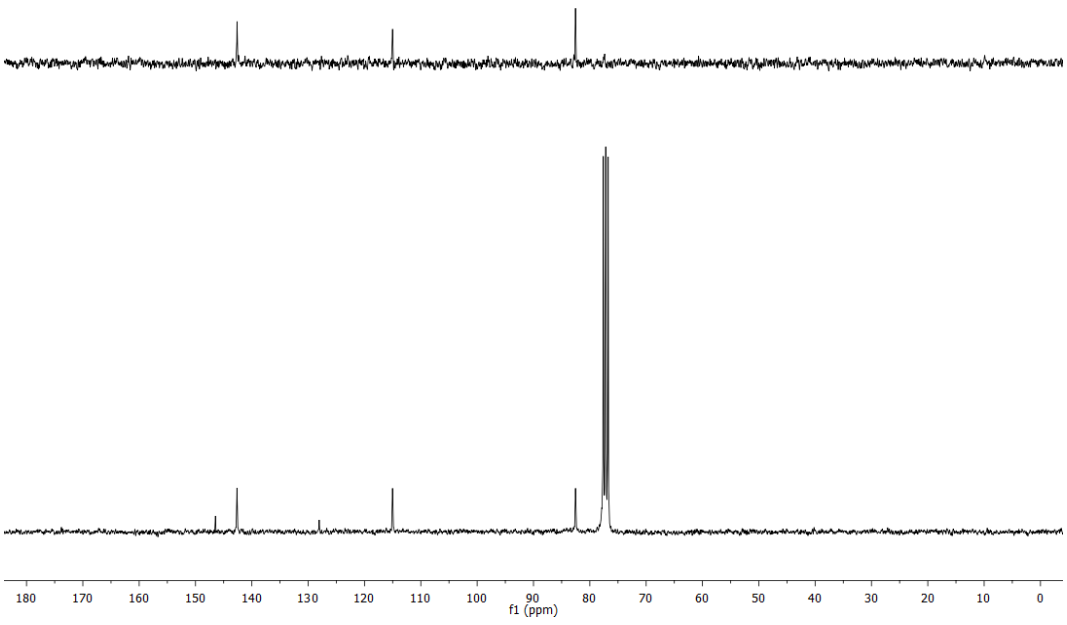

10.0 9.5 9.0 8.5 8.0 7.5 7.0 6.5 6.0 5.5 5.0 4.5 4.0 3.5 3.0 2.5 2.0 1.5 1.0 0.5 0.0
f1 (ppm)

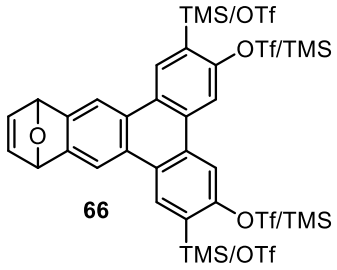

160 155 150 145 140 135 130 125 120 115 110 105
f1 (ppm)
180 170 160 150 140 130 120 110 100 90 80 70 60 50 40 30 20 10 0
f1 (ppm)



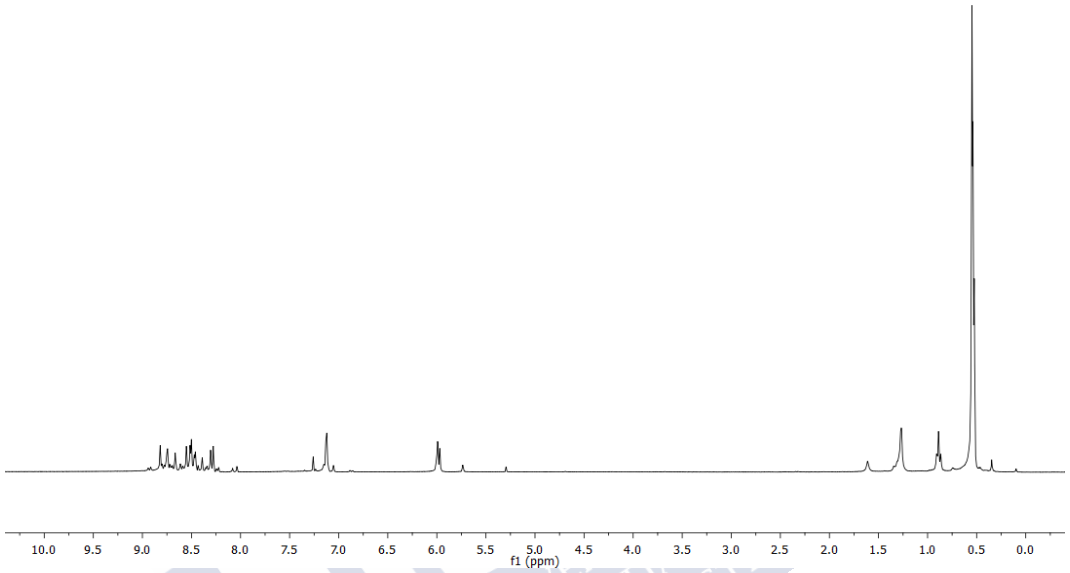
65

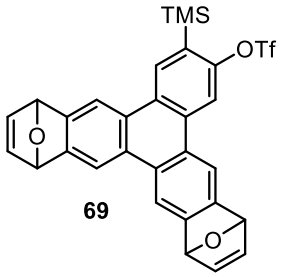

10.0
9.5
9.0
8.5
8.0
7.5
7.0
6.5
6.0
5.5
5.0
4.5
4.0
3.5
3.0
2.5
2.0
1.5
1.0
0.5
0.0
f1 (ppm)


180
170
160
150
140
130
120
110
100
90
80
70
60
50
40
30
20
10
0
f1 (ppm)

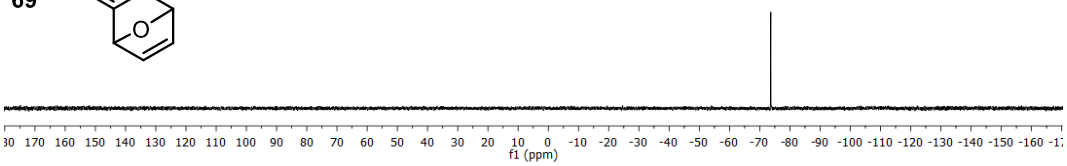

TMS/OTf
OTf/TMS
O
OTf/TMS
TMS/OTf

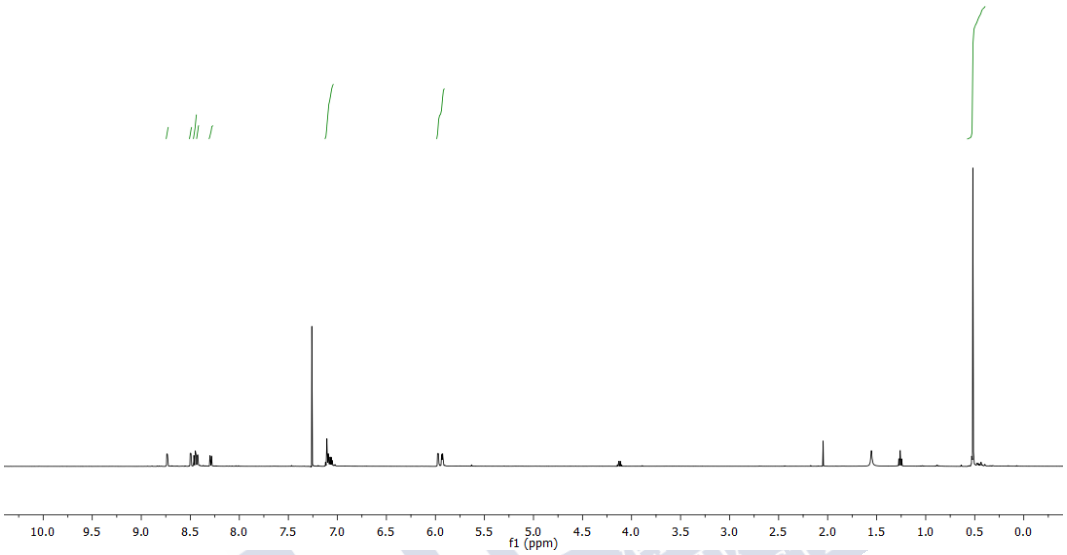
66

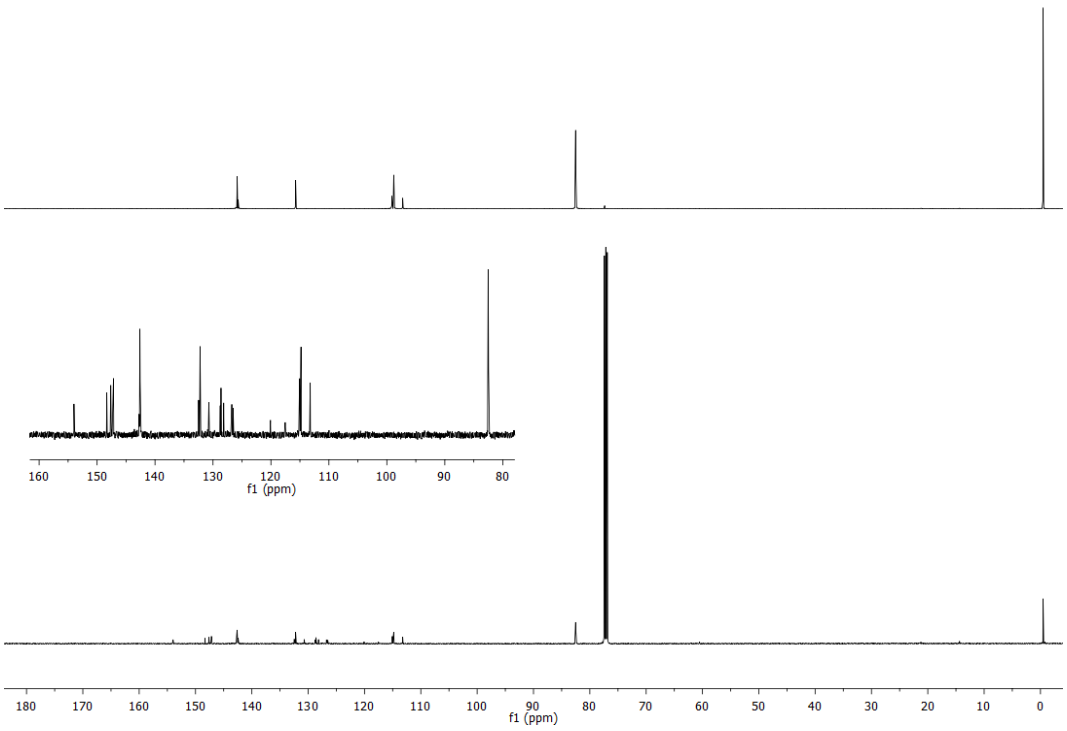

10.0
9.5
9.0
8.5
8.0
7.5
7.0
6.5
6.0
5.5
5.0
4.5
4.0
3.5
3.0
2.5
2.0
1.5
1.0
0.5
0.0
f1 (ppm)

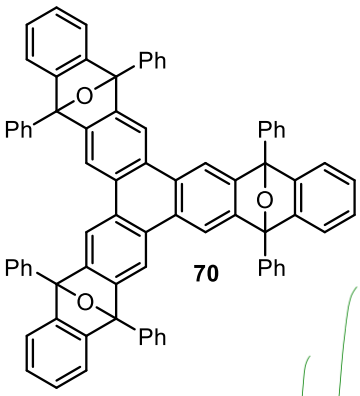


69

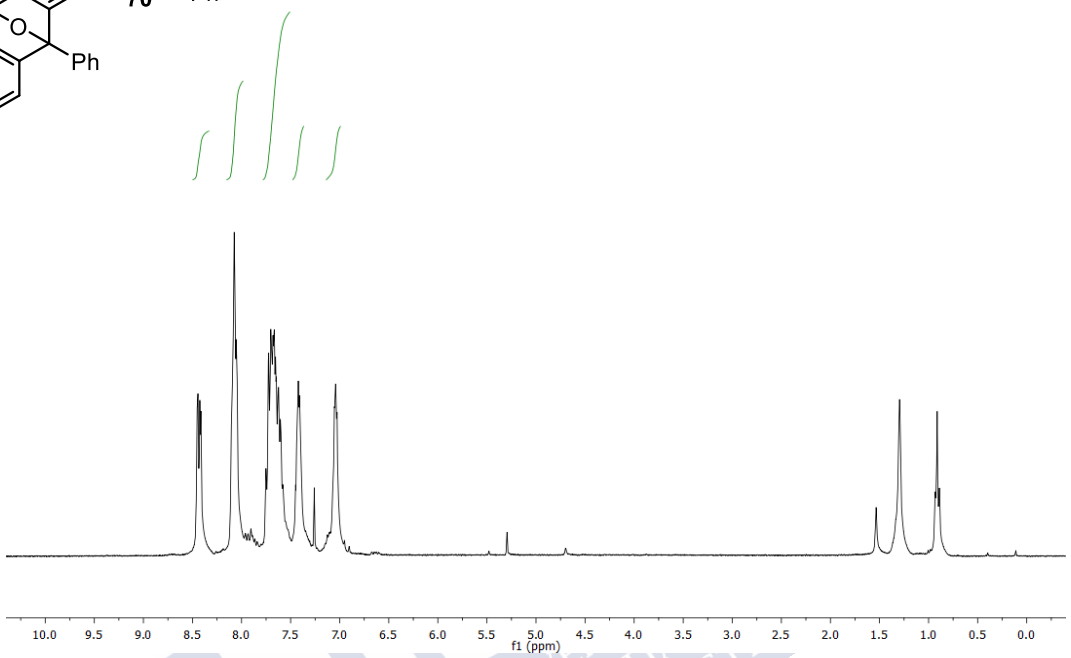


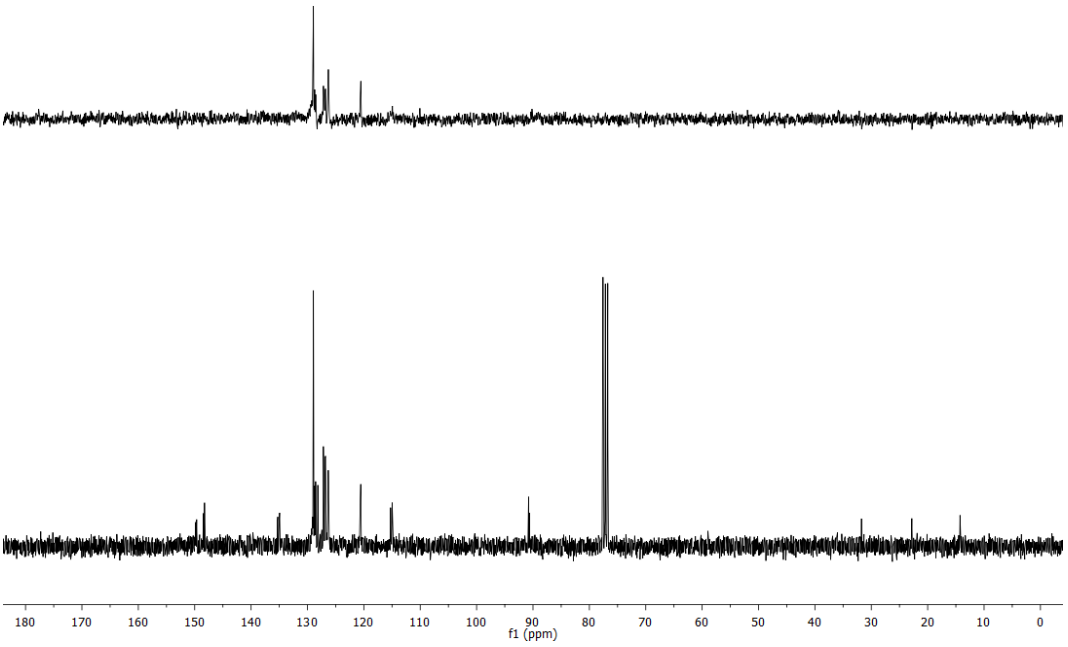


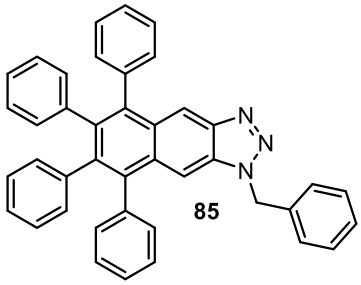



Ph
O
Ph
Ph
O
Ph
Ph
O
Ph

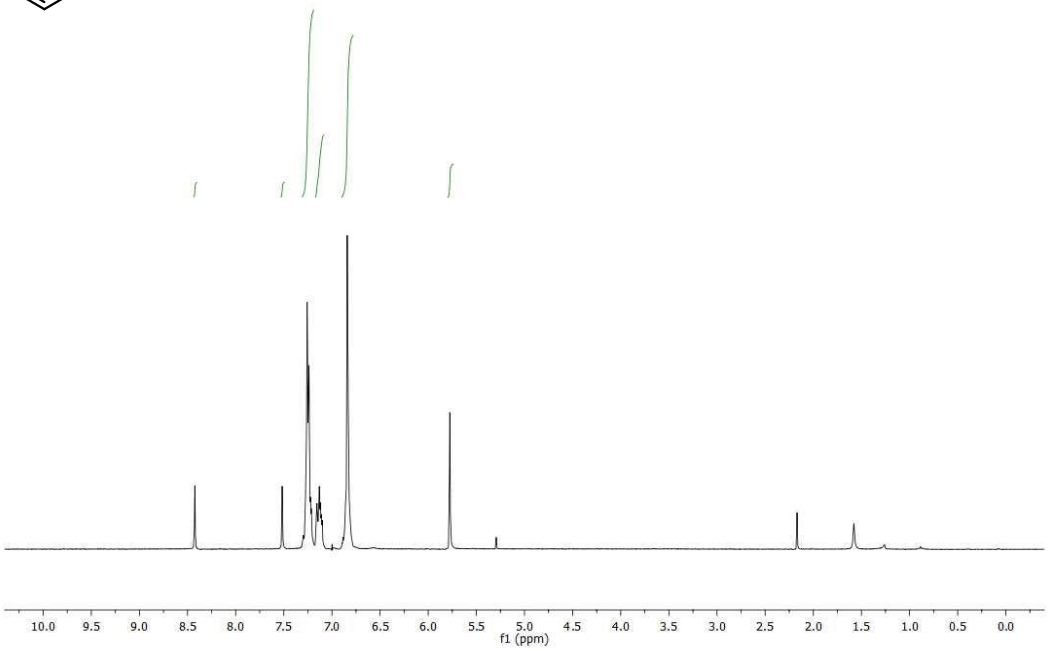
70

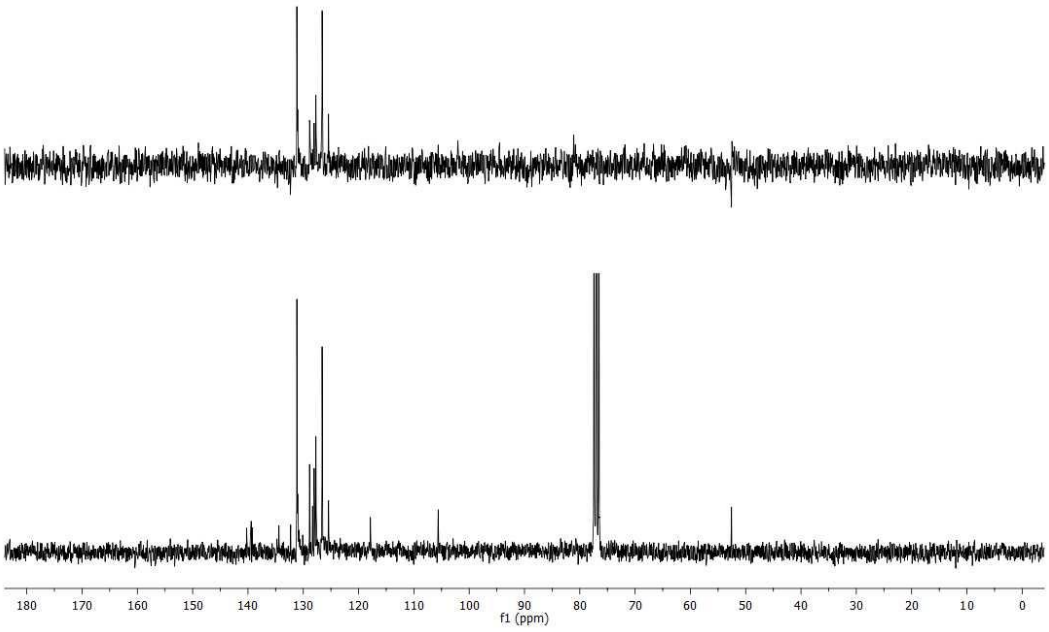

10.0 9.5 9.0 8.5 8.0 7.5 7.0 6.5 6.0 5.5 5.0 4.5 4.0 3.5 3.0 2.5 2.0 1.5 1.0 0.5 0.0
f1 (ppm)

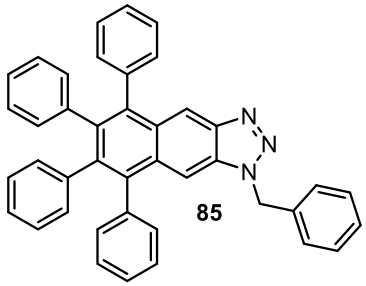

180 170 160 150 140 130 120 110 100 90 80 70 60 50 40 30 20 10 0
f1 (ppm)


N
N
N

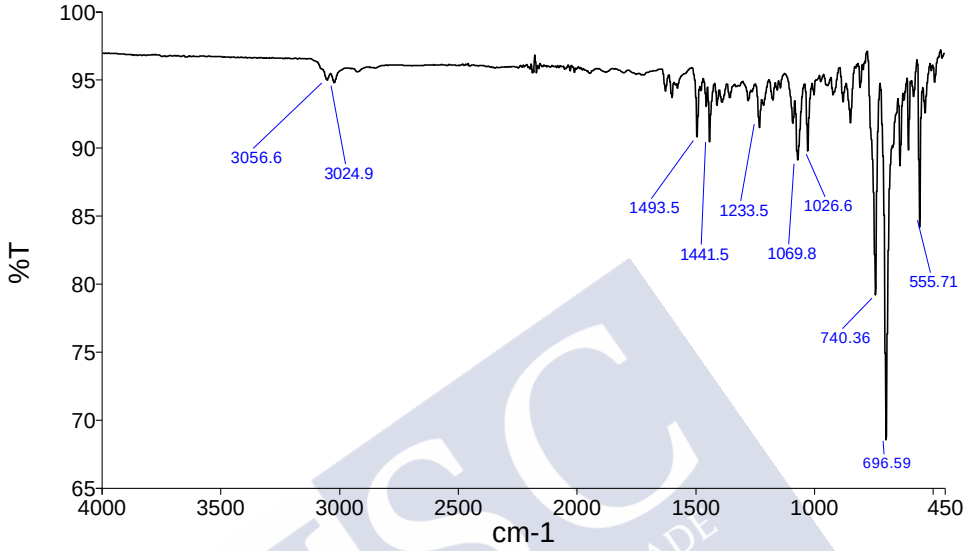
85

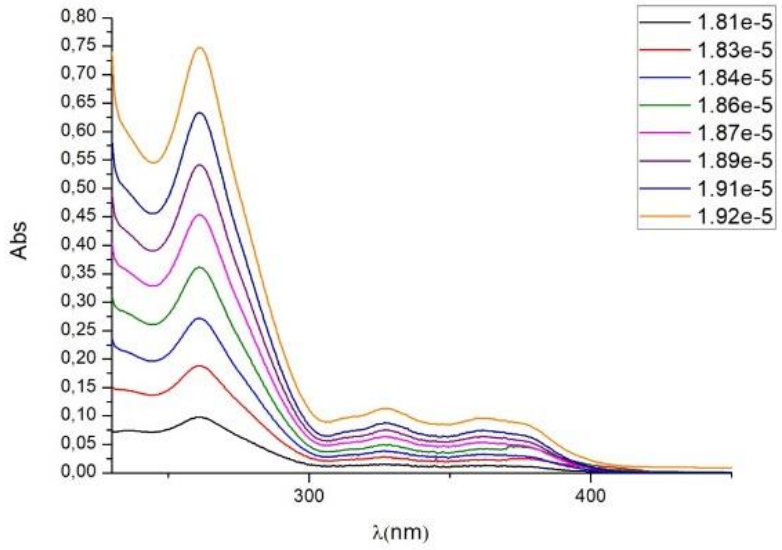

10.0 9.5 9.0 8.5 8.0 7.5 7.0 6.5 6.0 5.5 5.0 4.5 4.0 3.5 3.0 2.5 2.0 1.5 1.0 0.5 0.0
f1 (ppm)

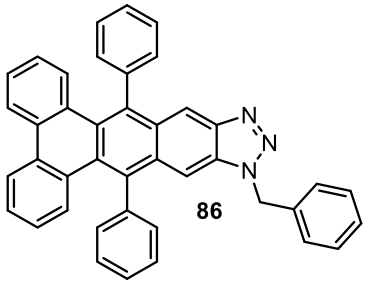

180 170 160 150 140 130 120 110 100 90 80 70 60 50 40 30 20 10 0
f1 (ppm)


N
N
N

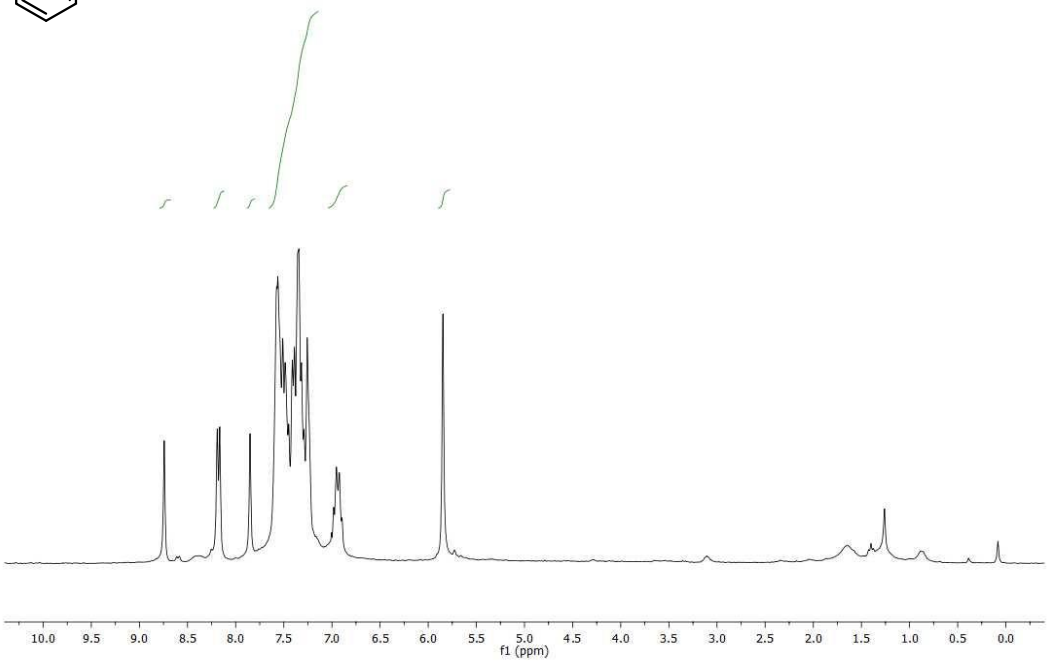
85

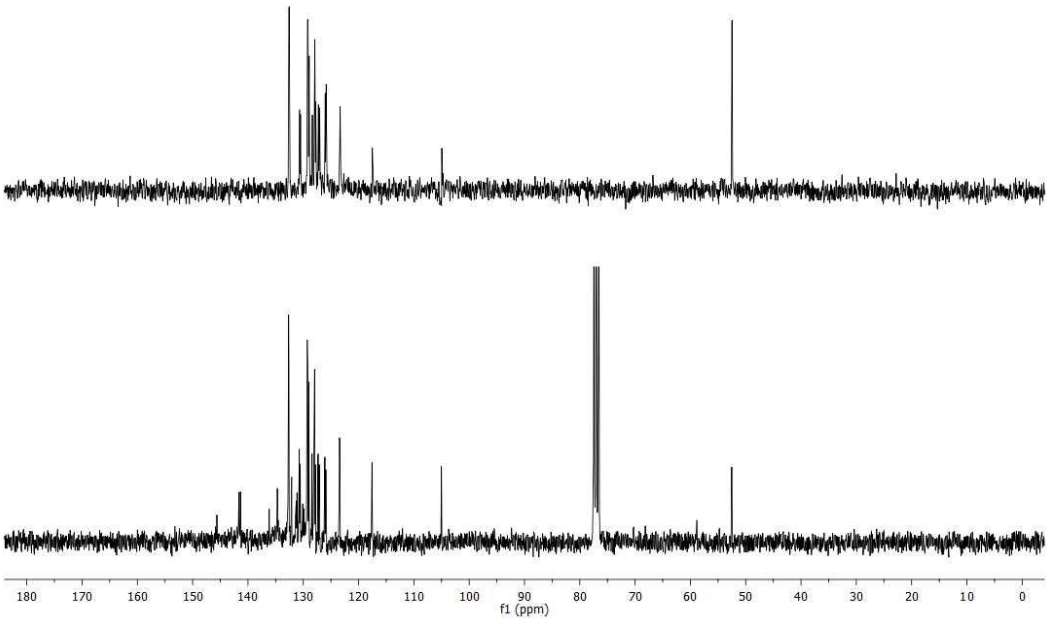

100
95
90
85
80
75
70
65
%T
3056.6
3024.9
1493.5
1441.5
1233.5
1069.8
1026.6
740.36
696.59
555.71
4000
3500
3000
2500
2000
1500
1000
450
cm-1

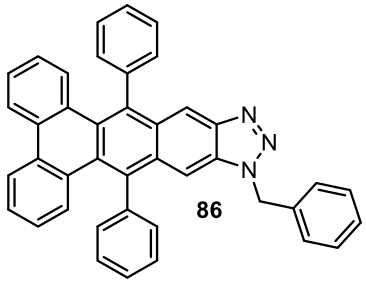

0,80
0,75
0,70
0,65
0,60
0,55
0,50
0,45
0,40
0,35
0,30
0,25
0,20
0,15
0,10
0,05
0,00
Abs
300
400
λ(nm)
1.81e-5
1.83e-5
1.84e-5
1.86e-5
1.87e-5
1.89e-5
1.91e-5
1.92e-5



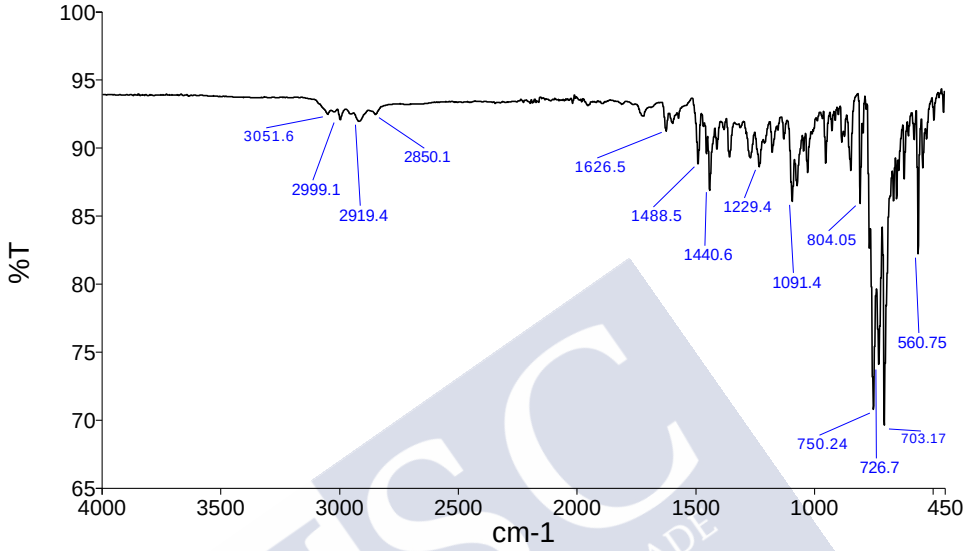
86

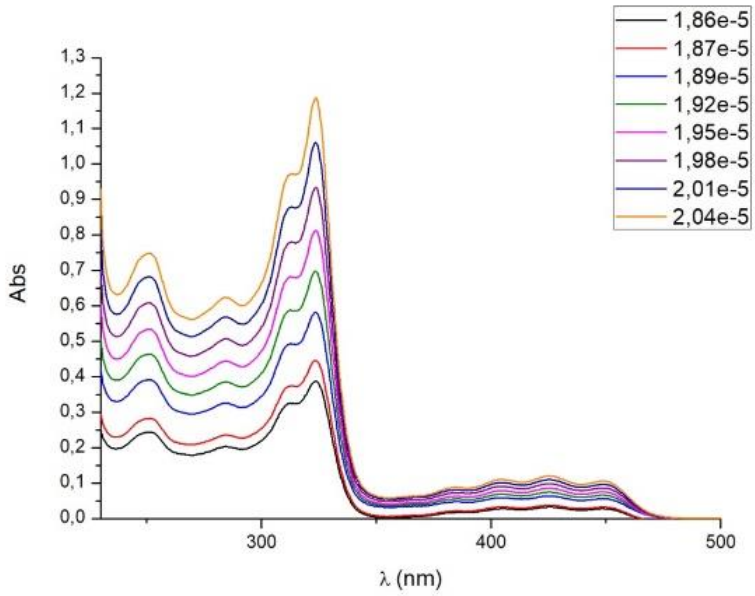

10.0 9.5 9.0 8.5 8.0 7.5 7.0 6.5 6.0 5.5 5.0 4.5 4.0 3.5 3.0 2.5 2.0 1.5 1.0 0.5 0.0
f1 (ppm)

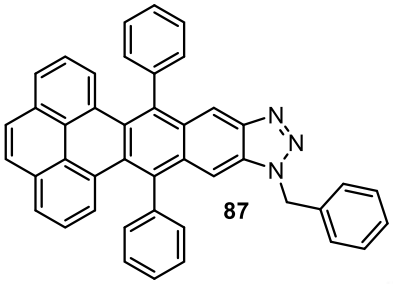

180 170 160 150 140 130 120 110 100 90 80 70 60 50 40 30 20 10 0
f1 (ppm)


N
N
N

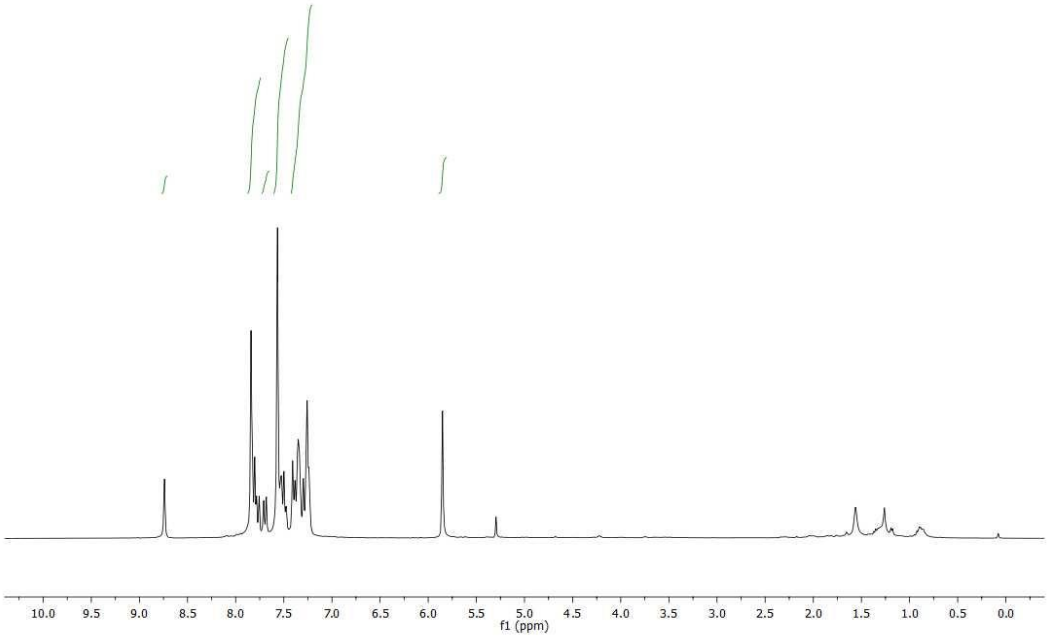
86

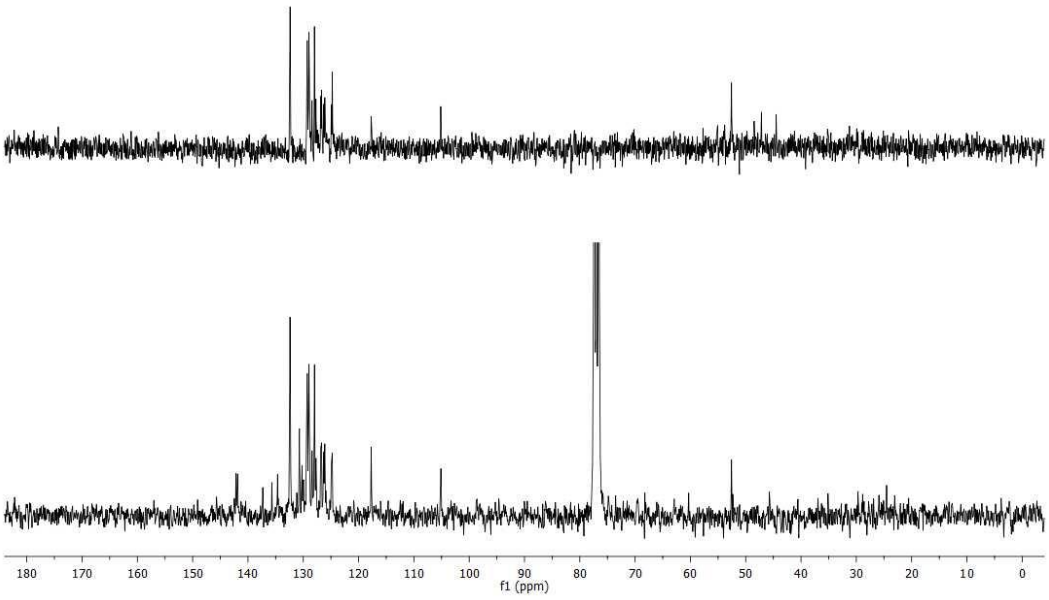

100
95
90
85
80
75
70
65
%T
3051.6
2999.1
2919.4
2850.1
1626.5
1488.5
1440.6
1229.4
1091.4
804.05
560.75
750.24
726.7
703.17
4000
3500
3000
2500
2000
1500
1000
450
cm-1

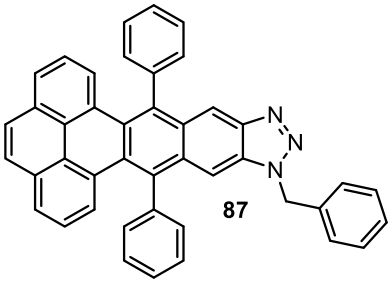

1,86e-5
1,87e-5
1,89e-5
1,92e-5
1,95e-5
1,98e-5
2,01e-5
2,04e-5
Abs
1,3
1,2
1,1
1,0
0,9
0,8
0,7
0,6
0,5
0,4
0,3
0,2
0,1
0,0
300
400
500
λ (nm)


N
N
N

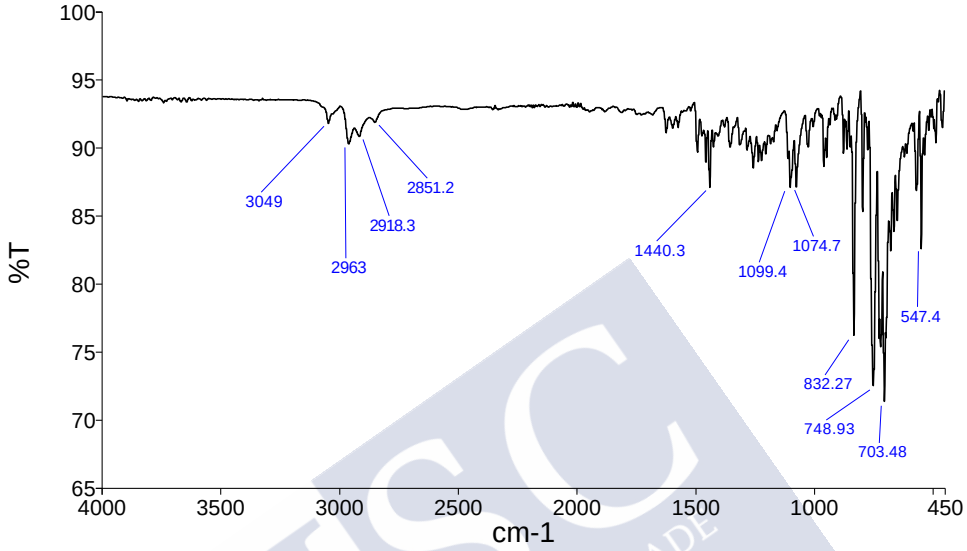
87

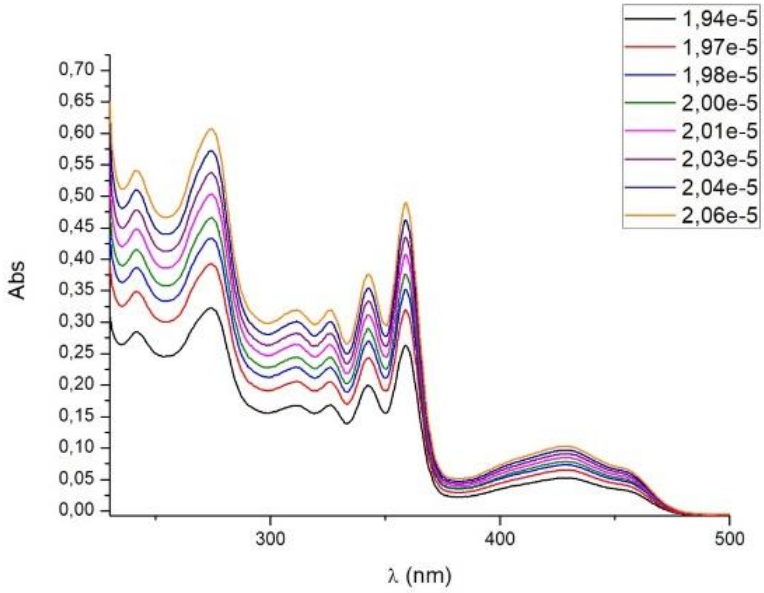

10.0 9.5 9.0 8.5 8.0 7.5 7.0 6.5 6.0 5.5 5.0 4.5 4.0 3.5 3.0 2.5 2.0 1.5 1.0 0.5 0.0
f1 (ppm)

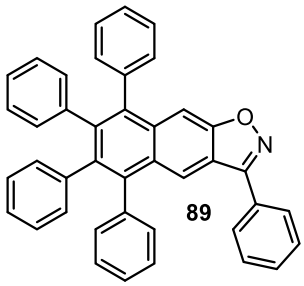

180 170 160 150 140 130 120 110 100 90 80 70 60 50 40 30 20 10 0
f1 (ppm)


N
N
N

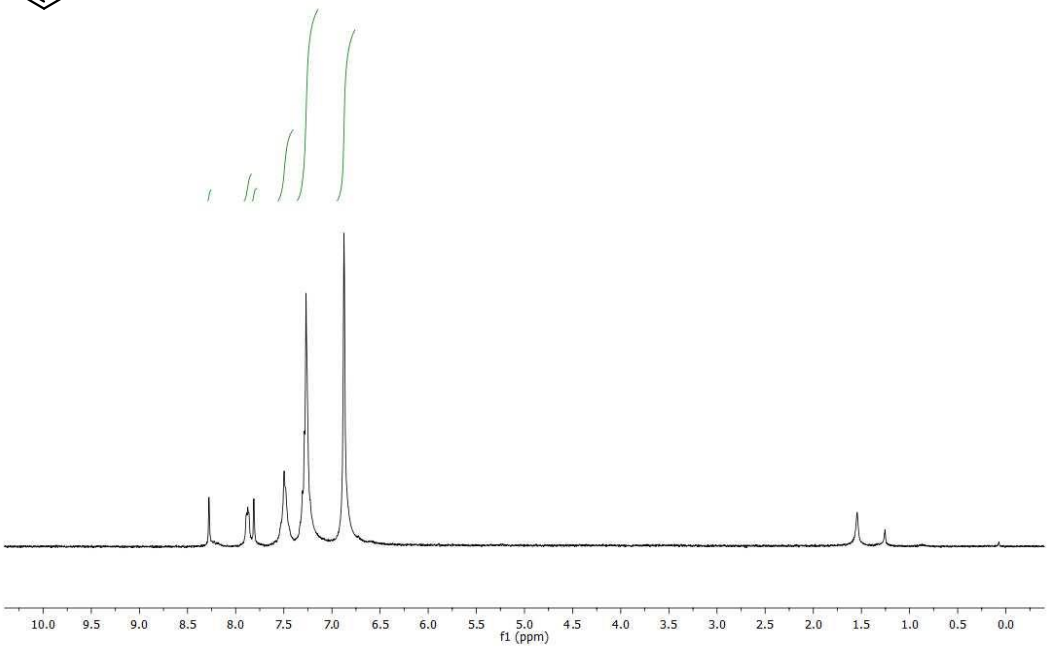
87

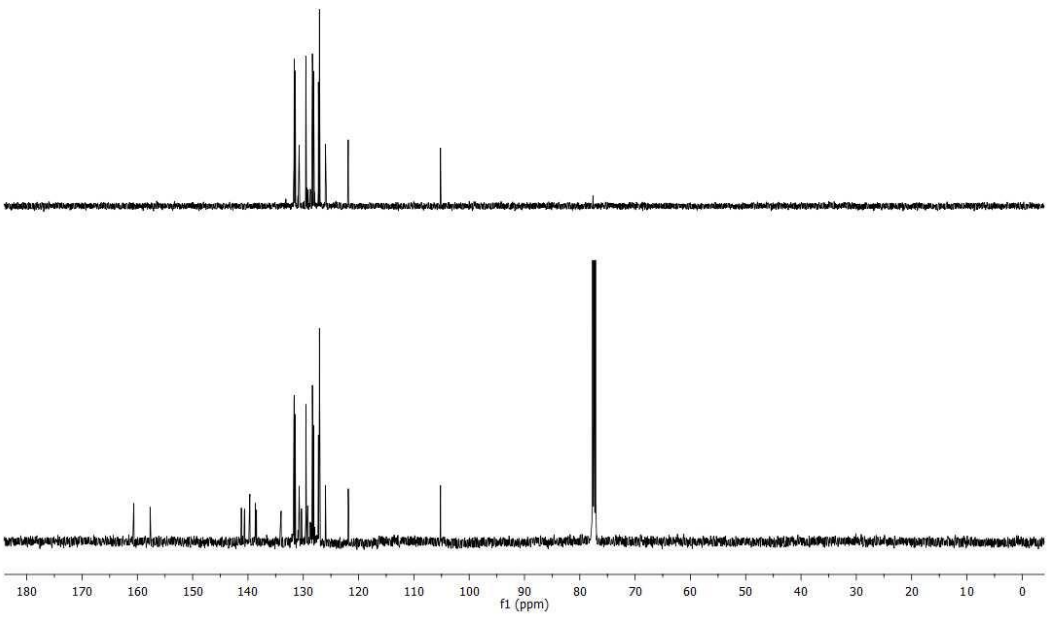

100
95
90
85
80
75
70
65
%T
3049
2963
2918.3
2851.2
1440.3
1099.4
1074.7
547.4
832.27
748.93
703.48
4000
3500
3000
2500
2000
1500
1000
450
cm-1

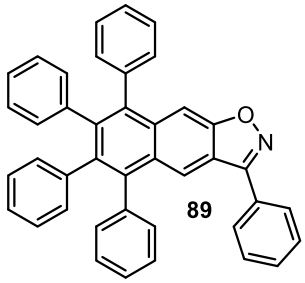

1,94e-5
1,97e-5
1,98e-5
2,00e-5
2,01e-5
2,03e-5
2,04e-5
2,06e-5
0,70
0,65
0,60
0,55
0,50
0,45
0,40
0,35
0,30
0,25
0,20
0,15
0,10
0,05
0,00
Abs
300
400
500
λ (nm)


O
N

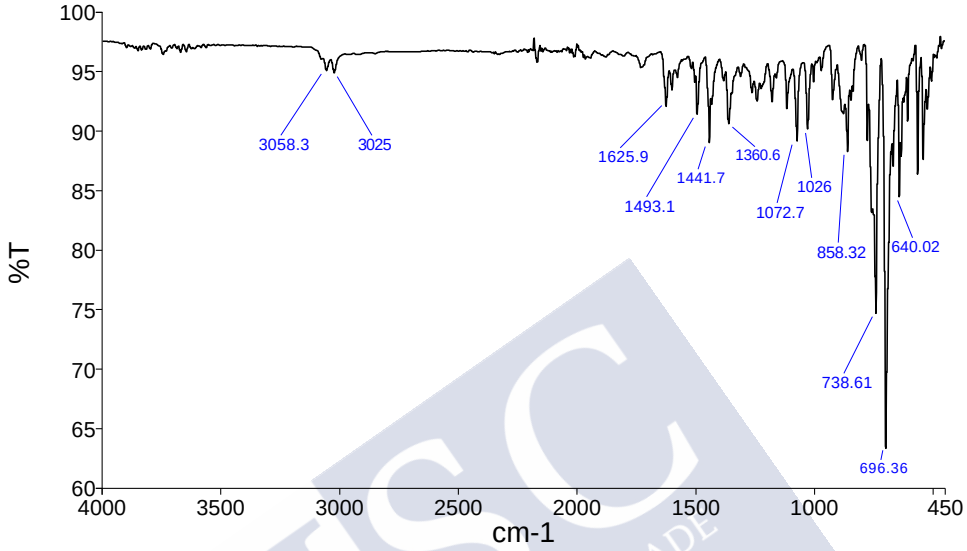
89

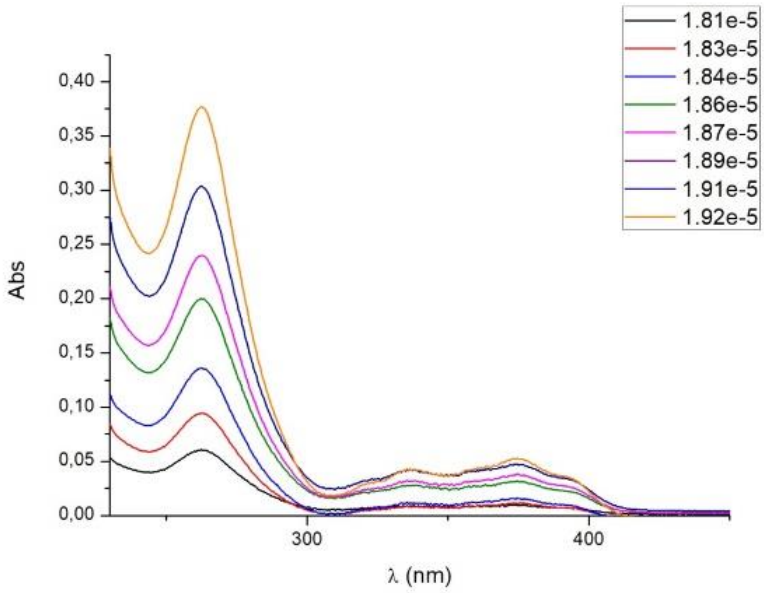

10.0 9.5 9.0 8.5 8.0 7.5 7.0 6.5 6.0 5.5 5.0 4.5 4.0 3.5 3.0 2.5 2.0 1.5 1.0 0.5 0.0
f1 (ppm)

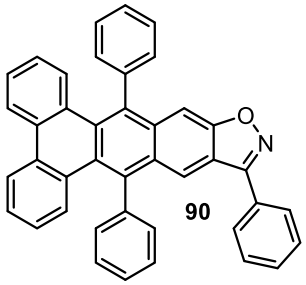

180 170 160 150 140 130 120 110 100 90 80 70 60 50 40 30 20 10 0
f1 (ppm)


O
N

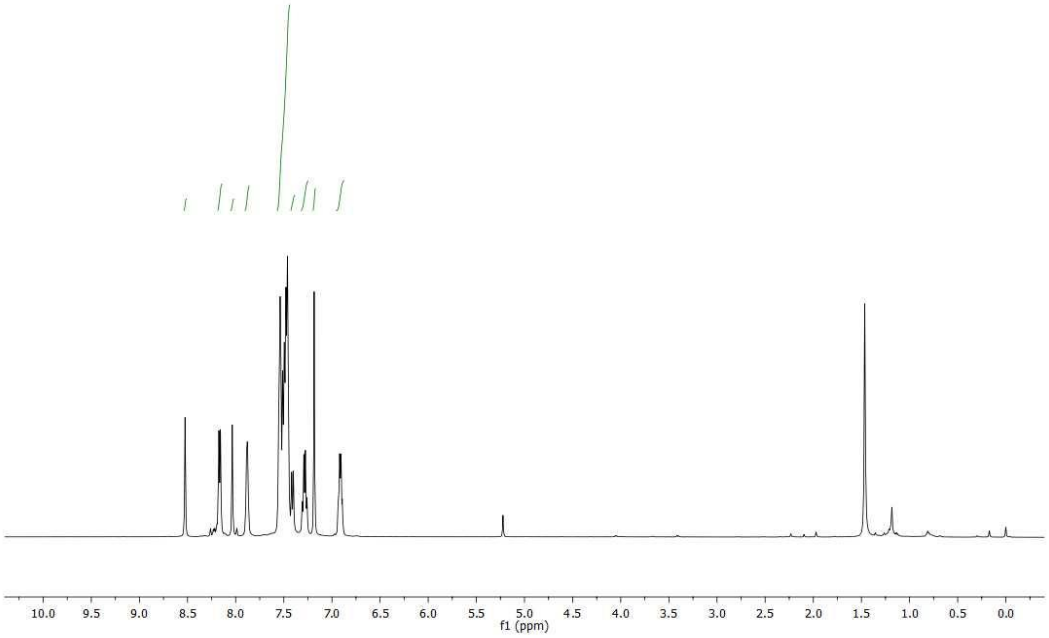
89

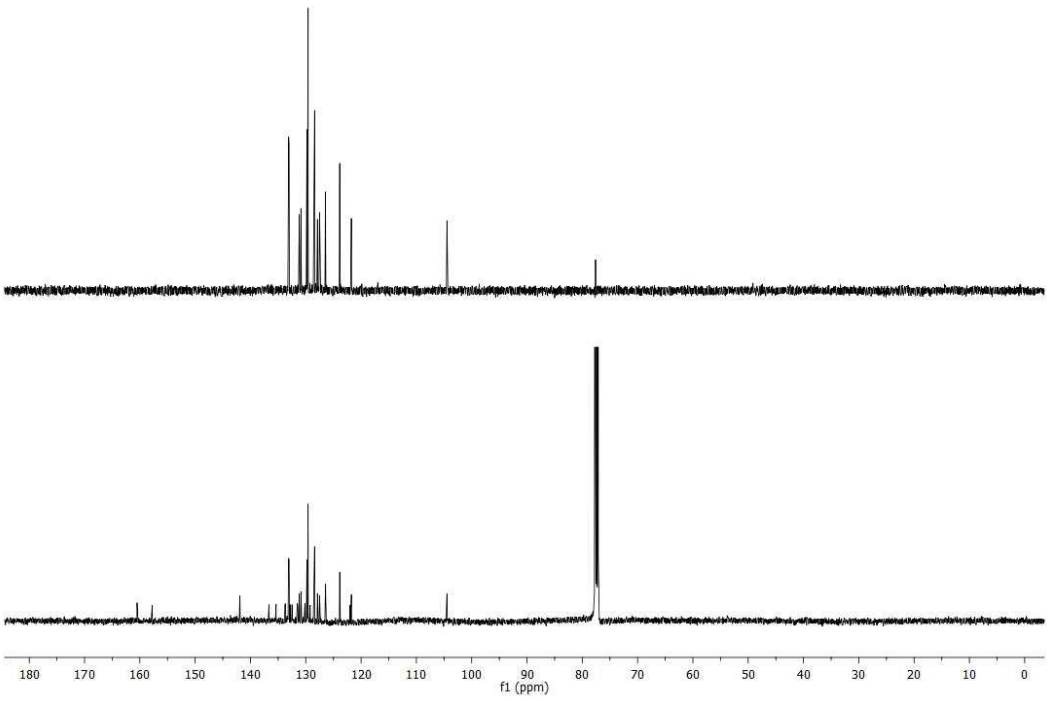

100
95
90
85
80
75
70
65
60
%T
3058.3
3025
1625.9
1493.1
1441.7
1360.6
1072.7
1026
858.32
738.61
696.36
640.02
4000
3500
3000
2500
2000
1500
1000
450
cm-1

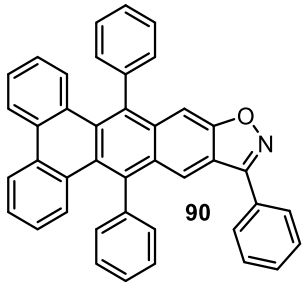

1.81e-5
1.83e-5
1.84e-5
1.86e-5
1.87e-5
1.89e-5
1.91e-5
1.92e-5
0,40
0,35
0,30
0,25
0,20
0,15
0,10
0,05
0,00
Abs
300
400
λ (nm)


O
N

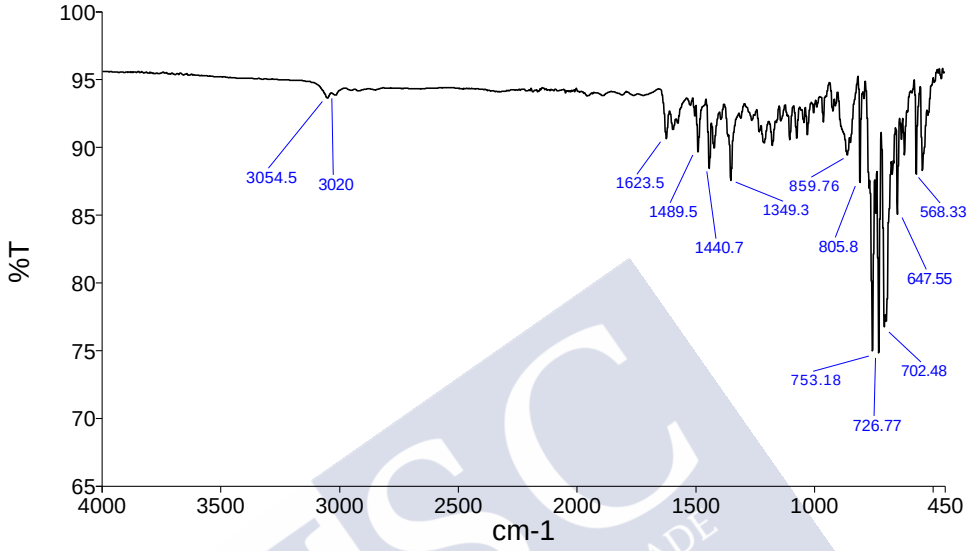
90

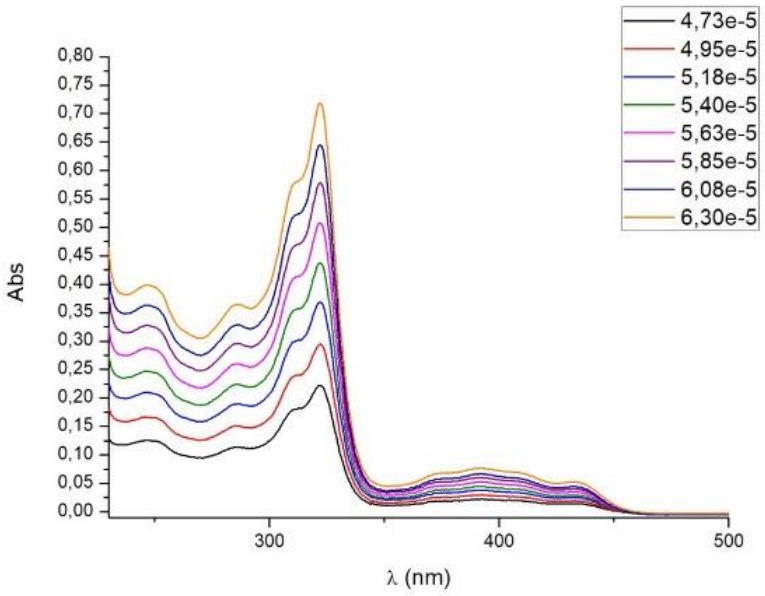

10.0 9.5 9.0 8.5 8.0 7.5 7.0 6.5 6.0 5.5 5.0 4.5 4.0 3.5 3.0 2.5 2.0 1.5 1.0 0.5 0.0
f1 (ppm)

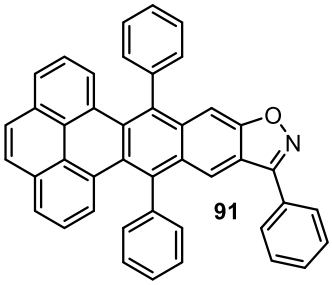

180 170 160 150 140 130 120 110 100 90 80 70 60 50 40 30 20 10 0
f1 (ppm)


O
N

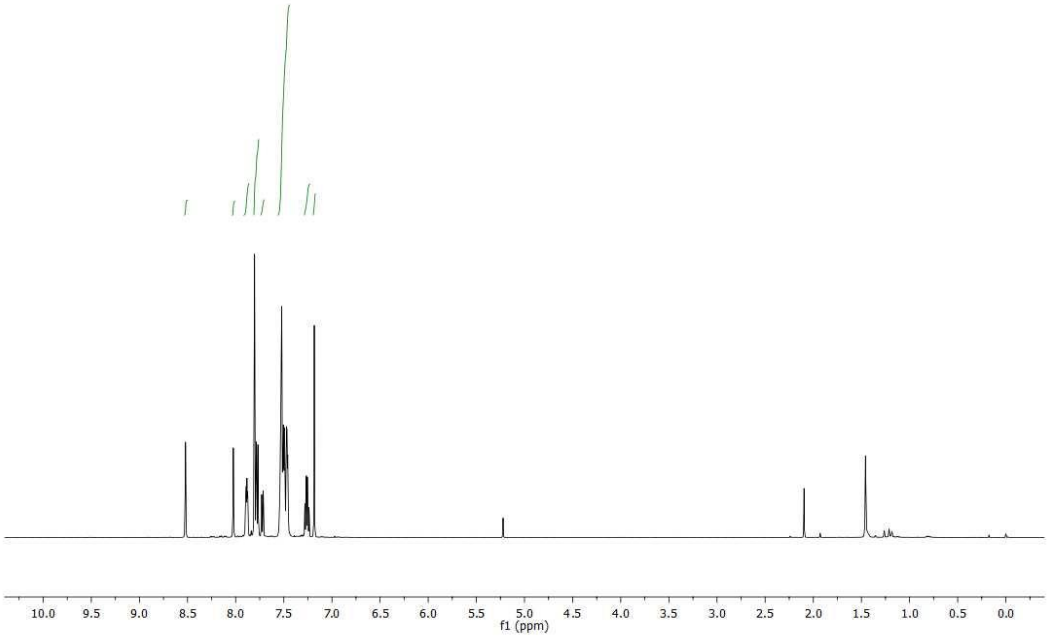
90

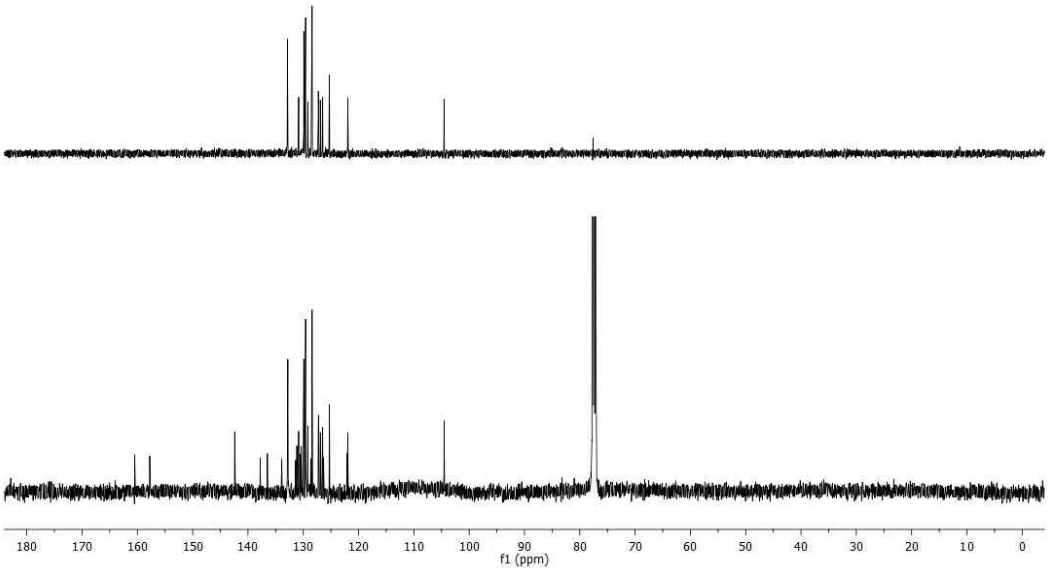

100
95
90
85
80
75
70
65
%T
4000
3500
3000
2500
2000
1500
1000
450
cm-1
3054.5
3020
1623.5
1489.5
1440.7
1349.3
859.76
805.8
568.33
647.55
753.18
726.77
702.48

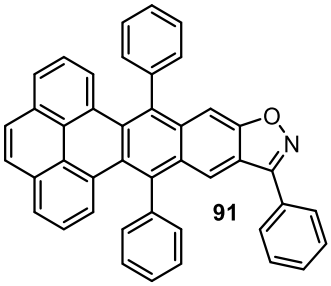

4,73e-5
4,95e-5
5,18e-5
5,40e-5
5,63e-5
5,85e-5
6,08e-5
6,30e-5
Abs
0,80
0,75
0,70
0,65
0,60
0,55
0,50
0,45
0,40
0,35
0,30
0,25
0,20
0,15
0,10
0,05
0,00
300
400
500
λ (nm)


O
N

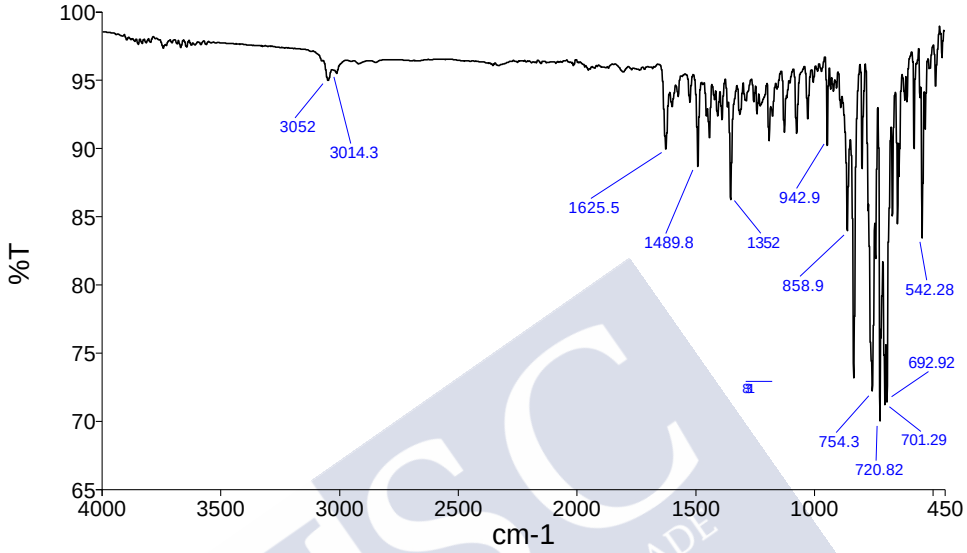
91

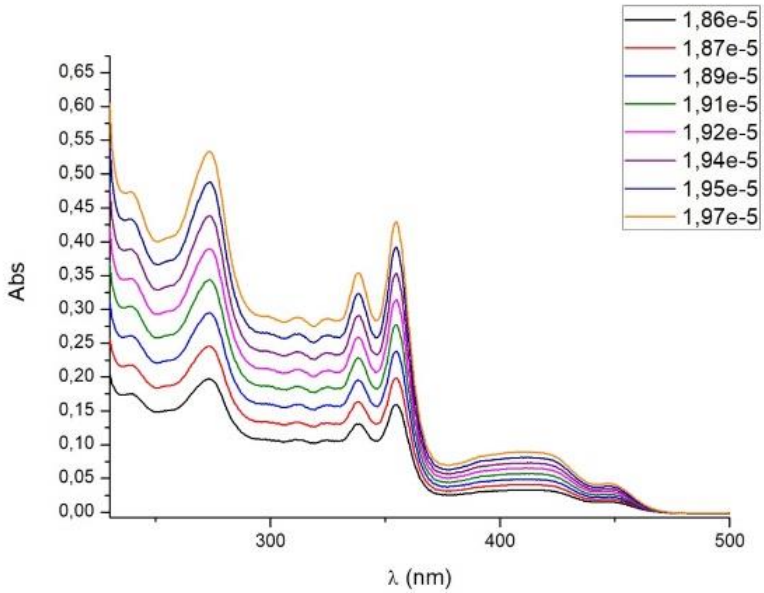

10.0 9.5 9.0 8.5 8.0 7.5 7.0 6.5 6.0 5.5 5.0 4.5 4.0 3.5 3.0 2.5 2.0 1.5 1.0 0.5 0.0
f1 (ppm)

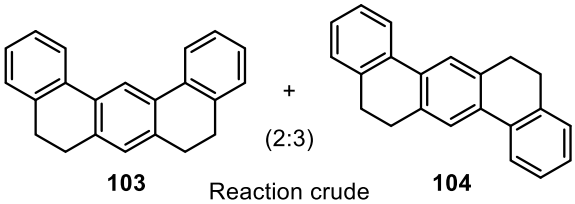

180 170 160 150 140 130 120 110 100 90 80 70 60 50 40 30 20 10 0
f1 (ppm)


O
N

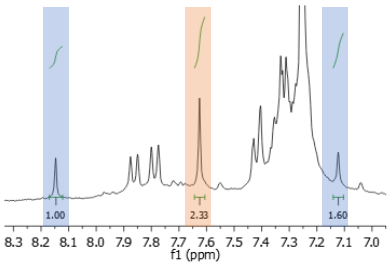
91

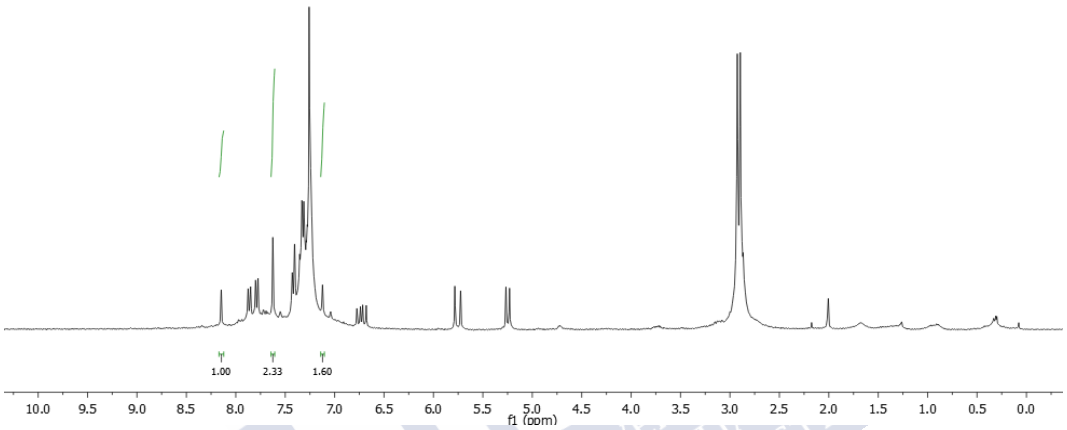

100
95
90
85
80
75
70
65
%T
4000
3500
3000
2500
2000
1500
1000
450
cm-1
3052
3014.3
1625.5
1489.8
1352
942.9
858.9
542.28
692.92
754.3
701.29
720.82

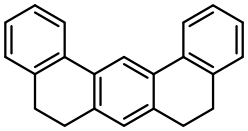

1,86e-5
1,87e-5
1,89e-5
1,91e-5
1,92e-5
1,94e-5
1,95e-5
1,97e-5
Abs
0,65
0,60
0,55
0,50
0,45
0,40
0,35
0,30
0,25
0,20
0,15
0,10
0,05
0,00
300
400
500
λ (nm)



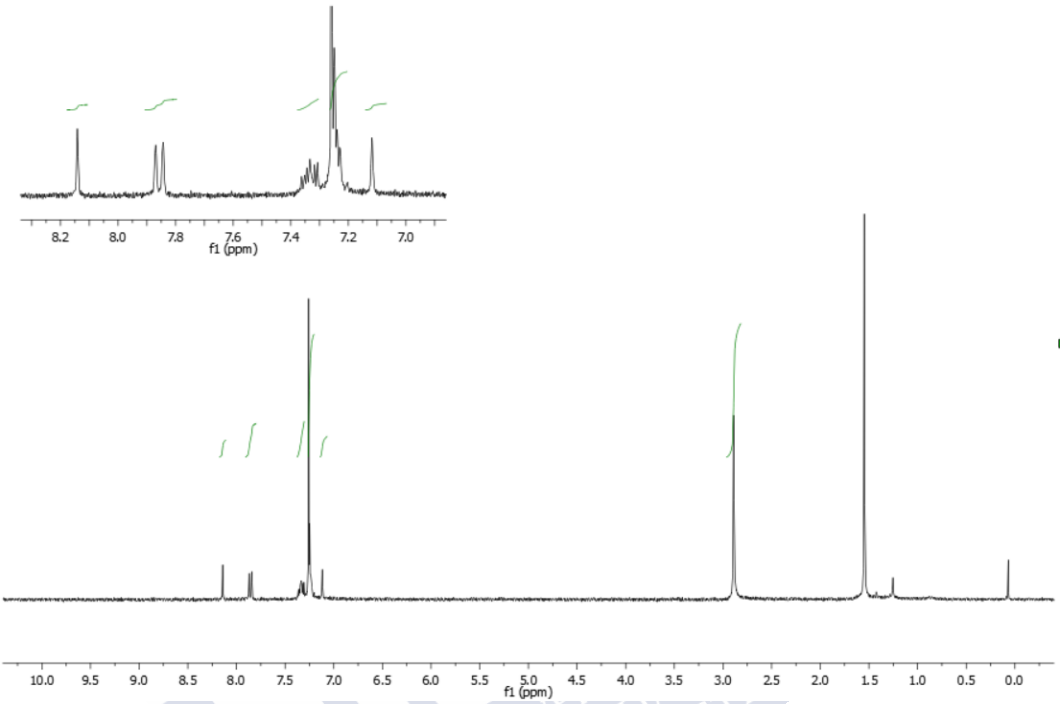
103 Reaction crude **104**

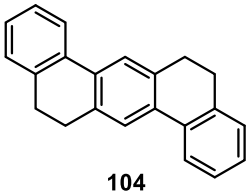




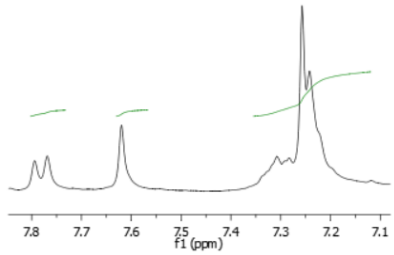


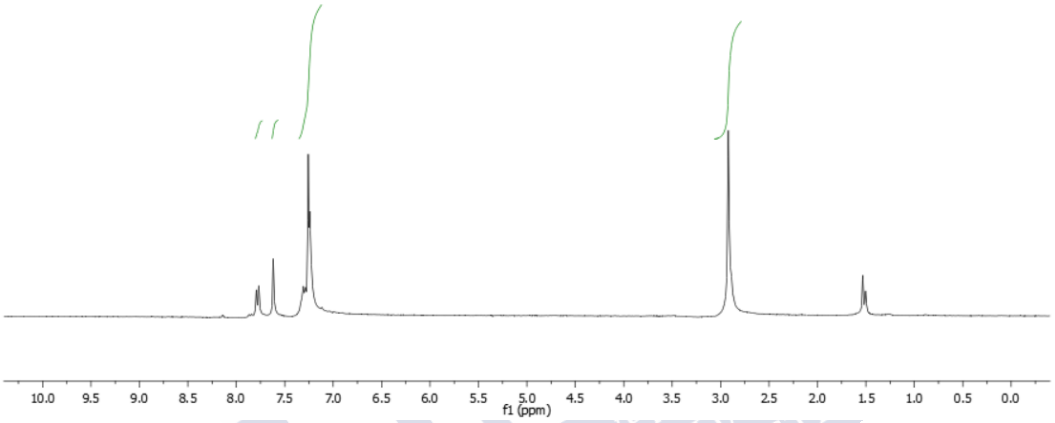
103


8.2
8.0
7.8
7.6
7.4
7.2
7.0
f1 (ppm)
10.0
9.5
9.0
8.5
8.0
7.5
7.0
6.5
6.0
5.5
5.0
4.5
4.0
3.5
3.0
2.5
2.0
1.5
1.0
0.5
0.0
f1 (ppm)



104


7.8
7.7
7.6
7.5
7.4
7.3
7.2
7.1
f1 (ppm)


10.0
9.5
9.0
8.5
8.0
7.5
7.0
6.5
6.0
5.5
5.0
4.5
4.0
3.5
3.0
2.5
2.0
1.5
1.0
0.5
0.0
f1 (ppm)

A.2 Arynes: chronology

Selected examples for this section are referred to specific publications cited in this thesis.

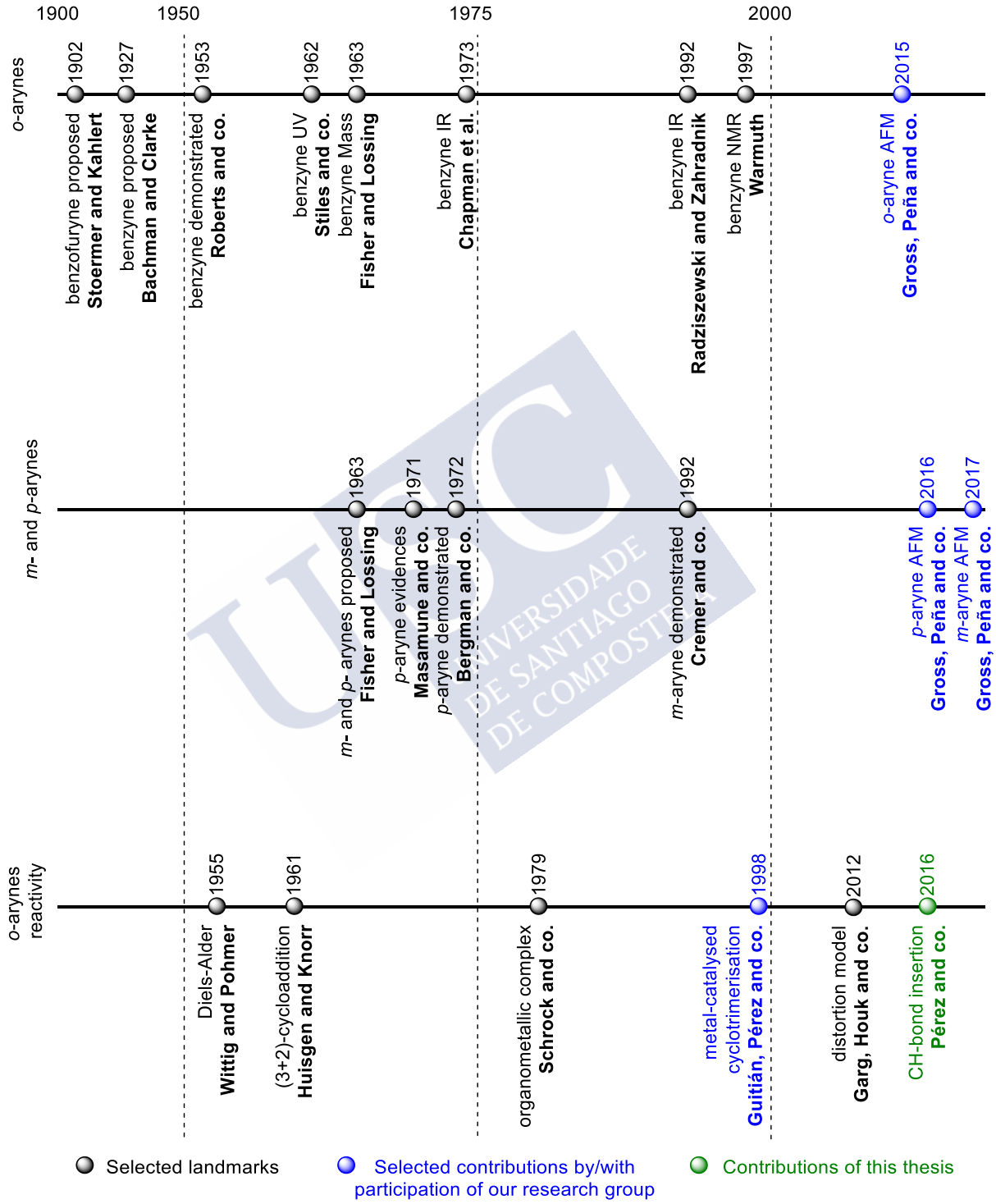


Figure A1. Selected achievements in the story of *o*-, *m* and *p*- arynes and their reactivity.

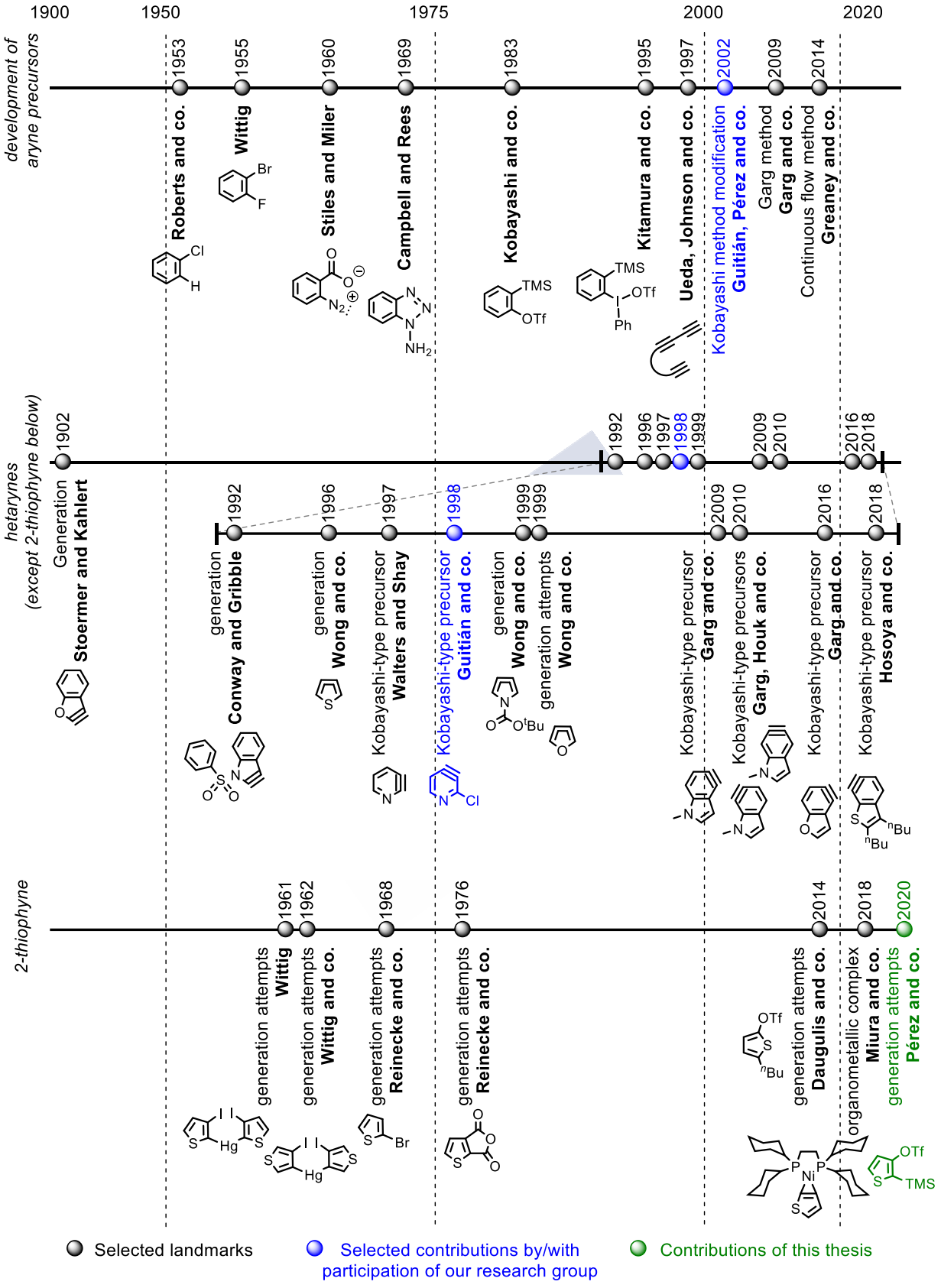


Figure A2. Selected achievements in the story of aryne precursors and hetarynes.

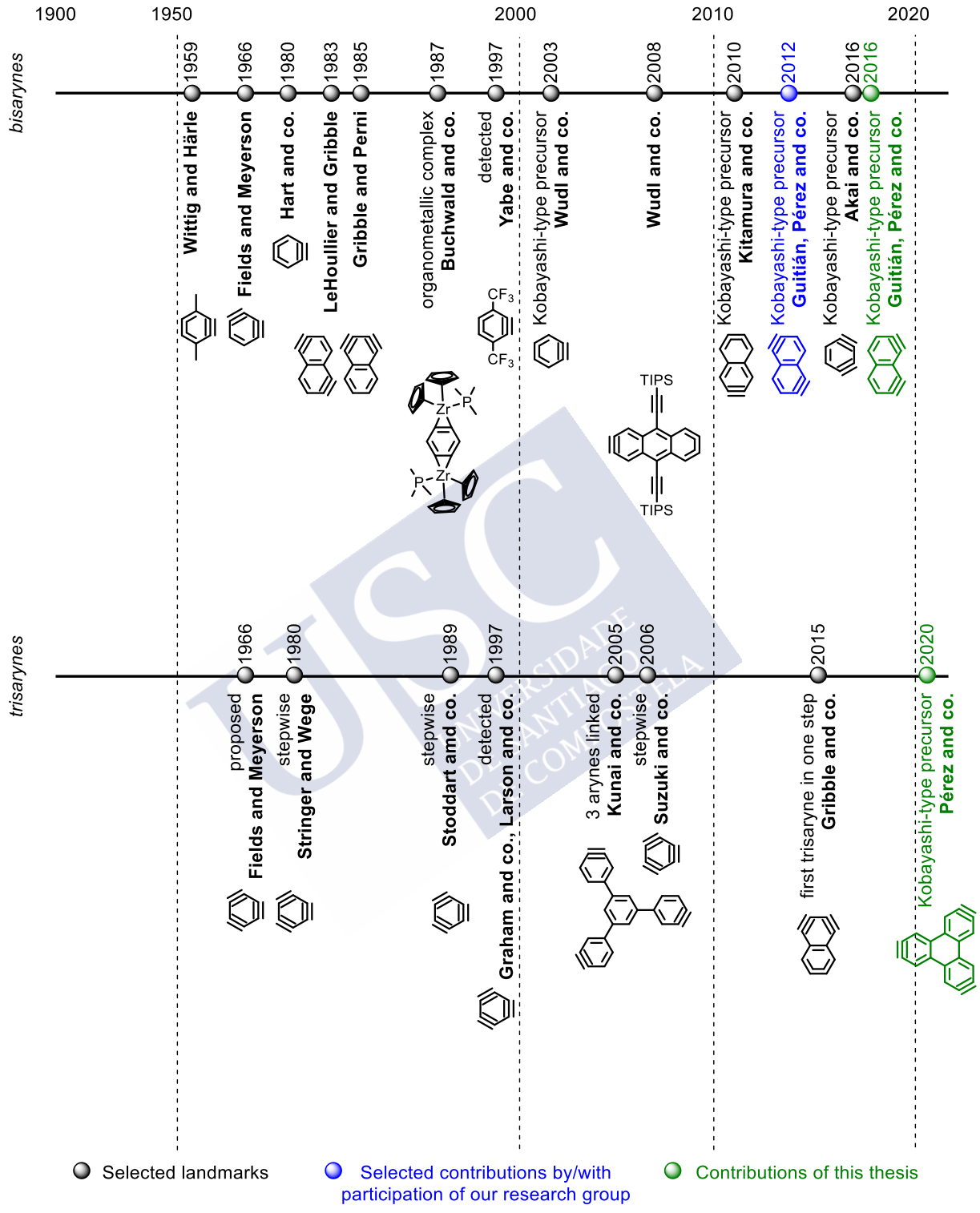


Figure A3. Selected achievements in the story of bisarynes and trisarynes.

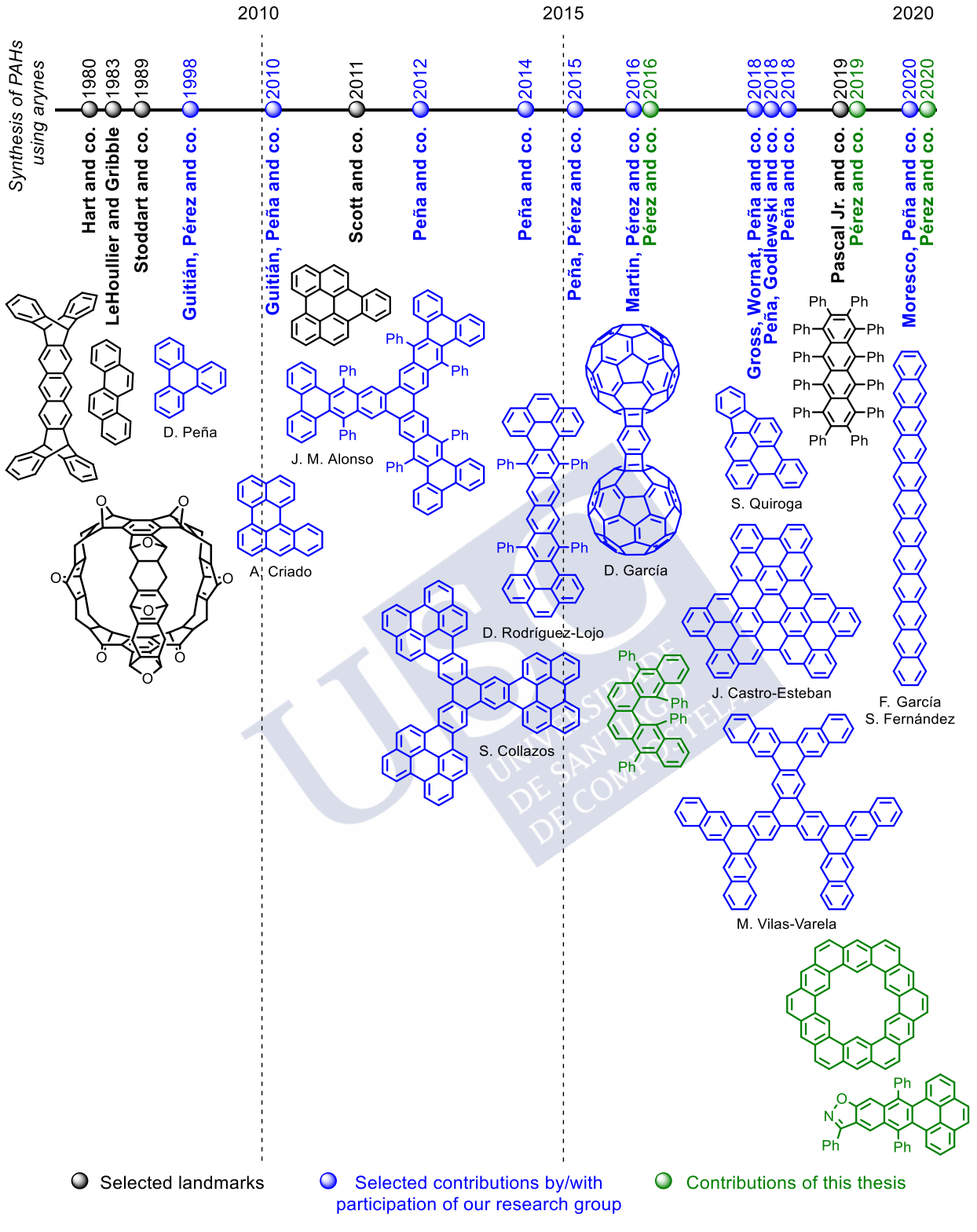


Figure A4. Selected examples of PAHs synthesised by using arynes.

A.3 Diederich and Staab's synthesis of kekulene

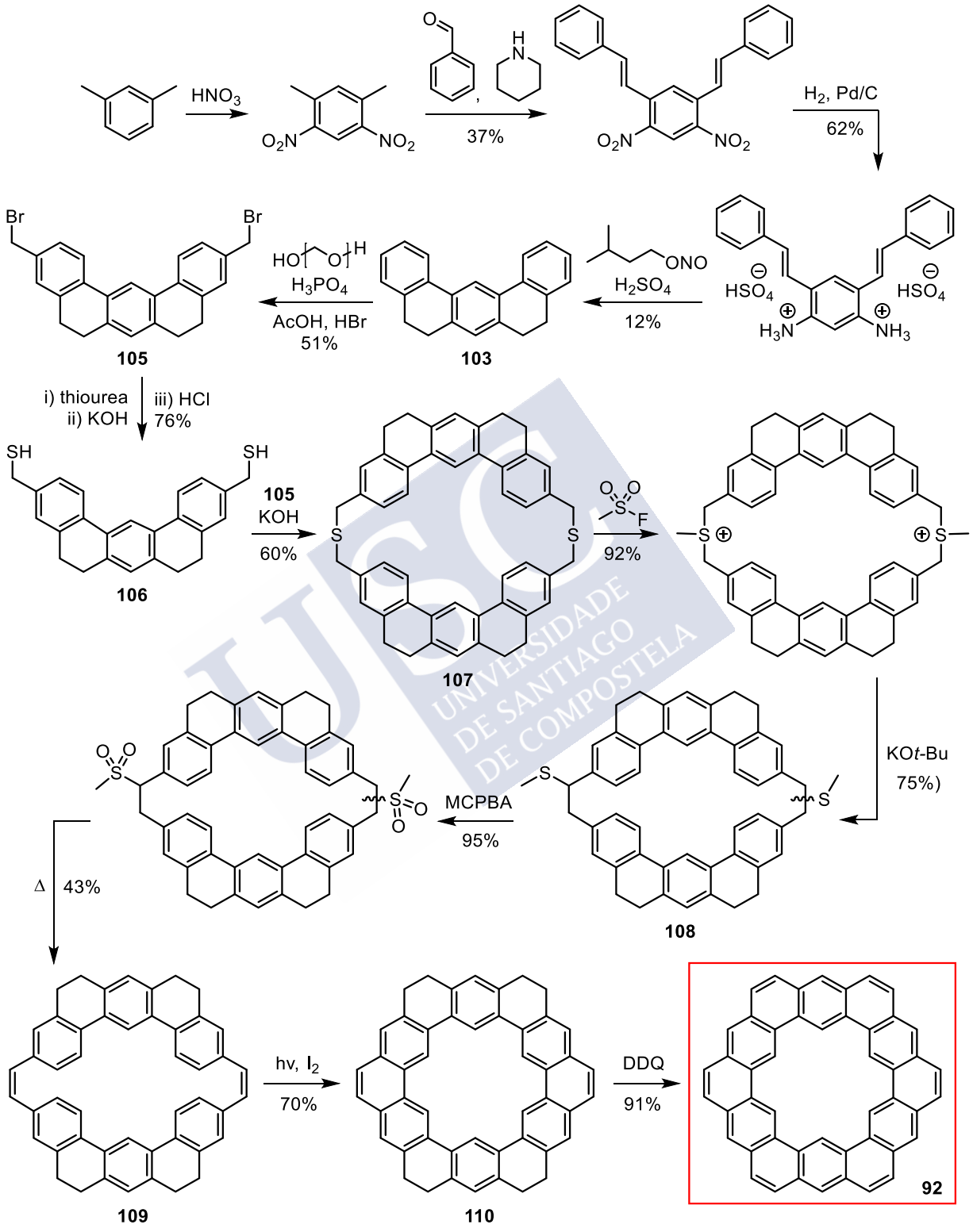


Figure A5. Original synthesis of kekulene (**92**) published by Diederich and Staab.[202]

USC
UNIVERSIDADE
DE SANTIAGO
DE COMPOSTELA

A.4 Cover image

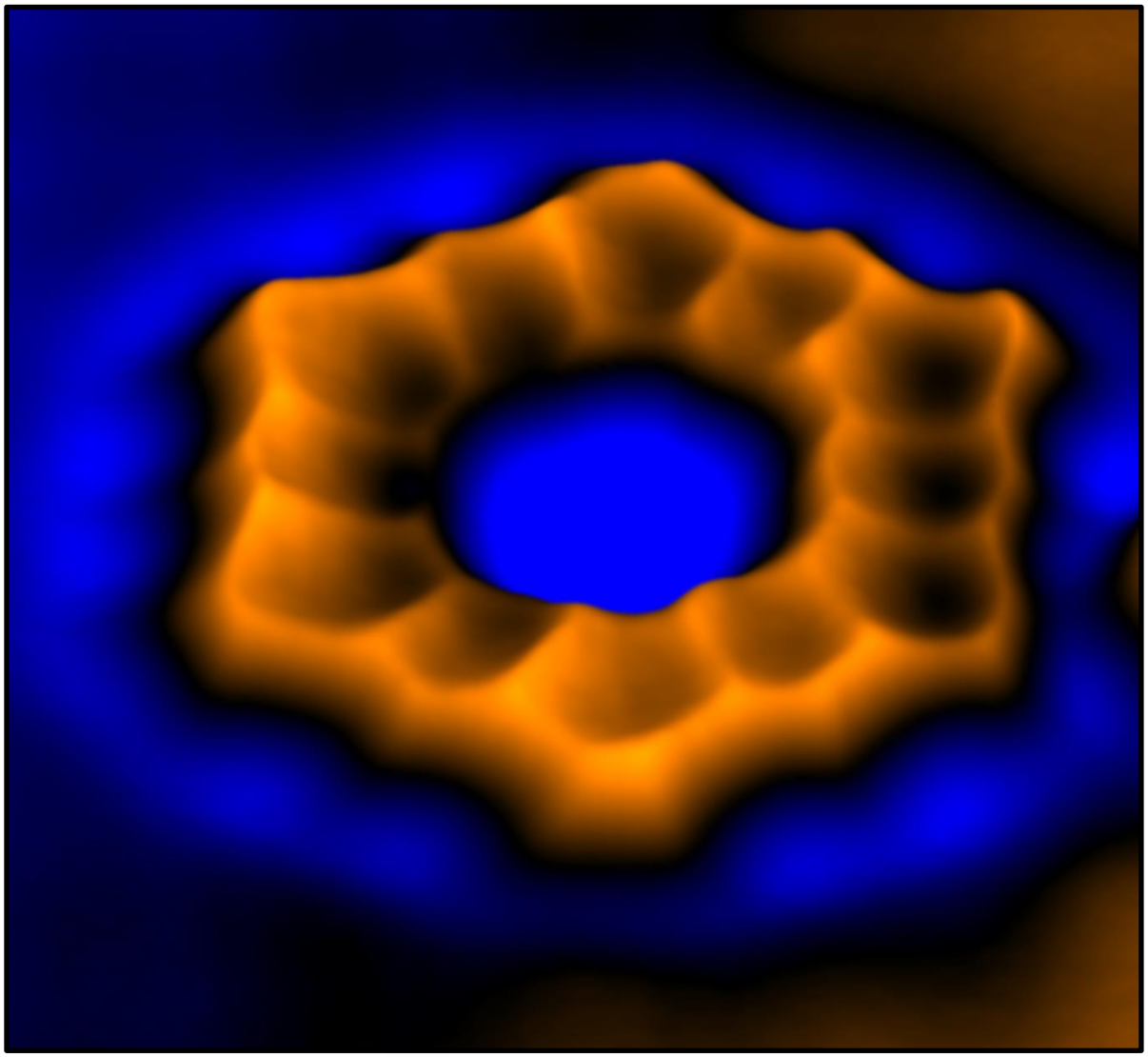


Figure A6. Selected cover image.

USC
UNIVERSIDADE
DE SANTIAGO
DE COMPOSTELA

Resumen de la tesis doctoral

Esta tesis doctoral recoge los resultados más relevantes obtenidos durante el desarrollo de nuevos arinos y su aplicación en la síntesis de hidrocarburos policíclicos aromáticos (HPAs) de interés en nanotecnología y ciencia de materiales. Consta de siete capítulos: el primero recoge la introducción, a continuación, cinco capítulos están dedicados a los cinco proyectos desarrollados en la tesis, y un último capítulo resume los detalles experimentales.

La introducción, Capítulo 1, resume la revisión bibliográfica realizada sobre química de arinos y síntesis de HPAs. Adicionalmente, se comentan algunos de los ejemplos actuales más representativos de la síntesis de HPAs mediante química de arinos.

El Capítulo 2, titulado “2-Tiofino”, engloba la síntesis de un compuesto que podría ser precursor potencial de este hetarino históricamente escurridizo y el estudio de su reactividad.

El Capítulo 3, “1,7-Naftodiino”, se centra en el desarrollo de un precursor de dicho bisarino. Además, se comenta el estudio de su reactividad y su utilidad como plataforma para obtener HPAs estéricamente congestionados.

El Capítulo 4, “2,6,10-Trifenilenotriino”, describe la síntesis de dos precursores de este arino. Se discuten los ensayos que prueban su reactividad y su idoneidad para la preparación de nanografenos trigonales.

El Capítulo 5, “Heteroacenos”, trata sobre la obtención de este tipo de compuestos mediante química de arinos. Se describe además el estudio preliminar de las propiedades de estas moléculas.

El Capítulo 6, “Kekuleno”, trata la optimización de la ruta de síntesis de esta emblemática molécula, ampliando su estudio mediante técnicas de microscopía de fuerza atómica.

El Capítulo 7 recoge los detalles experimentales más relevantes de los capítulos anteriores.

1 Introducción

Durante las últimas décadas, ha surgido un renovado interés acerca de los hidrocarburos policíclicos aromáticos (HPAs) debido a su similitud estructural con el grafeno y, por tanto, su potencial utilidad en nanotecnología y ciencia de materiales (Figura 1). Algunos de estos compuestos ya están siendo utilizados en dispositivos electrónicos, como diodos emisores de luz (OLEDs) o transistores de efecto campo (OFETs).

Las propiedades de los HPAs son muy variadas y están relacionadas con motivos específicos de su estructura. Algunas de estas características estructurales determinantes son su forma, tamaño o la presencia de heteroátomos (*doping*). Así, el desarrollo de procedimientos sintéticos para la obtención de nuevos HPAs es crucial para el estudio y comprensión de las relaciones estructura/propiedades existentes.

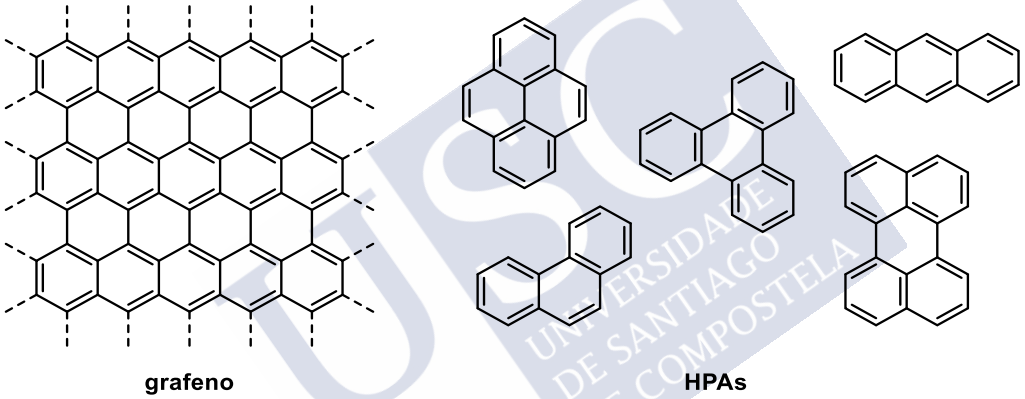
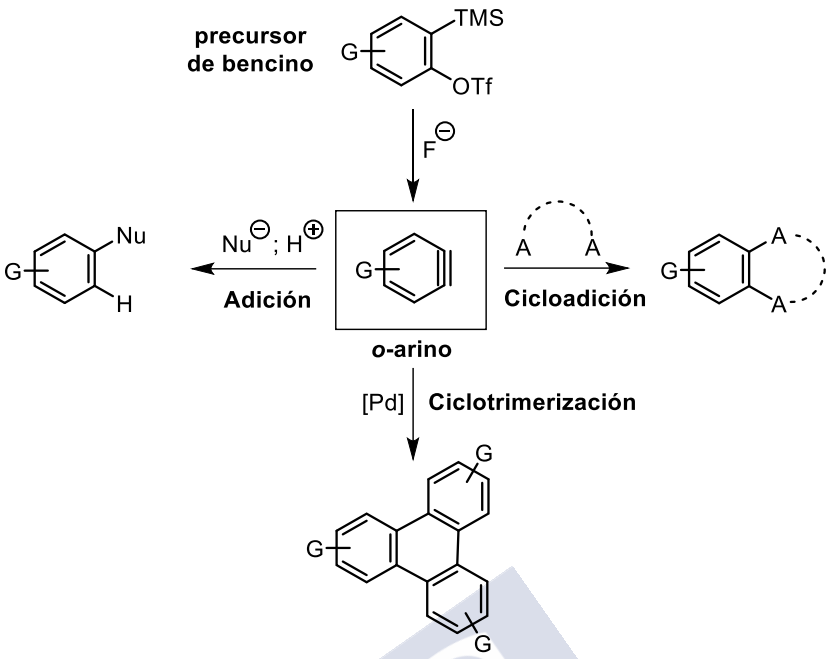


Figura 1. Estructura del grafeno y HPAs representativos.

Los arinos son intermedios de reacción efímeros, formalmente derivados de un areno por la pérdida de dos sustituyentes (Esquema 1). Dependiendo de las posiciones relativas en las que se hayan producido dichas pérdidas, pueden ser clasificados en *orto*-, *meta*- o *para*-arinos. Los *o*-arinos son los más utilizados en síntesis orgánica porque poseen una rica reactividad en ocasiones controlable. Principalmente, los arinos exhiben dos tipos de comportamiento; electrófilo y dienófilo. Así, su participación en reacciones de adición de nucleófilos y reacciones de cicloadición, ha sido ampliamente estudiada y utilizada en síntesis orgánica. Tras la gran expansión que experimentó la química organometálica, nuestro grupo de investigación desarrolló la primera reacción de arinos catalizada por metales en 1998, concretamente, la ciclotrimerización catalizada por paladio (Esquema 1).



Esquema 1. Estructura y reactividad de los *o*-arinos.

Debido a su reducido tiempo de vida media, los arinos deben ser generados en el propio medio de reacción. Para ello, es necesaria la utilización de precursores de arino adecuados. Los más empleados son los triflatos de *orto*-trimetilsililarilo, desarrollados por Kobayashi (Esquema 1). Estos compuestos son capaces de generar el arino correspondiente de manera selectiva, en rendimientos altos y condiciones de reacción suaves, mediante el tratamiento con iones fluoruro (Esquema 1).

Los hetarinos pueden definirse como arinos que incorporan en el mismo anillo aromático al menos un heteroátomo (Figura 2). Aunque los hetarinos derivados del tiofeno fueron ampliamente investigados durante las décadas de los 60 y 70, actualmente los más estudiados y utilizados son aquellos que derivan de la piridina. El estudio de estas especies es altamente interesante dado su inusual comportamiento y su potencial utilidad en síntesis orgánica.



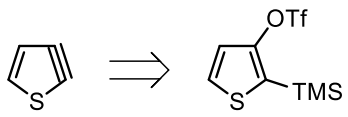
Figura 2. Ejemplos de hetarinos y poliarinos.

Los poliarinos, son compuestos que presentan dos o más insaturaciones arínicas en el mismo núcleo aromático (Figura 2). Aunque se han publicado algunos ejemplos de la observación directa de estas especies mediante técnicas espectroscópicas, en química sintética deben ser considerados como sintones. De esta manera, tras la generación de la primera insaturación arínica ésta reacciona *inmediatamente*, y en todo caso antes de la generación de la siguiente insaturación arínica. Los poliarinos que contienen dos insaturaciones arínicas, o bisarinos, son los más estudiados, especialmente aquellos localizados en los núcleos aromáticos de benceno y naftaleno. Ejemplos de otros poliarenos con un mayor número de insaturaciones arínicas, como los trisarinos, son escasos en la bibliografía. El uso de este tipo de especies en química orgánica tiene un gran interés asociado a su capacidad para crear un gran número de nuevos enlaces en un sola etapa sintética.

2 2-Tiofino

Probablemente, el hetarino más intrigante de los propuestos en la literatura científica sea el 2-tiofino (Figura 3). A pesar de ser uno de los más estudiados durante el siglo XX, su existencia sigue siendo una incógnita. Varios grupos de investigación han dedicado grandes esfuerzos para conseguir pruebas de su generación, sin haber podido aportar evidencias sólidas hasta la fecha. El interés en este hetarino transciende más allá del desafío que supone, ya que sería de gran utilidad para acceder a HPAs con un átomo de azufre de potencial aplicación como semiconductores orgánicos.

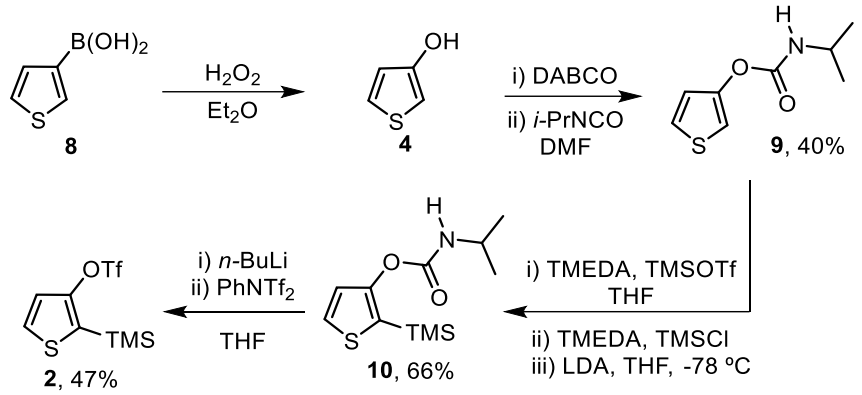
El objetivo de este capítulo es la generación del 2-tiofino. Decidimos afrontar este desafío basándonos en estudios computacionales recientes y apoyados por el desarrollo de los precursores arino de tipo Kobayashi.



2-tiofino (**1**) **2**

Figura 3. Propuesta retrosintética del 2-tiofino (**1**).

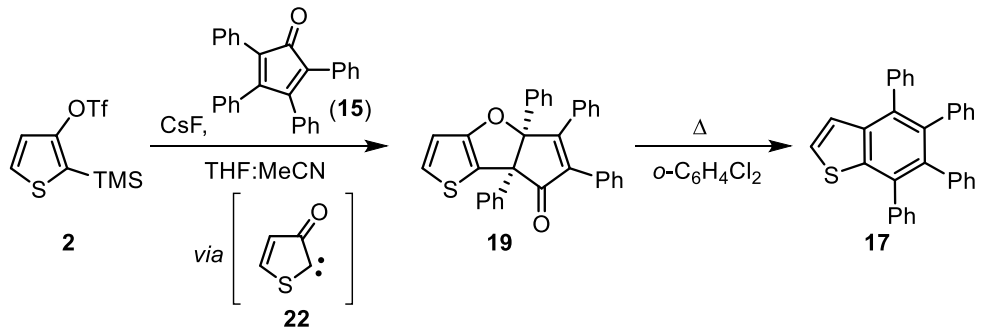
El primer paso fue la selección de un posible precursor de 2-tiofino (Figura 3) y el diseño una síntesis plausible para su obtención. El candidato seleccionado fue el triflato de trimetilsililtiofeno **2**. Su síntesis se realizó mediante un procedimiento similar al descrito por Garg y colaboradores para precursores de hetarinos nitrogenados, a través de cuatro etapas de reacción en rendimientos moderados (Esquema 2).



Esquema 2. Síntesis del 3-triflato de 2-trimetilsililtiofeno (**2**).

Una vez obtenido el compuesto **2**, estudiamos la generación del 2-tiofino (**1**). La reacción de **2** con CsF en presencia de diferentes dienos, adecuados para reaccionar con arinos, condujo a la descomposición del precursor. Finalmente, esta reacción utilizando 2,3,4,5-tetrafenilciclopentadienona (**15**) como dieno, permitió aislar un producto cuyo calentamiento en disolución condujo a la obtención del benzotiofeno tetrafenilado **17**. Este producto es el esperado de un mecanismo *via* arino, sin embargo, la falta de resultados adicionales que apoyasen la generación del 2-tiofino y su peculiar historia, nos motivaron a realizar un estudio mecanístico de esta transformación.

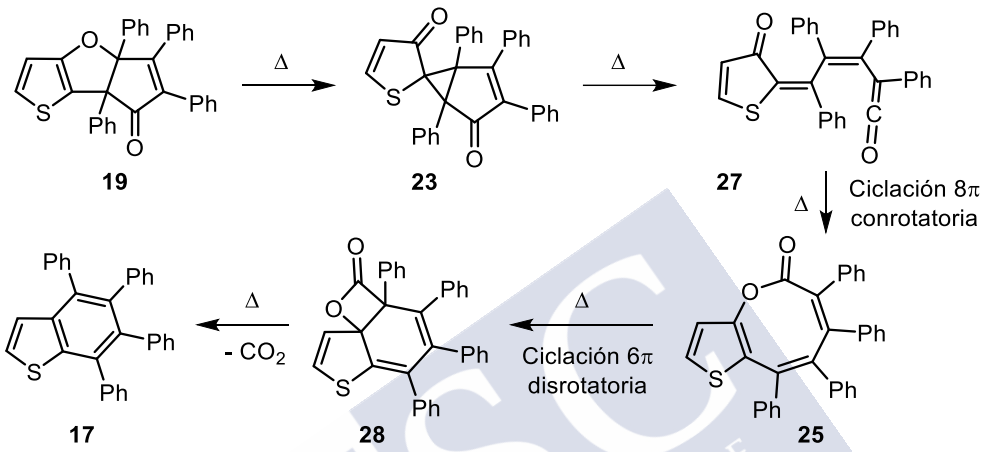
La realización de la reacción entre **2** y **15** a baja temperatura permitió el aislamiento y la caracterización inequívoca del producto intermedio **19**, mediante difracción de rayos X. Este resultado experimental descartó por completo la generación del arino **1** (Esquema 3). Experimentos adicionales basados en reacciones de atrapado y aislamiento de intermedios, nos llevaron a proponer una secuencia mecanística alternativa que decidimos evaluar computacionalmente.



Esquema 3. Síntesis de **17** a partir del triflato **2**.

El estudio teórico de estas transformaciones, realizado mediante cálculos DFT en colaboración con el Prof. A. Cobas, sugiere en primer lugar la formación del cetocarbeno **22**

(Esquema 3). El carbeno **22** daría una reacción de cicloadición (3+2) con uno de los dobles enlaces de la ciclopentadienona **15**, para formar el producto intermedio aislado **19**. Este compuesto podría evolucionar a través de un reagrupamiento para dar el ciclopropano **23**, y seguidamente, la apertura del sistema bicíclico de tres y cinco miembros fusionado conduciría a la cetena **27**. Finalmente, una cascada de reacciones pericíclicas, comprendiendo una ciclación 8π conrotatoria, una ciclación 6π disrotatoria y la extrusión de CO_2, permitiría la formación del producto aislado **17** (Esquema 4).



Esquema 4. Propuesta mecanística para la formación de **17**.

Se podría concluir que a pesar de haber sintetizado un "precursor formal de 2-tiofino apropiado" y de haber obtenido "evidencias de su generación" el enigma de su existencia todavía está por resolver.

3 1,7-Naftodiino

Los bisarinos han demostrado ser tremendamente útiles en síntesis, aportando un grado adicional de complejidad y versatilidad. Sin embargo, su generación conlleva a menudo rendimientos bajos, por lo que es imprescindible el empleo de precursores adecuados. Los bisarinos más utilizados hasta el momento han sido aquellos derivados del benceno y el naftaleno. Sin embargo, uno de ellos aún no había sido descrito al comienzo de esta tesis, el 1,7-naftodiino (**29**). Este sintón podría actuar como plataforma para acceder a los HPAs de geometría angular escasamente estudiados (Figura 4).

El objetivo de este capítulo es conseguir un precursor apropiado para la generación del 1,7-naftodiino.

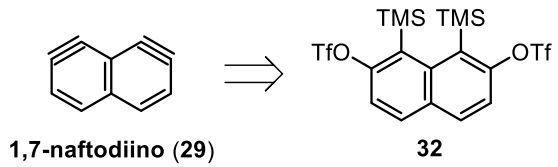
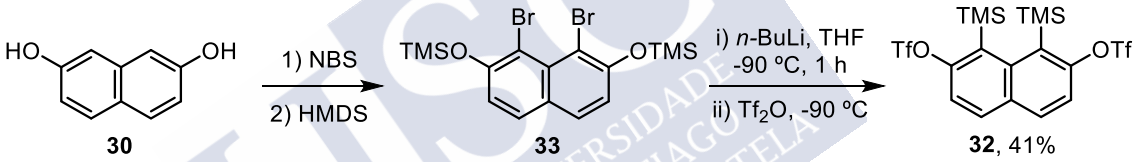


Figura 4. Propuesta retrosintética del 1,7-naftodiino (**29**).

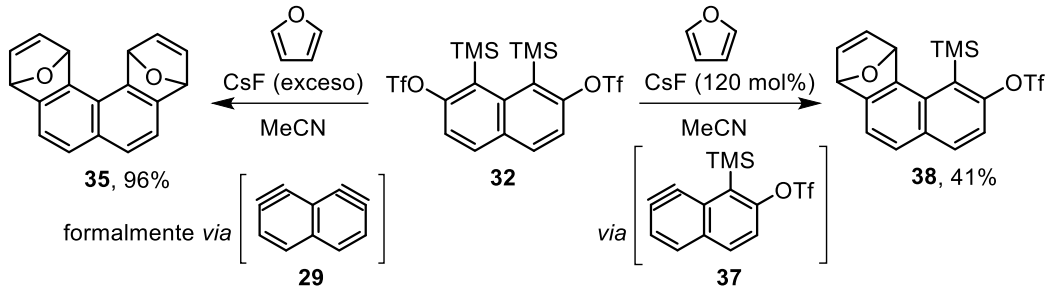
Al igual que en el capítulo anterior, la primera tarea realizada fue la selección del candidato ideal para actuar como precursor de **29** (Figura 4) y el diseño de una ruta sintética plausible para su obtención, basándonos en la experiencia de nuestro grupo de investigación. El compuesto seleccionado fue el naftaleno tetrasustituido **32**.

La síntesis del bistriflato **32** fue realizada en tres etapas a partir del 2,7-naftalenodiol (**30**) comercialmente disponible (Esquema 5). La primera etapa de la síntesis fue la *o*-dibromación selectiva del diol **30**. El producto obtenido fue tratado con HMDS dando lugar al compuesto **33** de manera cuantitativa. Finalmente, el tratamiento secuencial con *n*-BuLi y Tf_2O, permitió obtener **32** con un 41% de rendimiento.



Esquema 5. Síntesis del bistriflato **29**.

Una vez obtenido **32**, decidimos estudiar su capacidad para generar el bisarino correspondiente. Con este propósito realizamos en primer lugar reacciones de atrapado con furano, obteniendo la mezcla de aductos **35**, al utilizar CsF en exceso (Esquema 6). Este resultado demuestra la posibilidad de emplear **32** como un precursor del sintón 1,7-naftodiino (**29**). Cuando se realizó la misma reacción utilizando una cantidad determinada de CsF (120 mol%), obtuvimos los enantiómeros **38**, demostrando que es posible generar selectivamente una única insaturación arínica desde **32**. Esta característica permite el acceso a una gran diversidad de precursores de arinos complejos en una etapa sintética.



Esquema 6. Reacciones de **32** con CsF en presencia de furano.

Adicionalmente, decidimos estudiar la capacidad de **29** para participar en otro tipo de reacciones, como reacciones de inserción en enlaces σ o catalizadas por metales. Descubrimos que el nuevo sintón bisarínico (**29**) da lugar a HPAs de geometría angular a través de reacciones de Diels-Alder en rendimientos particularmente elevados, hecho que demuestra su utilidad como plataforma para acceder a este tipo estas estructuras (Figura 5).

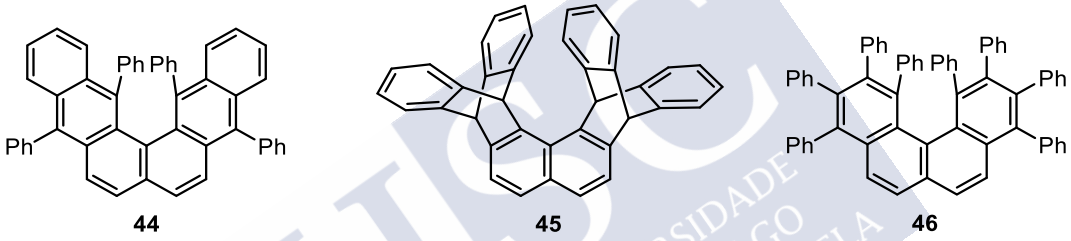
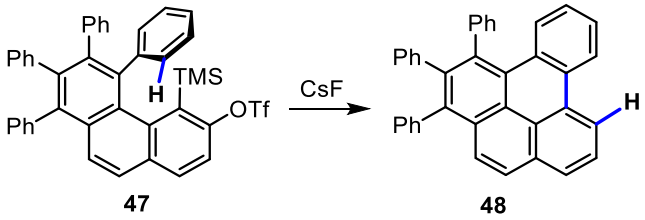


Figura 5. HPAs angulares sintetizados utilizando **32**.

En estudio de nuevos precursores de fenantrino complejos, como **47**, nos llevó a descubrir una nueva reacción de ciclación intramolecular, la cual implica la inserción formal de un arino en un enlace C-H (Esquema 7). La detección del producto clorado en la posición esperada al realizar experimentos de atrapado con CCl_4, sugiere que esta reacción podría transcurrir de forma radicalaria. El estudio teórico mediante cálculos DFT realizado en colaboración con el Prof. A. Cobas, apoya también un mecanismo radicalario para esta novedosa ciclación.



Esquema 7. Reacción de inserción formal de arinos en un enlace C-H.

En resumen, se ha desarrollado un precursor del sintón 1,7-naftodiino (**29**) y se ha demostrado su eficacia. Además, se ha estudiado su reactividad, encontrando una nueva reacción de arinos.

4 2,6,10-Trifenilenotriino

Los trisarinos son el siguiente peldaño en el campo de los poliarinos después de los bisarinos e implican una complejidad adicional con respecto a estos. Sin embargo, existen muy pocos precedentes sobre este tipo de especies en la bibliografía, y su existencia y utilidad en síntesis, apenas ha sido estudiadas.

En este contexto nos propusimos sintetizar un precursor eficiente de trisarino. Concretamente, nos centramos en el sintón 2,6,10-trifenilenotriino (**56**), dada su potencial aplicación para la síntesis de HPAs derivados del trifenileno (Figura 6).

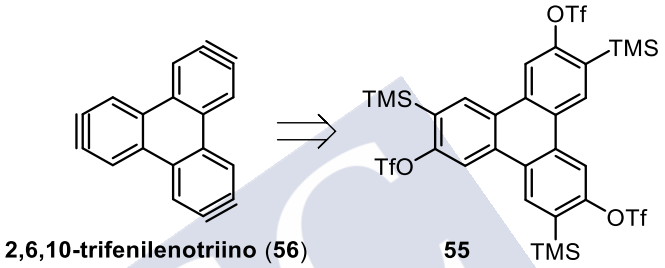
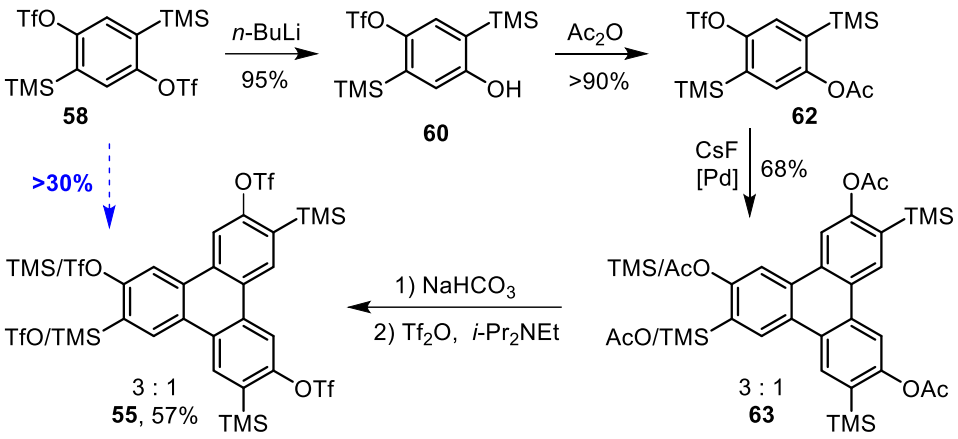


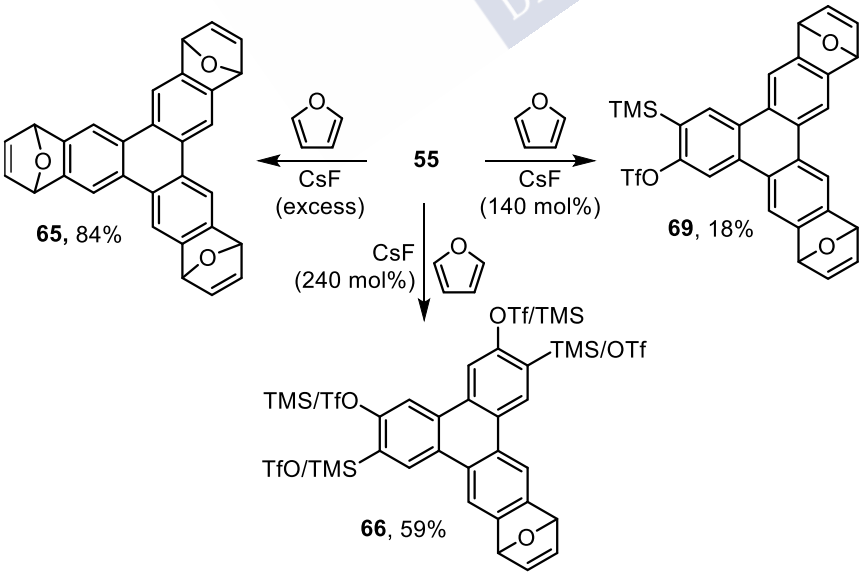
Figura 6. Propuesta retrosintética del 2,6,10-trifenilenotriino (**56**).

La síntesis de los potenciales precursores del 2,6,10-trifenilenotriino (**55**), comenzó a través de la *desprotección* selectiva de un grupo triflato del compuesto **58**, mediante la adición de *n*-BuLi. A continuación, el tratamiento del fenol obtenido (**60**) con anhidrido acético dio lugar al *precursor de bisarino enmascarado* **62** (Esquema 8). La reacción del acetato **62** con CsF en presencia de una pequeña cantidad de un catalizador de $Pd(PPh_3)_4$, condiciones generales para la ciclotrimerización de arinos desarrolladas en este grupo de investigación, permitió obtener los trímeros **63** con un 68% de rendimiento. Estos compuestos (**63**) fueron obtenidos en la proporción estadística 3:1, siendo minoritario el isómero con geometría C_3. Continuamos la síntesis mediante un protocolo de desprotección/esterificación hasta obtener los triflatos objetivo **55**. Resumiendo, hemos conseguido la síntesis de los potenciales precursores de trisarino **55** en cinco etapas y un rendimiento global del 34% a partir del compuesto comercialmente disponible **58** (Esquema 8).



Esquema 8. Síntesis de los tristriflatos **55**.

El siguiente paso fue el estudio de la capacidad de los triflatos **55** para la generación del sintón trisarínico **56**. En primer lugar, ensayamos la reacción de la mezcla de precursores **55** con furano, obteniendo la mezcla **65** con un excelente 84% de rendimiento (Esquema 9). Después, estudiamos la generación selectiva de una o dos de las insaturaciones arínicas de **55**, logrando aislar los correspondientes aductos, **66** y **69**, con un 59 y 18% de rendimiento respectivamente (Esquema 9). Con estos experimentos no sólo demostramos la capacidad de **55** para actuar como precursor del 2,6,10-trifenilenotriino (**56**), sino que también la posibilidad de generación selectiva de sus insaturaciones arínicas de manera independiente. Cabe destacar que es la primera vez que se consigue generar un arino, un bisarino y un trisarino desde un mismo precursor.



Esquema 9. Reacciones de **55** con CsF en presencia de furano.

Una vez probada la eficiencia de **55** como precursores del sintón trisarínico **56**, decidimos demostrar su utilidad como plataforma para acceder al HPAs derivados del trifenileno. La reacción de **55** con CsF en presencia de difenilisobenzofurano, antraceno o 2,3,4,5-tetrafenil ciclopentadienona permitió obtener los compuestos mostrados a continuación (Figura 7).

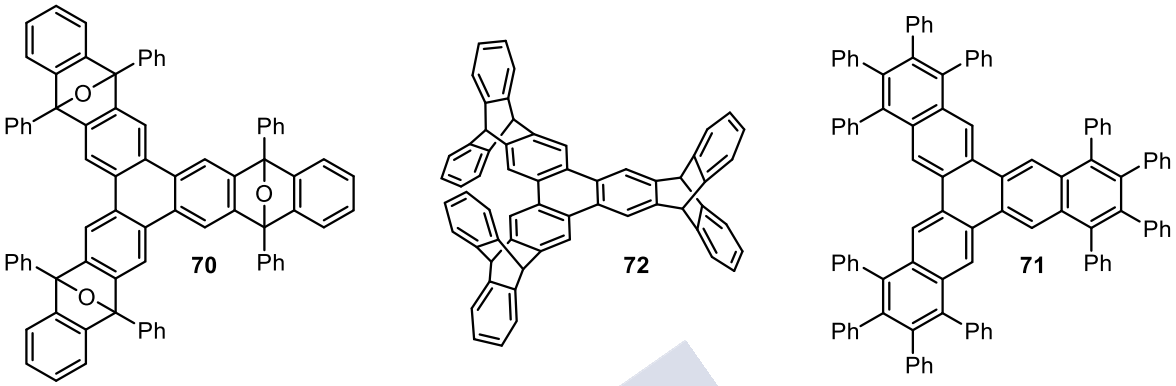


Figura 7. HPAs trigonales sintetizados utilizando **55**.

Para concluir, podemos destacar que se ha logrado la síntesis de dos precursores eficientes del 2,6,10-trifenilenotriino (**56**) que han permitido describir el segundo ejemplo de un trisarino utilizado en síntesis, el primero empleando el núcleo de trifenileno.

5 Síntesis de heteroacenos basada en arinos

Los acenos son una familia de moléculas formadas por la fusión lineal de anillos bencénicos. Algunos de ellos, como el pentaceno o el rubreno, han sido ampliamente utilizados como semiconductores en dispositivos electrónicos. Sus propiedades dependen de su tamaño, longitud y composición química entre otras características, por lo que es interesante la preparación de nuevos miembros de esta familia, que permitan estudiar y comprender la relación entre su estructura y propiedades.

El objetivo de este capítulo se centra en extender la metodología utilizada por nuestro grupo de investigación para la síntesis de acenos, basada en química de arinos. Concretamente, se propone la síntesis y el estudio de un grupo de heteroacenos que contengan un anillo terminal de triazol o isoxazol (Figura 8).

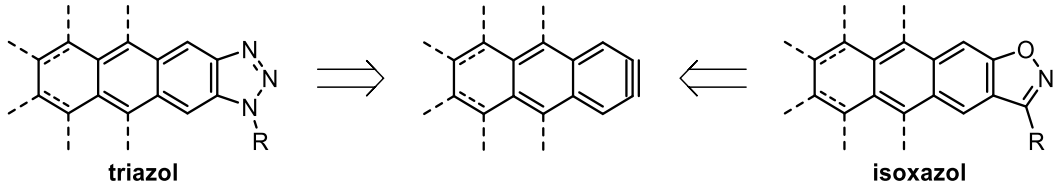
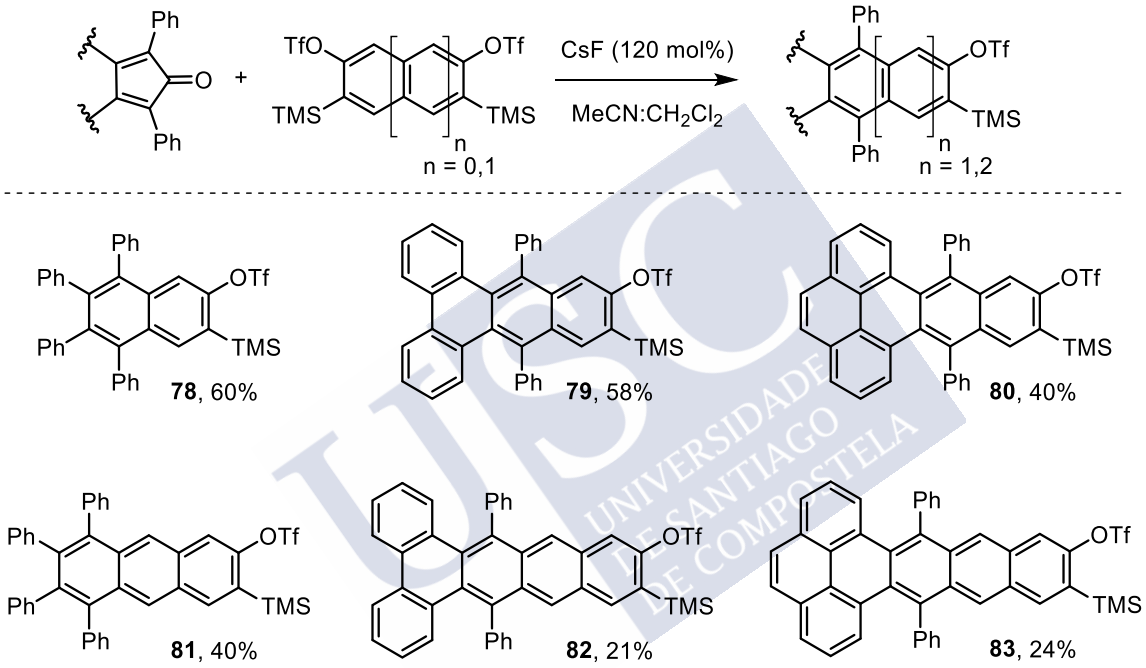


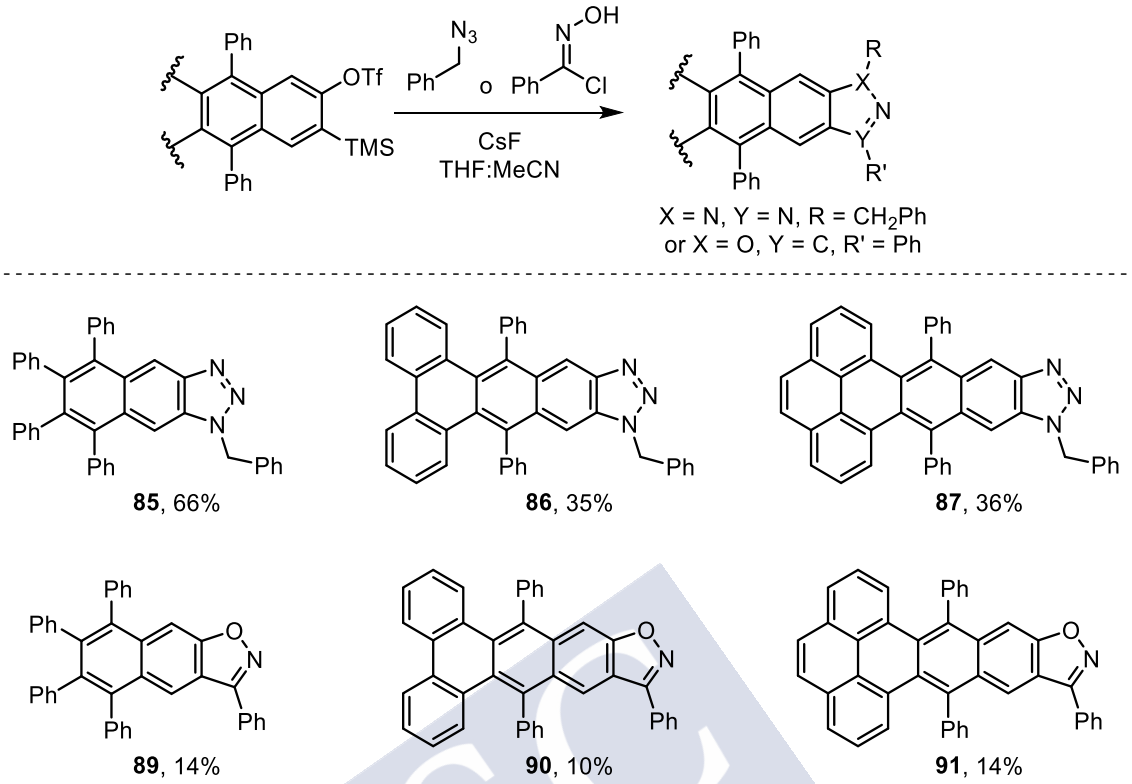
Figura 8. Propuesta retrosintética de heteroacenos triazólicos e isoxazólicos.

Para empezar, recurrimos al procedimiento previamente publicado y utilizado por nuestro grupo de investigación para sintetizar precursores de arinos estructuralmente complejos, **78**-**83** (Esquema 10), mediante el uso de precursores de bisarino y ciclopentadienonas.



Esquema 10. Síntesis de los precursores de arino estructuralmente complejos **78**-**83**.

Una vez dispusimos de los precursores requeridos, realizamos la reacción de cada uno de ellos con CsF en presencia de bencil azida. Desafortunadamente, las reacciones en las que se utilizaron los precursores **81**, **82** y **83**, dieron lugar a rendimientos bajos que impidieron el aislamiento y caracterización de los heteroacenos derivados de los mismos. Por este motivo continuamos el estudio de estas reacciones exclusivamente con los precursores de arino **78**, **79** y **80**, y obtuvimos los heteroacenos **85**, **86** y **87** con rendimientos moderados (Esquema 11). De manera análoga preparamos los isoxazoles **89**, **90** y **91** utilizando para ello fenil clorooxima (Esquema 11).



Esquema 11. Síntesis de heteroacenos.

Una vez obtenidos los heteroacenos mostrados anteriormente, se procedió al estudio preliminar de sus propiedades. El estudio mediante espectroscopía de absorción UV-vis, reveló valores de *gap* HOMO-LUMO entre 2.6 y 3.1 eV para todos ellos. Además, los análisis electroquímicos efectuados permitieron situar sus niveles energéticos HOMO y LUMO en valores cercanos a -5.6 y -2.6 eV, respectivamente. Ambos motivos estructurales, triazoles e isoxazoles, mostraron un comportamiento similar que se asocia al típico de los semiconductores orgánicos de tipo-*p*.

Podemos concluir que se han preparado seis heteroacenos de potencial interés como semiconductores orgánicos, a través de una nueva metodología basada en química de arinos.

6 Kekuleno

El estudio de la relación entre la estructura y las propiedades en moléculas orgánicas ha estado fuertemente ligado a algunas moléculas concretas que se emplearon como ejemplo. Inicialmente, el estudio de la aromaticidad se llevó a cabo en el benceno y anulenos. Posteriormente, el debate sobre la estructura electrónica de una molécula emblemática, el

kekuleno (**92**), captó la atención de la comunidad científica, que alcanzó su apogeo cuando en 1978 fue sintetizada y estudiada por Diederich y Staab.

El propósito de este capítulo se centra en el estudio del kekuleno desde una doble perspectiva; la exploración de una nueva síntesis mejorada (Figura 9), y la expansión del estudio de su estructura mediante microscopía de fuerza atómica de ultra alta resolución y la realización de cálculos teóricos.

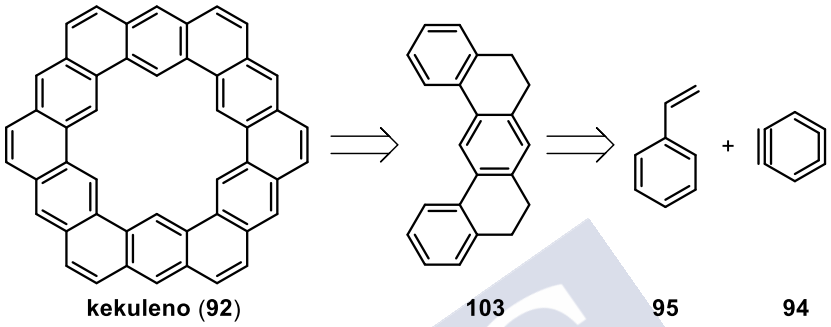
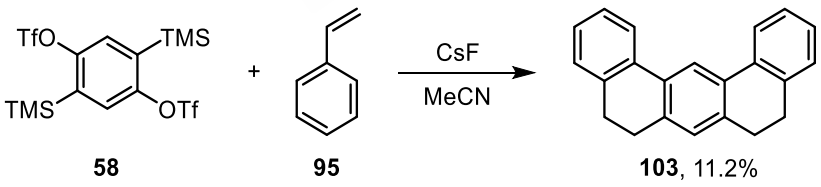


Figura 9. Propuesta retrosintética del kekuleno (**92**).

Siguiendo la ruta original de Diederich y Staab decidimos optimizar la síntesis del producto intermedio **103** mediante una doble reacción de Diels-Alder entre el bisarino **94** y dos moléculas de estireno (**95**) (Figura 9).

A pesar de la dificultad asociada a las reacciones entre arinos y estirenos, conseguimos obtener **103** y optimizar su síntesis hasta un 11.2% (Esquema 12). Este resultado supone un notable incremento del rendimiento, cuatro veces mayor que el previamente descrito y en un único paso. Además, esta aproximación evita el uso de condiciones de reacción drásticas y reactivos peligrosos.



Esquema 12. Síntesis del tetrahidrobenzotetrafeno **103**.

Una vez obtenido el compuesto **103**, y tras haber intentado varias alternativas sintéticas basadas en reacciones catalizadas por metales, continuamos la síntesis del kekuleno (**92**) siguiendo el procedimiento experimental publicado por Diederich y Staab. Esta resultó perfectamente reproducible en nuestras manos, incluso utilizando una escala considerablemente inferior. Muestras del kekuleno (**92**) fueron enviadas al grupo del Dr. Gross (IBM Research, Zurich), que consiguió obtener imágenes de AFM de alta resolución de

moléculas individuales. Estas imágenes permitieron observar que los enlaces C-C de mayor orden están situados en las regiones-*K*. Adicionalmente, la colaboración con el Prof. Melle-Franco, permitió estudiar computacionalmente la molécula de kekuleno en fase gas y sobre una superficie metálica, obteniendo resultados que coincidieron perfectamente con los datos obtenidos experimentalmente.

Los resultados confirman para moléculas individuales una estructura electrónica caracterizada por la presencia de sextetes aromáticos localizados denominada estructura de Clar, en lugar de dos corrientes electrónicas tipo anuleno (Figura 10), de acuerdo con las conclusiones obtenidas por Diederich y Staab anteriormente.

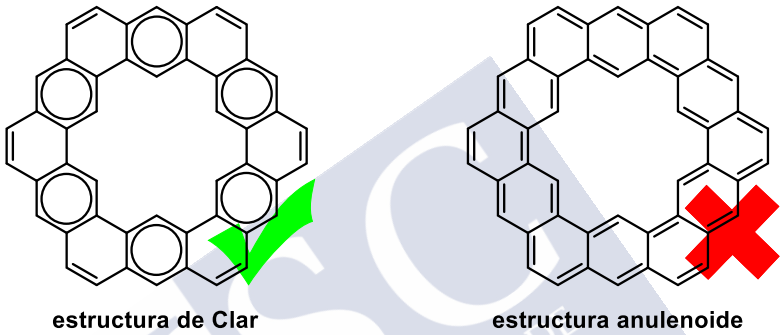


Figura 10. Estructuras electrónicas posibles para el kekuleno (**92**).